University of Alberta

UNDERSTANDING THE MOLECULAR BASIS OF SPINAL MUSCULAR ATROPHY

by

Victoria Elizabeth Cook

©

A thesis submitted to the Faculty of Graduate Studies and Research
in partial fulfillment of the requirements for the degree of

Master of Science

The Centre for Neuroscience

Edmonton, Alberta
Fall 2008

Library and
Archives Canada

Published Heritage
Branch

395 Wellington Street
Ottawa ON K1A 0N4
Canada

Bibliothèque et
Archives Canada

Direction du
Patrimoine de l'édition

395, rue Wellington
Ottawa ON K1A 0N4
Canada

Your file Votre référence
ISBN: 978-0-494-47196-8
Our file Notre référence
ISBN: 978-0-494-47196-8

NOTICE:
The author has granted a non-exclusive license allowing Library and Archives Canada to reproduce, publish, archive, preserve, conserve, communicate to the public by telecommunication or on the Internet, loan, distribute and sell theses worldwide, for commercial or non-commercial purposes, in microform, paper, electronic and/or any other formats.

The author retains copyright ownership and moral rights in this thesis. Neither the thesis nor substantial extracts from it may be printed or otherwise reproduced without the author's permission.

AVIS:
L'auteur a accordé une licence non exclusive permettant à la Bibliothèque et Archives Canada de reproduire, publier, archiver, sauvegarder, conserver, transmettre au public par télécommunication ou par l'Internet, prêter, distribuer et vendre des thèses partout dans le monde, à des fins commerciales ou autres, sur support microforme, papier, électronique et/ou autres formats.

L'auteur conserve la propriété du droit d'auteur et des droits moraux qui protège cette thèse. Ni la thèse ni des extraits substantiels de celle-ci ne doivent être imprimés ou autrement reproduits sans son autorisation.

In compliance with the Canadian Privacy Act some supporting forms may have been removed from this thesis.

While these forms may be included in the document page count, their removal does not represent any loss of content from the thesis.

Conformément à la loi canadienne sur la protection de la vie privée, quelques formulaires secondaires ont été enlevés de cette thèse.

Bien que ces formulaires aient inclus dans la pagination, il n'y aura aucun contenu manquant.

Canada

ABSTRACT

Spinal Muscular Atrophy (SMA) is a neuromuscular disorder caused by mutations in the *SMN1* gene. Analysis of ChAT, GAP-43 and MyHC proteins in a murine model of mild SMA indicated normal neuromuscular development and regeneration. However, we detected significant delays in denervation-induced muscle fiber atrophy in SMA muscles, which displayed a 29.4% reduction in average fiber CSA while that from WT animals was reduced by 52% 14d post-denervation. This finding may indicate alterations in PI3K/Akt signaling-mediated activation of the ubiquitin-proteasome system. Microarray analysis found substantial overlap of transcriptional changes between spinal cord and skeletal muscle of SMA animals, supporting a common molecular cause of disease in both tissues. We found significant overrepresentation of signaling-related genes, with KEGG pathway analysis specifically implicating MAPK and Wnt signaling. Collectively, findings implicate cell-signaling misregulation in development of SMA pathology. Further work will determine affectedness of PI3K/Akt, MAPK and Wnt signaling in SMA.

ACKNOWLEDGEMENTS

I would like to thank my supervisors, Drs. Tessa Gordon and Ted Putman, for their extensive help and guidance. I feel privileged to have learned from two individuals so enthusiastic about science. Dr. John Greer has also been very helpful through his role as committee member.

I feel extremely grateful for the technical assistance of Ian MacLean and Neil Tyreman, who were not only helpful in the lab, but have also played an important role as friends. I had the pleasure of working with Max Levine as a summer student, and Jo-An Padberg as a practicum student. Both were successful in contributing work for the completion of my thesis. I would like to express my appreciation for the help of Yang Shu, Dr. Esther Udina and Dr. Luke Harris, whose technical assistance and creative guidance were instrumental to the completion of this work. Finally, Karen Martins and Dr. Maria Gallo made the laboratory a positive place to work, and were excellent resources for technical information. I am also grateful to NSERC for their support in the form of a Canada Graduate Scholarship.

I am very lucky to have worked with such wonderful individuals, and would like to thank them for making my entire experience enjoyable. Finally, I would like to thank my amazing parents, Elizabeth and Alan, and my incredible friends, especially Dion and Troy. You have all been continually supportive of my work, and actually took the time to read my lengthy thesis drafts and provide constructive feedback. I hope to always make you proud!

TABLE OF CONTENTS

CHAPTER 1

1.1 INTRODUCTION 1

1.1.1 Clinical aspects of SMA 1

1.1.2 Genetic cause of SMA and modifier genes 3

1.1.3 Effects of SMN deficiency outside of the neuromuscular system 4

1.1.4 Expression and localization of SMN 5

1.1.5 SMN is essential for snRNP biogenesis 7

1.1.6 SMN functions in neurite outgrowth and mRNA trafficking 9

1.1.7 SMN plays a role in cytoskeletal integrity and actin organization 10

1.1.8 SMN affects actin dynamics in MN 11

1.1.9 SMN affects actin dynamics at the NMJ 13

1.1.10 Animal models of SMA 14

1.1.11 Mouse models used in the present study 17

1.1.12 Proteins integral to neuromuscular growth and development evaluated in the present study 17

1.2 STUDY RATIONALE 19

1.2.1 Delayed development hypothesis 19

1.2.2 Whole genome expression analysis 19

1.3 REFERENCES 20

CHAPTER 2: EVALUATION OF A DELAYED DEVELOPMENT HYPOTHESIS IN SMA

2.1 INTRODUCTION 37

2.2 METHODS AND MATERIALS 39

2.2.1 Animals 39

2.2.2 Surgeries and tissue removal 39

2.2.3 Choline acetyltransferase activity assay 39

2.2.4 Western blot analysis 40

2.2.5 Antibodies for immunohistochemistry 41

2.2.6 Immunohistochemistry 41

2.2.7 Immunohistochemical analyses 42

2.3 RESULTS 43

2.3.1 Choline acetyltransferase activity 43

2.3.2 Western blot analysis of GAP-43 in axotomized MN 45

2.3.3 Immunohistochemical analysis of muscle proteins 50

- 2.3.3.1. MyHC distribution 50
- 2.3.3.2. N-CAM expression 50
- 2.3.3.3. Cytoskeletal protein analysis 61
- 2.3.3.4. Analysis of muscle atrophy 68

2.4 DISCUSSION 73

2.4.1 Choline acetyltransferase expression 73

2.4.2 GAP-43 expression is not differentially expressed in SMAIII tissue and is upregulated similarly to WT after axotomy 73

2.4.3 Embryonic MyHC expression of does not persist, mature MyHC isoform distribution is unaffected in SMAIII skeletal muscle, and N-CAM staining provides no evidence for denervation in examined tissues 74

2.4.4 Staining for dystrophin, desmin and vimentin in skeletal muscle from Smn-/+-C57Bl/6 and smn-/-A2G-FVB is unremarkable 76

2.4.5 Denervation induced muscle atrophy as measured by fiber CSA is delayed in TA from 3 month smn-/-A2G-FVB mice 78

2.4.6 No evidence of developmental delays in nerve or skeletal muscle from SMAIII mice, but discovered delays in denervation-induced atrophy of skeletal muscle, and potential disorganization of the cytoskeletal protein dystrophin 81

2.4.7 Implication of present findings for delayed development hypothesis 82

2.5 REFERENCES 85

CHAPTER 3: GENE EXPRESSION ANALYSIS OF SMAIII MUSCLE AND NERVE

3.1 INTRODUCTION 96

3.2 METHODS 101

3.2.1 Animals 101

3.2.2 Tissue Removal and RNA extraction 101

3.2.3 cDNA labeling, array hybridization, and scanning 101

3.2.4 Data analysis 102

3.3 RESULTS 102

3.3.1 Microarray data quality assessment 102

3.3.2 Gene transcription in SMAIII Smn-/-A2G-FVB SpC and SkM relative to WT-FVB control tissues 104

3.3.3 Incorrect splicing of extracellular matrix and transporter-related genes in SMAII does not lead to overrepresentation of these genes among those affected in SMAIII SpC and SkM 106

3.3.4 Genes showing > 4 fold changes in expression are involved in protein breakdown, energy production, and signaling 108

3.3.5 Significant overlap exists between differentially regulated genes from SpC and SkM from SMAIII Smn-/-A2G-FVB mice 114

3.3.6 Functional grouping of differentially regulated genes in SpC and SkM from SMAIII Smn-/-A2G-FVB mice. 117

- 3.3.6.1. *Representation of genes with protein products involved in Development* 117
- 3.3.6.2. *Representation of genes with protein products involved in RNA transport and localization* 118
- 3.3.6.3. *Representation of genes with protein products involved in RNA processing and protein production* 119
- 3.3.6.4. *Representation of genes involved in cell cycle and apoptosis* 120
- 3.3.6.5. *Representation of genes with cytoskeleton-related protein Products* 121
- 3.3.6.6. *Representation of genes with signaling-related protein Products* 122

3.3.7 KEGG pathway analysis of differentially regulated genes in SMAIII $Smn^{-/-}$-A2G-FVB SpC and SkM 128

3.4 DISCUSSION 135

3.4.1 More genes were differentially regulated in SMAIII SpC than in SkM 135

3.4.1.1 No significant overlap between differentially regulated genes in SMAIII SpC and SkM and genes incorrectly spliced in SMAII SpC 136

3.4.1.2 Genes differentially regulated >4 fold in SMAIII SpC and SkM have roles in cell signaling, fatty acid oxidation and the proteasome pathway 136

3.4.1.3 Many transcriptional changes are shared and consistent between SMAIII SpC and SkM supporting the idea of a primary lesion common to both tissues in SMA 137

3.4.2 Differentially regulated genes in SMAIII SpC and SkM are NOT overrepresented among RNA-transport, RNA-processing, cell-death, or cytoskeletal-related functions 137

3.4.3 Signaling-related genes are overrepresented and MAPK and Wnt signaling pathways may be affected in SMA 139

3.4.3.1. Introduction to MAPK and Wnt signaling 140

3.4.3.2. MAPK and Wnt signaling are affected in neurodegenerative diseases 142

3.4.4. Differential regulation of signaling-related genes could result from reduced or altered ECM protein expression to explain aspects of molecular pathology observed in SMA 143

3.4.4.1 Defective signaling can explain reduced a reduced F:G-actin ratio in SMA cells 144

3.4.4.2 Signaling defects can explain aberrant AChR organization at the NMJ 147

3.4.5. Summary of findings 149

3.5 REFERENCES 150

CHAPTER 4

4.1 GENERAL DISCUSSION 162

4.2 REFERENCES 165

LIST OF TABLES

CHAPTER 3

Table 3.1 Summary of genes differentially regulated in SpC and SkM of SMAIII *Smn*$^{-/-}$*A2G*-FVB (n=3) compared with WT-FVB (n=3) based on pairwise analysis of microarray data generated by mouse whole genome cDNA microarrays from Agilent (log transformed data, Welch's t-test, adjusted p <0.05, Benjamini and Hochberg correction for FDR, quality=1) using GeneSifter software, and compared against genes incorrectly spliced in SMAII SpC according to Zhang *et al.*, 2008. 99

Table 3.2 Genes differentially regulated in SpC from SMAIII mice determined to be incorrectly spliced in SMAII spinal cord by Zhang *et al.*, 2008. 100

Table 3.3 Genes exhibiting a >4 fold change in expression levels in SpC from SMAIII *Smn*$^{-/-}$*A2G*-FVB mice compared to FVB-WT controls determined using GeneSifter (Welch's t-test, adjusted p<0.05, quality = 1, Benjamini and Hochberg correction for FDR, and >4 fold difference) 104

Table 3.4 Genes exhibiting a >4 fold change in expression levels in SkM from SMAIII *Smn*$^{-/-}$*A2G*-FVB mice compared to FVB-WT controls determined using GeneSifter (Welch's t-test, adjusted p<0.05, quality = 1, Benjamini and Hochberg correction for FDR, and >4 fold difference) 105

Table 3.5 Genes differentially regulated in both SpC and SkM from SMAIII *Smn*$^{-/-}$*A2G*-FVB mice compared to SpC and SkM from FVB-WT controls (log transformed data, Welch's t-test, adjusted p <0.05, Benjamini and Hochberg correction for FDR, quality=1) 108

Table 3.6 Genes involved in MAPK and Wnt signaling pathways differentially regulated in SpC from SMAIII *Smn*$^{-/-}$*A2G*-FVB mice compared to FVB-WT controls. 123

Table 3.7 Genes involved in MAPK and Wnt signaling pathways differentially regulated in SkM from SMAIII *Smn*$^{-/-}$*A2G*-FVB mice compared to FVB-WT controls. 126

LIST OF FIGURES

CHAPTER 1

Figure 1.1 (A) SMN demonstrates strong nuclear staining in human 20 week developing cortical plate and (B) preferentially localizes to the cytoplasm and gradually moves into axon processes during maturation. Figure from (Giavazzi *et al.*, 2006). 6

Figure 1.2 SMN colocalizes with GAP-43 in growth-cone-like structures of P19 cells. (A) SMN stains the cytoplasm and appears concentrated in growth-cone-like structures. (B) GAP-43 is located at soma edges and shows strongest staining in growth-cone-like structures. (C) Superimposition of SMN and GAP-43 labeling demonstrating strong colocalization in growth-cone-like structures. Scale bar is 10mm. Figure from Fan & Simard, 2002. 7

Figure 1.3 Simplified role of SMN in snRNP biogenesis. Figure from Kolb *et al.*, 2007. 8

Figure 1.4 Treadmilling effect of F-actin outgrowth showing depolymerization at the pointed end and polymerization at the barbed end. Figure from Pak *et al.*, 2008. 11

CHAPTER 2

Figure 2.1 There are no significant differences in ChAT levels between TA, BB and LC muscles from year old smn+/-C57Bl/6 and C57Bl/6-wild type or 3 month smn-/-A2G-FVB and FVB-wild type mice. ChAT levels in FM/ug/min. 44

Figure 2.2 Upregulation of GAP-43 in sciatic nerves from *Smn-/+*-C57Bl and C57Bl-wild type animals at 0, 3, 7 and 14 days post-axotomy (n=3 animals/condition) as determined by semi-quantitative western blot analysis. Each bar represents the average analysis of 12 sciatic nerves (n=3 mice). GAP-43 expression levels were normalized to those of the GAPDH loading control. 46

Figure 2.3 Increase in GAP-43 content of sciatic nerves as a function of days post-axotomy (0, 3, 7, and 14) in (A) C57Bl/6-WT and (B) *Smn-/+*-C57Bl/6 animals as determined by semi-quantitative western blot analysis. Each point on the graph represents an average of 4 sciatic nerves. Data were $\log_{10}$ transformed prior to linear regression analyses. 47

Figure 2.4 Upregulation of GAP-43 in sciatic nerves from *smn*$^{-/-}$-A2G-FVB and FVB-wild type animals at 0, 3, 7 and 14 days post-axotomy (n=3 animals/condition) as determined by semi-quantitative western blot analysis. Each bar represents the average analysis of 12 sciatic nerves (n=3 mice). GAP-43 expression levels were normalized to those of the GAPDH loading control. 48

Figure 2.5 Increase in GAP-43 content of sciatic nerves as a function of days post-axotomy (0, 3, 7, and 14) in (A) FVB-WT and (B) *Smn*$^{-/-}$-A2G-FVB animals as determined by semi-quantitative western blot analysis. Each time point on the graph represents an average of 4 sciatic nerves. Data were log$_{10}$ transformed prior to linear regression analyses. 49

Figure 2.6 Representative MyHC distribution in TA sections from year old smn+/-C57Bl/6 (A-D) and C57Bl/6-wild type (A'-D') mice. A/A' – Type I (BAD5); B/B' – Type IIB (BFF3); C/C' – Type IID/X (BF35); D/D' – Type IIA (SC71). Positive identification of type IID/X fibers (C/C') is indicated by the **absence** of staining. 52

Figure 2.7 Representative MyHC distribution in TA sections from 3 month smn-/-A2G-FVB (A-D) and FVB-wild type (A'-D') mice. A/A' – Type IIB (BFF3); B/B' – Type IID/X (BF35); C/C' – Type IIA (SC71). Positive identification of type IID/X fibers (C/C') is indicated by the **absence** of staining. Results for Type I (BAD5) were all negative and are not shown. 53

Figure 2.8 Percentage of tibialis anterior fibers expressing a given MyHC isoform from year old smn+/-C57Bl/6 mice and C57Bl/6-wild type controls and 3 month smn-/-A2G-FVB mice and FVB-wild type controls measured using immunohistochemistry. There are no significant differences in fiber type distribution between samples from either SMAIII strain and respective wild type controls. 54

Figure 2.9 Figure 2.9. Representative MyHC distribution in LC sections from 3 month smn-/-A2G-FVB (A-D) and FVB-wild type (A'-D') mice. A/A' – Type I (BAD5); B/B' – Type IIB (BFF3); C/C' – Type IID/X (BF35); D/D' – Type IIA (SC71). Positive identification of type IID/X fibers (C/C') is indicated by the **absence** of staining. 56

Figure 2.10 Percentage fibers expressing a given MyHC isoform in LC muscles from 3 month smn-/-A2G-FVB and FVB-wild type mice measured using immunohistochemistry. There are no significant differences in fiber type distribution between samples from SMAIII mice and wild type controls. 57

Figure 2.11 Representative MyHC distribution in Sol sections from 3 month smn-/-A2G-FVB (A-D) and FVB-wild type (A'-D') mice. A/A' – Type I (BAD5); B/B' – Type IIB (BFF3); C/C' – Type IID/X (BF35); D/D' – Type IIA (SC71). Positive identification of type IID/X fibers (C/C') is indicated by the absence of staining. 59

Figure 2.12 Percentage fibers expressing a given MyHC isoform in Sol muscles from 3 month smn-/-A2G-FVB and FVB-wild type mice measured using immunohistochemistry. There are no significant differences in fiber type distribution between samples from SMAIII mice and wild type controls. 60

Figure 2.13 Normal staining for cytoskeletal protein in superficial regions of quadriceps muscles from a year old smn+/-C57Bl/6 mouse. A/A' – desmin; B/B' – dystrophin; C/C' – vimentin. Images A-C were taken at 125X magnification, while A'-C' were taken at 312.5X. 62

Figure 2.14 Normal staining for cytoskeletal protein in superficial regions of quadriceps muscles from a year old C57Bl/6-wild type mouse. A/A' – desmin; B/B' – dystrophin; C/C' – vimentin. Images A-C were taken at 125X magnification, while A'-C' were taken at 312.5X. 63

Figure 2.15 Representative staining for the cytoskeletal proteins desmin (A/A'), dystrophin (B/B') and vimentin (C/C') in superficial regions of quadriceps muscle from a 3 month smn-/-A2G-FVB animals. Images A-C were taken at 125X magnification, while A'-C' were taken at 312.5X. 64

Figure 2.16 Representative staining for the cytoskeletal proteins desmin (A/A'), dystrophin (B/B') and vimentin (C/C') in superficial regions of quadriceps muscle from a 3 month smn-/-A2G-FVB animals. Some evidence of stronger staining, mostly in smaller fibers.Images A-C were taken at 125X magnification, while A'-C' were taken at 312.5X 65

Figure 2.17 Representative staining for the cytoskeletal proteins desmin (A/A'), dystrophin (B/B') and vimentin (C/C') in superficial regions of quadriceps muscle from a 3 month smn-/-A2G-FVB animals. Some evidence of stronger staining, mostly in smaller fibers.Images A-C were taken at 125X magnification, while A'-C' were taken at 312.5X 66

Figure 2.18 Representative staining for the cytoskeletal proteins desmin (A/A'), dystrophin (B/B') and vimentin (C/C') in superficial regions of quadriceps muscle from a 3 month FVB-wild type animal. Images A-C were taken at 125X magnification, while A'-C' were taken at 312.5X. 67

Figure 2.19 Percentage of tibialis anterior fibers expressing N-CAM 0, 3, 7 and 14 days after sciatic nerve axotomy in 3 month smn-/-A2G-FVB and FVB-wild type mice. 69

Figure 2.20 Denervation induced reduction in cross-sectional area of tibialis anterior muscle fibers from 3 month old smn-/-A2G and corresponding FVB wild type control mice at 0 and 3 days post-axotomy. In intact muscle average fiber CSA is extremely similar between FVB-WT (1606.9 μm^2) and smn-/-A2G (1601.4 μm^2) mice. Three days post-axotomy, the average fiber CSA is slightly smaller in FVB-WT (1367 μm^2) than in smn-/-A2G (1659.6 μm^2), but this difference is not significant (p=0.16). 70

Figure 2.21 Denervation induced reduction in cross-sectional area of tibialis anterior muscle fibers from 3 month old smn-/-A2G and corresponding FVB wild type control mice at 0 and 3 days post-axotomy. At 7d post-axotomy, the delay in denervation atrophy in smn-/-A2G muscles is more pronounced, with FVB-WT animals having an average fiber CSA of 940.7 μm^2, while smn-/-A2G average fiber CSA measured 1356.1 μm^2 (p=0.018). At 14d post-axotomy, the average fiber CSA of FVB-WT mice (662.6 μm^2) was much smaller than that measured in smn-/-A2G animals (1134.5 μm^2) although this difference did not reach significance (p=0.072). 71

Figure 2.22 Time course denervation induced reduction in cross-sectional area of tibialis anterior muscle fibers from 3 month old smn-/-A2G and corresponding FVB wild type control mice 0, 3, 7, and 14 days post-axotomy. Muscles from smn-/-A2G-FVB mice demonstrate a delayed response to denervation as measured by cross-sectional area although this difference is not significant (p=0.13). 72

Figure 2.23 Signaling responsible for regulation of anabolic (hypertrophic) and catabolic (atrophic) states in skeletal muscle. (Sandri *et al.*, 2004) 80

CHAPTER 3

Figure 3.1 Scatter plot of all data points from SpC (A) and SkM (B) microarray data illustrating genes differentially expressed in SMAIII *Smn*$^{-/-}$*A2G*-FVB animals (n=3) compared to WT-FVB controls (n=3). Genes that did not pass the filtering criteria are displayed in gray, upregulated genes are shown in red, while downregulated genes are shown in green. 97

Figure 3.2 Visual representation of overlap of differential expression in SpC and SkM from SMAIII *Smn*$^{-/-}$*A2G*-FVB mice with genes found to be incorrectly spliced in SpC from SMAII mice according to Zhang *et al.*, 2008. 99

Figure 3.3 Percentage of differentially regulated genes from SMAIII *Smn*$^{-/-}$*A2G*-FVB SpC and SkM, ALS 60d MN, and XLMTM SkM with protein product functions involved in transporter activity and the extracellular matrix as determined by GOTM. 101

Figure 3.4 Percentage of differentially regulated genes from SMAIII *Smn*$^{-/-}$*A2G*-FVB SpC and SkM, ALS 60d MN, and XLMTM SkM determined to have protein product functions related to development determined using GOTM. 112

Figure 3.5 Percentage of differentially regulated genes from SMAIII *Smn*$^{-/-}$*A2G*-FVB SpC and SkM, ALS 60d MN, and XLMTM SkM determined to have protein product functions related to RNA transport and localization using GOTM. 113

Figure 3.6 Percentage of differentially regulated genes from SMAIII *Smn*$^{-/-}$*A2G*-FVB SpC and SkM, ALS 60d MN, and XLMTM SkM with protein product functions related to RNA processing and protein production determined using GOTM. 114

Figure 3.7 Percentage of differentially regulated genes from SMAIII *Smn*$^{-/-}$*A2G*-FVB SpC and SkM, ALS 60d MN, and XLMTM SkM with protein product functions related to cell cycle and apoptosis determined using GOTM. 115

Figure 3.8 Percentage of differentially regulated genes from SMAIII *Smn*$^{-/-}$*A2G*-FVB SpC and SkM, ALS 60d MN, and XLMTM SkM with protein product functions related to the cytoskeleton determined using GOTM. 116

Figure 3.9 Chart describing functional classifications of differentially regulated genes involved in cell communication according to the Gene Ontology Consortium (http://www.geneontology.org). 117

Figure 3.10 Percentage of differentially regulated genes from SMAIII *Smn*$^{-/-}$*A2G*-FVB SpC and SkM, ALS 60d MN, and XLMTM SkM with protein product functions involved in cell-cell signaling and signal transduction as determined by GOTM. Numbers shown indicate the actual number of genes involved in a given function. 118

Figure 3.11 Percentage of differentially regulated genes from SMAIII *Smn*$^{-/-}$*A2G*-FVB SpC and SkM, ALS 60d MN, and XLMTM SkM with protein product functions involved in cell surface receptor linked signal transduction, the G-protein coupled receptor signaling pathway, enzyme linked receptor protein signaling pathways, and the Wnt receptor signaling pathway as determined by GOTM. Numbers shown indicate the actual number of genes involved in a given function. Numbers shown indicate the actual number of genes involved in a given function. 119

Figure 3.12 Percentage of differentially regulated genes from SMAIII *Smn*$^{-/-}$*A2G*-FVB SpC and SkM, ALS 60d MN, and XLMTM SkM with protein product functions involved in intracellular signaling cascades, small GTPase mediated signal transduction, and ras protein signal transduction as determined by GOTM. Numbers shown indicate the actual number of genes involved in a given function. 120

Figure 3.13 Percentage of differentially regulated genes from SMAIII *Smn*$^{-/-}$*A2G*-FVB SpC and SkM, ALS 60d MN, and XLMTM SkM with protein product functions involved in second-messenger-mediated signaling, phosphoinositide-mediated signaling, and the protein kinase cascade as determined by GOTM. Numbers shown indicate the actual number of genes involved in a given function. 121

Figure 3.14 Involvement of differentially regulated genes from SMAIII *Smn*$^{-/-}$*A2G*-FVB SpC in the MAPK signaling pathway. Affected genes are in red, and murine ortholog gene names and fold change in transcription are shown in red-lined boxes. 124

Figure 3.15 Involvement of differentially regulated genes from SMAIII *Smn*$^{-/-}$*A2G*-FVB SpC in the Wnt signaling pathway. Affected genes are in red, and murine ortholog gene names and fold change in transcription are shown in red-lined boxes. 125

Figure 3.16 Involvement of differentially regulated genes from SMAIII *Smn*$^{-/-}$*A2G*-FVB SkM in the MAPK signaling pathway. Affected genes are in red, and murine ortholog gene names and fold change in transcription are shown in red-lined boxes. 127

Figure 3.17 Involvement of differentially regulated genes from SMAIII *Smn-/-A2G*-FVB SkM in the Wnt signaling pathway. Affected genes are in red, and murine ortholog gene names and fold change in transcription are shown in red-lined boxes. 128

Figure 3.18 Simplified diagram of general (a) and classical (b) MAPK signaling pathways. ERKs, JNKs, and p38 MAPKs are the three main groups of MAP kinases which act as effectors for external signals in this pathway. 135

Figure 3.19 Summary of noncanonical and canonical Wnt signaling pathways. Canonical and calcium noncanonical pathways lead to transcriptional changes within the cell, while disheveled (DVL) acts through the small GTPases RhoA and Rac to influence cell polarity in the PCP noncanonical pathway. From (Chun *et al.*, 2008). 136

Figure 3.20 Review of canonical Wnt, PI3K/Akt and the classical MAPK pathway signaling occurring in response to integrin-ECM binding and external signals (GF and Wnt). Modified from (Takeuchi *et al.*, 2008). 139

Figure 3.21 Summary of RhoA-GTP actions in stress fiber formation via downstream effectors mDia (Dia1) and ROCK. Cofilin is not shown, but functions in depolymerizing the 'minus' end of the actin filament which faces away from the leading edge; its action is inhibited by RhoA-GTP. Stress fibers provide stabilization and allow conduction of mechanical signals and more efficient conduction of ligand-mediated signals (i.e. GFs). 140

Figure 3.22 Description of how losses or changes in ECM protein composition could cause aberrant signaling leading to failed AChR organization at the post-synaptic membrane of the NMJ. Reductions in ECM components, such as collagens and laminin, may lead to (a) inefficiencies in agrin binding for MuSK activation, and also to reduced activation of integrin proteins and subsequent down stream signaling (such as MAPK and PI3K), which would affect activation levels of small GTPases Rho (not depicted here), Rac, and Cdc42. Impaired activation of these important regulator proteins will prevent F-actin polymerization and bundling, which is a requirement for AChR stabilization and organizational movement within the membrane. Additionally, cofilin will remain active and continue F-actin depolymerization. Wnt signaling may also be involved, as Wnt activation promotes dispersal of AChR clusters, however increased levels of β-catenin alone promote clustering by acting as a linker molecule between rapsyn/AChRs and α-catenin/F-actin. Picture modified from (Luo *et al.*, 2003). 142

LIST OF ABBREVIATIONS

ACh	acetylcholine
AChR	acetylcholine receptor
ADF	actin depolymerizing factor (cofilin)
ALS	Amyotrophic Lateral Sclerosis
BB	biceps brachii
BSA	bovine serum albumin
CNS	central nervous system
CSA	cross sectional area
DeSyn	delayed synapse forming
EMG	electromyography
EMG	electron microscopy
ERK	extracellular signal related kinase
F-actin	filamentous actin
FaSyn	fast synapse forming
FL-SMN	full-length SMN
FMRP	Fragile X Mental Retardation Protein
G-actin	globular actin
GAP-43	growth associated protein 43
GAPDH	glyceraldehyde 3-phosphate dehydrogenase
GFP	green fluorescent protein
GO	gene ontology
GOTM	GO Tree Machine
GSK	glycogen synthase kinase
hnRNP	heterogeneous nuclear ribonucleoprotein
Ig	immunoglobulin
JNK	Jun N-terminal kinase
KEGG	Kyoto Encyclopedia of Genes and Genomes
LC	longus capitus
MAPK	MAP kinase
MAPKK	MAP kinase kinase
MAPKKK	MAP kinase kinase kinase
MG	medial gastrocnemius
MLC	myosin light chain
MMP	matrix metalloproteinase
MN	motoneuron
mRNA	messenger ribonucleic acid
MuSK	muscle specific tyrosine kinase
MyHC	myosin heavy chain
NAIP	neuronal apoptosis inhibitory protein
N-CAM	neural cell adhesion molecule
NMDA	N-methyl D-aspartate
NMJ	neuromuscular junction
PAGE	polyacrylamide gel electrophoresis
PBS	phosphoate buffered saline
PI3K	phosphoinositide 3 kinase
Q	quadriceps
qRT-PCR	quantitative reverse transcriptase polymerase chain reaction
RNA	ribonucleic acid

RPM	revolutions per minute
SDS	sodium dodecyl sulphate
SEM	standard error of the mean
SkM	skeletal muscle
SMA	Spinal Muscular Atrophy
SMAI	Type I SMA
SMAII	Type II SMA
SMAIII	Type III SMA
SMN	survival of motor neuron
snoRNP	small nucleolar ribonucleoprotein
snRNP	small nuclear ribonucleoprotein
Sol	soleus
SpC	spinal cord
SpC	spinal cord
TA	tibialis anterior
UTR	untranslated region
WASP	Wiskott-Aldrich Syndrome Protein
Wnt	wingless integration
WT	wild type
XLMTM	X-linked myotubular myopathy

CHAPTER 1: EVALUATION OF A DELAYED DEVELOPMENT HYPOTHESIS IN SMA

1.1 INTRODUCTION

1.1.1. Clinical aspects of SMA

Spinal Muscular Atrophy (SMA) was originally described by Werdnig and Hoffman in 1890. Patients, typically infants and young children, present with dramatic losses in muscle tone, and frequently die before 2 years. Disease progression and range of clinical symptoms are highly variable, and a classification system has been developed to loosely group clinical cases (Russman, 2007;Pearn, 1980). Type I SMA (SMAI), also known as Werdnig-Hoffman disease, is the most severe form with documented onset prior to 6 months and fast progression. SMAI patients are never able to sit independently, and die at a median age of 7 months. Type II SMA (SMAII) patients display first clinical signs around 2 years, and demonstrate highly variable rates of disease progression. These patients live into early to late childhood, and although they gain the ability to sit independently, they are never able to walk unaided. Type III SMA (SMAIII), also called Kugelberg-Welander Syndrome, is the mildest form of SMA,with age of onset ranging from childhood to late teens. Patients frequently live into adulthood and are able to walk independently. Progression is typically much slower than in SMAI and II. Publications also document occurrence of prenatal onset SMA (SMA0) (Nadeau *et al.*, 2007;Sarnat & Trevenen, 2007), leading to death *in utero* or immediately after birth, and adult onset SMA (SMAIV), where diagnosis is made in adulthood and lifespan is typically unaffected. For a recent classification review, please refer to (Russman, 2007).

Pathology visible with the naked eye in end-stage SMAI-III includes some visible axonal death in ventral roots although the brain and spinal cord remain mostly normal in appearance, and muscles appear small and pale (Batten *et al.*, 1911). Observations made using a light microscope revealed structural changes in some spinal motoneurons that are characteristic of those that have lost their connectivity with muscle and that have been referred to collectively as chromatolytic neurons. Degeneration of other motoneurons and progressive degenerative changes in the peripheral nerves have also been seen (Crawford & Pardo, 1996). Anterior spinal roots are significantly thinned (Simic *et al.*, 2000) and display losses of large myelinated fibers, while thin myelinated fibers are preserved. These findings are often accompanied by the presence of glial bundles (Chou & Nonaka, 1978). Chou & Nonaka (1978) and Omran *et al.* (1998) clearly demonstrate axonal degeneration of nerve fibers from anterior and posterior spinal roots, although Szliwowski & Drochmans (1975) failed to note abnormal axon pathology. Many axons contain myelin ovids, indicative of active axonal degeneration (Chou & Nonaka, 1978;Crawford & Pardo, 1996). Active apoptotic death in motoneurons (MN) in anterior horn sections was demonstrated by Soler-Botija *et al.* (2002), who suggested that selective neuromuscular degeneration in SMA might be caused by over-activation of naturally occurring apoptotic 'pruning' processes during development. Urbanits & Budka, (1996) investigated the role of cytoskeletal components in disease pathology in spinal cord sections of Amyotrophic Lateral Sclerosis (ALS) and SMA patients, and found that swollen MN axons from most SMA and a small number of ALS patients stained positively for phosphorylated neurofilament proteins. Authors noted that in comparison to ALS cases, neuronal cytoskeletal pathology was more prominent in SMA. Typically pathology has been confined to motoneurons. Patients experience no pain, and remain responsive to all cutaneous stimuli, although decreased conduction in sensory nerves has been documented in very severe cases (Anagnostou *et al.*, 2005)(Rudnik-Schoneborn *et al.*, 2003).

In muscle, spontaneous nocturnal cramps and minimal electromyography (EMG) abnormalities have been described as preclinical symptoms of SMA (Bussaglia *et al.*, 1997). EMG findings are typically unremarkable in SMAIII patients, but recordings in severe patients can display spontaneous activity, continuous activity at rest, and are often dominated by fibrillation potentials, indicative of atrophy and axonal degeneration (for reviews see Crawford & Pardo, 1996). Electron microscopy (EM) performed on skeletal muscle samples from SMAI patients found myofilament degeneration, focal proliferation of the sarcoplasmic reticulum, and mitochondrial degeneration (Roy *et al.*, 1971;Szliwowski & Drochmans, 1975). Muscles demonstrate widespread fiber atrophy and significant hypertrophy (increase of cross sectional area) of Type I and occasionally Type II fibers (Bobele *et al.*, 1996)(Kingma *et al.*, 1991). In SMA, weakness typically progresses from the shoulders→thighs→upper arms→forearm→legs (Deymeer *et al.*, 1997). Paralysis is characteristically proximal, with patients typically able to move fingers and toes despite arms and legs being completely paralyzed (Batten *et al.*, 1911). The diaphragm remains intact despite weakening of the intercostal muscles.

Immunohistochemical analysis of the muscles demonstrates presence of increased pathological desmin and vimentin staining in atrophic muscle fibers (Sarnat, 1992) and in some hypertrophic type I and IIA muscle fibers from SMAI patients (Goebel, 1995). Expression of these two intermediate filament proteins is common to numerous myopathies including X-linked recessive myotubular myopathy (XLMTM) and nemaline rod myopathy (Goebel, 1995)(Sarnat, 1992). Numerous studies have demonstrated that myosin heavy chain (MyHC) isoform distribution in skeletal muscle fibers is normal in SMAI-III, refuting the idea that SMA leads to a maturational arrest of fibers (Johnson & Kucukyalcin, 1978)(Sawchak *et al.*, 1990;Soubrouillard *et al.*, 1995;Soussi-Yanicostas *et al.*, 1992). Soubrouillard *et al.* (1992) noted developmental MyHC isoform and N-CAM expression in atrophic fibers from SMAI and II patients, a finding common to multiple forms of muscle degeneration (Smith *et al.*, 1999)(Stupka *et al.*, 2008), as well as the presence of an increased number of hybrid fibers in SMAI but not in SMAIII patient samples.

1.1.2. Genetic cause of SMA and modifier genes

SMA results from loss-of-function mutations in the *SMN1* gene, which is located at 5q13 and codes for a ubiquitously expressed 294 amino acid protein, SMN (survival of motor neuron) (Lefebvre *et al.*, 1995). A relatively recent duplication event in this region has made humans unique in the possession of a nearly identical centromeric copy of this gene, *SMN2* (van der *et al.*, 1996). Five base pair differences affect splicing enhancer and repression sites, causing alternative splicing of *SMN2*. This results in the skipping of exon 7 in ~90% of transcripts (Cartegni & Krainer, 2002)(Lorson *et al.*, 1999), leading to production of mostly truncated protein products, and very little full-length SMN (FL-SMN). Although *SMN2* cannot compensate for the loss of *SMN1*, it is considered a phenotypic modifier, as increased *SMN2* copy number is associated with decreased disease severity (Gavrilov *et al.*, 1998)(Parsons *et al.*, 1996). A second candidate gene was discovered for SMA: *NAIP*, coding for 'neuronal apoptosis inhibitory protein', and has since been classified as a modifier of phenotypic severity. NAIP prevents apoptosis through inhibition of caspases 3 and 7 and its overexpression has a protective effect on neurons provoked with pro-apoptotic stimuli (Maier *et al.*, 2002)(Xu *et al.*, 1997). *NAIP* is located in the same 5q region as *SMN1*, and large-scale deletions in this region frequently affect both genes (Roy *et al.*, 1995). Loss-of-function deletions in both *NAIP* and *SMN1* are associated with severe cases of SMAI (Al *et al.*, 1998)(Roy *et al.*, 1995)(Somerville *et al.*, 1997), likely because cells lacking *NAIP* have reduced ability to cope with negative stimuli, such as the loss of *SMN1*. Microarray studies comparing differential gene expression between affected and unaffected sibling pairs with identical *SMN1* deletions and *SMN2* copy number identified an additional phenotypic modifier gene, *plastin 3/T-plastin*, encoding a fibrin protein, T-plastin, involved in actin organization (Giganti *et al.*, 2005). Over-expression of *T-plastin* in individuals with *SMN1* deletions leads to near or complete amelioration of a disease phenotype (Oprea *et al.*, 2008).

1.1.3. Effects of SMN deficiency outside of the neuromuscular system

Effects of SMN deficiency in motoneurons and skeletal muscle have been amply documented. However, a small number of studies have focused on the role of SMN in other tissues. Vitte *et al.* (2004) used the Cre-loxP system to target deletion of murine *Smn* exon 7 to hepatocytes, resulting in a near-complete lack of full length FL-SMN produced in liver, a tissue asymptomatic in SMA patients. While other tissues remained unaffected, liver growth was stunted, function was impaired, and the liver exhibited mass iron overload, indicating that all tissues require at least low levels of FL-SMN. Bone fractures and hypercalcemia (elevated blood calcium levels) are frequent clinical features of SMA in human patients. Some studies suggest that these difficulties are not merely the result of reduced muscular activity (Felderhoff-Mueser *et al.*, 2002), indicating that SMN may play an important role in bone development and maintenance. This idea is supported by the observation that in SMA patients, bone mineral density decreases with age in a manner distinct from any decline in motor function (Kinali *et al.*, 2004). Multiple murine models of SMA display spinal column pathology (Hsieh-Li *et al.*, 2000)(Monani *et al.*, 2000)(Monani *et al.*, 2003), presenting with shortened, degenerating tails. (Shanmugarajan *et al.*, 2007) used dual energy x-ray absorptiometry analysis of the lower body of SMAIII animals (Hsieh-Li *et al.*, 2000) to discover a significant reduction of total bone area, mineral content, and mineral density in these animals compared to wild type (WT) counterparts. Authors interpret these findings as indicative of a functional role for SMN in development and remodeling of bone. There have also been reports of cardiac involvement in SMAI-III. Specifically, (Menke *et al.*, 2008) describe two cases of SMAI appearing with hypoplasia of the left heart, and present a review of 18 similar cases, indicating that occurrence of congenital heart defects in SMA is not merely coincidental. (Takahashi *et al.*, 2006) present a case study and review of cardiac abnormalities in SMAIII, in patients of ages 21-53. These studies indicate that atrial fibrillation and fibrosis of cardiac muscle are common findings in SMAIII, and may represent another aspect of pathology in this disease (Sugimura *et al.*, 1973)(Takahashi *et al.*, 2006)(Tanaka *et al.*, 1976).

1.1.4 Expression and localization of SMN

Unusual nuclear staining for SMN in HeLa cell nuclei led to the discovery of novel nuclear structures containing proteins involved in small nuclear ribonucleoprotein (snRNP) metabolism labeled 'gemini of coiled bodies' (gems) due to their proximity to Cajal bodies, which are nucleoli-associated circular structures containing proteins involved in transcription (Liu & Dreyfuss, 1996) (Lefebvre *et al.*, 1997). Subsequent research has demonstrated that gems exist only in fetal tissues and a small subset of cell lines (HeLa), but are indistinguishable from Cajal bodies in mature tissues (Young *et al.*, 2001). The fusion of these structures is the result of symmetrical arginine dimethylation of SMN that occurs late in development and increases its association with coilin, a major component of Cajal bodies (Hebert *et al.*, 2001)(Hebert *et al.*, 2002). Localization of SMN in the nucleus and in the cytoplasm at nuclear pore complexes associated with ribosomes has been confirmed in multiple studies, and is related to SMN function in snRNP biogenesis, described later (Bechade *et al.*, 1999).

SMN is a ubiquitously expressed protein that has been detected in many fetal tissues, including dorsal and ventral spinal cord, skeletal muscle, lungs, heart, kidney, liver and spleen (Novelli *et al.*, 1997). (Coovert *et al.*, 1997) assessed SMN levels in tissues from SMA patients and normal human controls. Control samples contained moderate levels of SMN in skeletal and cardiac muscle, and significantly higher levels in brain, kidney, and liver. This broad expression pattern is also observed in mice (Viollet *et al.*, 1997). SMN expression in all tissue types is maximal during early growth and development and diminishes with age, except in motoneurons where age-related reduction of SMN levels was smaller than that observed in other cell types (Pagliardini *et al.*, 2000). Phenotypic severity in SMA is dependent upon the degree of SMN reduction in SMA, with significant reduction of SMN in SMAI patient samples, and near normal levels in samples from SMAIII patients (Lefebvre *et al.*, 1997)(Vitte *et al.*, 2007). SMN mRNA and protein are expressed throughout the central nervous system (CNS), demonstrating strongest expression in motoneurons (Battaglia *et al.*, 1997). SMN is found in both nucleus and cytoplasm, but shows a preferential localization to the cytoplasm and subsequently to axons and dendrites with maturation (Figure 1.1) (Battaglia *et al.*, 1997)(Burlet *et al.*, 1998)(Giavazzi *et al.*, 2006), where it is associated with microtubules (Bechade *et al.*, 1999)(Pagliardini *et al.*, 2000). Within axons, SMN exhibits preferential localization to growth cones (Fan & Simard, 2002) (Figure 1.2). A series of studies by (Zhang *et al.*, 2003;Zhang *et al.*, 2006;Zhang *et al.*, 2007) using live cell imaging of expressing green fluorescent protein-tagged SMN (SMN-GFP) in PC12 neurons allowed visualization of "rapid, bi-directional and microtubule-dependent" movement of SMN along axons, as a component of either small (oscilliatory movement) or large complexes (which transversed long distances). In axons and growth cones, SMN targets to polyA mRNA-containing granules, indicating a function in site-specific mRNA processing in neurons (Zhang *et al.*, 2007). In skeletal muscle, SMN does not exhibit the general cytoplasmic localization observed in other tissues, and is found instead in large punctuate structures in the cytoplasm as a member of a heavy sedimenting complex (Burlet *et al.*, 1998). Further analysis in skeletal muscle revealed localization of SMN at the post-synaptic domain of the neuromuscular junction (Broccolini *et al.*, 1999).

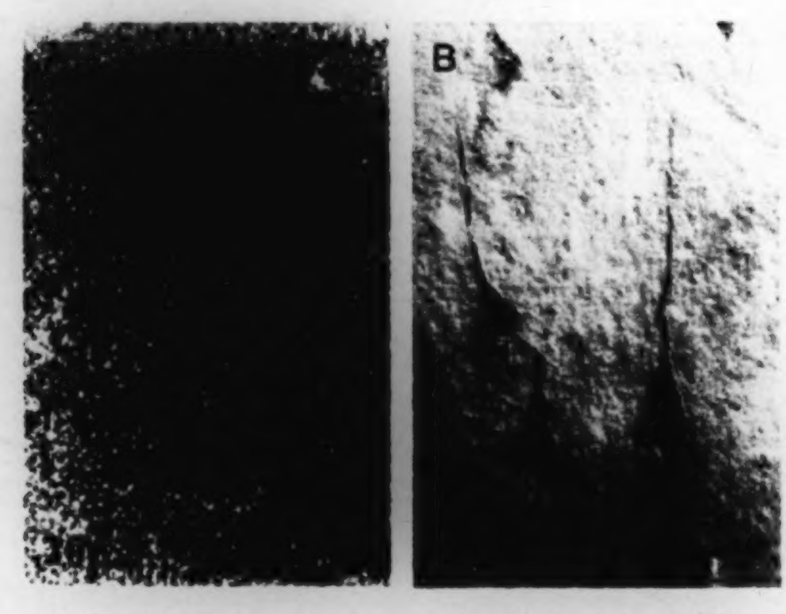

Figure 1.1. (A) SMN demonstrates strong nuclear staining in human 20 week developing cortical plate and (B) preferentially localizes to the cytoplasm and gradually moves into axon processes during maturation. Figure from (Giavazzi *et al.*, 2006).

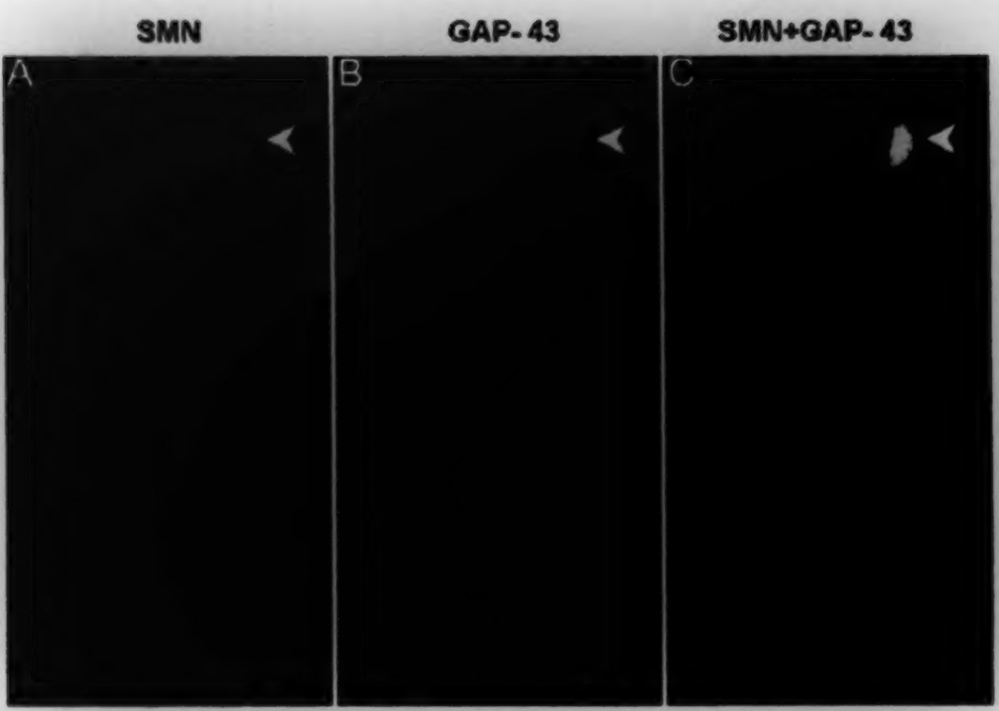

Figure 1.2. SMN colocalizes with GAP-43 in growth-cone-like structures of P19 cells. (A) SMN stains the cytoplasm and appears concentrated in growth-cone-like structures. (B) GAP-43 is located at soma edges and shows strongest staining in growth-cone-like structures. (C) Superimposition of SMN and GAP-43 labeling demonstrating strong colocalization in growth-cone-like structures. Scale bar is 10mm. Figure from Fan & Simard, 2002.

1.1.5. SMN is essential for snRNP biogenesis

The finding that SMN associates with snRNP-related proteins in the nucleus in either Cajal bodies or Gems (Liu & Dreyfuss, 1996) (Young *et al.*, 2001) led to the discovery of additional members of the "SMN complex" within the nucleus. In Cajal bodies, SMN self-associates and binds gemins 2-7 to form the 'snRNP assemblysome', which is additionally linked to small nucleolar RNA (snoRNA) proteins including fibrillarin and GAR1 (Baccon *et al.*, 2002) (Charroux *et al.*, 1999) (Charroux *et al.*, 2000) (Gubitz *et al.*, 2002) (Jones *et al.*, 2001) (Liu *et al.*, 1997) (Paushkin *et al.*, 2002) (Pellizzoni *et al.*, 2002). The 'snRNP assemblysome' is responsible for joining Sm protein and snRNA components to form snRNPs, which are essential constituents of the spliceosome (Battle *et al.*, 2006) (Battle *et al.*, 2007) (Feng *et al.*, 2005) (See (Kolb *et al.*, 2007) for review). Figure 1.3 (Kolb *et al.*, 2007) provides diagrammatic representation of this function. In addition to assembling snRNP core structure by placing correctly arranged Sm proteins on newly formed snRNAs, the SMN complex remains associated with newly assembled snRNPs through subsequent biogenesis processes in the cytoplasm, including monomethylated m^{7}GpppG (m^{7}G) cap addition to the snRNP 5' end, and translocation of the finished structure to the nuclear pore complex for subsequent nuclear import (Massenet *et al.*, 2002). snRNPs are integral components of the spliceosomal apparatus, which removes introns from pre-mRNA. For a review of splicing and alternative splicing in neurons, refer to(Li *et al.* 2007.

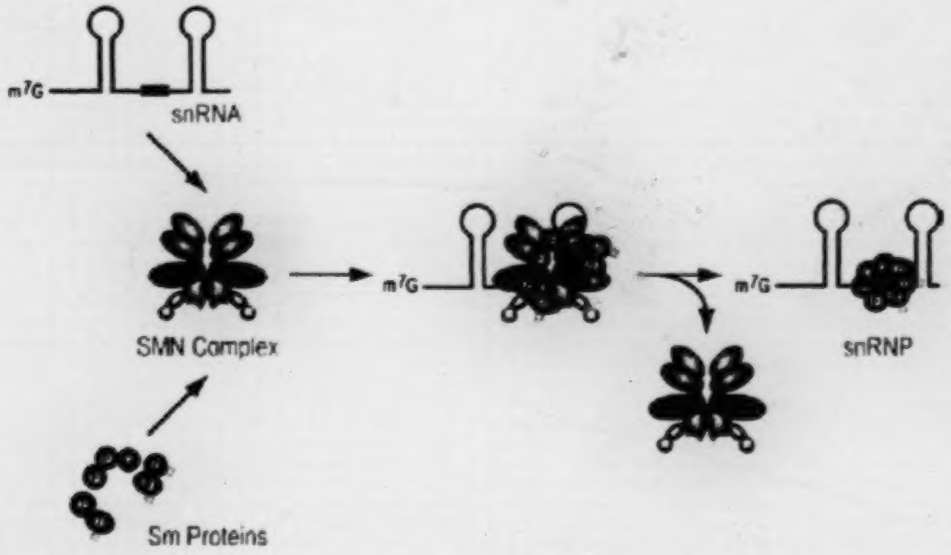

Figure 1.3. Simplified role of SMN in snRNP biogenesis. Figure from (Kolb *et al.*, 2007).

There is considerable debate whether the role of SMN in snRNP biogenesis leads to disease pathology in SMA. Development of a quantitative assay to measure snRNP assembly revealed that SMN is a limiting factor in this reaction, and reduced levels of SMN lead to reductions in snRNP formation (Wan *et al.*, 2005). In zebrafish, silencing of Gemin2 and pICln, two additional factors important in the snRNP biogenesis reaction, led to degeneration of motor axons similar to that observed during *Smn* silencing, providing the sole evidence linking impairments in snRNP biogenesis to pathology in SMA (Eggert *et al.*, 2006) (Winkler *et al.*, 2005). These results were striking in light of observations that Gemin 2 associates with SMN during snRNP assembly in the nucleus and cytoplasm near nuclear pore complexes, but *not* in axons and dendrites, and therefore does not contribute to the function of SMN in axon outgrowth (McWhorter *et al.*, 2008). Detailed analysis of the consequences of reduced snRNP biogenesis in neurons found that reductions in

SMN levels in the spinal cords of SMAI mice (Monani *et al.*, 2000) caused a reduction in expression of a subset of Gemin proteins, and further, led to a significant reduction in assembly of a small group of snRNPs in this tissue (Gabanella *et al.*, 2007). These findings were confirmed and expanded by (Zhang *et al.*, 2008), who documented tissue-specific differences in snRNAs (and subsequently formed snRNPs) in brain, spinal cord, kidney, heart, and skeletal muscle of SMAII mice (Le *et al.*, 2005). Additionally, the use of exon-specific microarrays on tissues from SMAII mice found tissue-specific splicing differences in the disease state, which were validated with quantitative reverse-transcriptase polymerase chain reaction (qRT-PCR) (Zhang *et al.*, 2008), prompting the authors to suggest that SMA is a "general splicing disease" common to all tissues. Cumulatively, these findings indicate that reduced levels of SMN lead to altered snRNP profiles in tissues of SMAI mice, which affect and impair intron splicing (Gabanella *et al.*, 2007) (Zhang *et al.*, 2008), and these defects may contribute to axonal pathology observed in SMA (Winkler *et al.*, 2005). While severely depleted levels of SMN obviously affect this aspect of SMN functioning causing phenotypic problems (a complete loss of SMN is embryonic lethal), there is not yet sufficient convincing evidence to support splicing deficits as the cause of neuromuscular degeneration in SMAI-III, and abnormal transcript production at less critical levels should be mediated by nonsense-mediated decay (Wen & Brogna, 2008).

1.1.6. SMN functions in neurite outgrowth and mRNA trafficking

Initial localization studies documenting the presence of SMN in axons and dendrites associated with microtubules suggested a role for SMN in molecular trafficking, distinct from its function in snRNP biogenesis (Battaglia *et al.*, 1997) (Burlet *et al.*, 1998). Clear evidence that SMN travels along neuritic processes either over long distances (as part of a large complex) or moving back and forth in a restricted region (as part of a smaller complex) in a manner dependent on microtubules indicates that SMN has neuron-specific functions within axons. SMN binds hnRNP-R and hnRNP-Q, two heterogeneous nuclear ribonucleoproteins (hnRNPs) that are involved in pre-mRNA processing and its subsequent translocation in the cell (Rossoll *et al.*, 2002). SMN has been found to colocalize with hnRNP-R in axons of motoneurons, implicating it in mRNA processing and localization in the cell (Rossoll *et al.*, 2002). hnRNP-R binds the 3' untranslated region (3'UTR) of β-actin mRNA and over-expression of SMN or hnRNP-R improved defects in axon outgrowth observed in cultured motoneurons from SMAI mice (Rossoll *et al.*, 2003). Together, these findings indicate that the SMN-hnRNP-R- β-actin mRNA complex travels to axon growth cones to influence axon growth, likely through provision of β-actin mRNA for localized translation (Rossoll *et al.*, 2003). In axons and growth cones, SMN targets to polyA mRNA-containing granules (Zhang *et al.*, 2007), providing additional support for these ideas.

1.1.7. SMN plays a role in cytoskeletal integrity and actin organization

Actin is a highly conserved 42kDa cytoskeletal protein that exists in two forms: free globular actin (G-actin), which is in either an 'active' GTP-bound state or an 'inactive' GDP-bound state, or polymers of filamentous actin (F-actin) called microfilaments. In microfilaments, 2 parallel F-actin strands are wound together to form a helix (Vandekerckhove & Weber, 1978). These filaments have a distinct polarity, and possess a fast-growing 'plus' end, facing the cell membrane, and a slow-growing 'minus' end, which faces the cytoplasm, and is generally subjected to depolymerization (Begg *et al.*, 1978). The ratio of G- to F-actin within cells and their compartments is tightly regulated. High G-actin levels promote the rapid addition of G-actin monomers to the plus end of a microfilament, while actin depolymerizing factors (ADFs) (such as cofilin, also known as ADF) act on the minus end, resulting in 'treadmilling' (Figure 1.4), where the actual length of the microfilament remains unchanged. G- to F-actin ratios are regulated by a host of actin binding proteins which include: cofilin/ADF for depolymerization, fibrins (such as T-plastin), filamin and villin for actin bundling, fibrins, vinculin and alpha-actinin are required to create an actin meshwork, and profilins, which regulate (both positively and negatively), the rate of actin polymerization (See (Dickinson, 2008)(Khurana & George, 2008)(Pak *et al.*, 2008) for review). Profilin binds and sequesters G-actin, preventing its incorporation into microfilaments. However, profilin acts like a guanine nucleotide exchange factor (GEF) for G-actin and promotes dissociation of GDP from inactive G-actin and subsequent GTP binding leading to active G-actin which increases its affinity for polymerization (See (Jockusch *et al.*, 2007) for review). Profilin also guides active actin monomers to the plus end of a microfilament and in this manner promotes controlled actin polymerization (Carlsson *et al.*, 1977). The actin cytoskeleton is controlled principally through intra- and extra-cellular signaling acting through small GTPase signaling cascades. Three major small GTPases, RhoA, Cdc42, and Rac1, all promote F-actin assembly and maintenance (for reviews see (Evers *et al.*, 2000)(Nikolic, 2002)(Koh, 2006)(Nobes & Hall, 1995). Cdc42 is involved in formation of filopodial structures (Kozma *et al.*, 1995) (necessary for cell outgrowth or migration) while RhoA activation leads to formation of F-actin filled stress fibers (necessary in cell adhesion) (Ridley & Hall, 1992). Rac1 activation is necessary for lamellopodial structures (Ridley *et al.*, 1992). Coordinate activation of these small proteins is essential for cytoskeletal modification, especially during growth and development (Linseman & Loucks, 2008).

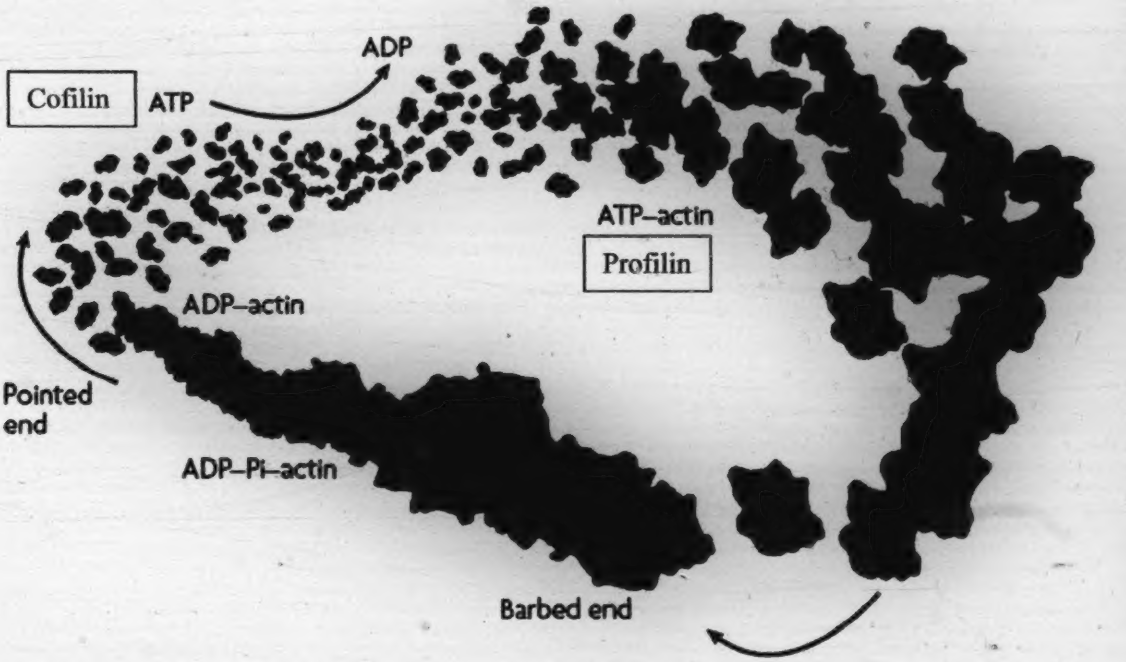

Figure 1.4. Treadmilling effect of F-actin outgrowth showing depolymerization at the pointed end and polymerization at the barbed end. Figure from Pak *et al.*, 2008.

1.1.8. SMN affects actin dynamics in motoneurons

Profilins are small proteins that sequester globular actin (G-actin) and in differentiating PC12 cells, they have been shown to bind SMN via proline-rich motifs in both the nucleus and neurites (Giesemann *et al.*, 1999)(Sharma *et al.*, 2005). SMN and profilin were determined to be part of distinct complexes in (a) the nucleus, associated with coilin p80 and Sm proteins (components of the snRNP-forming 'SMN complex'), and (b) in neurites, where coilin p80 and Sm were not detected (Sharma *et al.*, 2005), indicating that SMN is found in complexes with distinct components in different areas of the cell, likely involved in different functions. SMN is thought to increase actin polymerization by binding profilin and preventing them from sequestering G-actin for F-actin formation (Sharma *et al.*, 2005). This leads to the idea that reduced SMN levels in SMA may cause abnormal actin-organization by increasing levels of unbound profilin which could result in reduced actin polymerization.

SMN deficient cells contain elevated levels of unbound profilin due to (a) increased profilin expression and (b) the loss of the profilin binding partner SMN (Bowerman *et al.*, 2007). Loss of SMN was associated with misregulation in F-actin localization, increases in active RhoA (RhoA-GTP) and decreases in active Cdc42 (Cdc42-GTP) compared to normal cells. Overexpression of RhoA leads to bundling and retraction of F-actin into stress fibers, a process which inhibits neuritic outgrowth (Harrington *et al.*, 2005)(Delanote *et al.*, 2005). Increases in active RhoA result in activation of downstream effector proteins including Rho-kinase (ROCK), which phosphorylates myosin light chain (MLC), causing its activation, and subsequent F-actin accumulation (Amano *et al.*, 1996). Cdc42 promotes actin polymerization into F-actin through its effectors Wiskott-Aldrich Syndrome Protein (WASP) and its neural isoform, N-WASP and Arp2/3 which catalyses F-actin branching into filopodia (Rozelle *et al.*, 2000).

Increases in formation of a ROCK/profilin complex and RhoA activation to promote stress-fiber formation (da Silva *et al.*, 2003) in SMN deficient cells suggest that modulation of signaling pathways play a major role in observed impairments in neuritogenesis. Rac, another small GTPase important in neurite outgrowth, appears unaffected in SMA (Bowerman *et al.*, 2007). The importance of this information is made particularly apparent by the recent identification of *T-plastin* as a modifier gene in SMA, the upregulation of which was demonstrated to ameliorate symptoms in SMAII and III patients (Oprea *et al.*, 2008). Plastins (also known as fimbrins) are characterized as 'actin bundling proteins', which are generally localized to regions of the cell where actin polarization is necessary, and in areas with elevated actin filament turnover (Delanote *et al.*, 2005;Matsudaira, 1991). T-plastin promotes F-actin assembly and reduces activity of cofilin, an actin de-polymerizing protein (Giganti *et al.*, 2005). Expression of T-plastin in SMN-deficient cells prevents defects in axon outgrowth by reducing elevated G to F-actin ratios observed in these cells (Oprea *et al.*, 2008). T-plastin distribution is influenced by activity of small GTPases (RhoA, Cdc42 and Rac) (Dutartre *et al.*, 1996). Disturbances in actin organization have also been documented in skeletal muscle. Rajendra (2007) found reduced levels of F-actin and impairments in thin filament formation in flight muscles from a *D. melanogaster* model of SMA, and noted an association between SMN and α-actinin, another actin-binding protein (Rajendra *et al.*, 2007).

1.1.9. SMN affects actin dynamics at the neuromuscular junction

In skeletal muscle, SMN has been visualized at the post-synaptic domain of the neuromuscular junction (NMJ) (Broccolini *et al.*, 1999;Fan & Simard, 2002). The first evidence of neuromuscular junction impairments was provided by Braun *et al.* (1995) who found that innervating cultured myotubes from SMAI and II patients with spinal motoneurons from normal rats led to degeneration of both neurons and muscle fibers, suggesting that pathology in SMA could be related to defective neuromuscular transmission (Braun *et al.*, 1995). Cultured skeletal muscle from SMAI patients demonstrated problems in fusion of myotubes, and lacked normal organization of acetylcholine receptors (AChRs), an impairment that could not be rescued with application of neural agrin (Arnold *et al.*, 2004).

Impaired developmental organization of AChRs at the NMJ has been observed in a *D. melanogaster* model of SMA (Chan *et al.*, 2003) and has recently been observed in a murine model of SMAII (Kariya *et al.*, 2008). Defects in normal AChR expression and organization cause muscular degeneration independent of pathology in nerve: antibodies against AChRs or the muscle-specific receptor tyrosine kinase (MuSK), essential for formation of mature NMJ, cause Myasthenia Gravis leading to muscle fatigability and atrophy (Boneva *et al.*, 2006). It has been recently noted in murine models of SMAI and II that loss of motor endplates can occur independently of axonal defects, and endplates conforming to a fast-synapse forming (FaSyn) phenotype are more susceptible than those that are delayed-synapse forming (DeSyn) (Murray *et al.*, 2008). The identification of two distinct populations of NMJs (FaSyn and DeSyn) was based on assembly time during development and response to stimuli such as denervation. FaSyn synapse assembly occurs early during development and the synapses are not disassembled in response to denervation or paralysis unlike DeSyn synapses which take longer to reach mature assembly and remain plastic and responsive to such stimuli well into adulthood (Pun *et al.*, 2002). This finding of selective susceptibility of FaSyn motor units implicates NMJ formation as a pathological target in SMA. However, the NMJ deficiencies in DeSyn muscles indicate that the apparent selective susceptibility of FaSyn synapses is not necessarily important in SMA (Kariya *et al.*, 2008). Presynaptic pathology in SMA includes neurofilament accumulation in presynaptic regions at early stages of disease, and reduced branching of presynaptic outputs (fewer muscle-nerve contacts per motoneuron) (Chan *et al.*, 2003;Cifuentes-Diaz *et al.*, 2002;Kariya *et al.*, 2008;Murray *et al.*, 2008).

Interestingly, the significance of the abnormalities at the NMJ may relate directly to F-actin and misregulation of the small GTPases, RhoA and Cdc42, observed in SMA motoneurons. Cdc42 and Rac activation, and corresponding RhoA *in*activation, are essential for agrin-induced AChR clustering at the NMJ, and constitutively active Cdc42 and Rac are capable of inducing AChR aggregation in the absence of agrin (Weston *et al.*, 2000). Agrin promotes a signal transduction pathway through MuSK, which relies on phosphoinositide 3-kinase (PI3K) for activation of Cdc42 and Rac, leading to the actin reorganization necessary for proper arrangement of AChR organization (clustering) at the post-synaptic membrane (Nizhynska *et al.*, 2007). It is possible that reduced levels of SMN lead to similar misregulation of small GTPase activity in nerve and muscle, leading to analogous misregulation of small GTPase signaling and defects in F-actin organization and levels and in turn, the pathology of SMA.

1.1.10. Animal models of SMA

Work on SMA has been facilitated by the discovery of orthologous genes in other species, allowing for the development of animal models (see (Schmid & DiDonato, 2007) for review. *SMN* orthologues have been identified in yeast (*Saccharomyces pombe, ySMN*) (Paushkin *et al.*, 2000), nematode (*Caenorhabditis elegans, CeSMN)* (Talbot *et al.*, 1997), fruit fly (*Drosophila melanogaster, dSMN)* (Chan *et al.*, 2003); (Miguel-Aliaga *et al.*, 2000;Rajendra *et al.*, 2007), zebrafish (*Danio rerio, Smn*) (McWhorter *et al.*, 2003), and finally in the mouse, *Mus musculus*, in which a large number of distinct SMA models, described below, have been created. Findings in *S. pombe* and *C. elegans* have demonstrated that *Smn* is essential for viability even in lower organisms. N- and C-terminal domains of the protein are highly conserved (Paushkin *et al.*, 2000), emphasizing their importance in Smn functions and interactions. Burt *et al.* (2006)(Burt *et al.*, 2006) investigated CeSMN binding partners, and found interactions with DEAD/DEAH box helicases, a heat shock RNA polymerase, ankyrin repeat domains/G-patch domains (RNA-binding proteins), zinc finger domains, and a hyaluronan/mRNA binding protein. Functions are in agreement with reported roles of SMN in mammalian cells, including assembly of spliceosomal proteins and nuclear-cytoplasmic transport. Interestingly, the strongest interaction was between CeSMN and the hyaluronan/mRNA-binding protein (Drosophila vasa intronic gene ortholog protein 1 isoform a, Vig) (Caudy *et al.*, 2002). This gene product has been implicated in axonal repair during regeneration (Burt *et al.*, 2006). The significant body of work carried out in *D. melanogaster* further illustrated the essential nature of SMN for survival, and has highlighted the tissue-specific importance of dSMN in thoracic flight muscles (Rajendra *et al.*, 2007). All three studies (Chan *et al.*, 2003)(Miguel-Aliaga *et al.*, 2000)(Rajendra *et al.*, 2007) have shown that SMN deficiency in motoneurons results in disorganization of the NMJ, including impairments in glutamate receptor organization, and a frequent inability of the pre- and post-synaptic membranes to meet. Rajendra *et al.* (2007) documented a unique role for dSMN in actin organization and thin filament formation in flight muscles in normal flies. dSMN colocalizes with α-actinin in the muscles, and insufficient levels of dSMN in *d.melanogaster dSMN* knockdown models cause complete failure of thin-filament formation, a reduction in F-actin, and disorganization of α-actinin (Rajendra *et al.*, 2007). Studies in the zebrafish, *D. rerio,* utilize morpholinos to knock down *Smn*, and have found short, excessive axonal branching and path-finding defects, which are limited to neuronal tissue and do not impact muscle (McWhorter *et al.*, 2003). This zebrafish model has subsequently been used in investigation of relevance of SMN function in Sm protein synthesis (snRNP production) to clinical aspects of the disease (Eggert *et al.*, 2006;Gabanella *et al.*, 2007).

Murine *Smn* maps to chromosome 13 and demonstrates a high degree of homology with its human orthologue, but is not duplicated and does not undergo alternative splicing (Viollet *et al.*, 1997). A number of murine models have been created to facilitate the study of SMA disease progression. Monani *et al.* (2000) developed a homologous knockout of murine *Smn* carrying two copies of the human *SMN2* gene to prevent embryonic lethality caused by complete absence of SMN. *Smn* was removed through targeted mutation of exon 2, which without the addition of 1-2 copies of *SMN2* caused embryonic death at the 8 cell stage (Monani *et al.*, 2000). These mice (*Smn-/-*; *SMN2*) provide a model for the most severe human SMAI, and have been used to demonstrate that MN loss occurs after birth (Monani *et al.*, 2000), and that sensory neurons are mildly affected in severe SMA (Jablonka *et al.*, 2006). Gavrilina *et al.* (2008) directed expression of SMN specifically to motoneurons or skeletal muscle and determined that increased SMN expression in motoneurons but not skeletal muscle in these SMAI animals led to dramatic increases in lifespan, in support of the idea that motoneurons are more seriously affected by insufficient SMN than skeletal muscle (Gavrilina *et al.*, 2008). A modification of this model, SMA mice carrying both *SMN2* and *SMNΔ7* (a copy of human *SMN1* lacking exon 7, the deletion most common in human SMA patients) transgenes, was created by Le *et al.* (2005) and serves as a model of moderate SMAII. Decreased disease severity in these animals indicates that SMNΔ7 is still partially functional, and confirms that expression of a truncated SMN isoform does not exacerbate disease pathology (Le *et al.*, 2005). It was subsequently used by Azzouz *et al.* (2004) to assess efficacy of lentivector-mediated SMN replacement (Azzouz *et al.*, 2004), and by Avila *et al.* (2007) to provide evidence that trichostatin A improves survival (Avila *et al.*, 2007). Most recently, Murray *et al.* (2008) have employed the SMAI model designed by Monani (2000) and this model of SMAII to characterize pre-synaptic pathology at the neuromuscular junction in SMAI and II, finding significant neurofilament accumulations in pre-synaptic inputs at early and mid-symptomatic time points (Murray *et al.*, 2008). These findings additionally indicated a preferential susceptibility of FaSyn motor units in SMA pathology compared those with a DeSyn phenotype (Murray *et al.*, 2008).

Like Monani *et al.* (2000), Hsieh-Li *et al.* (2000) produced *Smn-/-; SMN2* mice, but disrupted exon 7 instead of exon 2. Homozygous deletion of murine *Smn* through exon 7 disruption allowed survival up to embryonic day 3.5. This group reported a range of SMA disease severity within a single litter, encompassing Type I, II or III based on clinical signs and phenotypic properties (Hsieh-Li *et al.*, 2000). This model has been used to show that oral administration of sodium butyrate decreased the severity of clinical signs of SMA (Chang *et al.*, 2001), to demonstrate the positive effect of exercise on the SMA phenotype (Grondard *et al.*, 2005) and the beneficial effects of removing Bax-dependent apoptosis (Tsai *et al.*, 2006b). A modified version of this model (Type III SMA-like mice only) was used to show moderate efficacy of valproic acid as treatment for SMA (Tsai *et al.*, 2006a).

The Cre-loxP recombination system was used to target murine *Smn* exon 7 deletion within neurons (Frugier *et al.*, 2000), and then skeletal muscle (Cifuentes-Diaz *et al.*, 2001). Examination of SMA mice created by neuron-specific deletion of *Smn* exon 8 showed neurofilament accumulation at motor endplates and an absence of axonal sprouting (Frugier *et al.*, 2000). This model has also been used to show progressive loss of motor axons and motoneurons in the spinal cord, to show the striking beneficial effects of cardiotrophin-1 gene transfer (Lesbordes *et al.*, 2003), and to demonstrate that oral administration of riluzole may attenuate SMA symptoms (Haddad *et al.*, 2003). Models where *Smn* exon 7 loss is targeted to skeletal muscle have proved interesting, providing evidence of a skeletal muscle-specific component in SMA (Cifuentes-Diaz *et al.*, 2001), an idea supported by earlier *in vitro* studies where degeneration of healthy rat motoneurons occurred after being co-cultured with skeletal muscle satellite cells from type I and II SMA patients (Braun *et al.*, 1995). This model has been used to evaluate the effects of bone marrow transplantation on muscle degeneration, supporting its use in SMA therapeutics (Salah-Mohellibi *et al.*, 2006).

1.1.11. Mouse models used in the present study

My research has employed two type III SMA murine models: (1) described by Jablonka *et al.* (2000) which is heterozygous for murine *Smn* (*Smn+/-C57Bl/6)*, and (2) by Monani *et al.* (2003) which has homologous loss of murine *Smn*, 1-2 copies of human *SMN2*, and a mutated form of *SMN1* which contains an A2G point mutation described by Parsons *et al.* (1998) (smn-/-A2G-FVB) (Monani *et al.*, 2003). Jablonka *et al.* (2000) found significant reduction of SMN protein content in the spinal cords of their 6 month old *Smn+/-* mice. Despite this, heterozygous *Smn* disruption does not appear to result in a dramatic reduction in the number of nuclear gemini of coiled bodies (Gem) and normal levels of correctly spliced Ich-1 mRNA in motoneurons indicate that limitations of pre-RNA splicing are not obvious in this model (Jablonka *et al.*, 2000). Nevertheless, 40% and 54% reductions of spinal motoneurons at 6 months and 12 months have been reported, along with a 23% reduction of facial motoneurons occurs at 12 months of age (Jablonka, *et al.*, 2000). However, findings in our lab using back-labeling of motoneurons, a much more sensitive approach, has revealed much more modest losses of spinal motoneurons (Udina *et al.*, unpublished data). Heterozygous loss of *Smn* does not result in a shortened lifespan, and there has been no observable negative impact on motor skills and behavior. Monani *et al.* (2003) created a slightly more severe SMAIII model (*Smn-/-*). They report generation of animals with statistically significant weight differences and a clinical phenotype of muscle weakness at as early as 1 month of age. They noted visible muscle atrophy in month old tissues, and documented a 29% loss in spinal MN by 3.5 months. While work in our laboratory has indicated that these traits are much milder than reported, these animals remain a suitable model for the study of mild SMAIII.

1.1.12. Proteins integral to neuromuscular growth and development evaluated in the present study

GAP-43 is a phosphoprotein substrate of protein kinase C (PKC) (Akers & Routtenberg, 1985) Aloyo *et al.*, 1983; Oestreicher *et al.*, 1981), and acts downstream of this signaling molecule to mediate effects on the actin cytoskeleton in axons/neurites during growth and regeneration. Overexpression of GAP-43 promotes axon outgrowth, while its loss prevents it, and it can be used as a marker of growth or regeneration (Aigner & Caroni, 1993) (Aigner & Caroni, 1995;Tetzlaff *et al.*, 1989). GAP-43 is phosphorylated and activated by PKC at the plasma membrane of growth cones, leading it to release its bound substrate, phosphoinositide (4,5) bisphosphate. This provokes recruitment of actin-modifying proteins and an increase in F-actin assembly and branching (Janmey & Lindberg, 2004) necessary for neurite/axon outgrowth. Expression of GAP-43 and additional proteins such as β-III-tubulin that are required for axon development are downregulated during postnatal maturation, a response dependent on active neuromuscular transmission (Caroni & Becker, 1992).

Choline acetyltransferase (ChAT) is the enzyme responsible for synthesis of the neurotransmitter acetylcholine (ACh). ACh synthesis by ChAT occurs in the cytoplasm of presynaptic nerve terminals, and Ach is packaged into vesicles for subsequent release (see (Parsons *et al.*, 1993) for review). ChAT is not expressed during development, but is upregulated during postnatal maturation in concordance with the onset of neuromuscular transmission (Lowrie *et al.*, 1985); (O'Brien *et al.*, 1978). Thus, ChAT expression can be used as a marker of phenotypic maturity in neurons since its expression is maximal in mature motoneurons capable of effective neurotransmission (Sharp *et al.*, 2003).

Neural cell adhesion molecule (N-CAM) is a membrane glycoprotein belonging to the immunoglobulin (Ig) superfamily (for reviews refer to Krog & Bock, 1992). N-CAM expression is minimal and restricted to the synapse in normal and innervated skeletal muscle. In contrast, in development and denervated muscle fibers, N-CAM expression is very high, and is expressed at the synapse as well as uniformly around on the surfaces of myoblasts, myotubes, and myofibers (in the case of regeneration) (Covault & Sanes, 1985;Gordon *et al.*, 2008).

1.2. STUDY RATIONALE

1.2.1. Delayed developmental hypothesis

SMA results from loss-of-function mutations in *SMN1*, which codes for the ubiquitously expressed SMN. SMN is essential for mRNA splicing through its role in snRNP biogenesis (Pellizzoni *et al.*, 1998), and has additionally been implicated in gene transcription through interactions with RNA helicase A and RNA polymerase II. Based on these functions, it is plausible that reduced SMN levels impair timely and effective expression of proteins, a deficit of significant importance during development, maturation and adaptation (ie regeneration post-injury). Replacement of immature proteins with mature isoforms is part of normal meuromuscular development, and this change, which permits the transition from a growth-to-transmitting phenotype is essential for survival of motoneurons, their axons, and associated muscle fibers. Reduction of SMN may impair these important alterations in protein expression profile, leading to developmental delays in the neuromuscular system, promoting instability and death in these tissues. This idea is supported by findings of immaturity in nerves from human patients, including low axon density, insufficient myelination, and continuous EMG activity at rest. The aim of the present project is to assess whether the transition from a growth-to-transmitting phenotype is impaired in SMA.

1.2.2. Whole genome expression analysis

Our evaluation of the delayed development hypothesis revealed that there is no evidence for impairment in growth-to-transmitting phenotypic changes during development in SMAIII murine models, and therefore widespread developmental delays are not responsible for selective neuromuscular degeneration in SMAIII (Chapter 2). These findings prompted us to undertake microarray studies on skeletal muscle and spinal cord tissues from a murine model of SMA III to characterize transcriptional differences between SMA and WT animals. Comparisons will allow determination of aspects of cellular function affected by decreased levels of SMN, and provide insight into the molecular basis of this complicated neuromuscular disease. DNA MAs offer a systematic approach for the assessment of genome-wide transcriptional changes caused by a biological condition. This technique can be an extremely beneficial approach to elucidating areas of concern in a multifaceted problem, such as that posed by SMA.

1.3. Reference List

Aigner L & Caroni P (1993). Depletion of 43-kD growth-associated protein in primary sensory neurons leads to diminished formation and spreading of growth cones. *J Cell Biol* **123**, 417-429.

Aigner L & Caroni P (1995). Absence of persistent spreading, branching, and adhesion in GAP-43-depleted growth cones. *J Cell Biol* **128**, 647-660.

Akers RF & Routtenberg A (1985). Protein kinase C phosphorylates a 47 Mr protein (F1) directly related to synaptic plasticity. *Brain Res* **334**, 147-151.

Al RS, Majumdar R, Awada A, Adeyokunnu A, Al JM, Al BM, & Snellen A (1998). Molecular analysis of the SMN and NAIP genes in Saudi spinal muscular atrophy patients. *J Neurol Sci* **158**, 43-46.

Amano M, Ito M, Kimura K, Fukata Y, Chihara K, Nakano T, Matsuura Y, & Kaibuchi K (1996). Phosphorylation and activation of myosin by Rho-associated kinase (Rho-kinase). *J Biol Chem* **271**, 20246-20249.

Anagnostou E, Miller SP, Guiot MC, Karpati G, Simard L, Dilenge ME, & Shevell MI (2005). Type I spinal muscular atrophy can mimic sensory-motor axonal neuropathy. *J Child Neurol* **20**, 147-150.

Arnold AS, Gueye M, Guettier-Sigrist S, Courdier-Fruh I, Coupin G, Poindron P, & Gies JP (2004). Reduced expression of nicotinic AChRs in myotubes from spinal muscular atrophy I patients. *Lab Invest* **84**, 1271-1278.

Avila AM, Burnett BG, Taye AA, Gabanella F, Knight MA, Hartenstein P, Cizman Z, Di Prospero NA, Pellizzoni L, Fischbeck KH, & Sumner CJ (2007). Trichostatin A increases SMN expression and survival in a mouse model of spinal muscular atrophy. *J Clin Invest* **117**, 659-671.

Azzouz M, Le T, Ralph GS, Walmsley L, Monani UR, Lee DC, Wilkes F, Mitrophanous KA, Kingsman SM, Burghes AH, & Mazarakis ND (2004). Lentivector-mediated SMN replacement in a mouse model of spinal muscular atrophy. *J Clin Invest* **114**, 1726-1731.

Baccon J, Pellizzoni L, Rappsilber J, Mann M, & Dreyfuss G (2002). Identification and characterization of Gemin7, a novel component of the survival of motor neuron complex. *J Biol Chem* **277**, 31957-31962.

Battaglia G, Princivalle A, Forti F, Lizier C, & Zeviani M (1997). Expression of the SMN gene, the spinal muscular atrophy determining gene, in the mammalian central nervous system. *Hum Mol Genet* **6**, 1961-1971.

Battle DJ, Kasim M, Wang J, & Dreyfuss G (2007). SMN-independent subunits of the SMN complex. Identification of a small nuclear ribonucleoprotein assembly intermediate. *J Biol Chem* **282**, 27953-27959.

Battle DJ, Kasim M, Yong J, Lotti F, Lau CK, Mouaikel J, Zhang Z, Han K, Wan L, & Dreyfuss G (2006). The SMN complex: an assembly machine for RNPs. *Cold Spring Harb Symp Quant Biol* **71**, 313-320.

Bechade C, Rostaing P, Cisterni C, Kalisch R, La B, V, Pettmann B, & Triller A (1999). Subcellular distribution of survival motor neuron (SMN) protein: possible involvement in nucleocytoplasmic and dendritic transport. *Eur J Neurosci* **11**, 293-304.

Begg DA, Rodewald R, & Rebhun LI (1978). The visualization of actin filament polarity in thin sections. Evidence for the uniform polarity of membrane-associated filaments. *J Cell Biol* **79**, 846-852.

Bobele GB, Feeback DL, Leech RW, & Brumback RA (1996). Hypertrophic intrafusal muscle fibers in infantile spinal muscular atrophy. *J Child Neurol* **11**, 246-248.

Boneva N, Frenkian-Cuvelier M, Bidault J, Brenner T, & Berrih-Aknin S (2006). Major pathogenic effects of anti-MuSK antibodies in myasthenia gravis. *J Neuroimmunol* **177**, 119-131.

Bowerman M, Shafey D, & Kothary R (2007). Smn depletion alters profilin II expression and leads to upregulation of the RhoA/ROCK pathway and defects in neuronal integrity. *J Mol Neurosci* **32**, 120-131.

Braun S, Croizat B, Lagrange MC, Warter JM, & Poindron P (1995). Constitutive muscular abnormalities in culture in spinal muscular atrophy. *Lancet* **345**, 694-695.

Broccolini A, Engel WK, & Askanas V (1999). Localization of survival motor neuron protein in human apoptotic-like and regenerating muscle fibers, and neuromuscular junctions. *NeuroReport* **10**, 1637-1641.

Burlet P, Huber C, Bertrandy S, Ludosky MA, Zwaenepoel I, Clermont O, Roume J, Delezoide AL, Cartaud J, Munnich A, & Lefebvre S (1998). The distribution of SMN protein complex in human fetal tissues and its alteration in spinal muscular atrophy. *Hum Mol Genet* **7**, 1927-1933.

Burt EC, Towers PR, & Sattelle DB (2006). Caenorhabditis elegans in the study of SMN-interacting proteins: a role for SMI-1, an orthologue of human Gemin2 and the identification of novel components of the SMN complex. *Invert Neurosci* **6**, 145-159.

Bussaglia E, Tizzano EF, Illa I, Cervera C, & Baiget M (1997). Cramps and minimal EMG abnormalities as preclinical manifestations of spinal muscular atrophy patients with homozygous deletions of the SMN gene. *Neurol* **48**, 1443-1445.

Carlsson L, Nystrom LE, Sundkvist I, Markey F, & Lindberg U (1977). Actin polymerizability is influenced by profilin, a low molecular weight protein in non-muscle cells. *J Mol Biol* **115**, 465-483.

Caroni P & Becker M (1992). The downregulation of growth-associated proteins in motoneurons at the onset of synapse elimination is controlled by muscle activity and IGF1. *J Neurosci* **12**, 3849-3861.

Cartegni L & Krainer AR (2002). Disruption of an SF2/ASF-dependent exonic splicing enhancer in SMN2 causes spinal muscular atrophy in the absence of SMN1. *Nat Genet* **30**, 377-384.

Caudy AA, Myers M, Hannon GJ, & Hammond SM (2002). Fragile X-related protein and VIG associate with the RNA interference machinery. *Genes Dev* **16**, 2491-2496.

Chan YB, Miguel-Aliaga I, Franks C, Thomas N, Trulzsch B, Sattelle DB, Davies KE, & van den HM (2003). Neuromuscular defects in a Drosophila survival motor neuron gene mutant. *Hum Mol Genet* **12**, 1367-1376.

Chang JG, Hsieh-Li HM, Jong YJ, Wang NM, Tsai CH, & Li H (2001). Treatment of spinal muscular atrophy by sodium butyrate. *Proc Natl Acad Sci U S A* **98**, 9808-9813.

Charroux B, Pellizzoni L, Perkinson RA, Shevchenko A, Mann M, & Dreyfuss G (1999). Gemin3: A novel DEAD box protein that interacts with SMN, the spinal muscular atrophy gene product, and is a component of gems. *J Cell Biol* **147**, 1181-1194.

Charroux B, Pellizzoni L, Perkinson RA, Yong J, Shevchenko A, Mann M, & Dreyfuss G (2000). Gemin4. A novel component of the SMN complex that is found in both gems and nucleoli. *J Cell Biol* **148**, 1177-1186.

Chou SM & Nonaka I (1978). Werdnig-Hoffmann disease: proposal of a pathogenetic mechanism. *Acta Neuropathol* **41**, 45-54.

Cifuentes-Diaz C, Frugier T, Tiziano FD, Lacene E, Roblot N, Joshi V, Moreau MH, & Melki J (2001). Deletion of murine SMN exon 7 directed to skeletal muscle leads to severe muscular dystrophy. *J Cell Biol* **152**, 1107-1114.

Cifuentes-Diaz C, Nicole S, Velasco ME, Borra-Cebrian C, Panozzo C, Frugier T, Millet G, Roblot N, Joshi V, & Melki J (2002). Neurofilament accumulation at the motor endplate and lack of axonal sprouting in a spinal muscular atrophy mouse model. *Hum Mol Genet* **11**, 1439-1447.

Coovert DD, Le TT, McAndrew PE, Strasswimmer J, Crawford TO, Mendell JR, Coulson SE, Androphy EJ, Prior TW, & Burghes AH (1997). The survival motor neuron protein in spinal muscular atrophy. *Hum Mol Genet* **6**, 1205-1214.

Covault J & Sanes JR (1985). Neural cell adhesion molecule (N-CAM) accumulates in denervated and paralyzed skeletal muscles. *Proc Natl Acad Sci U S A* **82**, 4544-4548.

Crawford TO & Pardo CA (1996). The neurobiology of childhood spinal muscular atrophy. *Neurobiol Dis* **3**, 97-110.

da Silva JS, Medina M, Zuliani C, Di NA, Witke W, & Dotti CG (2003). RhoA/ROCK regulation of neuritogenesis via profilin IIa-mediated control of actin stability. *J Cell Biol* **162**, 1267-1279.

Delanote V, Vandekerckhove J, & Gettemans J (2005). Plastins: versatile modulators of actin organization in (patho)physiological cellular processes. *Acta Pharmacol Sin* **26**, 769-779.

Deymeer F, Serdaroglu P, Poda M, Gulsen-Parman Y, Ozcelik T, & Ozdemir C (1997). Segmental distribution of muscle weakness in SMA III: implications for deterioration in muscle strength with time. *Neuromuscul Disord* **7**, 521-528.

Dickinson RB (2008). Models for actin polymerization motors. *J Math Biol*.

Dutartre H, Davoust J, Gorvel JP, & Chavrier P (1996). Cytokinesis arrest and redistribution of actin-cytoskeleton regulatory components in cells expressing the Rho GTPase CDC42Hs. *J Cell Sci* **109 (Pt 2)**, 367-377.

Eggert C, Chari A, Laggerbauer B, & Fischer U (2006). Spinal muscular atrophy: the RNP connection. *Trends Mol Med* **12**, 113-121.

Evers EE, Zondag GC, Malliri A, Price LS, ten Klooster JP, van der Kammen RA, & Collard JG (2000). Rho family proteins in cell adhesion and cell migration. *Eur J Cancer* **36**, 1269-1274.

Fan L & Simard LR (2002). Survival motor neuron (SMN) protein: role in neurite outgrowth and neuromuscular maturation during neuronal differentiation and development. *Hum Mol Genet* **11**, 1605-1614.

Felderhoff-Mueser U, Grohmann K, Harder A, Stadelmann C, Zerres K, Buhrer C, & Obladen M (2002). Severe spinal muscular atrophy variant associated with congenital bone fractures. *J Child Neurol* **17**, 718-721.

Feng W, Gubitz AK, Wan L, Battle DJ, Dostie J, Golembe TJ, & Dreyfuss G (2005). Gemins modulate the expression and activity of the SMN complex. *Hum Mol Genet* **14**, 1605-1611.

Frugier T, Tiziano FD, Cifuentes-Diaz C, Miniou P, Roblot N, Dierich A, Le Meur M, & Melki J (2000). Nuclear targeting defect of SMN lacking the C-terminus in a mouse model of spinal muscular atrophy. *Hum Mol Genet* **9**, 849-858.

Gabanella F, Butchbach ME, Saieva L, Carissimi C, Burghes AH, & Pellizzoni L (2007). Ribonucleoprotein assembly defects correlate with spinal muscular atrophy severity and preferentially affect a subset of spliceosomal snRNPs. *PLoS ONE* **2**, e921.

Gavrilina TO, McGovern VL, Workman E, Crawford TO, Gogliotti RG, DiDonato CJ, Monani UR, Morris GE, & Burghes AH (2008). Neuronal SMN expression corrects spinal muscular atrophy in severe SMA mice while muscle-specific SMN expression has no phenotypic effect. *Hum Mol Genet* **17**, 1063-1075.

Gavrilov DK, Shi X, Das K, Gilliam TC, & Wang CH (1998). Differential SMN2 expression associated with SMA severity. *Nat Genet* **20**, 230-231.

Giavazzi A, Setola V, Simonati A, & Battaglia G (2006). Neuronal-specific roles of the survival motor neuron protein: evidence from survival motor neuron expression patterns in the developing human central nervous system. *J Neuropathol Exp Neurol* **65**, 267-277.

Giesemann T, Rathke-Hartlieb S, Rothkegel M, Bartsch JW, Buchmeier S, Jockusch BM, & Jockusch H (1999). A role for polyproline motifs in the spinal muscular atrophy protein SMN. Profilins bind to and colocalize with smn in nuclear gems. *J Biol Chem* **274**, 37908-37914.

Giganti A, Plastino J, Janji B, Van TM, Lentz D, Ampe C, Sykes C, & Friederich E (2005). Actin-filament cross-linking protein T-plastin increases Arp2/3-mediated actin-based movement. *J Cell Sci* **118**, 1255-1265.

Goebel HH (1995). Desmin-related neuromuscular disorders. *Muscle Nerve* **18**, 1306-1320.

Gordon T, Ly V, Hegedus J, & Tyreman N (2008). Early detection of denervated muscle fibers in hindlimb muscles after sciatic nerve transection in wild type mice and in the G93A mouse model of amyotrophic lateral sclerosis. *Neurol Res*.

Grondard C, Biondi O, Armand AS, Lecolle S, della GB, Pariset C, Li H, Gallien CL, Vidal PP, Chanoine C, & Charbonnier F (2005). Regular exercise prolongs survival in a type 2 spinal muscular atrophy model mouse. *J Neurosci* **25**, 7615-7622.

Gubitz AK, Mourelatos Z, Abel L, Rappsilber J, Mann M, & Dreyfuss G (2002). Gemin5, a novel WD repeat protein component of the SMN complex that binds Sm proteins. *J Biol Chem* **277**, 5631-5636.

Haddad H, Cifuentes-Diaz C, Miroglio A, Roblot N, Joshi V, & Melki J (2003). Riluzole attenuates spinal muscular atrophy disease progression in a mouse model. *Muscle Nerve* **28**, 432-437.

Harrington EO, Shannon CJ, Morin N, Rowlett H, Murphy C, & Lu Q (2005). PKCdelta regulates endothelial basal barrier function through modulation of RhoA GTPase activity. *Exp Cell Res* **308**, 407-421.

Hebert MD, Shpargel KB, Ospina JK, Tucker KE, & Matera AG (2002). Coilin methylation regulates nuclear body formation. *Dev Cell* **3**, 329-337.

Hebert MD, Szymczyk PW, Shpargel KB, & Matera AG (2001). Coilin forms the bridge between Cajal bodies and SMN, the spinal muscular atrophy protein. *Genes Dev* **15**, 2720-2729.

Hsieh-Li HM, Chang JG, Jong YJ, Wu MH, Wang NM, Tsai CH, & Li H (2000). A mouse model for spinal muscular atrophy. *Nat Genet* **24**, 66-70.

Jablonka S, Karle K, Sandner B, Andreassi C, von AK, & Sendtner M (2006). Distinct and overlapping alterations in motor and sensory neurons in a mouse model of spinal muscular atrophy. *Hum Mol Genet* **15**, 511-518.

Jablonka S, Schrank B, Kralewski M, Rossoll W, & Sendtner M (2000). Reduced survival motor neuron (Smn) gene dose in mice leads to motor neuron degeneration: an animal model for spinal muscular atrophy type III. *Hum Mol Genet* **9**, 341-346.

Janmey PA & Lindberg U (2004). Cytoskeletal regulation: rich in lipids. *Nat Rev Mol Cell Biol* **5**, 658-666.

Jockusch BM, Murk K, & Rothkegel M (2007). The profile of profilins. *Rev Physiol Biochem Pharmacol* **159**, 131-149.

Johnson MA & Kucukyalcin DK (1978). Patterns of abnormal histochemical fibre type differentitation in human muscle biopsies. *J Neurol Sci* **37**, 159-178.

Jones KW, Gorzynski K, Hales CM, Fischer U, Badbanchi F, Terns RM, & Terns MP (2001). Direct interaction of the spinal muscular atrophy disease protein SMN with the small nucleolar RNA-associated protein fibrillarin. *J Biol Chem* **276**, 38645-38651.

Kariya S, Park GH, Maeno-Hikichi Y, Leykekhman O, Lutz C, Arkovitz MS, Landmesser LT, & Monani UR (2008). Reduced SMN protein impairs maturation of the neuromuscular junctions in mouse models of spinal muscular atrophy. *Hum Mol Genet* **17**, 2552-2569.

Khurana S & George SP (2008). Regulation of cell structure and function by actin-binding proteins: villin's perspective. *FEBS Lett* **582**, 2128-2139.

Kinali M, Banks LM, Mercuri E, Manzur AY, & Muntoni F (2004). Bone mineral density in a paediatric spinal muscular atrophy population. *Neuropediatrics* **35**, 325-328.

Kingma DW, Feeback DL, Marks WA, Bobele GB, Leech RW, & Brumback RA (1991). Selective type II muscle fiber hypertrophy in severe infantile spinal muscular atrophy. *J Child Neurol* **6**, 329-334.

Koh CG (2006). Rho GTPases and their regulators in neuronal functions and development. *Neurosignals* **15**, 228-237.

Kolb SJ, Battle DJ, & Dreyfuss G (2007). Molecular functions of the SMN complex. *J Child Neurol* **22**, 990-994.

Kozma R, Ahmed S, Best A, & Lim L (1995). The Ras-related protein Cdc42Hs and bradykinin promote formation of peripheral actin microspikes and filopodia in Swiss 3T3 fibroblasts. *Mol Cell Biol* **15**, 1942-1952.

Krog L & Bock E (1992). Glycosylation of neural cell adhesion molecules of the immunoglobulin superfamily. *APMIS Suppl* **27**, 53-70.

Le TT, Pham LT, Butchbach ME, Zhang HL, Monani UR, Coovert DD, Gavrilina TO, Xing L, Bassell GJ, & Burghes AH (2005). SMNDelta7, the major product of the centromeric survival motor neuron (SMN2) gene, extends survival in mice with spinal muscular atrophy and associates with full-length SMN. *Hum Mol Genet* **14**, 845-857.

Lefebvre S, Burglen L, Reboullet S, Clermont O, Burlet P, Viollet L, Benichou B, Cruaud C, Millasseau P, Zeviani M, & . (1995). Identification and characterization of a spinal muscular atrophy-determining gene. *Cell* **80**, 155-165.

Lefebvre S, Burlet P, Liu Q, Bertrandy S, Clermont O, Munnich A, Dreyfuss G, & Melki J (1997). Correlation between severity and SMN protein level in spinal muscular atrophy. *Nat Genet* **16**, 265-269.

Lesbordes JC, Cifuentes-Diaz C, Miroglio A, Joshi V, Bordet T, Kahn A, & Melki J (2003). Therapeutic benefits of cardiotrophin-1 gene transfer in a mouse model of spinal muscular atrophy. *Hum Mol Genet* **12**, 1233-1239.

Li Q, Lee JA, & Black DL (2007). Neuronal regulation of alternative pre-mRNA splicing. *Nat Rev Neurosci* **8**, 819-831.

Linseman DA & Loucks FA (2008). Diverse roles of Rho family GTPases in neuronal development, survival, and death. *Front Biosci* **13**, 657-676.

Liu Q & Dreyfuss G (1996). A novel nuclear structure containing the survival of motor neurons protein. *EMBO J* **15**, 3555-3565.

Liu Q, Fischer U, Wang F, & Dreyfuss G (1997). The spinal muscular atrophy disease gene product, SMN, and its associated protein SIP1 are in a complex with spliceosomal snRNP proteins. *Cell* **90**, 1013-1021.

Lorson CL, Hahnen E, Androphy EJ, & Wirth B (1999). A single nucleotide in the SMN gene regulates splicing and is responsible for spinal muscular atrophy. *Proc Natl Acad Sci U S A* **96**, 6307-6311.

Lowrie MB, O'Brien RA, & Vrbová G (1985). The effect of altered peripheral field on motoneurone function in developing rat soleus muscles. *J Physiol* **368**, 513-524.

Maier JK, Lahoua Z, Gendron NH, Fetni R, Johnston A, Davoodi J, Rasper D, Roy S, Slack RS, Nicholson DW, & MacKenzie AE (2002). The neuronal apoptosis inhibitory protein is a direct inhibitor of caspases 3 and 7. *J Neurosci* **22**, 2035-2043.

Massenet S, Pellizzoni L, Paushkin S, Mattaj IW, & Dreyfuss G (2002). The SMN complex is associated with snRNPs throughout their cytoplasmic assembly pathway. *Mol Cell Biol* **22**, 6533-6541.

Matsudaira P (1991). Modular organization of actin crosslinking proteins. *Trends Biochem Sci* **16**, 87-92.

McWhorter ML, Boon KL, Horan ES, Burghes AH, & Beattie CE (2008). The SMN binding protein Gemin2 is not involved in motor axon outgrowth. *Dev Neurobiol* **68**, 182-194.

McWhorter ML, Monani UR, Burghes AH, & Beattie CE (2003). Knockdown of the survival motor neuron (Smn) protein in zebrafish causes defects in motor axon outgrowth and pathfinding. *J Cell Biol* **162**, 919-931.

Menke LA, Poll-The BT, Clur SA, Bilardo CM, van der Wal AC, Lemmink HH, & Cobben JM (2008). Congenital heart defects in spinal muscular atrophy type I: a clinical report of two siblings and a review of the literature. *Am J Med Genet A* **146A**, 740-744.

Miguel-Aliaga I, Chan YB, Davies KE, & van den HM (2000). Disruption of SMN function by ectopic expression of the human SMN gene in Drosophila. *FEBS Lett* **486**, 99-102.

Monani UR, Pastore MT, Gavrilina TO, Jablonka S, Le TT, Andreassi C, DiCocco JM, Lorson C, Androphy EJ, Sendtner M, Podell M, & Burghes AH (2003). A transgene carrying an A2G missense mutation in the SMN gene modulates phenotypic severity in mice with severe (type I) spinal muscular atrophy. *J Cell Biol* **160**, 41-52.

Monani UR, Sendtner M, Coovert DD, Parsons DW, Andreassi C, Le TT, Jablonka S, Schrank B, Rossol W, Prior TW, Morris GE, & Burghes AH (2000). The human centromeric survival motor neuron gene (SMN2) rescues embryonic lethality in Smn(-/-) mice and results in a mouse with spinal muscular atrophy. *Hum Mol Genet* **9**, 333-339.

Murray LM, Comley LH, Thomson D, Parkinson N, Talbot K, & Gillingwater TH (2008). Selective vulnerability of motor neurons and dissociation of pre- and post-synaptic pathology at the neuromuscular junction in mouse models of spinal muscular atrophy. *Hum Mol Genet* **17**, 949-962.

Nadeau A, D'Anjou G, Debray G, Robitaille Y, Simard LR, & Vanasse M (2007). A newborn with spinal muscular atrophy type 0 presenting with a clinicopathological picture suggestive of myotubular myopathy. *J Child Neurol* **22**, 1301-1304.

Nikolic M (2002). The role of Rho GTPases and associated kinases in regulating neurite outgrowth. *Int J Biochem Cell Biol* **34**, 731-745.

Nizhynska V, Neumueller R, & Herbst R (2007). Phosphoinositide 3-kinase acts through RAC and Cdc42 during agrin-induced acetylcholine receptor clustering. *Dev Neurobiol* **67**, 1047-1058.

Nobes CD & Hall A (1995). Rho, rac and cdc42 GTPases: regulators of actin structures, cell adhesion and motility. *Biochem Soc Trans* **23**, 456-459.

Novelli G, Calza L, Amicucci P, Giardino L, Pozza M, Silani V, Pizzuti A, Gennarelli M, Piombo G, Capon F, & Dallapiccola B (1997). Expression study of survival motor neuron gene in human fetal tissues. *Biochem Mol Med* **61**, 102-106.

O'Brien RA, Ostberg A, & Vrbova G (1978). Persistent polyneuronal innervation in hyperinnervated skeletal muscle [proceedings]. *J Physiol* **280**, 38P.

Omran H, Ketelsen UP, Heinen F, Sauer M, Rudnik-Schoneborn S, Wirth B, Zerres K, Kratzer W, & Korinthenberg R (1998). Axonal neuropathy and predominance of type II myofibers in infantile spinal muscular atrophy. *J Child Neurol* **13**, 327-331.

Oprea GE, Krober S, McWhorter ML, Rossoll W, Muller S, Krawczak M, Bassell GJ, Beattie CE, & Wirth B (2008). Plastin 3 is a protective modifier of autosomal recessive spinal muscular atrophy. *Science* **320**, 524-527.

Pagliardini S, Giavazzi A, Setola V, Lizier C, Di Luca M, DeBiasi S, & Battaglia G (2000). Subcellular localization and axonal transport of the survival motor neuron (SMN) protein in the developing rat spinal cord. *Hum Mol Genet* **9**, 47-56.

Pak CW, Flynn KC, & Bamburg JR (2008). Actin-binding proteins take the reins in growth cones. *Nat Rev Neurosci* **9**, 136-147.

Parsons DW, McAndrew PE, Monani UR, Mendell JR, Burghes AH, & Prior TW (1996). An 11 base pair duplication in exon 6 of the SMN gene produces a type I spinal muscular atrophy (SMA) phenotype: further evidence for SMN as the primary SMA-determining gene. *Hum Mol Genet* **5**, 1727-1732.

Parsons SM, Prior C, & Marshall IG (1993). Acetylcholine transport, storage, and release. *Int Rev Neurobiol* **35**, 279-390.

Paushkin S, Charroux B, Abel L, Perkinson RA, Pellizzoni L, & Dreyfuss G (2000). The survival motor neuron protein of Schizosacharomyces pombe. Conservation of survival motor neuron interaction domains in divergent organisms. *J Biol Chem* **275**, 23841-23846.

Paushkin S, Gubitz AK, Massenet S, & Dreyfuss G (2002). The SMN complex, an assemblyosome of ribonucleoproteins. *Curr Opin Cell Biol* **14**, 305-312.

Pearn J (1980). Classification of spinal muscular atrophies. *Lancet* **1**, 919-922.

Pellizzoni L, Baccon J, Rappsilber J, Mann M, & Dreyfuss G (2002). Purification of native survival of motor neurons complexes and identification of Gemin6 as a novel component. *J Biol Chem* **277**, 7540-7545.

Pellizzoni L, Kataoka N, Charroux B, & Dreyfuss G (1998). A novel function for SMN, the spinal muscular atrophy disease gene product, in pre-mRNA splicing. *Cell* **95**, 615-624.

Pun S, Sigrist M, Santos AF, Ruegg MA, Sanes JR, Jessell TM, Arber S, & Caroni P (2002). An intrinsic distinction in neuromuscular junction assembly and maintenance in different skeletal muscles. *Neuron* **34**, 357-370.

Rajendra TK, Gonsalvez GB, Walker MP, Shpargel KB, Salz HK, & Matera AG (2007). A Drosophila melanogaster model of spinal muscular atrophy reveals a function for SMN in striated muscle. *J Cell Biol* **176**, 831-841.

Ridley AJ & Hall A (1992). The small GTP-binding protein rho regulates the assembly of focal adhesions and actin stress fibers in response to growth factors. *Cell* **70**, 389-399.

Ridley AJ, Paterson HF, Johnston CL, Diekmann D, & Hall A (1992). The small GTP-binding protein rac regulates growth factor-induced membrane ruffling. *Cell* **70**, 401-410.

Rossoll W, Jablonka S, Andreassi C, Kroning AK, Karle K, Monani UR, & Sendtner M (2003). Smn, the spinal muscular atrophy-determining gene product, modulates axon growth and localization of beta-actin mRNA in growth cones of motoneurons. *J Cell Biol* **163**, 801-812.

Rossoll W, Kroning AK, Ohndorf UM, Steegborn C, Jablonka S, & Sendtner M (2002). Specific interaction of Smn, the spinal muscular atrophy determining gene product, with hnRNP-R and gry-rbp/hnRNP-Q: a role for Smn in RNA processing in motor axons? *Hum Mol Genet* **11**, 93-105.

Roy N, Mahadevan MS, McLean M, Shutler G, Yaraghi Z, Farahani R, Baird S, Besner-Johnston A, Lefebvre C, Kang X, & . (1995). The gene for neuronal apoptosis inhibitory protein is partially deleted in individuals with spinal muscular atrophy. *Cell* **80**, 167-178.

Roy S, Dubowitz V, & Wolman L (1971). Ultrastructure of muscle in infantile spinal muscular atrophy. *J Neurol Sci* **12**, 219-232.

Rozelle AL, Machesky LM, Yamamoto M, Driessens MH, Insall RH, Roth MG, Luby-Phelps K, Marriott G, Hall A, & Yin HL (2000). Phosphatidylinositol 4,5-bisphosphate induces actin-based movement of raft-enriched vesicles through WASP-Arp2/3. *Curr Biol* **10**, 311-320.

Rudnik-Schoneborn S, Goebel HH, Schlote W, Molaian S, Omran H, Ketelsen U, Korinthenberg R, Wenzel D, Lauffer H, Kreiss-Nachtsheim M, Wirth B, & Zerres K (2003). Classical infantile spinal muscular atrophy with SMN deficiency causes sensory neuronopathy. *Neurol* **60**, 983-987.

Russman BS (2007). Spinal muscular atrophy: clinical classification and disease heterogeneity. *J Child Neurol* **22**, 946-951.

Salah-Mohellibi N, Millet G, ndre-Schmutz I, Desforges B, Olaso R, Roblot N, Courageot S, Bensimon G, Cavazzana-Calvo M, & Melki J (2006). Bone marrow transplantation attenuates the myopathic phenotype of a muscular mouse model of spinal muscular atrophy. *Stem Cells* **24**, 2723-2732.

Sarnat HB (1992). Vimentin and desmin in maturing skeletal muscle and developmental myopathies. *Neurol* **42**, 1616-1624.

Sarnat HB & Trevenen CL (2007). Motor neuron degeneration in a 20-week male fetus: spinal muscular atrophy type 0. *Can J Neurol Sci* **34**, 215-220.

Sawchak JA, Benoff B, Sher JH, & Shafiq SA (1990). Werdnig-Hoffmann disease: myosin isoform expression not arrested at prenatal stage of development. *J Neurol Sci* **95**, 183-192.

Schmid A & DiDonato CJ (2007). Animal models of spinal muscular atrophy. *J Child Neurol* **22**, 1004-1012.

Shanmugarajan S, Swoboda KJ, Iannaccone ST, Ries WL, Maria BL, & Reddy SV (2007). Congenital bone fractures in spinal muscular atrophy: functional role for SMN protein in bone remodeling. *J Child Neurol* **22**, 967-973.

Sharma A, Lambrechts A, Hao lT, Le TT, Sewry CA, Ampe C, Burghes AH, & Morris GE (2005). A role for complexes of survival of motor neurons (SMN) protein with gemins and profilin in neurite-like cytoplasmic extensions of cultured nerve cells. *Exp Cell Res* **309**, 185-197.

Sharp PS, Dekkers J, Dick JR, & Greensmith L (2003). Manipulating transmitter release at the neuromuscular junction of neonatal rats alters the expression of ChAT and GAP-43 in motoneurons. *Brain Res Dev Brain Res* **146**, 29-38.

Simic G, Seso-Simic D, Lucassen PJ, Islam A, Krsnik Z, Cviko A, Jelasic D, Barisic N, Winblad B, Kostovic I, & Kruslin B (2000). Ultrastructural analysis and TUNEL demonstrate motor neuron apoptosis in Werdnig-Hoffmann disease. *J Neuropathol Exp Neurol* **59**, 398-407.

Smith HK, Plyley MJ, Rodgers CD, & McKee NH (1999). Expression of developmental myosin and morphological characteristics in adult rat skeletal muscle following exercise-induced injury. *Eur J Appl Physiol Occup Physiol* **80**, 84-91.

Soler-Botija C, Ferrer I, Gich I, Baiget M, & Tizzano EF (2002). Neuronal death is enhanced and begins during foetal development in type I spinal muscular atrophy spinal cord. *Brain* **125**, 1624-1634.

Somerville MJ, Hunter AG, Aubry HL, Korneluk RG, MacKenzie AE, & Surh LC (1997). Clinical application of the molecular diagnosis of spinal muscular atrophy: deletions of neuronal apoptosis inhibitor protein and survival motor neuron genes. *Am J Med Genet* **69**, 159-165.

Soubrouillard C, Pellissier JF, Lepidi H, Mancini J, Rougon G, & Figarella-Branger D (1995). Expression of developmentally regulated cytoskeleton and cell surface proteins in childhood spinal muscular atrophies. *J Neurol Sci* **133**, 155-163.

Soussi-Yanicostas N, Ben HC, Bejaoui K, Hentati F, Ben HM, & Butler-Browne GS (1992). Evolution of muscle specific proteins in Werdnig-Hoffman's disease. *J Neurol Sci* **109**, 111-120.

Stupka N, Schertzer JD, Bassel-Duby R, Olson EN, & Lynch GS (2008). Stimulation of calcineurin A{alpha} activity attenuates muscle pathophysiology in mdx dystrophic mice. *Am J Physiol Regul Integr Comp Physiol* **294**, R983-R992.

Sugimura F, Iijima M, Ozawa Y, Oki Y, & Watanabe S (1973). [2 cases of Kugelberg-Welander disease with cardiopathy]. *Rinsho Shinkeigaku* **13**, 79-86.

Szliwowski HB & Drochmans P (1975). Ultrastructural aspects of muscle and nerve in Werdnig-Hoffmann disease. *Acta Neuropathol* **31**, 281-296.

Takahashi N, Shimada T, Ishibashi Y, Sugamori T, Hirano Y, Oyake N, & Murakami Y (2006). Cardiac involvement in Kugelberg-Welander disease: a case report and review. *Am J Med Sci* **332**, 354-356.

Talbot K, Ponting CP, Theodosiou AM, Rodrigues NR, Surtees R, Mountford R, & Davies KE (1997). Missense mutation clustering in the survival motor neuron gene: a role for a conserved tyrosine and glycine rich region of the protein in RNA metabolism? *Hum Mol Genet* **6**, 497-500.

Tanaka H, Uemura N, Toyama Y, Kudo A, & Ohkatsu Y (1976). Cardiac involvement in the Kugelbert-Welander syndrome. *Am J Cardiol* **38**, 528-532.

Tetzlaff W, Lederis KL, Cassar L, & Bisby MA (1989). Axonal transport and localization of B-50/GAP-43-like immunoreactivity in regnerating sciatic and facial nerves of the rat. *J Neurosci* **9**, 1303-1313.

Tsai LK, Tsai MS, Lin TB, Hwu WL, & Li H (2006a). Establishing a standardized therapeutic testing protocol for spinal muscular atrophy. *Neurobiol Dis* **24**, 286-295.

Tsai MS, Chiu YT, Wang SH, Hsieh-Li HM, Lian WC, & Li H (2006b). Abolishing Bax-dependent apoptosis shows beneficial effects on spinal muscular atrophy model mice. *Mol Ther* **13**, 1149-1155.

Urbanits S & Budka H (1996). [Spinal pathology in spinal muscular atrophy in comparison with amyotrophic lateral sclerosis]. *Wien Med Wochenschr* **146**, 199-200.

van der SG, Grootscholten PM, Cobben JM, Zappata S, Scheffer H, den Dunnen JT, van Ommen GJ, Brahe C, & Buys CH (1996). Apparent gene conversions involving the SMN gene in the region of the spinal muscular atrophy locus on chromosome 5. *Am J Hum Genet* **59**, 834-838.

Vandekerckhove J & Weber K (1978). Comparison of the amino acid sequences of three tissue-specific cytoplasmic actins with rabbit skeletal muscle actin [proceedings]. *Arch Int Physiol Biochim* **86**, 891-892.

Viollet L, Bertrandy S, Bueno Brunialti AL, Lefebvre S, Burlet P, Clermont O, Cruaud C, Guenet JL, Munnich A, & Melki J (1997). cDNA isolation, expression, and chromosomal localization of the mouse survival motor neuron gene (Smn). *GENOMICS* **40**, 185-188.

Vitte J, Fassier C, Tiziano FD, Dalard C, Soave S, Roblot N, Brahe C, Saugier-Veber P, Bonnefont JP, & Melki J (2007). Refined characterization of the expression and stability of the SMN gene products. *Am J Pathol* **171**, 1269-1280.

Vitte JM, Davoult B, Roblot N, Mayer M, Joshi V, Courageot S, Tronche F, Vadrot J, Moreau MH, Kemeny F, & Melki J (2004). Deletion of murine Smn exon 7 directed to liver leads to severe defect of liver development associated with iron overload. *Am J Pathol* **165**, 1731-1741.

Wan L, Battle DJ, Yong J, Gubitz AK, Kolb SJ, Wang J, & Dreyfuss G (2005). The survival of motor neurons protein determines the capacity for snRNP assembly: biochemical deficiency in spinal muscular atrophy. *Mol Cell Biol* **25**, 5543-5551.

Wen J & Brogna S (2008). Nonsense-mediated mRNA decay. *Biochem Soc Trans* **36**, 514-516.

Weston C, Yee B, Hod E, & Prives J (2000). Agrin-induced acetylcholine receptor clustering is mediated by the small guanosine triphosphatases Rac and Cdc42. *J Cell Biol* **150**, 205-212.

Winkler C, Eggert C, Gradl D, Meister G, Giegerich M, Wedlich D, Laggerbauer B, & Fischer U (2005). Reduced U snRNP assembly causes motor axon degeneration in an animal model for spinal muscular atrophy. *Genes Dev* **19**, 2320-2330.

Xu DG, Korneluk RG, Tamai K, Wigle N, Hakim A, Mackenzie A, & Robertson GS (1997). Distribution of neuronal apoptosis inhibitory protein-like immunoreactivity in the rat central nervous system. *J Comp Neurol* **382**, 247-259.

Young PJ, Le TT, Dunckley M, Nguyen TM, Burghes AH, & Morris GE (2001). Nuclear gems and Cajal (coiled) bodies in fetal tissues: nucleolar distribution of the spinal muscular atrophy protein, SMN. *Exp Cell Res* **265**, 252-261.

Zhang H, Xing L, Rossoll W, Wichterle H, Singer RH, & Bassell GJ (2006). Multiprotein complexes of the survival of motor neuron protein SMN with Gemins traffic to neuronal processes and growth cones of motor neurons. *J Neurosci* **26**, 8622-8632.

Zhang H, Xing L, Singer RH, & Bassell GJ (2007). QNQKE targeting motif for the SMN-Gemin multiprotein complexin neurons. *J Neurosci Res* **85**, 2657-2667.

Zhang HL, Pan F, Hong D, Shenoy SM, Singer RH, & Bassell GJ (2003). Active transport of the survival motor neuron protein and the role of exon-7 in cytoplasmic localization. *J Neurosci* **23**, 6627-6637.

Zhang Z, Lotti F, Dittmar K, Younis I, Wan L, Kasim M, & Dreyfuss G (2008). SMN deficiency causes tissue-specific perturbations in the repertoire of snRNAs and widespread defects in splicing. *Cell* **133**, 585-600.

CHAPTER 2: EVALUATION OF A DELAYED DEVELOPMENT HYPOTHESIS IN SMA

2.1. INTRODUCTION

SMN is a ubiquitously expressed protein, making the selective neuromuscular degeneration characteristic of SMA especially puzzling. SMN self-associates to facilitate formation of large multiprotein SMN complexes, determined to be of variable composition depending on location, and presumably function, within the cell (Zhang *et al.*, 2006). The best characterized function of SMN is its role in snRNP biogenesis (for review, please refer to (Kolb *et al.*, 2007). In addition to this, SMN plays a role in transcription, pre-mRNA splicing, and in the metabolism of ribosomal and small nucleolar RNA (snoRNA) (Jones *et al.*, 2001;Pellizzoni *et al.*, 1998;Pellizzoni *et al.*, 2001a;Pellizzoni *et al.*, 2001b). Studies have found direct interactions between SMN and apoptotic proteins Bcl-2 and p53, in support of a dated hypothesis that excessive naturally occurring apoptosis during development is the cause of selective neuromuscular defects observed in SMA (Soler-Botija *et al.*, 2002b;Tews & Goebel, 1997). More recent associations of SMN with hnRNPs and β-actin mRNA (Rossoll *et al.*, 2003;Tadesse *et al.*, 2008) have implicated SMN in trafficking of mRNAs for localized translation purposes including those in the soma and within the axons. Despite the wide array of SMN functions, none of these individually can explain selective death of nerve and muscle caused by its loss. Adding to disease complexity, SMN is (a) found in the nucleus and cytoplasm of most cell types (Liu & Dreyfuss, 1996;Burlet *et al.*, 1998), (b) may be differentially spliced in different tissues (Hsieh-Li *et al.*, 2000), (c) occurs in two different isoforms that are post-translationally modified (La, V *et al.*, 2000;La, V *et al.*, 2004), and (d) has an impressive number of confirmed binding partners in both the cytoplasm and the nucleus. The implications of this myriad of findings to disease pathology have yet to be determined.

Insufficient production of FL-SMN may prevent motoneurons and associated muscle fibers from effectively completing the developmental transition from a growth-to-transmitting phenotype, and may additionally impair transition from transmitting-to-growth that is required for regeneration. SMN indirectly regulates pre-translational mRNA processing through mediation of snRNP assembly, particles which form part of the spliceosome necessary for pre-mRNA processing. Based on this function, a logical hypothesis to explain selective neuromuscular degeneration in SMA is that low levels of SMN may prevent timely and effective protein expression, a functional deficiency of great importance during development and adaptation (i.e., response to injury).

Transition of protein expression from developmental to mature isoforms is critical during growth and development of motoneurons and skeletal muscle. Significant evidence supporting this hypothesis can be found in studies of SMA patients. Specifically, surviving motoneurons in SMA patients are typically smaller, and contain less rough endoplasmic reticulum and associated ribosomes as detected by Nissl staining than motoneurons from normal subjects of the same age (Fidzianska *et al.*, 1984a). Motoneurons from some SMA patients show incessant EMG activity at rest, a condition also observed after interrupted neuromuscular contact in rats (Navarrete & Vrbova, 1984). Motor axons display numerous signs of immaturity: ventral roots of some patients exhibit low axon density, multiple axons can be wrapped by a single Schwann cell, and insufficient myelination of thin axons is frequently observed. These axons additionally display a delayed increase in excitability and conduction compared to ventral root axons of healthy patients (Krajewska & Hausmanowa-Petrusewicz, 2002;Simic *et al.*, 2000). Evidence in support of immaturity in muscle is less convincing. Pathological features which could be attributed to a delayed developmental phenotype include presence of small fibers with a single, centrally placed nucleus (Fidzianska *et al.*, 1990), and an apoptotic response to injury as opposed to the necrotic reaction displayed by normal skeletal muscle (Fidzianska *et al.*, 1984b).

The objective of the present study is to test the hypothesis of developmental delay in SMA by investigating in murine models of SMAIII whether decreased levels of SMN impair the normal developmental transition from growth-to-transmitting phenotypes in motoneurons and the maturation of skeletal muscles with transition from developmental to adult phenotype, leading to the selective neuromuscular degeneration observed in SMA. The first question that we asked was whether ChAT is upregulated postnatally in SMA as it is normally. Second, we determined whether, after nerve injury, the motoneurons upregulate growth associated proteins such as GAP-43 as do normal motoneurons. If there is a delay in the protein isoform switch, we cut the peripheral nerve to axotomize motoneurons and to denervate the skeletal muscles and determined whether the time course of protein expression in muscle is affected.

2.2. METHODS AND MATERIALS

2.2.1. Animals

Breeding pairs of *Smn-/+*-C57Bl/6, C57Bl/6-WT, *Smn-/-*A2G-FVB and FVB-WT were obtained from Jackson Laboratories and housed in HSLAS at the University of Alberta. Animals were genotyped by PCR amplification of DNA extracted from ear biopsies according to protocols specified by Jackson Laboratories. All animal procedures were performed with approval from the University of Alberta Health Sciences Animal Welfare and Policy Committee.

2.2.2. Surgeries and Tissue Removal

Smn-/+-C57Bl/6 (n=24), C57Bl/6-WT (n=24), *Smn-/-*A2G-FVB (n=24) and FVB-WT (n=24) animals were anaesthetized with a ketamine (100mg/ml) and atravet (10mg/ml) cocktail according to weight (17.5ul/g). Sciatic nerves were bilaterally transected at mid-thigh level just above the division of the sciatic into tibial and common peroneal nerves, and nerve stumps were sewn into fascia to prevent regeneration and reinnervation of target tissue. At 0, 3, 7, and 14d post-axotomy, animals were again anaesthetized. Right and left sciatic nerves were extracted and flash frozen in liquid nitrogen. The following muscles were bilaterally extracted: *longus capitus* (LC), *biceps brachii* (BB), *tibialis anterior* (TA), *quadriceps* (Q), *medial gastrocnemius* (MG) and *soleus* (Sol). Right sides were embedded in Tissue-Tek (O.C.T. Compound, Miles Scientific, USA), frozen in melting isopentane, and stored at -80°C for subsequent sectioning and immunohistochemistry. Left muscles were flash frozen in liquid nitrogen for subsequent genetic and enzymatic analyses.

2.2.3. Choline Acetyltransferase Activity Assay

Enzymatic activity of ChAT was assessed using a sensitive radiochemical procedure described by Sharp *et al.* (2003). Intact LC, BB and TA muscles from *Smn-/+*-C57Bl/6 (n=3), C57Bl/6-WT (n=6), *Smn-/-*A2G-FVB (n=4) and FVB-WT (n=4) animals were pulverized over liquid nitrogen and homogenized, and the assay was carried out exactly as described previously (Sharp *et al.*, 2003a). After assay completion, homogenate protein content was measured using a Bradford assay (Bio-Rad). Enzymatic activity was calculated as fmol/μg protein/minute. All samples were tested in duplicate to ensure similar, reproducible patterns of ChAT activity. Mean results were calculated for each condition and muscle, and significance was assessed using a student's t-test. Data are expressed as means ± standard error of the mean (SEM). Differences were considered significant when $P<0.05$.

2.2.4. Western Blot Analysis of GAP-43

The effect of axotomy on GAP-43 expression was assessed with western blotting. Right and left sciatic nerves from 2 animals were pooled (4 nerves total) and homogenized as described previously (Sharp *et al.*, 2003b). Homogenates were centrifuged at 2300 X g for 2 min to remove debris, and supernatants were transferred to new microcentrifuge tubes. Protein concentrations were determined using a Bradford assay (Bio-Rad). Sodium dodecyl sulphate (SDS) was added to bovine serum albumin (BSA) (Sigma) standards to control for detergent effects on absorbance readings. Equal amounts of protein (20 μg) were diluted 1:1 in SDS-polyacrylamide gel electrophoresis (PAGE) sample buffer (0.5M Tris-HCl, pH 6.8, glycerol 10% (w/v), SDS, 5% β-mercaptoethanol and 1.0% bromophenol blue), heated at 80°C for 10 min, and electrophoresed in a 12% acrylamide SDS gel (Laemmli, 1970). Proteins were subsequently electroblotted onto a PVDF membrane (Immobilon) in transfer buffer containing 25mM Tris, 192mM glycine, and 20% (v/v) methanol. Membranes were blocked in 3% BSA (Sigma) in phosphate buffered saline/0.1% Triton (PBS-T) for 1h at room temperature (RT). After washing 3 times with PBS, signal amplification was performed by incubating membranes 10' in Avidin-D PBS (1 drop/5mL) (Vector Labs), rinsing 3 times in PBS, and subsequently incubating membranes in Biotin-PBS (1 drop/5mL) (Vector Labs). Membranes were rinsed 3 times in PBS-T, and then incubated overnight at 4°C in primary polyclonal antibodies for GAP-43 (AB5220, Chemicon International Inc.) and GAPDH diluted 1:6000 and 1:2000 respectively in PBS-T. Blots were washed 3 times in PBS-T prior to incubation 1h at RT in biotinylated secondary antibody, AB-1000 (Vector Labs) diluted 1:200 in PBS-T. Blots were then rinsed three times in PBS-T and incubated 1h at RT in a streptavidin-HRP conjugate (Millipore) diluted 1:500 in PBS-T. Blots were visualized using chemiluminescent detection reagents (ECL, Amersham). Protein identity was determined by comparison with standard molecular weight markers (PrecisionPlus Protein standards, Bio-Rad). All blots were completed in duplicate, and immunoblots were evaluated with integrating densitometry using Gene Snap and Gene Tools (Chemigenius Gel Documentation System, Syngene, UK). GAP-43 band intensities were normalized to intensities of glyceraldehydes 3-phosphate dehydrogenase (GAPDH) loading control.

2.2.5. Antibodies for Immunohistochemistry

Monoclonal antibodies directed against adult MyHC were harvested from hybridoma cell lines obtained from the American Type Culture Collection (Manassas, VA, USA): BA-D5 (IgG, anti-MHCI), SC-71 (IgG, anti-MHCIIa), BF-F3 (IgM, anti-MHCIIb), BF-35 (IgG, binds all but MyHCIId/x), BF-45 (IgG), binds embryonic MyHC. N-CAM (IgG, AB5032, Chemicon International). Antibodies for cytoskeletal elements were: dystrophin (IgG, VPD505, Vector Laboratories, Inc.), desmin (IgG, D1033, Sigma), and vimentin (IgG, V6630, Sigma). Biotinylated goat-anti-rabbit IgG, biotinylated horse anti-mouse IgG and goat-anti-mouse IgM were obtained from Vector Laboratories Inc. (Burlingame, CA, USA).

2.2.6. Immunohistochemistryg

MyHC composition (staining for I, IIa, not IId/x, IIb and embryonic fiber types) was assessed in intact TA muscles from 2 month and 1 year old *Smn-/+*-C57Bl/6 (n=6) and C57Bl/6-WT controls (n=6). MyHC composition was also evaluated in 0, 3, 7, and 14d denervated skeletal muscles from 3 month *Smn-/-*A2G-FVB (n=12) and FVB-WT counterparts (n=12). Immunohistochemical staining on these same tissues was also performed for neural cell adhesion molecule (N-CAM) for assessment of denervation, and for cytoskeletal proteins dystrophin, desmin, and vimentin.

Frozen serial cross-sections (10μm) were collected from muscle mid-point of frozen embedded tissue at -22°C. Immunohistochemical staining was completed according to Putman *et al.* (2003). Briefly, sections were air-dried, washed in PBS-T (**note:** all PBS-T washes prior to blocking were omitted for dystrophin, desmin, and vimentin stains), and incubated for 15 minutes in 3% H_2O_2 in methanol. Serial sections stained for MyHC I, IIa, and not IId/x were incubated overnight at 4°C in blocking solution (BS-1: 1% BSA, 10% horse serum in PBS-T, pH 7.4) containing Avidin-D blocking reagent (Vector Laboratories, Inc.); on sections staining for IIb and N-CAM, goat serum was substituted for horse serum (BS-2). Sections were incubated 1h RT with primary antibody diluted in its corresponding blocking solution containing a Biotin blocking reagent (Vector Laboratories, Inc.). Antibodies were diluted as follows: BA-D5, 1:400; SC-71, 1:100; BF-35, 1:10,000; BF-45, 1:50; BF-F3, 1:400; N-CAM, 1:400; dystrophin, 1:10; desmin, 1:100; vimentin, 1:20. Sections were rinsed with PBS-T and then incubated 1h RT with the appropriate secondary antibody from Vector Laboratories: BA2001 (goat-anti-mouse IgM) (BF-35, 1:400; BF-45, 1:400; BA-D5, 1:400; SC-71, 1:400; Dystrophin, 1:200; Desmin, 1:500, Vimentin, 1:200), BA2020 (BF-F3, 1:400) or BA1000 (goat-anti-rabbit IgG) (N-CAM, 1:200). Sections were washed as before and incubated with Vectastain ABC reagent (avidin-biotin horseradish peroxidase (HRP) complex, Vector Laboratories, Inc.), and immunoreactivity was developed by incubating with a solution containing diaminobenzidine, H_2O_2, and $NiCl_2$ (omitted for vimentin staining) in 50mM Tris-HCl (pH 7.5) (Vector Laboratories, Inc.). All sections were dehydrated by successive immersions in 70%, 95%, and 100% ethanol, immersed in xylene, and mounted in Entallan (Merck, Darmstadt, Germany).

2.2.7. Immunohistochemical Analyses

Photographs of all muscle sections were taken using a Leica DMRBE microscope with aid of ImagePro software, and semi-quantitative analysis of MyHC content and fiber size was carried out with a custom designed analytical imaging program (Putman *et al.*, 2000). Muscles fibers stained for MyHC isoforms were examined from three distinct cross-sectional areas of the TA (deep, middle, and superficial). Type I, IIa, IIb, embryonic and N-CAM expressing fibers were identified by positive staining, while IId/x fibers were identified by the absence of staining.

2.3. RESULTS

2.3.1. ChAT Activity

Analysis of ChAT levels was performed to assess functional maturity of MN in SMAIII mice. Evaluation of ChAT activity in nerve terminals at the NMJ was performed using a sensitive radiometric assay (Sharp *et al.*, 2003c) on skeletal muscle homogenates (TA, BB, and LC) from *Smn*-/+-C57Bl/6 (n=4) and *Smn*-/-A2G-FVB (n=3) SMAIII mice and corresponding WT controls, C57Bl/6 (n=4) and FVB (n=6) animals. Statistical analysis revealed that these were not significant, and therefore there are no significant differences in ChAT activity between muscles from either strain of SMAIII mice and their controls (Figure 2.1).

Figure 2.1. There are no significant differences in ChAT levels between TA, BB and LC muscles from year old smn+/-C57Bl/6 and C57Bl/6-wild type or 3 month smn-/-A2G-FVB and FVB-wild type mice. ChAT levels in FM/ug/min.

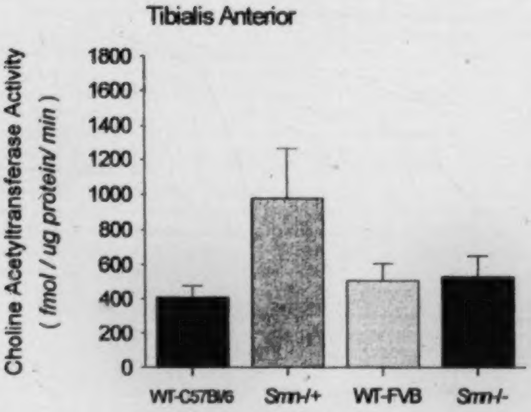
Tibialis Anterior

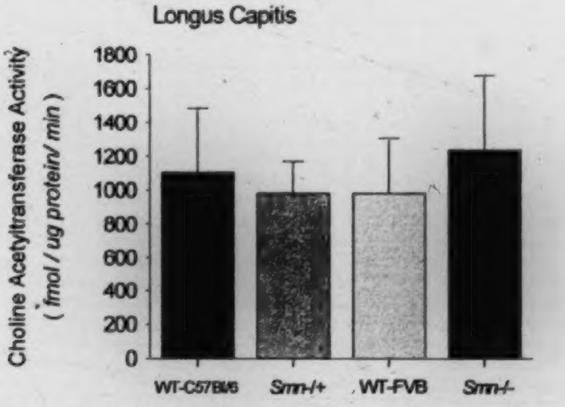
Longus Capitis

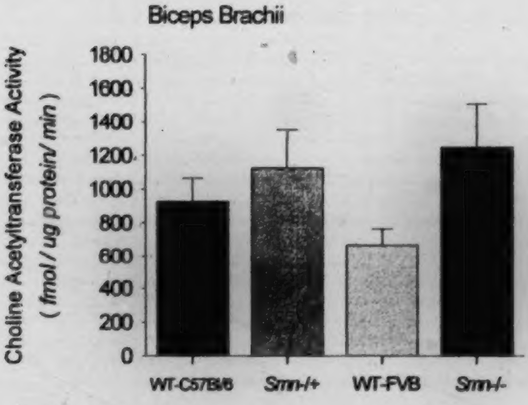
Biceps Brachii

2.3.2. Western blot analysis of GAP-43 in normal and axotomized MN

GAP-43 western blots were performed in two mouse models of SMAIII, smn+/-C57Bl/6 and smn-/-A2G-FVB and their corresponding control mice, C57Bl/6-wild type and FVB-wild type respectively to compare baseline protein expression levels, and to measure degree and rate at which these levels are upregulated in response to injury (sciatic axotomy). Comparison of GAP-43 levels in *Smn-/+*-C57Bl and C57Bl-WT control axotomized sciatic nerves up to 14 days did not reveal significant differences with regard to upregulation of GAP-43 post-axotomy (Figure 2.2). Subsequent multilinear regression analyses (Figure 2.3) found an increased rate of upregulation in *Smn-/+*-C57Bl animals compared to C57Bl-WT counterparts ($P<0.05$). We compared of GAP-43 levels in the more severe *Smn-/-*A2G-FVB animals with FVB-WT controls. Again there were no differences in GAP-43 upregulation in axotomized motoneurons of normal and SMAIII mice (Figure 2.4), and multilinear regression analyses showed that there was no significant difference in the rate of upregulation between SMAIII animals and WT (Figure 2.5).

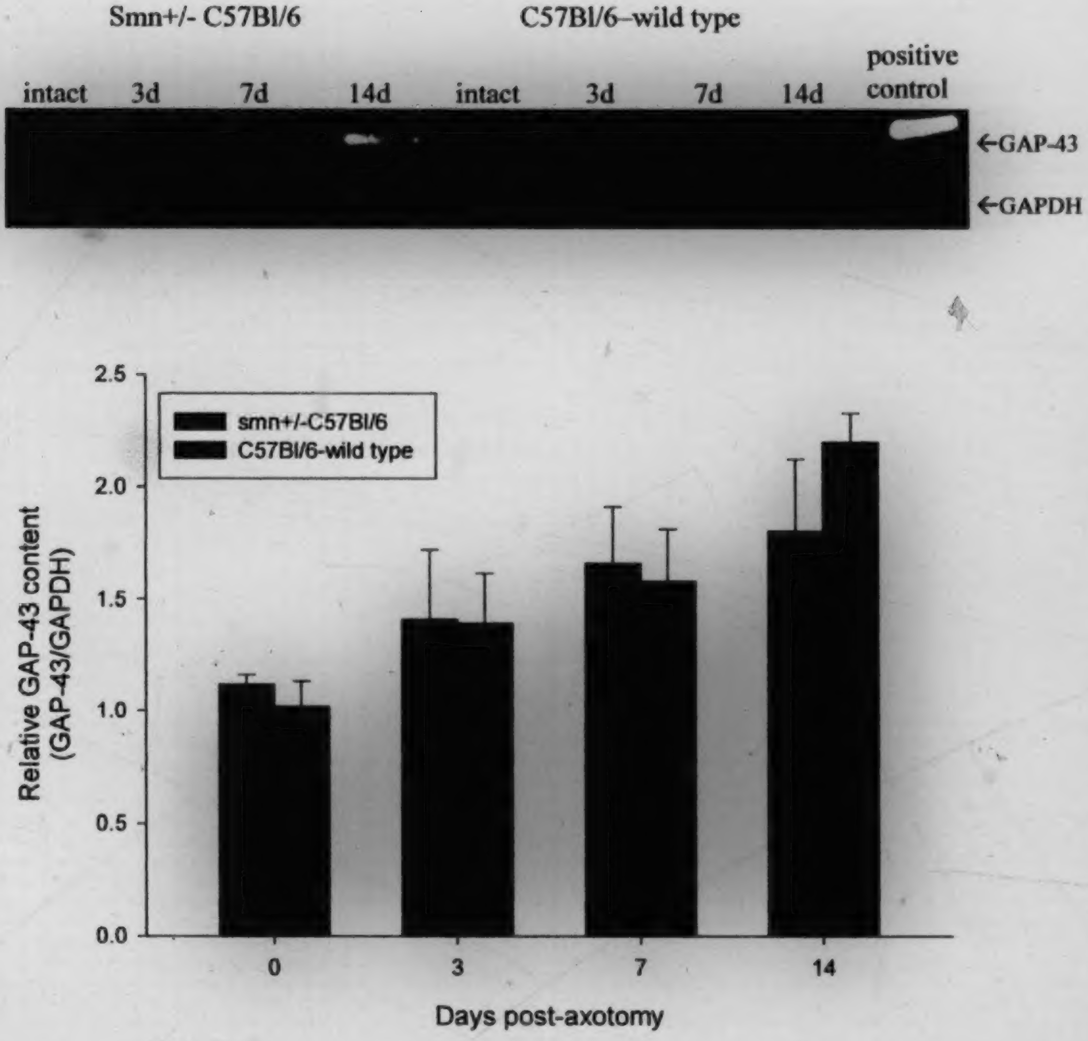

Figure 2.2. Upregulation of GAP-43 in sciatic nerves from year old *Smn-/+*-C57Bl and C57Bl-wild type animals at 0, 3, 7 and 14 days post-axotomy (n=3 animals/condition) as determined by semi-quantitative western blot analysis. Each bar represents the average analysis of 12 sciatic nerves (n=3 mice). GAP-43 expression levels were normalized to those of the GAPDH loading control.

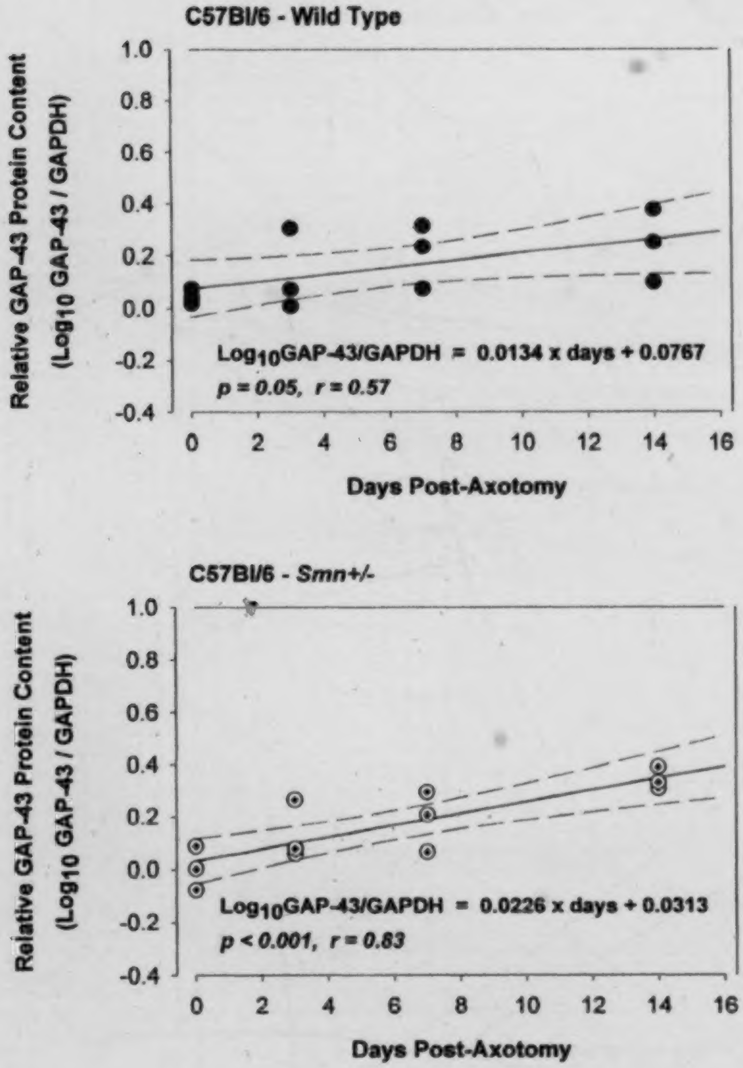

Figure 2.3. Increase in GAP-43 content of sciatic nerves as a function of days post-axotomy (0, 3, 7, and 14) in year old C57Bl/6-WT and *Smn*-/+-C57Bl/6 animals as determined by semi-quantitative western blot analysis. Each point on the graph represents an average of 4 sciatic nerves. Data were $\log_{10}$ transformed prior to linear regression analyses.

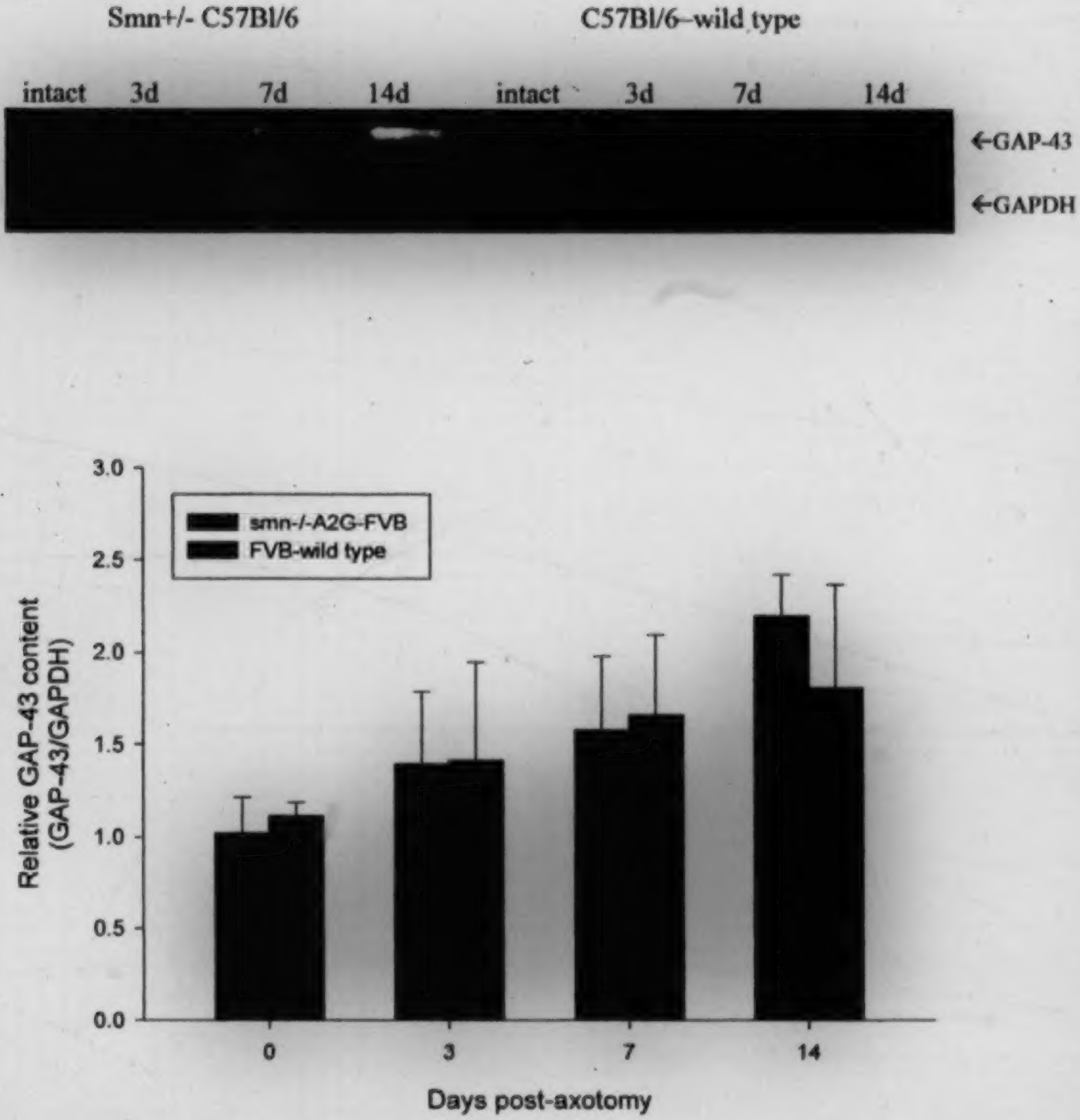

Figure 2.4. Upregulation of GAP-43 in sciatic nerves from *smn-/-*A2G-FVB and FVB-wild type animals at 0, 3, 7 and 14 days post-axotomy (n=3 animals/condition) as determined by semi-quantitative western blot analysis. Each bar represents the average analysis of 12 sciatic nerves (n=3 mice). GAP-43 expression levels were normalized to those of the GAPDH loading control.

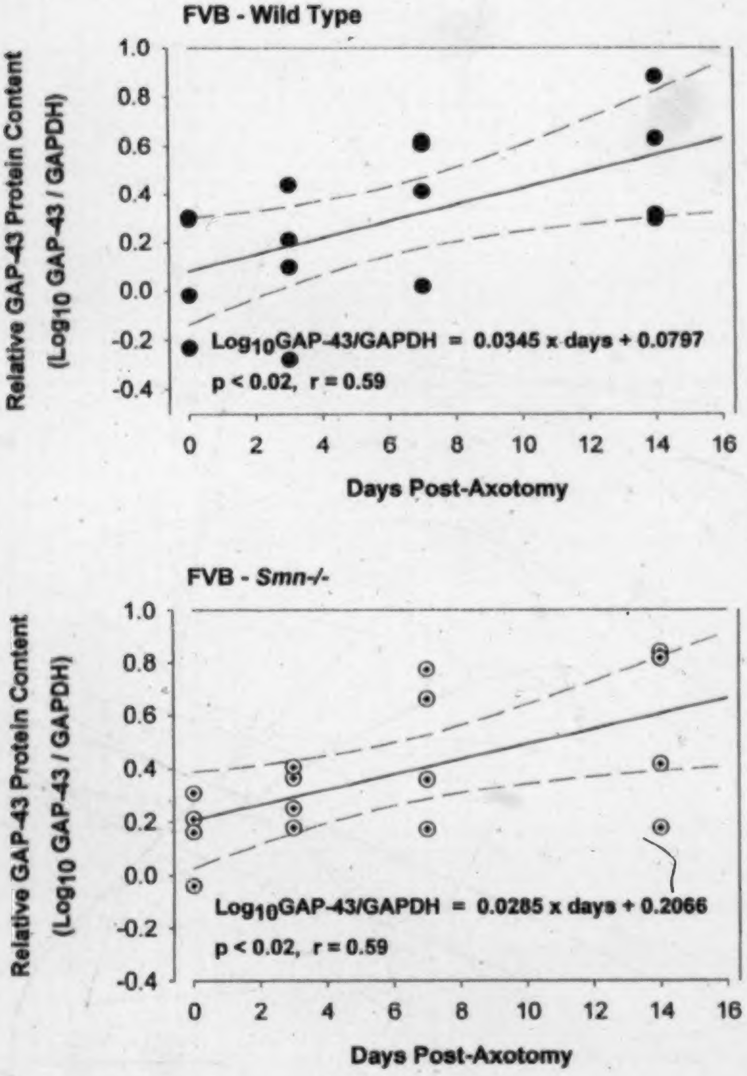

Figure 2.5. Increase in GAP-43 content of sciatic nerves as a function of days post-axotomy (0, 3, 7, and 14) in FVB-WT and *Smn-/-*A2G-FVB animals as determined by semi-quantitative western blot analysis. Each time point on the graph represents an average of 4 sciatic nerves. Data were $\log_{10}$ transformed prior to linear regression analyses.

2.3.3. Immunohistochemical analysis of muscle proteins

2.3.3.1. MyHC distribution

TA muscles from SMAIII mice were analyzed to test the hypothesis that expression of developmental protein isoforms will persist in mature muscle fibers. Analysis of immunohistochemical staining for embryonic MyHC (BF-45) in TA muscles from year old smn+/-C57Bl/6 and C57Bl/6-wild type controls and TA muscles from 3 month smn-/-A2G-FVB and FVB-wild type controls (Figures 2.6 and 2.7) demonstrated that embryonic MyHC is not expressed in these adult tissues (data not shown). The distribution of MyHCs I, IIA, IID/X and IIB fiber types were not significantly different in TA muscles from year old smn+/-C57Bl/6 and C57Bl/6-wild type controls and TA muscles from 3 month smn-/-A2G-FVB and FVB-wild type controls (Figure 2.8) . We expanded our analysis of 3 month smn-/-A2G-FVB to include a mixed fiber postural muscle, the LC, and the slow Sol. MyHC distribution was not significantly different than that observed in FVB-wild type controls in either the LC (Figure 2.9 and 2.10) or Sol (Figure 2.11 and 2.12).

2.3.3.2. N-CAM expression

Immunohistochemical staining of N-CAM was carried out to detect any presence of denervated fibers and/or inappropriate continuation developmental N-CAM expression in intact BB, LC, TA, Q, Mg and Sol muscles from mature 2 month and 1 year smn+/-C57Bl/6 and 3 month smn-/-A2G-FVB mice compared to C57Bl/6 and FVB wild type controls, respectively. No significant N-CAM expression was visible, and the small number of denervated fibers was not significantly different between SMAIII and control muscles (data not shown).

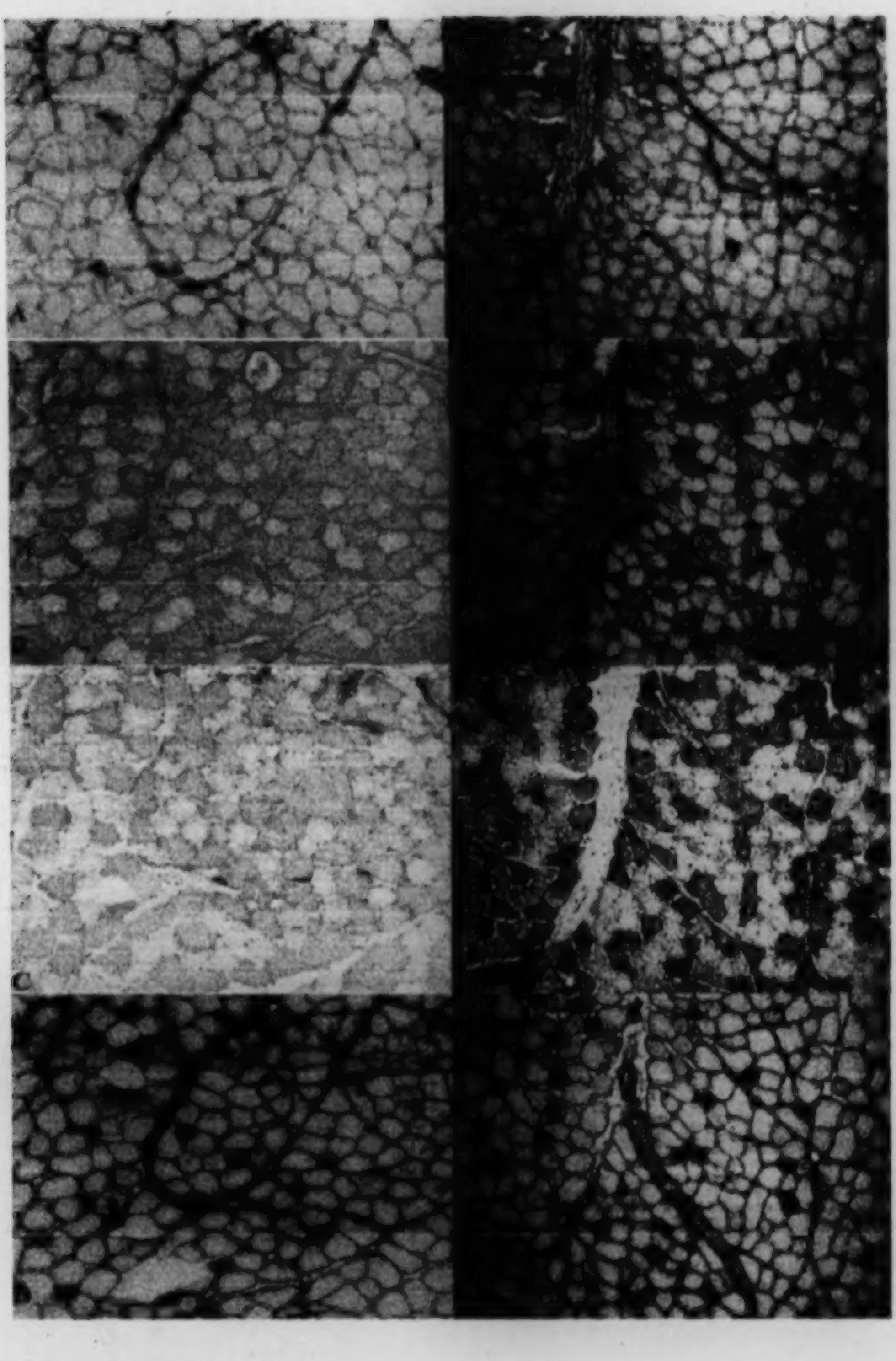
A
C

Figure 2.6. Representative MyHC distribution in TA muscle sections from year old smn+/- C57Bl/6 (A-D) and C57Bl/6-wild type (A'-D') mice. A/A' – Type I (BAD5); B/B' – Type IIB (BFF3); C/C' – Type IID/X (BF35); D/D' – Type IIA (SC71). Positive identification of type IID/X fibers (C/C') is indicated by the **absence** of staining.

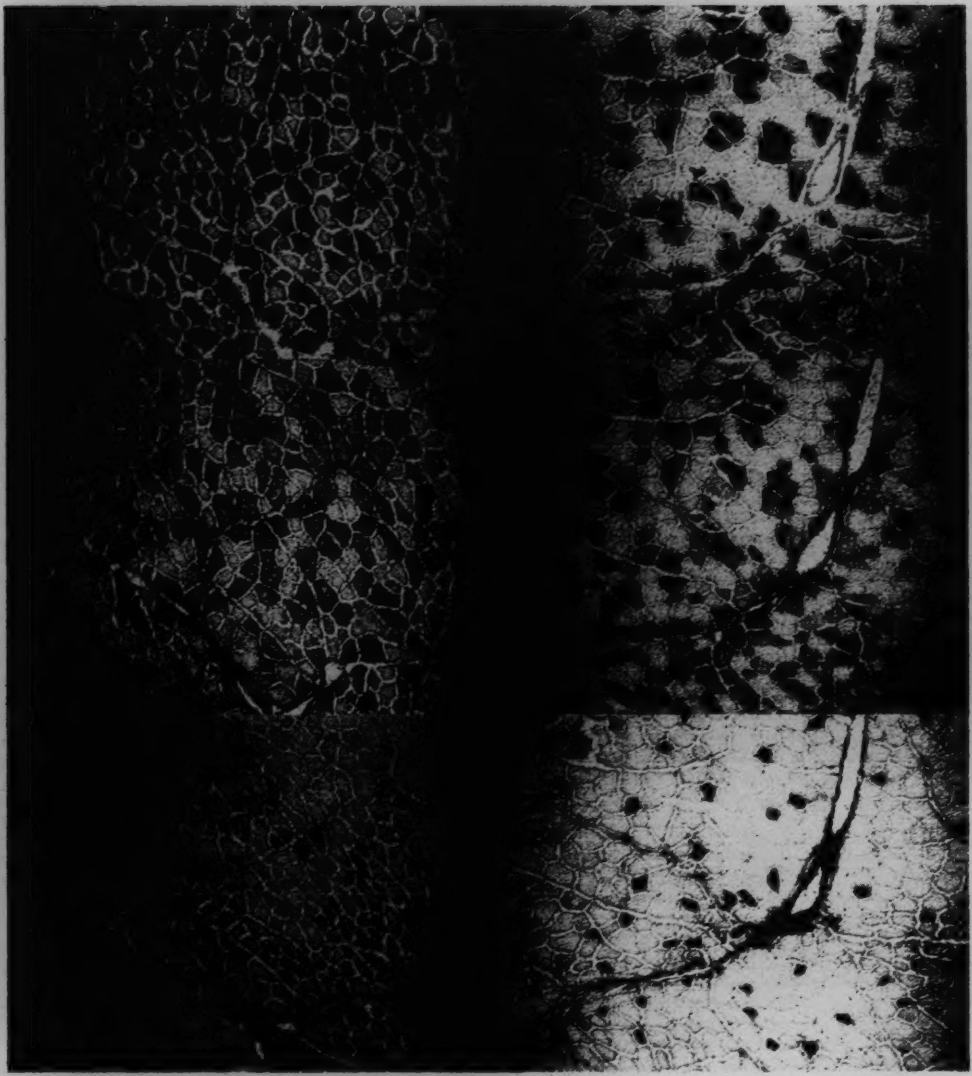

Figure 2.7. Representative MyHC distribution in TA muscle sections from 3 month smn-/-A2G-FVB (A-D) and FVB-wild type (A'-D') mice. A/A' – Type IIB (BFF3); B/B' – Type IID/X (BF35); C/C' – Type IIA (SC71). Positive identification of type IID/X fibers (C/C') is indicated by the **absence** of staining. Results for Type I (BAD5) were all negative and are not shown.

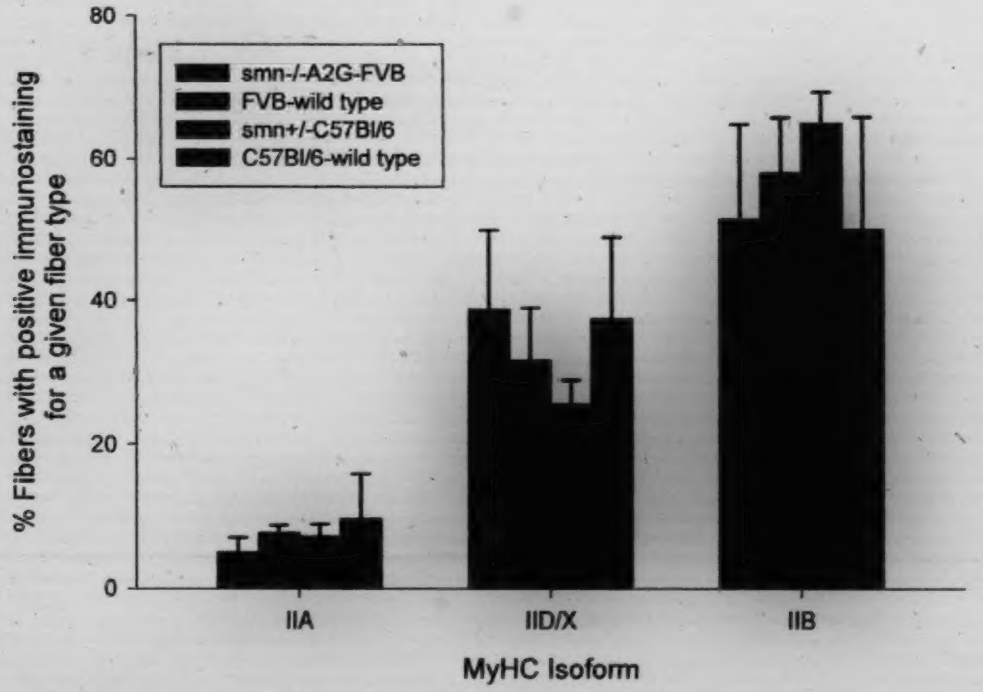

Figure 2.8. Percentage of tibialis anterior fibers expressing a given MyHC isoform from year old smn+/-C57Bl/6 mice (n=3) and C57Bl/6-wild type controls (n=3) and 3 month smn-/-A2G-FVB mice (n=3) and FVB-wild type controls (n=3) measured using immunohistochemistry. There are no significant differences in fiber type distribution between samples from either SMAIII strain and respective wild type controls.

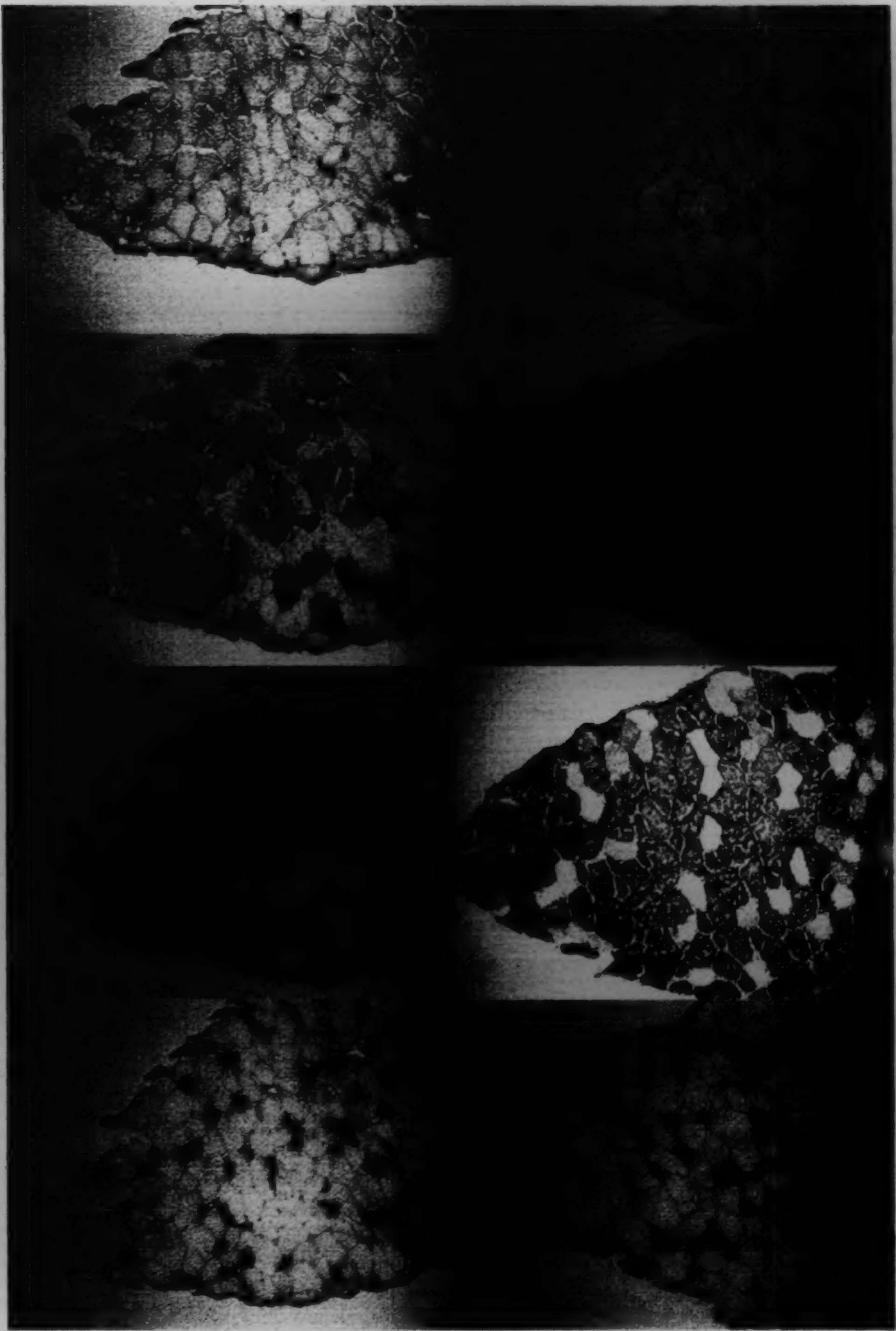

Figure 2.9. Representative MyHC distribution in LC muscle sections from 3 month smn-/-A2G-FVB (A-D) and FVB-wild type (A'-D') mice. A/A' – Type I (BAD5); B/B' – Type IIB (BFF3); C/C' – Type IID/X (BF35); D/D' – Type IIA (SC71). Positive identification of type IID/X fibers (C/C') is indicated by the **absence** of staining.

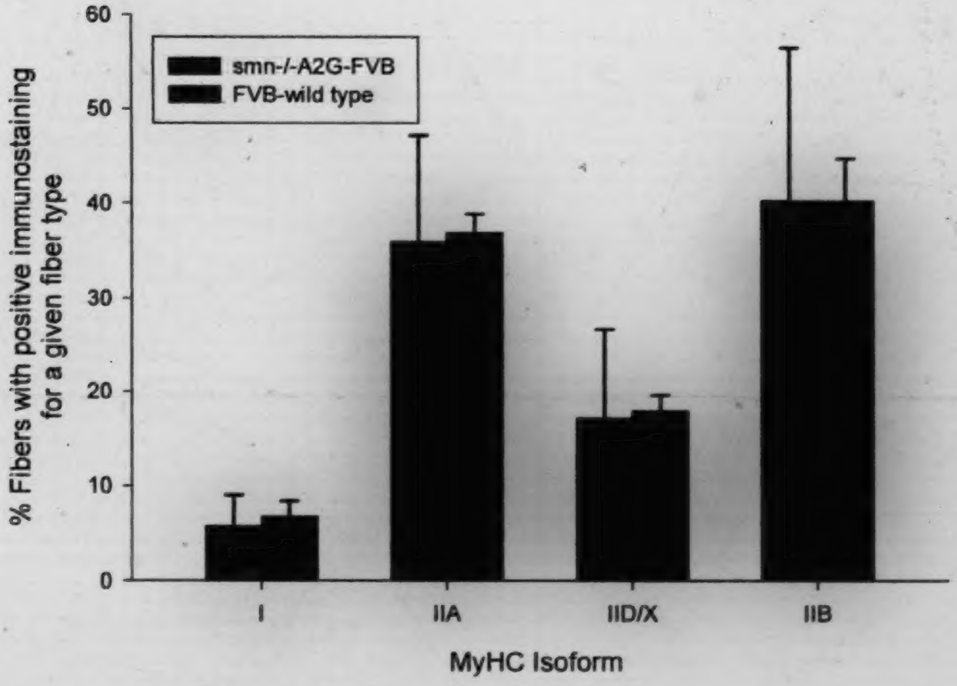

Figure 2.10. Percentage fibers expressing a given MyHC isoform in LC muscles from 3 month smn-/-A2G-FVB and FVB-wild type mice measured using immunohistochemistry. There are no significant differences in fiber type distribution between samples from SMAIII mice and wild type controls.

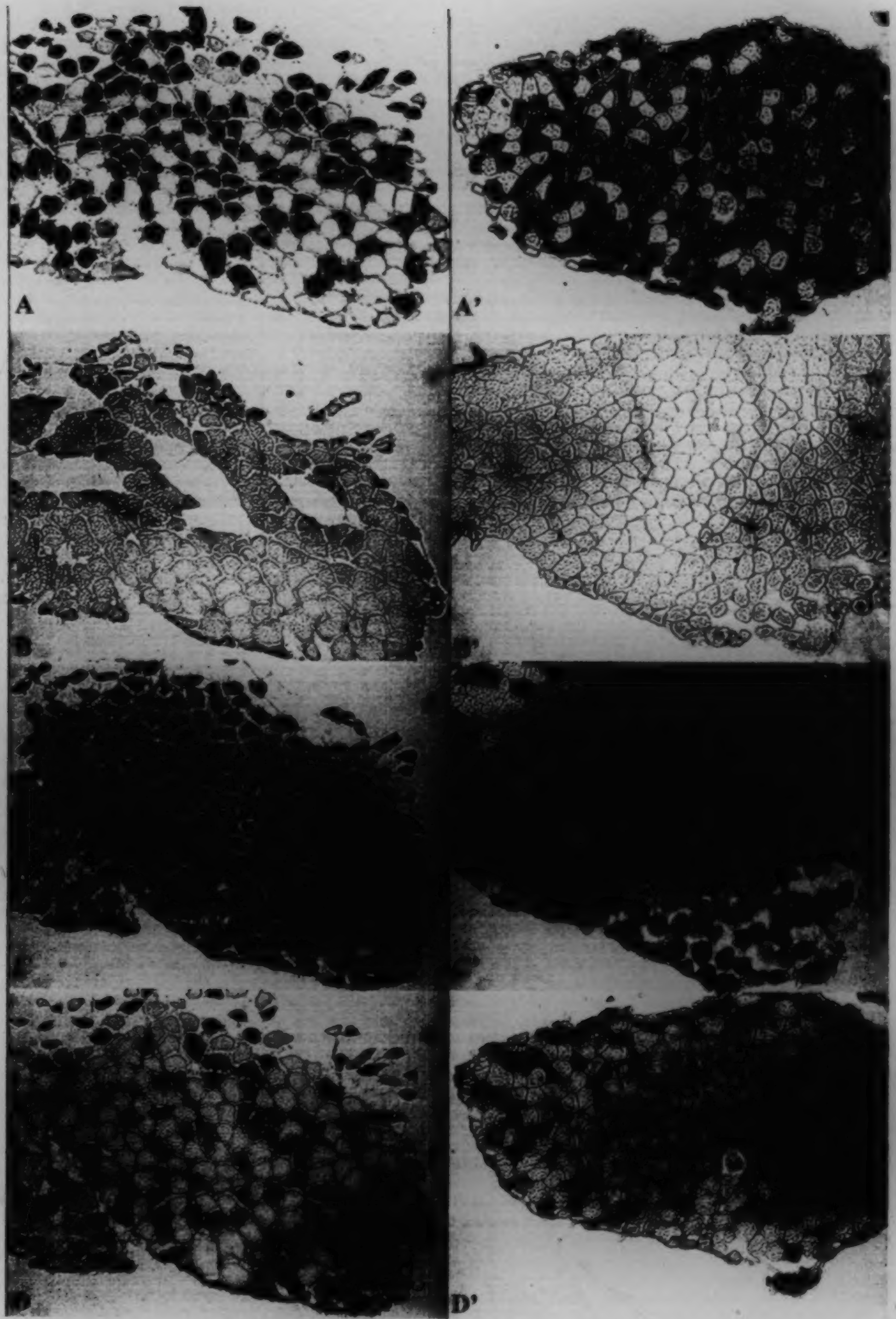
A
A'
D'

Figure 2.11. Representative MyHC distribution in Sol muscle sections from 3 month smn-/-A2G-FVB (A-D) and FVB-wild type (A'-D') mice. A/A' – Type I (BAD5); B/B' – Type IIB (BFF3); C/C' – Type IID/X (BF35); D/D' – Type IIA (SC71). Positive identification of type IID/X fibers (C/C') is indicated by the **absence** of staining.

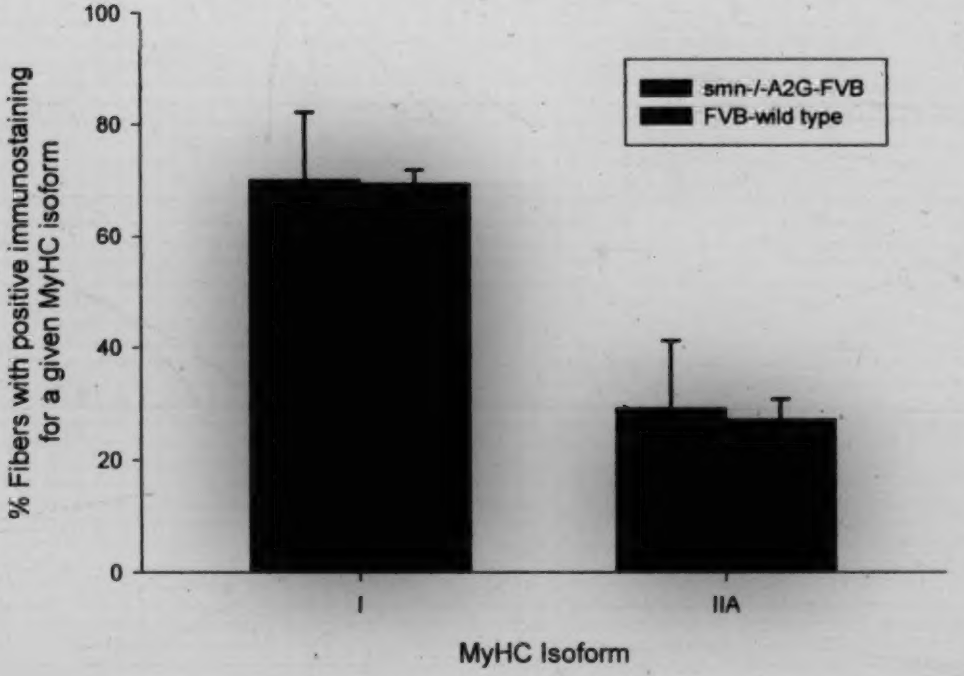

Figure 2.12. Percentage fibers expressing a given MyHC isoform in Sol muscles from 3 month smn-/-A2G-FVB and FVB-wild type mice measured using immunohistochemistry. There are no significant differences in fiber type distribution between samples from SMAIII mice and wild type controls.

2.3.3.3. Cytoskeletal protein expression

No differences between year old Q muscles from smn+/-C57Bl/6 and C57Bl/6-wild type control mice were noted in staining for desmin, dystrophin and vimentin (Figure 2.13 and 2.14). However, analysis of cytoskeletal proteins in Q muscles from 3 month smn-/-A2G-FVB and FVB-wild type controls revealed interesting findings including increased staining for desmin, dystrophin and vimentin (Figures 2.15, 2.16, 2.17, 2.18). Elevated staining levels were observed primarily in smaller fibers, and may not be attributable to disease pathology.

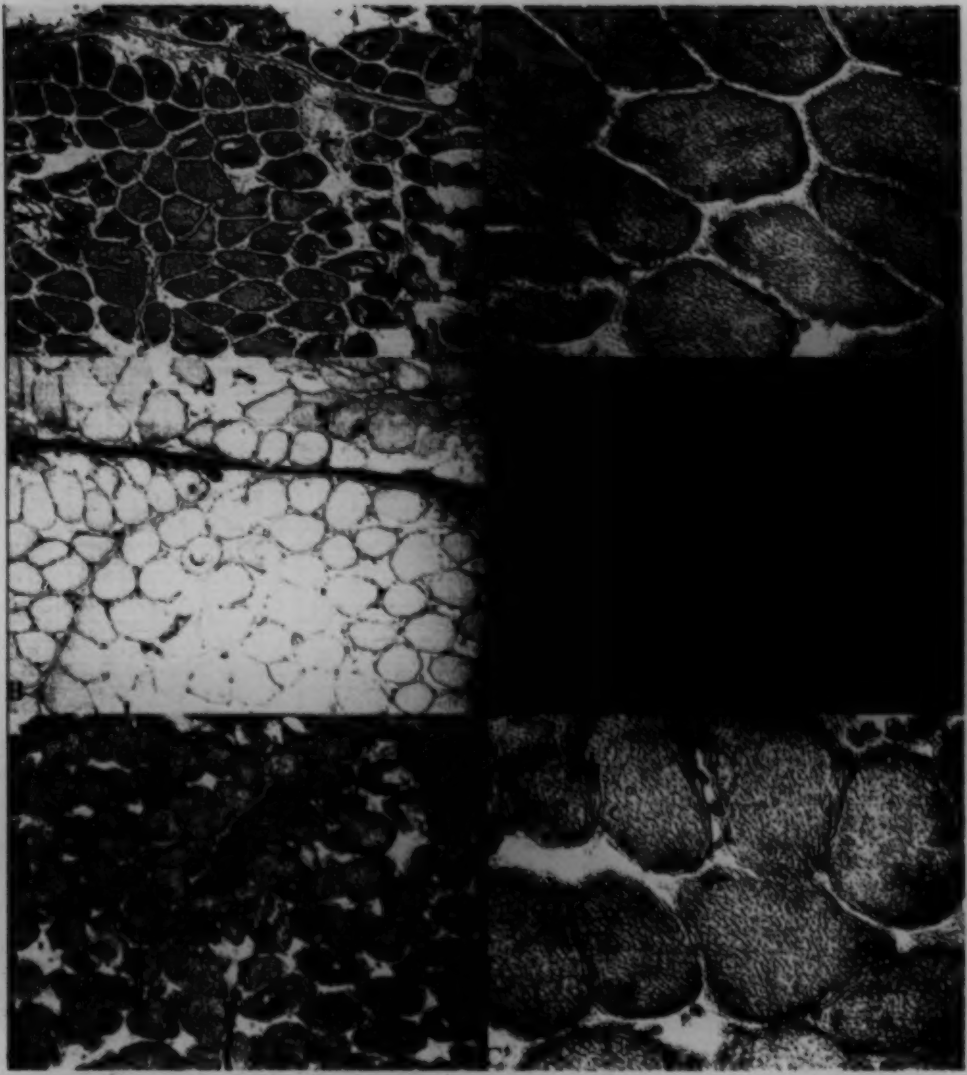

Figure 2.13. Normal staining for cytoskeletal protein in superficial regions of quadriceps muscles from a year old smn+/-C57Bl/6 mouse. A/A' – desmin; B/B' – dystrophin; C/C' – vimentin. Images A-C were taken at 125X magnification, while A'-C' were taken at 312.5X.

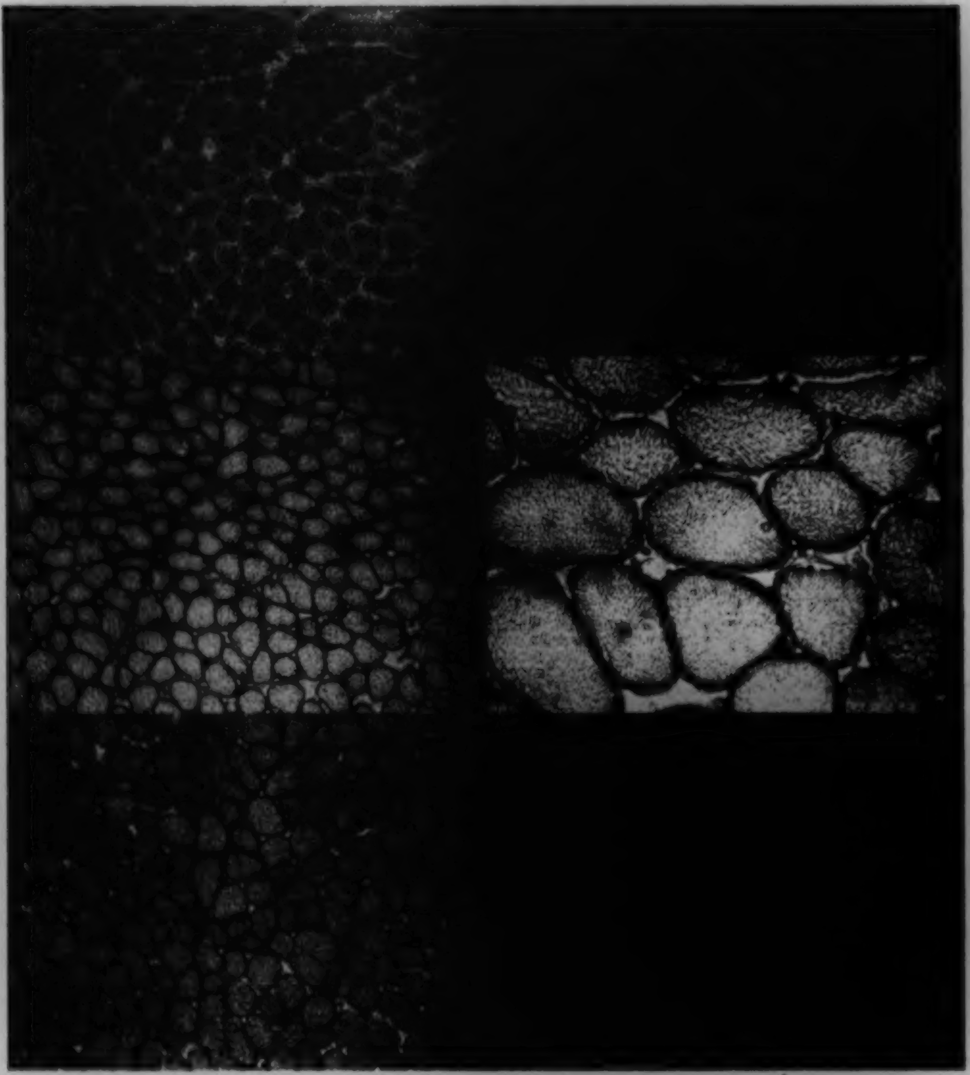

Figure 2.14. Normal staining for cytoskeletal protein in superficial regions of quadriceps muscles from a year old C57Bl/6-wild type mouse. A/A' – desmin; B/B' – dystrophin; C/C' – vimentin. Images A-C were taken at 125X magnification, while A'-C' were taken at 312.5X.

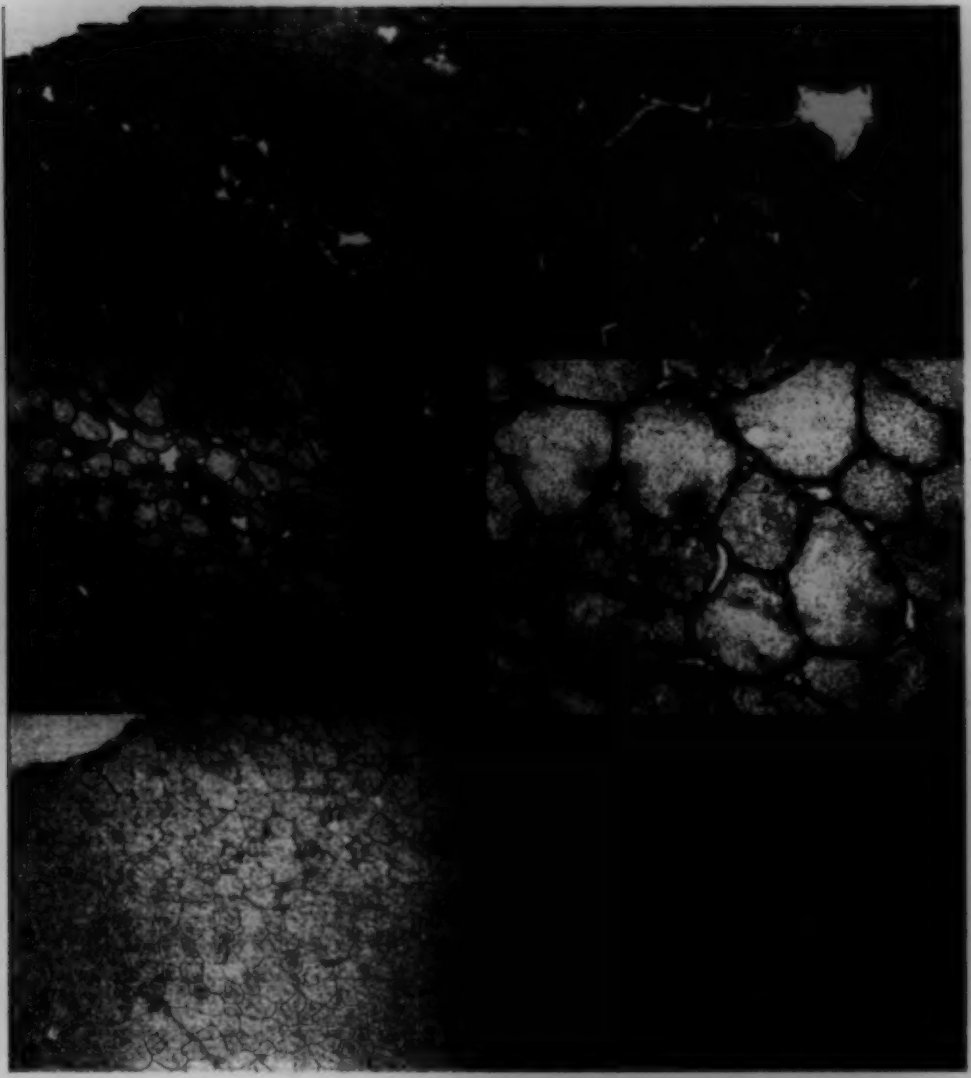

Figure 2.15. Representative staining for the cytoskeletal proteins desmin (A/A'), dystrophin (B/B') and vimentin (C/C') in superficial regions of quadriceps muscle from a 3 month smn-/- A2G-FVB animals. Images A-C were taken at 125X magnification, while A'-C' were taken at 312.5X.

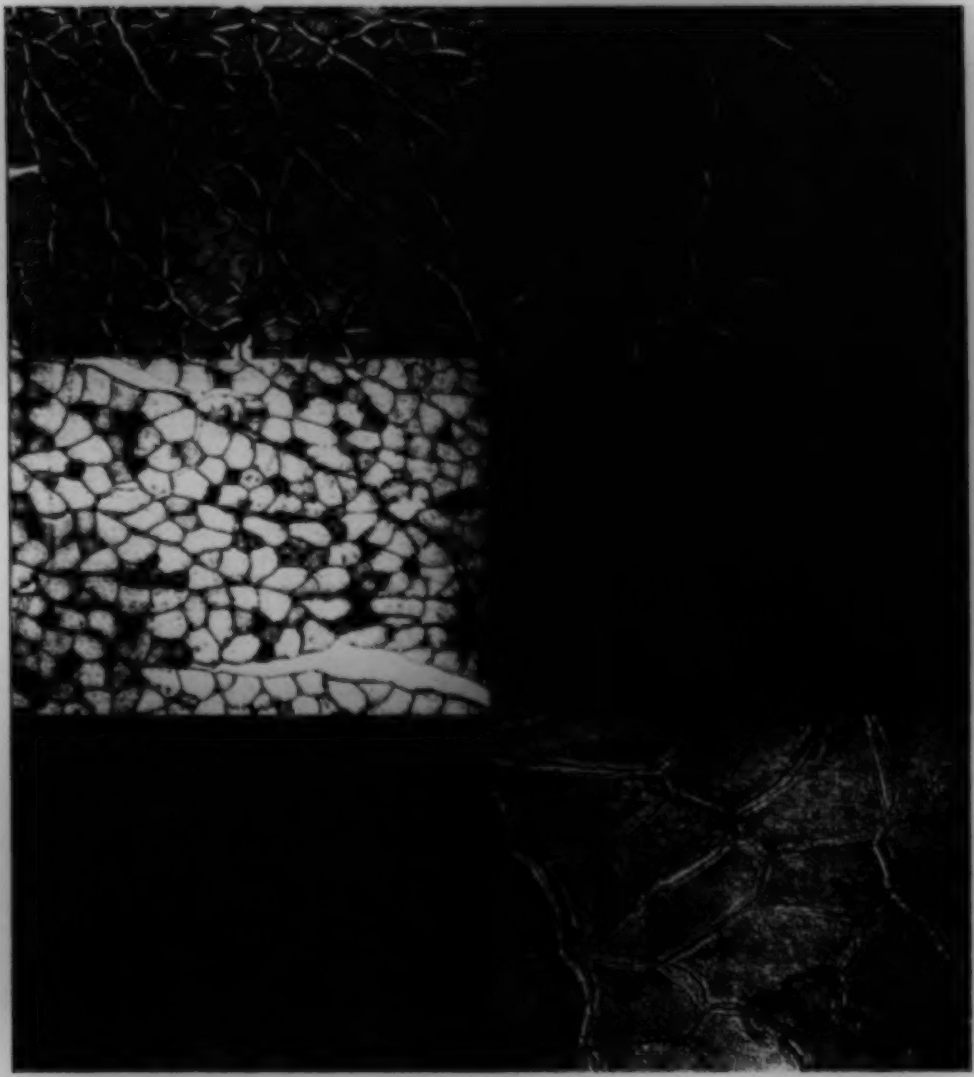

Figure 2.16. Representative staining for the cytoskeletal proteins desmin (A/A'), dystrophin (B/B') and vimentin (C/C') in superficial regions of quadriceps muscle from a 3 month smn-/- A2G-FVB animals. Some evidence of stronger staining, mostly in smaller fibers.Images A-C were taken at 125X magnification, while A'-C' were taken at 312.5X. Asterisk (*) indicates fibers displaying increased

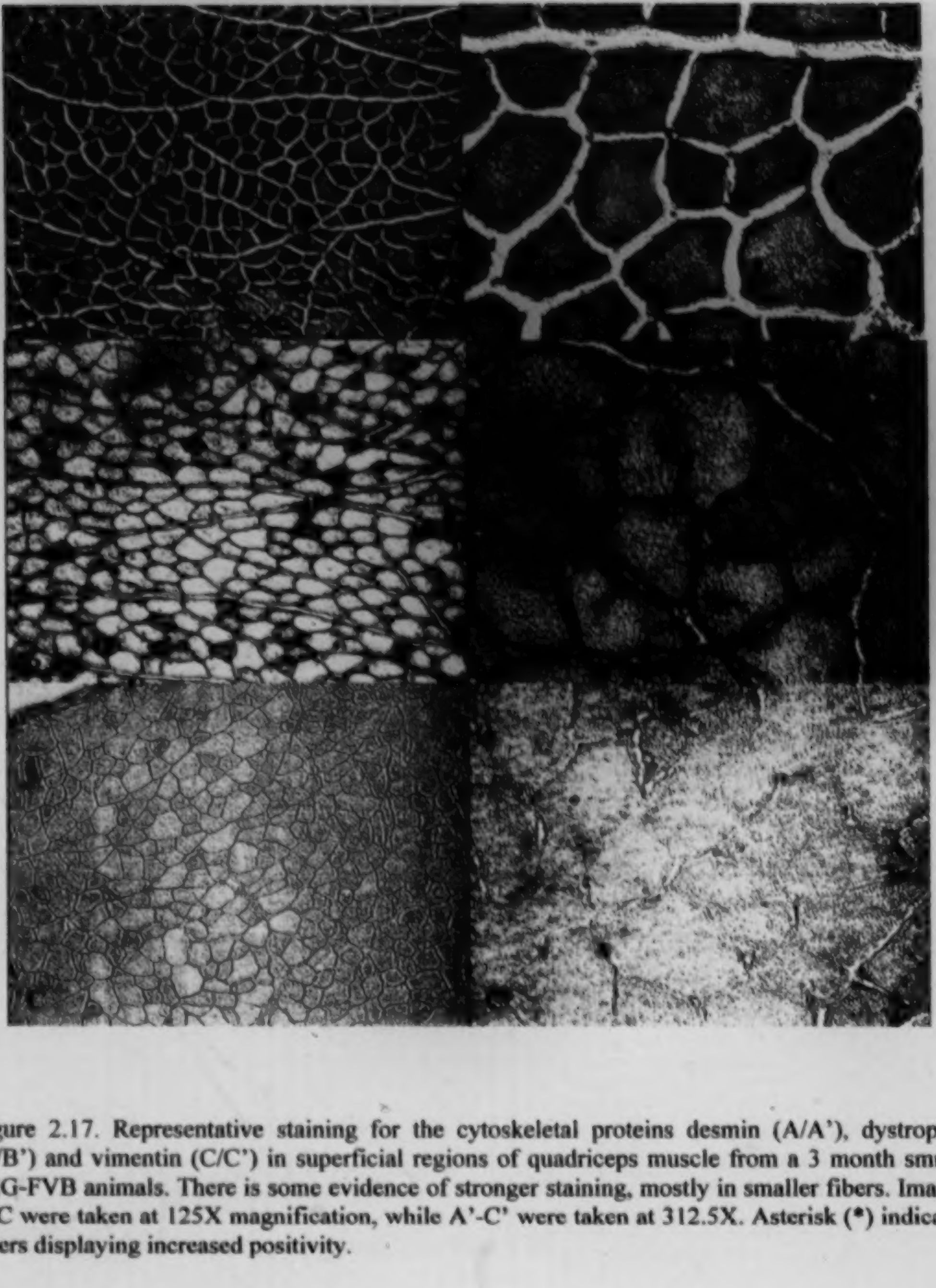

Figure 2.17. Representative staining for the cytoskeletal proteins desmin (A/A'), dystrophin (B/B') and vimentin (C/C') in superficial regions of quadriceps muscle from a 3 month smn-/- A2G-FVB animals. There is some evidence of stronger staining, mostly in smaller fibers. Images A-C were taken at 125X magnification, while A'-C' were taken at 312.5X. Asterisk (*) indicates fibers displaying increased positivity.

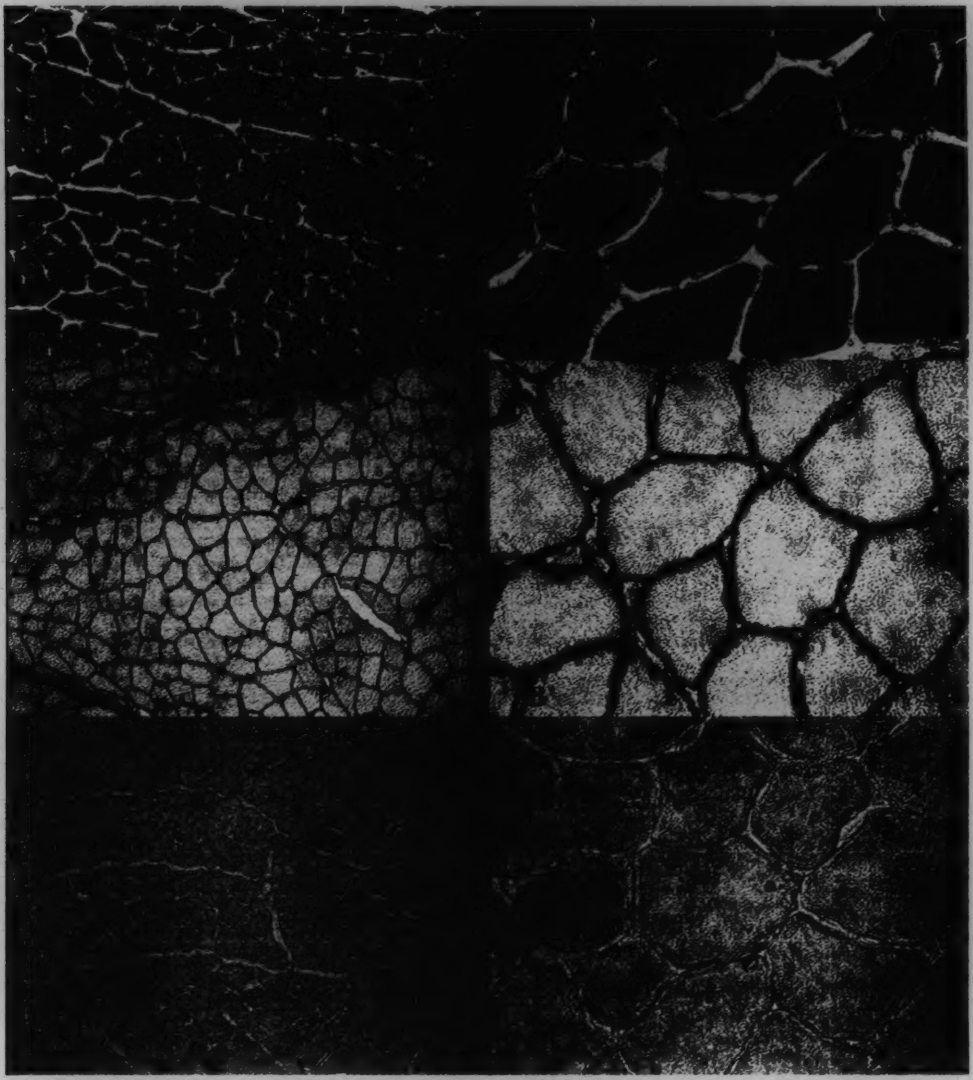

Figure 2.18. Representative staining for the cytoskeletal proteins desmin (A/A'), dystrophin (B/B') and vimentin (C/C') in superficial regions of quadriceps muscle from a 3 month FVB-wild type animal. Images A-C were taken at 125X magnification, while A'-C' were taken at 312.5X.

2.3.3.4. Analysis of muscle atrophy

We assessed the response of TA from 3 month smn-/-A2G-FVB to denervation by sciatic nerve transection. N-CAM staining shows that N-CAM expression is upregulated dramatically by 3d post-axotomy, and this upregulation was nearly identical between smn-/-A2G-FVB and FVB-wild type control samples (Figure 2.19). MyHC distribution changes in response to axotomy were similar between smn-/-A2G-FVB and FVB-wild type control samples (data not shown).

Analysis of muscle fiber cross sectional area (CSA) at 0, 3, 7, and 14d post-denervation revealed the exciting finding that normal reductions in CSA (atrophy) in response to denervation occur at a lower rate (Figure 2.20-2.22) in smn-/-A2G-FVB TA than in FVB-WT TA, indicating impairments in initiation of protein degradation.

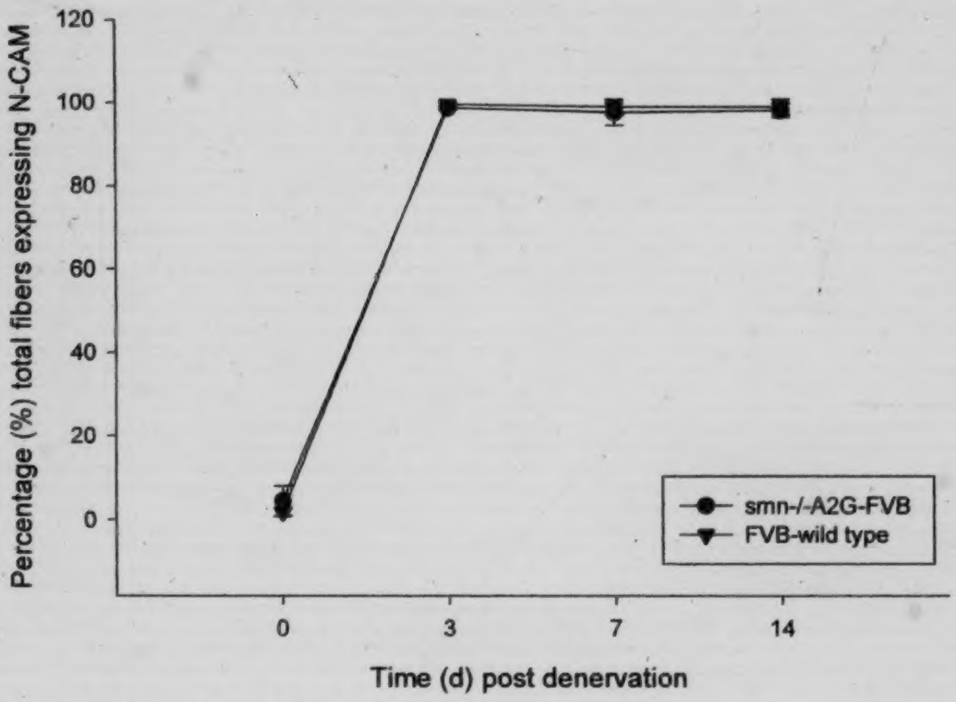

Figure 2.19. Percentage of tibialis anterior fibers expressing N-CAM 0, 3, 7 and 14 days after sciatic nerve axotomy in 3 month smn-/-A2G-FVB and FVB-wild type mice.

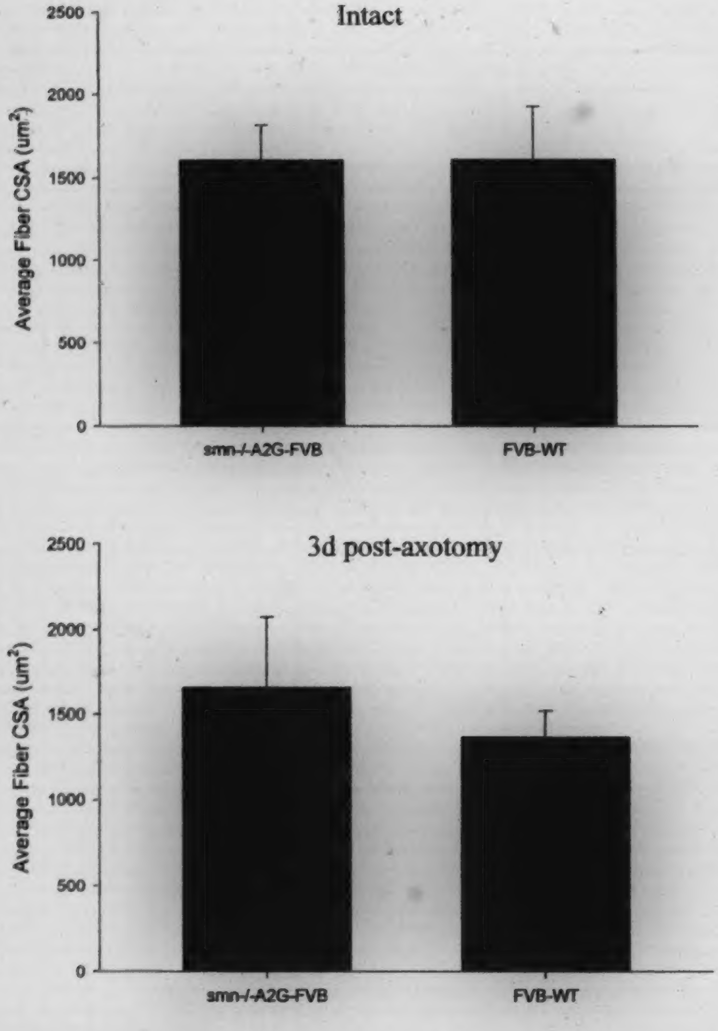

Figure 2.20. Denervation induced reduction in cross-sectional area of tibialis anterior muscle fibers from 3 month old smn-/-A2G and corresponding FVB wild type control mice at 0 and 3 days post-axotomy. In intact muscle average fiber CSA is extremely similar between FVB-WT (1606.9 μm^2) and smn-/-A2G (1601.4 μm^2) mice. Three days post-axotomy, the average fiber CSA is slightly smaller in FVB-WT (1367 μm^2) than in smn-/-A2G (1659.6 μm^2), but this difference is not significant ($p=0.16$).

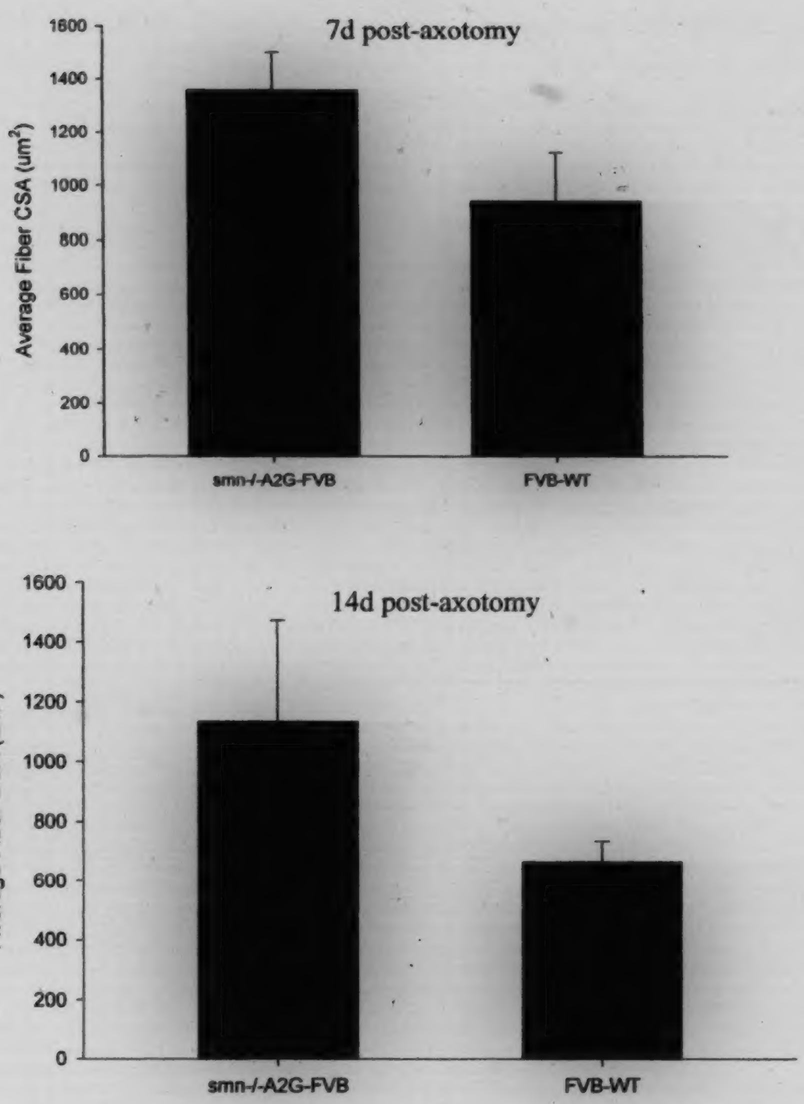

Figure 2.21. Denervation induced reduction in cross-sectional area of tibialis anterior muscle fibers from 3 month old smn-/-A2G and corresponding FVB wild type control mice at 0 and 3 days post-axotomy. At 7d post-axotomy, the delay in denervation atrophy in smn-/-A2G muscles is more pronounced, with FVB-WT animals having an average fiber CSA of 940.7 μm^2, while smn-/-A2G average fiber CSA measured 1356.1 μm^2 ($p=0.018$). At 14d post-axotomy, the average fiber CSA of FVB-WT mice (662.6 μm^2) was much smaller than that measured in smn-/-A2G animals (1134.5 μm^2) although this difference did not reach significance ($p=0.072$).

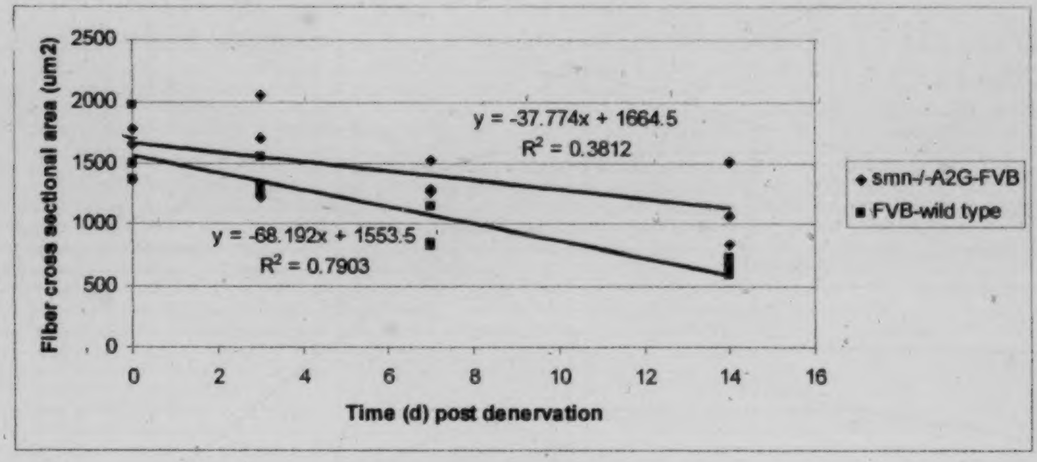

Figure 2.22. Time course denervation induced reduction in cross-sectional area of tibialis anterior muscle fibers from 3 month old smn-/-A2G and corresponding FVB wild type control mice 0, 3, 7, and 14 days post-axotomy. Muscles from smn-/-A2G-FVB mice demonstrate a delayed response to denervation as measured by cross-sectional area although this difference is not significant (p=0.13).

2.4. DISCUSSION

2.4.1. ChAT expression measured in BB, LC, and TA tissues is not significantly different in SMAIII and WT animals

Analysis of ChAT levels was performed to assess functional maturity of motoneurons in SMAIII mice. No statistically significant differences in ChAT activity were detected between SMAIII and WT controls. We **did not** observe, as expected, decreased ChAT expression levels in SMAIII tissues that would demonstrate a failure to sufficiently upregulate transmission-related proteins during development. In fact, ChAT levels appear to be greater in the 3 month *Smn-/-*A2G-FVB than in FVB-WT counterparts in BB, LC and (minimally) in TA muscles, although these differences are not statistically significant (Figure 2.1). In confirmation of this, splicing deficits documented in Zhang *et al.* (2008) do not indicate that the gene encoding ChAT is affected. Results are in agreement with findings of Soler-Botija *et al.* (2005), showing that ChAT expression was unaffected in SMAI fetuses (Soler-Botija *et al.*, 2002a), where impairments caused by depleted SMN levels are much more severe than those observed in the mild SMAIII murine models employed in this study. We conclude that neuromuscular transmission defects in SMA disease pathology do not result from a failure to synthesize acetylcholine. Present results indicate that upregulation of ChAT with the onset of neuromuscular activity during postnatal development is not impaired in SMA. Defective neuromuscular transmission observed in SMA is more likely attributable to other observed molecular defects in SMA including: impaired excitability due to insufficient concentrations of L-type calcium channels present in the membrane (Jablonka *et al.*, 2007), neurofilament accumulation in the pre-synaptic terminal, or insufficient AChR number and disorganization of these at the post-synaptic membrane (Kariya *et al.*, 2008a;Murray *et al.*, 2008a).

2.4.2. GAP-43 expression is not differentially expressed in SMAIII tissue and is upregulated similarly to WT after axotomy

Western blots for semi-quantitation of GAP-43 production in intact nerves indicate that baseline expression of this protein is not significantly different in SMAIII than in WT sciatic nerves (Figures 2.2 and 2.4). Results were not as expected, that high GAP-43 expression would be perpetuated in SMAIII tissue. Sharp *et al.* (2005) noted that developing motoneurons, when challenged by a second stimulus (in this case, sciatic axotomy) frequently cannot respond adequately and are more susceptible to death (Sharp *et al.*, 2005). The robust upregulation of GAP-43 in motoneurons of both SMAIII models (Figures 2.2-2.5) indicates that tissues are amply equipped to respond to axotomy, supporting the conclusion that a developmental state is not perpetuated in motoneurons from SMAIII mice. Comparison of upregulation rate between *Smn-/+*-C57Bl/6 and C57Bl/6-WT controls indicates an increased rate of upregulation in *Smn-/+*-C57Bl/6 animals (P<0.05) (Figure 2.3). While an increased rate of upregulation in GAP-43 might be a response compensating for impairments in axonal outgrowth (Gaudreault *et al.*, 2005), it is more likely to be biologically insignificant in the present situation, as Figure 2.2 indicates that this 'rate increase' was created solely by measured expression differences between days 7 and 14 post axotomy, and replicate experiments in the more severe smn-/-A2G-FVB SMAIII model (Figure 2.5) do not provide evidence for rate of upregulation differences between *Smn-/-*A2G-FVB animals and FVB-WT control tissues.

Zhang *et al.* (2008) documented widespread splicing deficits in tissues from a murine model of SMAII (Le *et al.*, 2005). GAP-43 was not among genes determined to be inappropriately spliced, implying that the subset of snRNPs produced by SMN are not required for its splicing. While mis-splicing of genes coding for additional proteins essential in axonogenesis may occur, this situation appears less likely in light of findings from our lab that sprouting occurs normally in motoneurons from smn+/-C57Bl/6 and smn-/-A2G-FVB animals (Harris *et al.*, unpublished work). It is more probable that motoneuron outgrowth is not significantly impaired by modest reductions of SMN.

SMN trafficks along the length of developing axons, and has been shown to co-localize with GAP-43 in growth cones (Zhang *et al.*, 2003). Reduced levels of SMN in the two SMAIII models evaluated here did not prevent GAP-43 upregulation in axotomized sciatic nerves, indicating that although they colocalize, GAP-43 is not dependent upon SMN for its expression or localization in the axon.

2.4.3. Embryonic MyHC expression of does not persist, mature MyHC isoform distribution is unaffected in SMAIII skeletal muscle, and N-CAM staining provides no evidence for denervation in examined tissues

TA muscles from SMAIII mice were analyzed to detect persistence of developmental protein isoform expression in mature tissues. Embryonic MyHC is normally expressed during development and sometimes in fibers undergoing atrophy or regeneration (Stupka *et al.*, 2008). Immunohistochemical staining for embryonic MyHC in B, LC, TA, Mg, Q and Sol muscles from two murine models of SMAIII was negative (data not shown), indicating that expression of this developmental MyHC isoform does not persist inappropriately in mature tissues. Previous documentation of developmental myosin isoforms in SMA patient tissues has been limited to expression of neonatal myosin (nMyHC) in very small, atrophied fibers (Compton *et al.*, 2005b). nMyHC is expressed in response to fiber damage in tissues of multiple muscular disorders (Arnardottir *et al.*, 2004) (Yuasa *et al.*, 2008), and does not represent persistence of a developmental phenotype. Present findings indicate (a) a lack of perpetuation of developmental protein expression and (b) a lack of evidence for degeneration/regeneration as indicated by absence of embryonic MyHC expression, staining for which has been previously documented in more severe forms of the disease (Compton *et al.*, 2005a;Soubrouillard *et al.*, 1995a).

Evaluation of adult MyHC distribution found no differences between TA from year old smn+/-C57Bl/6 and 3 month smn-/-A2G-FVB animals and their corresponding wild type controls (Figures 2.6-2.8). A recent study found that more proximal postural muscles are affected earlier and more severely in SMA (Murray *et al.*, 2008c). Based on this, analysis of the LC, a mixed fiber postural muscle, and the Sol, a predominantly slow muscle in the hindlimb, was undertaken. (See figures 2.9 and 2.11 for representative pictures). Figures 2.10 and 2.12 clearly show that MyHC distribution in both muscles was similarly unaffected in smn-/-A2G-FVB mice. These findings are consistent with multiple reports that found MyHC isoform content to be unimpaired in SMA patient samples (Sawchak *et al.*, 1990;Soubrouillard *et al.*, 1995b;Soussi-Yanicostas *et al.*, 1992). In the *D. melanogaster* model, thick filament formation was also determined to be unimpaired (Rajendra *et al.*, 2007b).

Immunohistochemical staining of N-CAM was carried out to observe presence of denervated fibers and/or inappropriate continued developmental N-CAM expression in intact B, LC, TA, Q, MG and Sol muscles from mature 2 month and 1 year smn+/-C57Bl/6 and 3 month smn-/-A2G-FVB mice compared to C57Bl/6 and FVB wild type controls, respectively. No significant N-CAM staining was observed, indicating (a) the absence of perpetuation of developmental N-CAM expression, and (b) the lack of denervated fibers in these mild SMAIII murine models. These results indicate that at time points examined in the mild SMAIII models assessed (2 months and 1 year in *Smn-/+*-C57Bl/6 animals, and 3 months in *Smn-/-*A2G-FVB animals), no significant denervation has occurred, illustrating a mild phenotype resulting from a modest reduction of SMN in SMAIII mice.

2.4.4. Staining for dystrophin, desmin and vimentin in skeletal muscle from Smn-/+-C57Bl/6 and smn-/-A2G-FVB is unremarkable

Staining for the cytoskeletal proteins dystrophin, desmin and vimentin was unremarkable in muscles from 2 month (data not shown) and year old *Smn-/+*-C57Bl/6 animals (Figure 2.13), and did not differ from that observed in C57Bl/6-WT controls (Figure 2.14). Similarly, muscles from 3 month *Smn-/-*A2G-FVB animals demonstrated strong dystrophin staining and no positive pathological staining of desmin or vimentin, indicating a lack of denervation and regeneration in these muscles, in confirmation of results for N-CAM and embryonic MyHC immunohistochemistry. Some unusual dystrophin staining can be observed in TA and Q muscles from 3 month smn-/-A2G-FVB mice, although it is difficult to determine whether this is a staining artifact or a real effect.

Dystrophin is one of the major proteins comprising costameric structures in skeletal muscle. The costamere (also referred to as the dystrophin-associated protein complex, DAPC) is a sub-sarcolemmal assembly which appears as transverse stripes over sarcomeres, aligned with Z-disks of peripheral myofibrils (Pardo *et al.*, 1983). These assemblies function to couple sarcomeric force-generation with the sarcolemma in skeletal muscle (Straub & Campbell, 1997;Ervasti, 2003). The costamere is a macromolecular assembly that has many functions, with members including dystroglycans (which link the costamere to extracellular proteins such as laminin), and F-actin, which binds to dystrophin (another member) (Ervasti & Campbell, 1993), and the intermediate filament (IF) protein desmin (See Ervasti, 2003 for review). Vimentin and nestin are the primary expressed IF proteins expressed during prenatal development, but are quickly downregulated during maturation. Desmin production begins later and persists in adult tissue (Sejersen & Lendahl, 1993). Work by Vaittinen *et al.* (2001) suggests that nestin and vimentin are essential in early phases of myofiber development and regeneration, participating in migration, fusion and remodeling events (Vaittinen *et al.*, 2001). The later upregulation of desmin was interpreted to indicate its necessity in structural maintenance of mature myofibers.

In the present study, immunostaining for desmin and vimentin did not provide evidence of any positively-expressing fibers. Goeble (1995) noted that desmin pathology in human neuromuscular disorders is always marked by either diffuse or focally increased amounts of protein (Goebel, 1995). Desmin upregulation has previously been noted in subsarcolemmal regions of small fibers of infantile SMA (SMAI) (Sarnat, 1992), attributable to immaturity, denervation, or both. Borneman & Schmalbruch (1992) also noted desmin overexpression, but always in very small atrophied fibers (Bornemann & Schmalbruch, 1992). The absence of pathological (extremely dark or foci of positivity) desmin staining indicates that there are no atrophying or regenerating fibers present in these tissue sections. Manta *et al.* (2006) report significant vimentin staining in X-linked Myotubular Myopathy (XLMTM) samples, supportive of a delayed developmental phenotype in this disease (Manta *et al.*, 2006). Lack of positive vimentin staining demonstrates that abnormal expression of developmental proteins in mature tissues does not occur in SMAIII mice, and provides further evidence that developmental delays in protein production are not a hallmark of SMA pathology.

Staining for dystrophin in muscles (LC, BB, TA, Mg, Q, Sol) from smn-/-A2G-FVB SMAIII mice showed presence of diffuse sarcoplasmic labeling in smaller fibers in addition to strong normal sarcolemmal immunolabelling. Sarcoplasmic dystrophin immunoreactivity has previously been documented in *quadriceps femoris* muscle biopsies from a patient with servere neonatal XLMTM, along with positive staining for vimentin (Manta *et al.*, 2006). Many of the generalized splicing defects described in Zhang *et al.* (2008) involve genes coding for protein components of the extracellular matrix (ECM). The dystroglycan complex (DGC) provides a connection between the extracellular matrix (ECM) and cytoskeleton in skeletal muscle, a linkage essential for both structural stability and for passage of extracellular cues and messages into the cell to be communicated via cell signaling pathways acting through this complex. It is logical that general splicing defects in mRNAs for ECM components could lead to impaired production of ECM proteins that would in turn affect organization of cytoskeletal proteins such as dystrophin. Thus it is possible that if the altered distribution of dystrophin observed here is a real effect of SMA, it may be the result of splicing defects in SMA.

Arnold *et al.* (2004) created primary muscle cultures using tissue from SMAI patients to observe the process of muscle fiber differentiation in the absence of a nerve component (Arnold *et al.*, 2004b). Their observations included disabled myotube fusion accompanied by an inability to form multinucleated myotubes. They also noted that application of neural agrin was insufficient to promote AChR organization. Although the radiometric binding assay employed in this study determined decreased AChR expression, it can only measure assembled, functioning AChR levels and cannot assess transcription and translation of subunit components. Both mRNA encoding AChR subunits, and subsequently translated AChR subunit proteins, require accurate localization in the region of the neuromuscular junction for functional AChR assembly and accurate organization within the membrane. Deficiencies in SMN could impair either mRNA or protein trafficking, or lead to cytoskeletal instabilities affecting mRNA and protein localization (Bowerman *et al.*, 2007;Rajendra *et al.*, 2007a). AChR aggregation relies on actin filaments. Mitsui *et al.* (2000) determined that actin and desmin support AChR organization, and function to mediate excitation of AChR through the sarcomeric contraction system (costameres/dystrophin) (Mitsui *et al.*, 2000). Bezakova & Lomo (2001) found that muscle activity and agrin application (neural and muscular) regulate cytoskeletal proteins (specifically dystrophin) and the organization of their attached AChR aggregates in skeletal muscle (Bezakova *et al.*, 2001;Bezakova & Lomo, 2001). In light of this information, and findings by Rajendra *et al.* (2007) and Olaso *et al.* (2008) documenting misregulation of F-actin in SMA, our results indicate that AChR disorganization observed in SMA (Arnold *et al.*, 2004a;Biondi *et al.*, 2008c) might be explained by differential organization of dystrophin.

It is difficult to resolve impairments in cytoskeletal protein organization with the immunohistochemical stains of muscle cross-sections employed in this study. To confirm these findings and to determine how dytrophin is differentially organized, studies using much greater resolution and immunofluoresence staining should be employed. Immunofluorescence offers an excellent alternative to the immunohistochemistry performed here, as it allows target protein distribution to be observed without being confounded by background and general staining of the tissue. Co-immunofluorescence for components of the DGC as well as F-actin and AChR receptors would provide insight into any disorganization of important cytoskeletal components in these tissues.

2.4.5. Denervation induced muscle atrophy as measured by fiber CSA is delayed in TA from 3 month smn-/-A2G-FVB mice

Denervation of skeletal muscle causes a growth-to-regeneration phenotypic change involving drastic alterations in the muscle's protein expression profile. N-CAM expression is upregulated immediately following denervation, and its levels remain high until regeneration occurs or muscle fibers die and disappear. Prolonged denervation induces atrophy mediated by the ubiquitin (Ub) proteasome system and invokes a catabolic state characterized by marked protein degradation and resultant shrinkage of the muscle (Medina *et al.*, 1995;Jagoe & Goldberg, 2001).

Evaluation of N-CAM expression 3, 7 and 14d post-denervation using immunohistochemistry found that even at 3d post-denervation, >98% of all fibers from 3 month smn-/-A2G-FVB and FVB-wild type control TA muscles were N-CAM positive (Figure 2.19), once again indicating that mild reductions in SMN levels and resulting splicing deficits do not impair efficient protein upregulation in SMAIII tissues. MyHC distribution in denervated TA fibers was not different between smn-/-A2G-FVB and FVB-wild type controls (data not shown).

Analysis of fiber CSA post-denervation revealed a delay in the rate of denervation induced muscle atrophy in smn-/-A2G-FVB mice (Figure 2.20). Reduction in CSA over time occurs 1.8X slower in fibers from SMAIII mice. These results provide the first evidence for a delayed physiological response resulting from reduced levels of SMN in a mild SMAIII murine model. Our findings of delayed denervation-induced atrophy may relate to a unique pathological feature of SMA in human patients: the presence of hypertrophic (enlarged) muscle fibers (Bobele *et al.*, 1996b). Muscle response to denervation involves increased protein degradation by the Ub proteasome system, which is activated by transcription of atrophy-related genes, termed 'atrogenes' (Jagoe and Goldberg, 2001; Lecker *et al.*, 2004). In normal skeletal muscle, atrogene expression is inhibited (Figure 2.23): Phosphoinositide-3-kinase (PI3K) phosphorylates and activates Akt (protein kinase B), which phosphorylates F-box (FOXO) transcription factors, a modification which prevents them from entering the nucleus to stimulate atrogene transcription (Mammucari *et al.*, 2007). In the event of an atrophy-promoting stimulus, such as denervation of starvation, Akt is *inactivated* and the muscle enters a catabolic state in which protein synthesis is decreased in favor of protein degradation. The F-box proteins are now able to enter the nucleus to promote atrogene transcription, leading to production of ubiquitin ligases such as Atrogin-1, which tags and marks many cellular proteins for degradation by the Ub proteasome system. Reduced rates of denervation atrophy have previously been documented in neonatal tissue (in comparison with adult tissue) (Vrbova, personal communication). The PI3K/Akt pathway is strongly activated during development, providing a very likely explanation for slower denervation atrophy observed in this instance (Florini *et al.*, 1996).

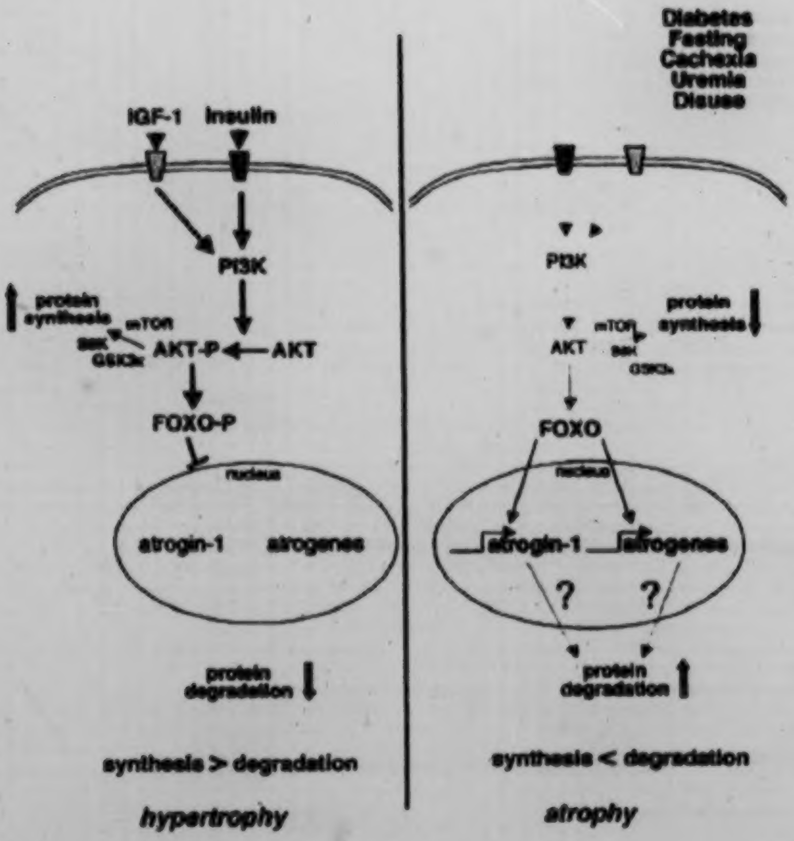
Diabetes
Fasting
Cachexia
Uremia
Disuse
IGF-1
Insulin
PI3K
protein synthesis
mTOR
S6K
GSK3β
AKT-P
AKT
FOXO-P
nucleus
atrogin-1
atrogenes
protein degradation
synthesis > degradation
hypertrophy
PI3K
AKT
mTOR
S6K
GSK3β
protein synthesis
FOXO
nucleus
atrogin-1
atrogenes
?
?
protein degradation
synthesis < degradation
atrophy

Figure 2.23. Signaling responsible for regulation of anabolic (hypertrophic) and catabolic (atrophic) states in skeletal muscle. (Sandri *et al.*, 2004).

In the present study, a delayed reduction in CSA indicates impaired protein breakdown in smn-/-A2G-FVB tissues. This could be caused by (a) inappropriate splicing and therefore inappropriate expression of proteins essential for atrophy induction, such as Atrogin-1, which is the primary ubiquitin ligase responsible for decreases in muscle mass during atrophy (Bodine *et al.*, 2001), or (b) misregulation of some component in the signaling pathway essential for the induction of atrogene transcription (Figure 2.23).

It may also be possible to relate misregulation of Akt, a primary component of this signaling pathway, to decreased levels of F-actin documented in SMA tissues (Olaso *et al.*, 2008). Akt contains a plekstrin homology (PH) domain which mediates its binding to membrane phospholipids, usually phosphoinositol (3,4,5) triphosphate (PtIns3,4,5P3), which is synthesized by PI3K. PI3K is activated by G protein coupled receptors (GPCRs) or tyrosine kinase receptors (TRKs). Akt binding to PtIns3,4,5P3 leads to its phosphorylation and activation by phosphoinositide-dependent kinase 1 and an additional kinase (mTOR, integrin-linked kinase, or mitogen activated protein kinase activated kinase-2). Phospholipids are very important to cell signaling and are typically clustered in highly organized cholesterol-rich lipid rafts which are linked to the cell via the F-actin cytoskeleton. Reduction in F-actin levels have been demonstrated to disrupt lipid rafts and associated signaling (Head *et al.*, 2006), therefore it seems possible that reduced F-actin levels in SMA could lead to a situation where Akt cannot be easily de-activated by the phosphatase, PTEN, which associates with lipid rafts and appropriate signaling molecules (such as Akt) after an atrophy-inducing stimulus. These ideas should be tested in future experiments and could easily be assessed by first determining that the F-to-G-actin ratio is low in skeletal muscle from SMA animals as it is in nerve (Oprea *et al.*, 2008), and then assess levels of the various phoshpolipid signaling molecules to determine whether or not they deviate from levels observed in wild type animals. Additionally, Akt activation levels can be easily assessed.

The present findings are in the process of further evaluation with qRT-PCR to quantify mRNA levels of atrogenes (i.e. *atrogin-1*), and confirm findings with western blotting. If atrogene mRNA levels are decreased in tissues from smn-/-A2G-FVB animals, exon-specific mRNA quantitation will be carried out to determine whether decreased mRNA levels are caused by splicing defects, which would provide the first evidence for physiological defects caused directly by splicing impairments in SMA. If this is not the case, then further experiments will be done to assess proteins within the signaling pathway outlined in Figure 2.23 (i.e. Akt).

2.4.6. No evidence of developmental delays in nerve or skeletal muscle from SMAIII mice, but discovered delays in denervation-induced atrophy of skeletal muscle, and potential disorganization of the cytoskeletal protein dystrophin

Present experimental findings have determined that a developmental phenotype does not persist in tissues from two murine models of SMAIII, and that effective expression of GAP-43, ChAT, and adult MyHC proteins occurs in these tissues. These findings indicate that snRNP biogenesis and subsequent splicing activity do not affect production of these important proteins and suggest that impairments in this function do not contribute to neuromuscular disease pathology in these models. Gabanella *et al.* (2007) recently employed a zebrafish model of SMA to demonstrate that provision of externally produced snRNPs corrected splicing deficits and improved disease phenotype by correcting axonal pathfinding defects (Gabanella *et al.*, 2007). However, pathology observed in zebrafish models of SMA is distinct from that seen in humans, as even in severe SMAI patients, axons manage to find and innervate target muscles. Since a morpholino approach is used to knock down *Smn* expression in zebrafish, varying levels of Smn can be present throughout the animal's life. If levels are reduced too drastically, aspects of Smn function that are normally unimpaired in SMA patients (where low levels of FL-SMN are always present) might be affected. Studies in mouse models directing exon 7 deletion to *Smn* in tissues other than nerve and muscle have proven that complete loss of Smn causes defects in tissues typically unaffected in SMA, such as liver (Vitte *et al.*, 2004). It is possible that snRNP biogenesis is an essential function that is normally unimpaired in the disease due to sufficient production of FL-SMN. So far, no evidence has been published to support existence of splicing impairment in SMA patient pathology. A recent publication by Zhang *et al.* (2008) documented widespread splicing defects in spinal cord, brain, kidney and liver from SMAII animals. However, this study did not provide evidence that these problems were directly responsible for disease pathology. Our findings of delayed denervation-induced atrophy may provide a causal relationship between a splicing defect (in atrogenes) and pathological features of the disease, specifically presence of hypertrophic fibers in muscle biopsies from SMA patients (Bobele *et al.*, 1996a) and delayed reductions in CSA during denervation-induced atrophy (Figure 2.23). This idea will be further evaluated in ongoing experiments described above.

2.4.7. Implication of present findings for delayed development hypothesis

Present results do not support the presence of developmental delays in SMAIII animals. However, these findings do not necessarily invalidate this idea. Support for incomplete maturation of motoneurons in SMA is strong in patient samples (for review see (Hausmanowa-Petrusewicz & Vrbova, 2005), and multiple publications detail molecular evidence for developmental delays. Grondard *et al.* (2007), Biondi *et al.* (2008), Kariya *et al.* (2008) and Murray *et al.* (2008) describe a similar neuromuscular junction immaturity in SMAII mice, although AChR clustering rather than expression was determined to be impaired (Grondard *et al.*, 2005;Biondi *et al.*, 2008b;Kariya *et al.*, 2008b;Murray *et al.*, 2008b). These studies also implicate reduced and delayed expression of the N-methyl-D-aspartic acid (NMDA) receptor subunit NR2A in motoneurons of SMAII mice (Biondi *et al.*, 2008a), a deficiency which can be repaired through exercise and leads to a temporary improvement in motor capabilities of these animals along with a moderate lifespan increase. Such developmental delays have been noted only in

SMAI-II patients and models, and similar observations in SMAIII tissues have not been published. It is possible that minor developmental delays, specifically receptor expression and organization as described, are hallmarks of disease pathology in severe SMA, leading to an inability of the neuromuscular system to cope with adult functional demands. However, there is also a possibility that although initial developmental delays are noted, such impairments are not permanent. Although SMA tissues may not develop at the same rate, it is possible that at later stages they are able to catch up and complete normal development. Biondi *et al.* (2008) assessed neuromuscular junction maturation at 9 and 12 days. It would be interesting to repeat these experiments at a later time point to determine whether major developmental differences persist. It is also feasible that, while developmental attributes may remain in mature SMAI and II patients and animals, they may not be solely responsible for specific neuromuscular degeneration observed in SMA. Although Biondi *et al.* (2008) report significant improvement in maturation of both neuromuscular junctions and motoneurons in exercise-trained SMAII mice, these animals still die at a very early age, indicating that near-rescue of developmental delays is insufficient to save the neuromuscular system in SMA.

The evidence of widespread splicing defects in SMA (Zhang *et al.*, 2008) does not provide a connection between these impairments and neuromuscular pathology in SMA. Results presented in the current study show that there is no abnormal persistent expression of developmental proteins (GAP-43, vimentin, N-CAM, embryonic MyHC) in mature nerve and skeletal muscle from two models of SMAIII, and that these animals are capable of timely and effective protein upregulation after axotomy (GAP-43) and denervation (N-CAM), although we find a striking delay in the rate of denervation-induced atrophy, an impairment which may be the result of splicing inefficiencies. It is possible that although widespread splicing impairments exist, these do not have a severe impact on SMA disease pathology when reductions in SMN levels are relatively modest, as in SMAIII. An appealing explanation is that of a dosage response: different aspects of SMN function are affected with decreasing levels of the protein (from SMAIII to I), and so deficiencies in a greater number of SMN functions contribute to disease pathology with increasing severities of SMN. This idea helps to account for the highly variable disease pathology between SMAI, II and III. At modest reductions of SMN (i.e. in SMAIII), splicing deficits may have only minor, if any, effects on pathology, and neuromuscular degeneration might be the result of another aspect of SMN function, such as mRNA trafficking for localized translation, or altered F-to-G-actin ratios leading to cytoskeletal and/or signaling problems. When SMN levels are more severely reduced (SMAII and I), it is possible that splicing defects account for more of the disease pathology observed. Studies where a complete loss of SMN is directed to individual tissues (Cifuentes-Diaz *et al.*, 2001), prove that all tissues require at least small amounts of SMN for viability, and the necessary function likely affected in these cases is splicing.

2.5. Reference List

Arnardottir, S., Borg, K., & Ansved, T. (2004). Sporadic inclusion body myositis: morphology, regeneration, and cytoskeletal structure of muscle fibres. *J Neurol Neurosurg.Psychiatry* **75**, 917-920.

Arnold, A. S., Gueye, M., Guettier-Sigrist, S., Courdier-Fruh, I., Coupin, G., Poindron, P., & Gies, J. P. (2004a). Reduced expression of nicotinic AChRs in myotubes from spinal muscular atrophy I patients. *Lab Invest* **84**, 1271-1278.

Arnold, A. S., Gueye, M., Guettier-Sigrist, S., Courdier-Fruh, I., Coupin, G., Poindron, P., & Gies, J. P. (2004b). Reduced expression of nicotinic AChRs in myotubes from spinal muscular atrophy I patients. *Lab Invest* **84**, 1271-1278.

Bezakova, G., Helm, J. P., Francolini, M., & Lomo, T. (2001). Effects of purified recombinant neural and muscle agrin on skeletal muscle fibers in vivo. *J Cell Biol.* **153**, 1441-1452.

Bezakova, G. & Lomo, T. (2001). Muscle activity and muscle agrin regulate the organization of cytoskeletal proteins and attached acetylcholine receptor (AchR) aggregates in skeletal muscle fibers. *J Cell Biol.* **153**, 1453-1463.

Biondi, O., Grondard, C., Lecolle, S., Deforges, S., Pariset, C., Lopes, P., Cifuentes-Diaz, C., Li, H., della, G. B., Chanoine, C., & Charbonnier, F. (2008a). Exercise-induced activation of NMDA receptor promotes motor unit development and survival in a type 2 spinal muscular atrophy model mouse. *J Neurosci* **28**, 953-962.

Biondi, O., Grondard, C., Lecolle, S., Deforges, S., Pariset, C., Lopes, P., Cifuentes-Diaz, C., Li, H., della, G. B., Chanoine, C., & Charbonnier, F. (2008c). Exercise-induced activation of NMDA receptor promotes motor unit development and survival in a type 2 spinal muscular atrophy model mouse. *J Neurosci* **28**, 953-962.

Biondi, O., Grondard, C., Lecolle, S., Deforges, S., Pariset, C., Lopes, P., Cifuentes-Diaz, C., Li, H., della, G. B., Chanoine, C., & Charbonnier, F. (2008b). Exercise-induced activation of NMDA receptor promotes motor unit development and survival in a type 2 spinal muscular atrophy model mouse. *J Neurosci* **28**, 953-962.

Bobele, G. B., Feeback, D. L., Leech, R. W., & Brumback, R. A. (1996a). Hypertrophic intrafusal muscle fibers in infantile spinal muscular atrophy. *J Child Neurol* **11**, 246-248.

Bobele, G. B., Feeback, D. L., Leech, R. W., & Brumback, R. A. (1996b). Hypertrophic intrafusal muscle fibers in infantile spinal muscular atrophy. *J Child Neurol* **11**, 246-248.

Bodine, S. C., Stitt, T. N., Gonzalez, M., Kline, W. O., Stover, G. L., Bauerlein, R., Zlotchenko, E., Scrimgeour, A., Lawrence, J. C., Glass, D. J., & Yancopoulos, G. D. (2001). Akt/mTOR pathway is a crucial regulator of skeletal muscle hypertrophy and can prevent muscle atrophy in vivo. *Nat.Cell Biol.* **3**, 1014-1019.

Bornemann, A. & Schmalbruch, H. (1992). Desmin and vimentin in regenerating muscles. *Muscle Nerve* **15**, 14-20.

Bowerman, M., Shafey, D., & Kothary, R. (2007). Smn depletion alters profilin II expression and leads to upregulation of the RhoA/ROCK pathway and defects in neuronal integrity. *J Mol.Neurosci* **32**, 120-131.

Burlet, P., Huber, C., Bertrandy, S., Ludosky, M. A., Zwaenepoel, I., Clermont, O., Roume, J., Delezoide, A. L., Cartaud, J., Munnich, A., & Lefebvre, S. (1998). The distribution of SMN protein complex in human fetal tissues and its alteration in spinal muscular atrophy. *Hum.Mol.Genet.* **7**, 1927-1933.

Cifuentes-Diaz, C., Frugier, T., Tiziano, F. D., Lacene, E., Roblot, N., Joshi, V., Moreau, M. H., & Melki, J. (2001). Deletion of murine SMN exon 7 directed to skeletal muscle leads to severe muscular dystrophy. *J Cell Biol.* **152**, 1107-1114.

Compton, A. G., Cooper, S. T., Hill, P. M., Yang, N., Froehner, S. C., & North, K. N. (2005a). The syntrophin-dystrobrevin subcomplex in human neuromuscular disorders. *J Neuropathol.Exp.Neurol* **64**, 350-361.

Compton, A. G., Cooper, S. T., Hill, P. M., Yang, N., Froehner, S. C., & North, K. N. (2005b). The syntrophin-dystrobrevin subcomplex in human neuromuscular disorders. *J Neuropathol.Exp.Neurol* **64**, 350-361.

Ervasti, J. M. (2003). Costameres: the Achilles' heel of Herculean muscle. *J Biol.Chem.* **278**, 13591-13594.

Ervasti, J. M. & Campbell, K. P. (1993). A role for the dystrophin-glycoprotein complex as a transmembrane linker between laminin and actin. *J Cell Biol.* **122**, 809-823.

Fidzianska, A., Goebel, H. H., & Warlo, I. (1990). Acute infantile spinal muscular atrophy. Muscle apoptosis as a proposed pathogenetic mechanism. *Brain* **113 (Pt 2)**, 433-445.

Fidzianska, A., Rafalowska, J., & Glinka, Z. (1984b). Ultrastructural study of motoneurons in Werdnig-Hoffmann disease. *Clin.Neuropathol.* **3**, 260-265.

Fidzianska, A., Rafalowska, J., & Glinka, Z. (1984a). Ultrastructural study of motoneurons in Werdnig-Hoffmann disease. *Clin.Neuropathol.* **3**, 260-265.

Gabanella, F., Butchbach, M. E., Saieva, L., Carissimi, C., Burghes, A. H., & Pellizzoni, L. (2007). Ribonucleoprotein assembly defects correlate with spinal muscular atrophy severity and preferentially affect a subset of spliceosomal snRNPs. *PLoS.ONE.* **2**, e921.

Gaudreault, S. B., Blain, J. F., Gratton, J. P., & Poirier, J. (2005). A role for caveolin-1 in post-injury reactive neuronal plasticity. *J Neurochem.* **92**, 831-839.

Goebel, H. H. (1995). Desmin-related neuromuscular disorders. *Muscle Nerve* **18**, 1306-1320.

Grondard, C., Biondi, O., Armand, A. S., Lecolle, S., della, G. B., Pariset, C., Li, H., Gallien, C. L., Vidal, P. P., Chanoine, C., & Charbonnier, F. (2005). Regular exercise prolongs survival in a type 2 spinal muscular atrophy model mouse. *J Neurosci* **25**, 7615-7622.

Hausmanowa-Petrusewicz, I. & Vrbova, G. (2005). Spinal muscular atrophy: a delayed development hypothesis. *NeuroReport* **16**, 657-661.

Head, B. P., Patel, H. H., Roth, D. M., Murray, F., Swaney, J. S., Niesman, I. R., Farquhar, M. G., & Insel, P. A. (2006). Microtubules and actin microfilaments regulate lipid raft/caveolae localization of adenylyl cyclase signaling components. *J Biol.Chem.* **281**, 26391-26399.

Hsieh-Li, H. M., Chang, J. G., Jong, Y. J., Wu, M. H., Wang, N. M., Tsai, C. H., & Li, H. (2000). A mouse model for spinal muscular atrophy. *Nat.Genet.* **24**, 66-70.

Jablonka, S., Beck, M., Lechner, B. D., Mayer, C., & Sendtner, M. (2007). Defective Ca2+ channel clustering in axon terminals disturbs excitability in motoneurons in spinal muscular atrophy. *J Cell Biol.* **179**, 139-149.

Jagoe, R. T. & Goldberg, A. L. (2001). What do we really know about the ubiquitin-proteasome pathway in muscle atrophy? *Curr.Opin.Clin.Nutr.Metab Care* **4**, 183-190.

Jones, K. W., Gorzynski, K., Hales, C. M., Fischer, U., Badbanchi, F., Terns, R. M., & Terns, M. P. (2001). Direct interaction of the spinal muscular atrophy disease protein SMN with the small nucleolar RNA-associated protein fibrillarin. *J Biol.Chem.* **276**, 38645-38651.

Kariya, S., Park, G. H., Maeno-Hikichi, Y., Leykekhman, O., Lutz, C., Arkovitz, M. S., Landmesser, L. T., & Monani, U. R. (2008b). Reduced SMN protein impairs maturation of the neuromuscular junctions in mouse models of spinal muscular atrophy. *Hum.Mol.Genet.* **17**, 2552-2569.

Kariya, S., Park, G. H., Maeno-Hikichi, Y., Leykekhman, O., Lutz, C., Arkovitz, M. S., Landmesser, L. T., & Monani, U. R. (2008a). Reduced SMN protein impairs maturation of the neuromuscular junctions in mouse models of spinal muscular atrophy. *Hum.Mol.Genet.* **17**, 2552-2569.

Kolb, S. J., Battle, D. J., & Dreyfuss, G. (2007). Molecular functions of the SMN complex. *J Child Neurol* **22**, 990-994.

Krajewska, G. & Hausmanowa-Petrusewicz, I. (2002). Abnormal nerve conduction velocity as a marker of immaturity in childhood muscle spinal atrophy. *Folia Neuropathol.* **40**, 67-74.

La, B., V, Kallenbach, S., & Pettmann, B. (2000). Expression and subcellular localization of two isoforms of the survival motor neuron protein in different cell types. *J Neurosci Res* **62**, 346-356.

La, B., V, Kallenbach, S., & Pettmann, B. (2004). Post-translational modifications in the survival motor neuron protein. *Biochem.Biophys.Res Commun.* **324**, 288-293.

Laemmli, U. K. (1970). Cleavage of structural proteins during the assembly of the head of bacteriophage T4. *Nature* **227**, 680-685.

Le, T. T., Pham, L. T., Butchbach, M. E., Zhang, H. L., Monani, U. R., Coovert, D. D., Gavrilina, T. O., Xing, L., Bassell, G. J., & Burghes, A. H. (2005). SMNDelta7, the major product of the centromeric survival motor neuron (SMN2) gene, extends survival in mice with spinal muscular atrophy and associates with full-length SMN. *Hum.Mol.Genet.* **14**, 845-857.

Liu, Q. & Dreyfuss, G. (1996). A novel nuclear structure containing the survival of motor neurons protein. *EMBO J* **15**, 3555-3565.

Mammucari, C., Milan, G., Romanello, V., Masiero, E., Rudolf, R., Del, P. P., Burden, S. J., Di, L. R., Sandri, C., Zhao, J., Goldberg, A. L., Schiaffino, S., & Sandri, M. (2007). FoxO3 controls autophagy in skeletal muscle in vivo. *Cell Metab* **6**, 458-471.

Manta, P., Mamali, I., Zambelis, T., Aquaviva, T., Kararizou, E., & Kalfakis, N. (2006). Immunocytochemical study of cytoskeletal proteins in centronuclear myopathies. *Acta Histochem.* **108,** 271-276.

Medina, R., Wing, S. S., & Goldberg, A. L. (1995). Increase in levels of polyubiquitin and proteasome mRNA in skeletal muscle during starvation and denervation atrophy. *Biochem.J* **307 (Pt 3),** 631-637.

Mitsui, T., Kawajiri, M., Kunishige, M., Endo, T., Akaike, M., Aki, K., & Matsumoto, T. (2000). Functional association between nicotinic acetylcholine receptor and sarcomeric proteins via actin and desmin filaments. *J Cell Biochem.* **77,** 584-595.

Murray, L. M., Comley, L. H., Thomson, D., Parkinson, N., Talbot, K., & Gillingwater, T. H. (2008a). Selective vulnerability of motor neurons and dissociation of pre- and post-synaptic pathology at the neuromuscular junction in mouse models of spinal muscular atrophy. *Hum.Mol.Genet.* **17,** 949-962.

Murray, L. M., Comley, L. H., Thomson, D., Parkinson, N., Talbot, K., & Gillingwater, T. H. (2008c). Selective vulnerability of motor neurons and dissociation of pre- and post-synaptic pathology at the neuromuscular junction in mouse models of spinal muscular atrophy. *Hum.Mol.Genet.* **17,** 949-962.

Murray, L. M., Comley, L. H., Thomson, D., Parkinson, N., Talbot, K., & Gillingwater, T. H. (2008b). Selective vulnerability of motor neurons and dissociation of pre- and post-synaptic pathology at the neuromuscular junction in mouse models of spinal muscular atrophy. *Hum.Mol.Genet.* **17,** 949-962.

Navarrete, R. & Vrbova, G. (1984). Differential effect of nerve injury at birth on the activity pattern of reinnervated slow and fast muscles of the rat. *J Physiol* **351,** 675-685.

Pardo, J. V., Siliciano, J. D., & Craig, S. W. (1983). A vinculin-containing cortical lattice in skeletal muscle: transverse lattice elements ("costameres") mark sites of attachment between myofibrils and sarcolemma. *Proc.Natl.Acad.Sci.U.S.A* **80,** 1008-1012.

Pellizzoni, L., Baccon, J., Charroux, B., & Dreyfuss, G. (2001a). The survival of motor neurons (SMN) protein interacts with the snoRNP proteins fibrillarin and GAR1. *Curr.Biol.* **11,** 1079-1088.

Pellizzoni, L., Charroux, B., Rappsilber, J., Mann, M., & Dreyfuss, G. (2001b). A functional interaction between the survival motor neuron complex and RNA polymerase II. *J Cell Biol.* **152,** 75-85.

Pellizzoni, L., Kataoka, N., Charroux, B., & Dreyfuss, G. (1998). A novel function for SMN, the spinal muscular atrophy disease gene product, in pre-mRNA splicing. *Cell* **95,** 615-624.

Rajendra, T. K., Gonsalvez, G. B., Walker, M. P., Shpargel, K. B., Salz, H. K., & Matera, A. G. (2007a). A Drosophila melanogaster model of spinal muscular atrophy reveals a function for SMN in striated muscle. *J Cell Biol.* **176,** 831-841.

Rajendra, T. K., Gonsalvez, G. B., Walker, M. P., Shpargel, K. B., Salz, H. K., & Matera, A. G. (2007b). A Drosophila melanogaster model of spinal muscular atrophy reveals a function for SMN in striated muscle. *J Cell Biol.* **176,** 831-841.

Rossoll, W., Jablonka, S., Andreassi, C., Kroning, A. K., Karle, K., Monani, U. R., & Sendtner, M. (2003). Smn, the spinal muscular atrophy-determining gene product, modulates axon growth and localization of beta-actin mRNA in growth cones of motoneurons. *J Cell Biol.* **163**, 801-812.

Sandri, M., Sandri, C., Gilbert, A., Skurk, C., Calabria, E., Picard, A., Walsh, K., Schiaffino, S., Lecker, S. H., & Goldberg, A. L. (2004). Foxo transcription factors induce the atrophy-related ubiquitin ligase atrogin-1 and cause skeletal muscle atrophy. *Cell* **117**, 399-412.

Sarnat, H. B. (1992). Vimentin and desmin in maturing skeletal muscle and developmental myopathies. *Neurol* **42**, 1616-1624.

Sawchak, J. A., Benoff, B., Sher, J. H., & Shafiq, S. A. (1990). Werdnig-Hoffmann disease: myosin isoform expression not arrested at prenatal stage of development. *J Neurol Sci.* **95**, 183-192.

Sejersen, T. & Lendahl, U. (1993). Transient expression of the intermediate filament nestin during skeletal muscle development. *J Cell Sci.* **106 (Pt 4)**, 1291-1300.

Sharp, P. S., Dekkers, J., Dick, J. R., & Greensmith, L. (2003c). Manipulating transmitter release at the neuromuscular junction of neonatal rats alters the expression of ChAT and GAP-43 in motoneurons. *Brain Res.Dev.Brain Res.* **146**, 29-38.

Sharp, P. S., Dekkers, J., Dick, J. R., & Greensmith, L. (2003b). Manipulating transmitter release at the neuromuscular junction of neonatal rats alters the expression of ChAT and GAP-43 in motoneurons. *Brain Res.Dev.Brain Res.* **146**, 29-38.

Sharp, P. S., Dekkers, J., Dick, J. R., & Greensmith, L. (2003a). Manipulating transmitter release at the neuromuscular junction of neonatal rats alters the expression of ChAT and GAP-43 in motoneurons. *Brain Res.Dev.Brain Res.* **146**, 29-38.

Sharp, P. S., Dick, J. R., & Greensmith, L. (2005). The effect of peripheral nerve injury on disease progression in the SOD1((G93A)) mouse model of amyotrophic lateral sclerosis. *Neurosci* **130**, 897-910.

Simic, G., Seso-Simic, D., Lucassen, P. J., Islam, A., Krsnik, Z., Cviko, A., Jelasic, D., Barisic, N., Winblad, B., Kostovic, I., & Kruslin, B. (2000). Ultrastructural analysis and TUNEL demonstrate motor neuron apoptosis in Werdnig-Hoffmann disease. *J Neuropathol.Exp.Neurol* **59**, 398-407.

Soler-Botija, C., Ferrer, I., Gich, I., Baiget, M., & Tizzano, E. F. (2002a). Neuronal death is enhanced and begins during foetal development in type I spinal muscular atrophy spinal cord. *Brain* **125**, 1624-1634.

Soler-Botija, C., Ferrer, I., Gich, I., Baiget, M., & Tizzano, E. F. (2002b). Neuronal death is enhanced and begins during foetal development in type I spinal muscular atrophy spinal cord. *Brain* **125**, 1624-1634.

Soubrouillard, C., Pellissier, J. F., Lepidi, H., Mancini, J., Rougon, G., & Figarella-Branger, D. (1995b). Expression of developmentally regulated cytoskeleton and cell surface proteins in childhood spinal muscular atrophies. *J Neurol Sci.* **133**, 155-163.

Soubrouillard, C., Pellissier, J. F., Lepidi, H., Mancini, J., Rougon, G., & Figarella-Branger, D. (1995a). Expression of developmentally regulated cytoskeleton and cell surface proteins in childhood spinal muscular atrophies. *J Neurol Sci.* **133**, 155-163.

Soussi-Yanicostas, N., Ben, H. C., Bejaoui, K., Hentati, F., Ben, H. M., & Butler-Browne, G. S. (1992). Evolution of muscle specific proteins in Werdnig-Hoffman's disease. *J Neurol Sci.* **109**, 111-120.

Straub, V. & Campbell, K. P. (1997). Muscular dystrophies and the dystrophin-glycoprotein complex. *Curr.Opin.Neurol* **10**, 168-175.

Stupka, N., Schertzer, J. D., Bassel-Duby, R., Olson, E. N., & Lynch, G. S. (2008). Stimulation of calcineurin A{alpha} activity attenuates muscle pathophysiology in mdx dystrophic mice. *Am.J Physiol Regul.Integr.Comp Physiol* **294**, R983-R992.

Tadesse, H., schenes-Furry, J., Boisvenue, S., & Cote, J. (2008). KH-type splicing regulatory protein interacts with survival motor neuron protein and is misregulated in spinal muscular atrophy. *Hum.Mol.Genet.* **17**, 506-524.

Tews, D. S. & Goebel, H. H. (1997). Apoptosis-related proteins in skeletal muscle fibers of spinal muscular atrophy. *J Neuropathol.Exp.Neurol* **56**, 150-156.

Vaittinen, S., Lukka, R., Sahlgren, C., Hurme, T., Rantanen, J., Lendahl, U., Eriksson, J. E., & Kalimo, H. (2001). The expression of intermediate filament protein nestin as related to vimentin and desmin in regenerating skeletal muscle. *J Neuropathol.Exp.Neurol* **60**, 588-597.

Vitte, J. M., Davoult, B., Roblot, N., Mayer, M., Joshi, V., Courageot, S., Tronche, F., Vadrot, J., Moreau, M. H., Kemeny, F., & Melki, J. (2004). Deletion of murine Smn exon 7 directed to liver leads to severe defect of liver development associated with iron overload. *Am.J Pathol.* **165**, 1731-1741.

Yuasa, K., Nakamura, A., Hijikata, T., & Takeda, S. (2008). Dystrophin deficiency in canine X-linked muscular dystrophy in Japan (CXMDJ) alters myosin heavy chain expression profiles in the diaphragm more markedly than in the tibialis cranialis muscle. *BMC.Musculoskelet.Disord.* **9**, 1.

Zhang, H., Xing, L., Rossoll, W., Wichterle, H., Singer, R. H., & Bassell, G. J. (2006). Multiprotein complexes of the survival of motor neuron protein SMN with Gemins traffic to neuronal processes and growth cones of motor neurons. *J Neurosci* **26**, 8622-8632.

Zhang, H. L., Pan, F., Hong, D., Shenoy, S. M., Singer, R. H., & Bassell, G. J. (2003). Active transport of the survival motor neuron protein and the role of exon-7 in cytoplasmic localization. *J Neurosci* **23**, 6627-6637.

Zhang, Z., Lotti, F., Dittmar, K., Younis, I., Wan, L., Kasim, M., & Dreyfuss, G. (2008). SMN deficiency causes tissue-specific perturbations in the repertoire of snRNAs and widespread defects in splicing. *Cell* **133**, 585-600.

CHAPTER 3: GENE EXPRESSION ANALYSIS OF SMAIII MUSCLE AND NERVE

3.1. INTRODUCTION

The broad body of research on SMN functions fails to reach a consensus regarding the cause of selective neuromuscular degeneration in SMA. There are numerous well-published and highly valid hypotheses that require careful consideration in the study of SMA and additionally, a few very important questions that must be answered before significant progress can be made. Specifically, the primary lesion in SMA has yet to be identified. There is significant literature supporting location of causative defects in nerve (subsequently causing muscle atrophy) (Monani *et al.*, 2000)(Roy *et al.*, 1971), and in muscle (Arnold *et al.*, 2004;Braun *et al.*, 1995). Recent works highlight impairments in cell-specific functions of SMN that may cause degeneration independently in nerve and muscle (Bowerman *et al.*, 2007;Rajendra *et al.*, 2007), and some demonstrate functions of SMN that might cause parallel degeneration in both tissues (Dahm *et al.*, 2007;Tadesse *et al.*, 2008a).

Gene expression studies have been carried out previously in SMA research. Anderson *et al.* (2004) used a microarray to study the expression profile of embryonic spinal MN from a spinal cord removed from a murine model of mild SMAIII described previously (Jablonka *et al.*, 2000), and additionally performed MA analysis on primary muscle culture cells derived from a single SMA II patient. In transgenic mice, they describe up-regulation of a group of RNA-binding proteins, a few of which were also determined to be differentially regulated in the muscle cultures. This work focused on Brunol3/ETR-3, an RNA binding protein involved in splicing (Ladd & Cooper, 2004), and did not offer detailed information on additional differentially regulated genes. Although these findings bear further investigation in SMA, this study was limited in terms of biological replicates and tissue types analyzed, as cultured cells are limited in their ability to model a whole system response (Dere *et al.*, 2006).

Olaso *et al.* (2006) used cDNA MAs to evaluate differential expression of genes from animals with loss of *Smn* directed specifically either to neurons or muscle (Cifuentes-Diaz *et al.*, 2001) (Frugier *et al.*, 2000). They found that 5% of differentially regulated genes were involved in pre-mRNA splicing, ribosomal RNA (rRNA) processing, or RNA decay. Subsequent analysis of human SMA patient samples using qRT-PCR and western blotting failed to confirm their results, perhaps because the amount of FL-SMN present in tissues from human patients is sufficient to cover these functions of SMN, preventing these genes from being affected. This is a rational explanation given that severe depletion of SMN in any tissue causes significant defects related to RNA metabolism, specifically snRNA expression, snRNP assembly and subsequent splicing (Gabanella *et al.*, 2007;Zhang *et al.*, 2008). An additional consideration is that the affected infants whose samples were analyzed in their study, were all severe SMAI cases which were either miscarriaged preterm or died soon after birth. The differences in severity of SMA, as well as distinctions in developing versus more mature tissues, might also play a role in this discrepancy.

Balabanian (2007) used a murine model of mild SMAIII, also employed by Anderson (2004), to carry out MA analysis on whole spinal cord samples (Balabanian *et al.*, 2007). Although a number of genes involved in apoptosis were differentially regulated in SMAIII compared to WT mice, these changes were not consistently pro- or anti-apoptotic, and therefore do not provide evidence for apoptotic involvement in motoneuron death in SMAIII. The authors suggested that decreased expression of genes with products involved in calcium dependent signaling in spinal cord from these SMAIII animals might indicate a decrease in overall calcium levels, misregulation of which could impair axon outgrowth and pathfinding (Balabanian *et al.*, 2007). However, assessment of calcium levels in motoneurons from these samples was not performed to substantiate this idea. Finally, this analysis indicated a general misregulation of genes coding actin interacting proteins, which might lead to cytoskeletal impairments, a promising idea given that such deficits have already been demonstrated in SMA and play a role in motor axon pathology (Bowerman *et al.*, 2007).

A recently published paper studied gene expression in a *D. melanogaster* model of SMA (Lee *et al.*, 2008). SMA *D. melanogaster* mutants display highly defective neuromuscular junctions (NMJs) (Chan *et al.*, 2003;Miguel-Aliaga *et al.*, 2000;Rajendra *et al.*, 2007). In accordance with this, MA results found a general downregulation of genes coding for proteins involved in NMJ physiology, while genes coding for rRNA metabolism involved proteins were upregulated. In skeletal muscle, significant findings included downregulation of genes coding for proteins involved in cellular transport and protein degradation, and upregulation of genes encoding proteins involved in RNA metabolism. A general decrease in metabolic activity of affected organisms was indicated by consistent downregulation of genes coding for metabolic enzymes, although this finding was not validated with additional experimentation.

Transcriptional studies carried out in SMA to date have failed to mine important data to specifically evaluate the validity of the broad array of hypotheses which strive to explain the molecular basis of the disease. Microarray analysis performed here will prove beneficial by helping to elucidate the location of the primary lesion in SMA, and through evaluating the most promising hypotheses explaining the molecular bases of selective neuromuscular degeneration in SMA: (i) delayed development (Hausmanowa-Petrusewicz & Vrbova, 2005), (ii) mRNA trafficking deficits leading to impairments in localized translation (Rossoll *et al.*, 2003;Sharma *et al.*, 2005;Tadesse *et al.*, 2008b;Dahm *et al.*, 2007), (iii) defects in snRNP biogenesis (Gabanella *et al.*, 2007), and (iv) impairments in neuronal and muscular cytoskeletal integrity affecting synapses and the NMJ (Anderson *et al.*, 2004;Belanger *et al.*, 2003) (Bowerman *et al.*, 2007;Rajendra *et al.*, 2007), and

Microarray analysis will prove beneficial by helping to determine the location of the primary lesion in SMA. Determination of disease-related transcriptional changes in nerve compared to those observed in muscle will allow us to observe which tissue exhibits changes that are merely responsive to lesions in the other, or will indicate that lesions in nerve and muscle occur (a) in parallel due to a common molecular basis or (b) occur distinctly from one another due to loss/impairment in cell-specific functions of SMN. Additionally, such observations can be compared to recently published gene profiling information from motoneurons and skeletal muscle of a murine model of amyotrophic lateral sclerosis (ALS) (Ferraiuolo *et al.*, 2007;Gonzalez de Aguilar *et al.*, 2008). If, as many researchers believe, the primary SMA lesion is nerve, and muscle atrophy occurs secondary to this, then we would expect similarities in transcriptional profiles between muscle in SMA and ALS.

(i) Delayed Development

In SMAI-III, MN death occurs after the establishment of neuromuscular connections (Frugier, 2000), indicating that SMN deficiency negatively impacts necessary interaction between nerve and target muscle. Immature MNs are more susceptible to cell death than mature MNs (Greensmith and Vrbova, 1996), and so defects in motor axon growth, and incomplete maturation from growth-to-transmitting phenotype of the neuromuscular system, may compromise MN survival, explaining selective vulnerability of MNs and their associated muscle fibers in SMA. As described in Chapter 2, techniques employed to date in this lab (western blotting for GAP-43, radioimmunoassay for Choline acetyltransferase (ChAT) levels) have been unable to determine impairments related to development. However, transcriptional data collected from whole genome mouse MAs can be used to detect signs of incomplete development, and can assess many developmental genes with great efficiency, although less accurately than more involved methods.

(ii) mRNA Trafficking Defects

Many papers have illustrated the role of SMN in axonal and dendritic transport (Rossoll *et al.*, 2003;Zhang *et al.*, 2003), and likely involvement in mRNA localization in neurons. These findings occur in concert with a growing awareness of the importance of localized mRNA translation in highly compartmentalized nerve and muscle cells. For reviews please refer to (Hengst *et al.*, 2006;Hengst & Jaffrey, 2007) (Dahm *et al.*, 2007). Impairment of mRNA localization offers an enticing explanation for specific neuromuscular degeneration involving failings in a single function of SMN which is of extreme importance in both nerve and muscle. Many proteins are involved in these complex processes, making individual evaluation of each highly time consuming and inefficient. However, whole genome transcriptional analysis offers an attractive alternative, and allows assessment of any differential regulation of genes involved in these processes. Interestingly, SMA is not the only disease where impaired mRNA localization is implicated in disease pathology. Fragile X syndrome, the most common inherited form of human mental retardation, is caused by decreased levels of an RNA binding protein (FMRP), and translational dysregulation of mRNAs normally translocated by this protein may be responsible for disease pathology (Brown *et al.*, 2001). Whole genome microarray analysis has recently been published in subjects with Fragile X syndrome (Bittel *et al.*, 2007). If mRNA localization does indeed play a role in SMA disease progression, we would expect to observe some similarities between transcriptional profiles.

(iii) snRNP biogenesis defects

Gabanella *et al.* (2007) demonstrated that snRNP activity is dramatically reduced in spinal cord samples from severe SMAI mice. This strong snRNP biogenesis impairment was more pronounced in neural tissue, and the extent of reduction of snRNP activity correlates with disease severity. However, it is also possible that since SMN levels also correlate with disease severity, snRNP activity will decrease, but other SMN functions might also be affected and lead to neurodegeneration. The authors note that their findings strongly support the hypothesis that SMN loss affects splicing machinery and the splicing pathway of a rare class of introns which lead to selective neuromuscular degeneration, and generalized splicing defects, observed in all tissues, was recently confirmed by Zhang *et al.* (2008). Determination of differential expression of genes involved in coping with elevated numbers of mRNAs containing nonsense stop codons (genes involved in the nonsense mediated decay pathway) might indicate that such generalized splicing defects are causative of disease pathology in SMA.

(iv) Impairments in Neuronal and Muscular Cytoskeletal Integrity

Impairment of cytoskeletal integrity has been suggested as an explanation for the pathology of SMA observed in both muscle and nerve. Rajendra (2007) used a *D. melanogaster* model of SMA (dSMA) which exhibited axon routing and arborization defects. Most surprising, however, were the findings in mutant myofibers: there was no thin filament formation, indicating problems involving actin dynamics. They also found that in WT flies, *Smn* colocalized with sarcomeric actin and formed complexes with α-actinin, the thin-filament cross-linker. In neurons, Sharma (2005) demonstrated a neuron-specific interaction between SMN and profilin II, an actin-binding protein involved in cytoskeletal reorganization (actin sequestering). Bowerman *et al.* (2007) expanded on these findings by performing SMN knock-down (KD) experiments in PC12 cells. They found that SMN KD cells exhibited beading and swelling along neuronal processes, indicative of cytoskeletal perturbation and impaired axonal transport (Nakayama & Aoki, 2000). They demonstrated that increased availability of unbound profillin IIa (a binding partner of SMN) in SMN deficient cells allowed an unnatural increase in the binding of profillin IIa to Rho kinase (ROCK), and subsequent over-activation of RhoA, leading to cytoskeletal instability (due to increases in stress-fiber formation) and defects in neuritogenesis. Interestingly, this pathway is also implicated in NMJ formation through its positive regulator, agrin, which induces activation of Rac and Cdc42 to promote F-actin formation and outgrowth. Rac and Cdc42 are antagonized by the RhoA/ROCK pathway, and if their actions are disrupted, AChR cluster formation is prevented (Bloch *et al.*, 1997;Weston *et al.*, 2003), which might relate to findings that AChR numbers in post-synaptic folds of the NMJ are reduced in cultured myotubes from SMA patients (Arnold *et al.*, 2004). Recent work has provided confirmation that actin organization is critical to disease pathology in SMA, as upregulation of the modifier gene *T-plastin*, encoding a protein that promotes F-actin formation, can completely ameliorate disease phenotype in individuals with moderate to mild decreases in SMN levels (SMAII and III patients) (Oprea *et al.*, 2008).

In the present study, we carry out microarray analysis to compare transcriptional differences in quadriceps and spinal cords of SMAIII animals and WT controls in order to evaluate the validity of the previously described hypothesis, and to allow interpretation of the delay in denervation-induced atrophy observed in TA muscles from SMAIII mice (Chapter 2).

3.2 METHODS

3.2.1. Animals

Breeding pairs of SMAIII *Smn-/-A2G*-FVB animals and WT-FVB controls were obtained from Jackson Labs and housed in HSLAS at the University of Alberta. Animals were genotyped by PCR amplification of DNA extracted from ear biopsies according to protocols specified by Jackson Labs. All animal procedures were performed with approval from the University of Alberta Health Sciences Animal Welfare and Policy Committee (HSAWPC).

3.2.2. Tissue Removal and RNA extraction

Animals were anaesthetized with a ketamine (100mg/ml) and atravet (10mg/ml) cocktail according to weight (17.5ul/g), and T11-L1 spinal cord sections and quadriceps femoris muscles were extracted from 40d old male, litter-matched SMAIII *Smn-/-A2G*-FVB animals (n=3) and WT-FVB controls (n=3) and immediately frozen in liquid nitrogen (-196°C), and stored at -80°C. Quadriceps muscles were pulverized under liquid nitrogen. Total RNA was extracted using Trizol reagent (Invitrogen) according to the manufacturer's instructions, and subsequently purified using RNeasy mini columns (Qiagen). Further removal of phenolic contamination was carried out by ethanol precipitation. Briefly, 1/10 volume of 3M NaOAc pH 5.2 and 2 volumes 95% ethanol were added to the sample and allowed to stand for 30 minutes. Samples were then spun at 13,000 X g for 10 minutes, and washed twice with 500µl 75% ethanol. Samples were air dried for 5 minutes and re-suspended in nuclease-free water for one hour before concentration determination. RNA concentration was determined using a NanoDrop-1000 spectrophotometer, and RNA integrity was assessed using Lab-On-a-Chip technology, on an Agilent 2100 Bioanalyzer, paired with Agilent's RNA Nano chips.

3.2.3. cDNA labeling, array hybridization, and scanning

The low amp linear amplification kit from Agilent was used in the synthesis of cyanine 3 (Cy3) and cyanine 5 (cy5) labeled cDNA. Cy3-labeled SMAIII *Smn-/-A2G*-FVB cDNA was mixed with Cy-5 labeled WT-FVB cDNA and hybridized to Agilent 4X44K whole genome mouse DNA microarrays for 17h at 65°C. Slides were washed and dried, and images were read using a Molecular Devices GenePix 4000B scanner at 5µm resolution using the GenePix Pro 6.0 imaging software. A dye swap experiment, with Cy5-labeled SMAIII *Smn-/-A2G*-FVB cDNA and Cy3-labeled WT-FVB cDNA was performed to control for dye bias.

3.2.4. Data analysis

Agilent Feature Extraction software v10 was used to extract ratio data from microarray images and normalize spot intensities. Control spots present on the slide are used by the software to calculate population statistics for spot intensities and background levels, and employ a 99% confidence level. Data analysis was performed using GeneSifter (VizX Lab) software. Initial analysis of data from spinal cord and quadriceps arrays, to remove genes that were not significantly expressed, was carried out by applying Welch's t-tests with an adjusted p-value of 0.05, applying the Benjamini and Hochberg correction for false discovery rate (Reiner et al 2003), and quality value cutoff of 1. Genes with less than a 1.5 fold change were not analyzed further. Significantly expressed genes were further examined using the Ontology Report and KEGG report in GeneSifter.

3.3 RESULTS

3.3.1. Microarray data quality assessment

Figure 3.1 shows that log transformed array data for both spinal cord (SpC) and skeletal muscle (SkM) arrays appears linear along the 45° identity line and intersects at zero. Pairwise analysis conditions (Welch's t-test, adjusted $p<0.05$, quality=1, Benjamini and Hochberg correction for FDR, at least 1.5 fold regulation difference) were stringent enough to eliminate most genes, as evidenced by the large number of grey (excluded) points.

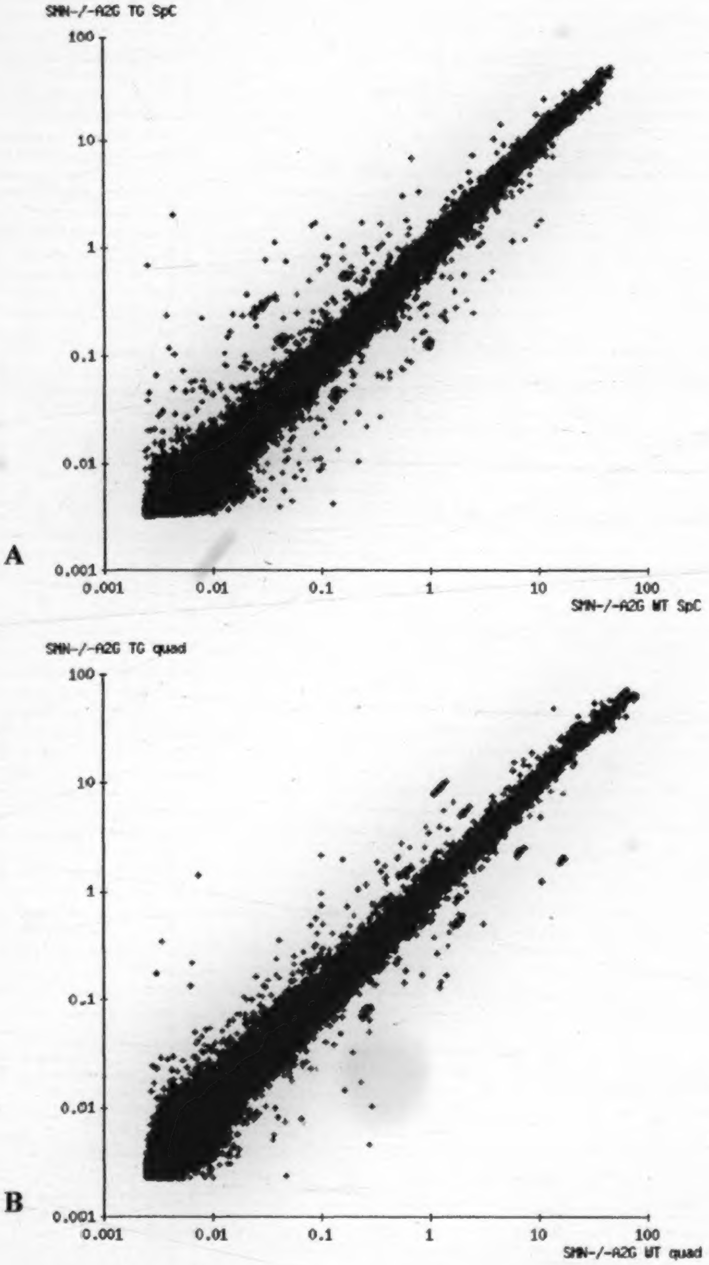

Figure 3. 1. Scatter plot of all data points from SpC (A) and SkM (B) microarray data illustrating genes differentially expressed in SMAIII *Smn-/-A2G*-FVB animals (n=3) compared to WT-FVB controls (n=3). Genes that did not pass the filtering criteria are displayed in gray, upregulated genes are shown in red, while downregulated genes are shown in green.

3.3.2. Gene transcription in SMAIII Smn-/-A2G-FVB SpC and SkM relative to WT-FVB control tissues

Table 3.1 contains the number of genes determined to be differentially regulated in SMAIII *Smn-/-A2G*-FVB Spc and SkM compared to WT-FVB controls based on the following pairwise analysis conditions: Welch's t-test, adjusted $p<0.05$, quality = 1, Benjamini and Hochberg correction for false discovery rate (FDR), and at least 1.5 fold regulation difference. Reduced levels of SMN in SMAIII tissues led to a greater number of transcriptional changes in SpC (421) than in SkM (207) (Table 3.1). For complete listings of these developmentally regulated genes refer to Appendix 1. Genes exhibiting a >4 fold change in expression from SpC and SkM tissues are summarized in tables 3.3 and 3.4 respectively. There were 79 genes differentially regulated in both SpC and SkM from SMAIII mice compared to FVB-WT (Table 3.1 and Figure 3.2). This large degree of overlap in gene regulation between tissues indicates that common changes resulting from SMN deficiency occur in multiple tissues.

A recent publication by Zhang *et al.* (2008) utilizes a murine model of SMAII to assess deficiencies in gene splicing. Impairments in gene splicing are likely to cause changes in mRNA levels of an incorrectly spliced gene, because these should be quickly degraded by nonsense-mediated decay (NMD) within the cell (Wen & Brogna, 2008), therefore lowering overall levels of this type of mRNA. To determine whether observed changes in gene expression could be attributed to incorrect splicing, we compared our list of differentially regulated genes with those determined to be incorrectly spliced in SpC by Zhang *et al.* (2008). This analysis revealed minimal overlap between these two gene sets (Table 3.1 and Figure 3.2), indicating that differential regulation of only a small number of genes, 8 in SpC and 3 in SkM, could potentially be attributed to incorrect splicing. Table 3.2 provides a full list of these genes.

Table 3.1. Summary of genes differentially regulated in SpC and SkM of SMAIII *Smn-/-A2G*-FVB (n=3) compared with WT-FVB (n=3) based on pairwise analysis of microarray data generated by mouse whole genome cDNA microarrays from Agilent (log transformed data, Welch's t-test, adjusted $p < 0.05$, Benjamini and Hochberg correction for FDR, quality=1) using GeneSifter software, and compared against genes incorrectly spliced in SMAII SpC according to Zhang *et al.*, 2008.

Tissue Type	**Genes differentially regulated**	**Up-regulated**	**Down-regulated**	**Genes found to be mis-spliced according to Zhang *et al.*, 2008**
Spinal Cord	421	245	176	8
Quadriceps	207	118	89	3
Spinal Cord and Quadriceps	79	57	22	2

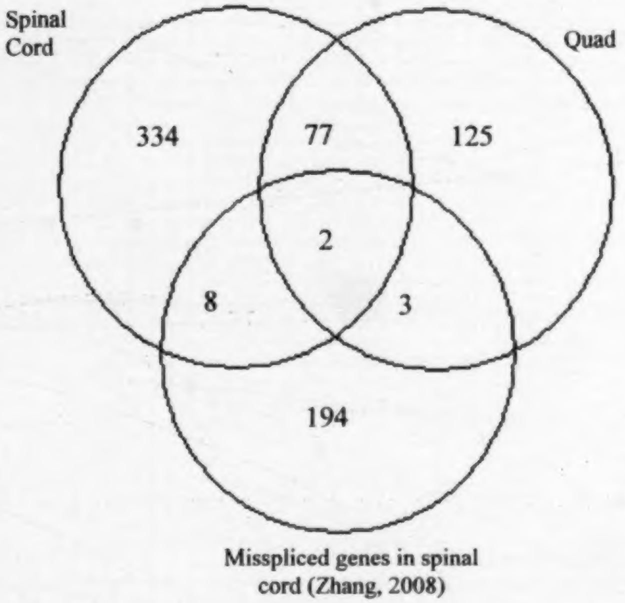

Figure 3. 2. Visual representation of overlap of differential expression in SpC and SkM from SMAIII *Smn-/-A2G*-FVB mice with genes found to be incorrectly spliced in SpC from SMAII mice according to Zhang *et al.*, 2008.

Table 3.2. Genes differentially regulated in SpC from SMAIII mice determined to be incorrectly spliced in SMAII spinal cord by Zhang *et al.*, 2008.

Tissue Type	**Gene ID**	**Gene Name**	**Fold Change in Expression**
Spinal Cord	*Eif3s10*	Eukaryotic translation initiation factor 3, subunit 10 (theta)	-2.49
	Fbn2	Fibrillin 2	-1.54
	Gpr126	G protein-coupled receptor 126	-1.88
	Lbp	Lipopolysaccharide binding protein	-1.75
	Map3k6	Mitogen activated protein kinase kinase kinase 6	1.56
	Mcc1	Methylcrotonoyl-Coenzyme A carboxylase 1 (alpha)	1.6
	Mmp14	Matrix metallopeptidase 14 (membrane-inserted)	-1.69
	Tpm1	Tropomyosin 1, alpha	-1.7
Quadriceps	*Gpr126*	G protein-coupled receptor 126	-2.15
	Mmp14	Matrix metallopeptidase 14 (membrane-inserted)	-2.03
	Pdk4	Pyruvate dehydrogenase kinase, isoenzyme 4	2.09

3.3.3. Incorrect splicing of extracellular matrix and transporter-related genes in SMAII does not lead to overrepresentation of these genes among those affected in SMAIII SpC and SkM

Zhang *et al.* (2008) report that splicing of transporter and extracellular matrix (ECM) genes was significantly altered in SpC, brain, and kidney tissues from SMAII mice. Figure 3.3 confirms that genes with protein products involved in transporter activity are notably represented among transcripts found to be incorrectly spliced (Zhang *et al.*, 2008), and percentage of affected genes from SMAII SpC was greater than that observed in ALS 60d MN and XLMTM SkM. The percentage of affected genes from SMAIII SkM was similar to that observed in ALS and XLMTM tissues. The percentage of differentially regulated genes related to the ECM was quite high among incorrectly spliced genes from SMAII SpC (10.6%), but not from kidney (2.8%). This functional group appears moderately affected in XLMTM SkM, but is not highly represented among differentially regulated genes from ALS 60d MN, or SpC and SkM from SMAIII mice.

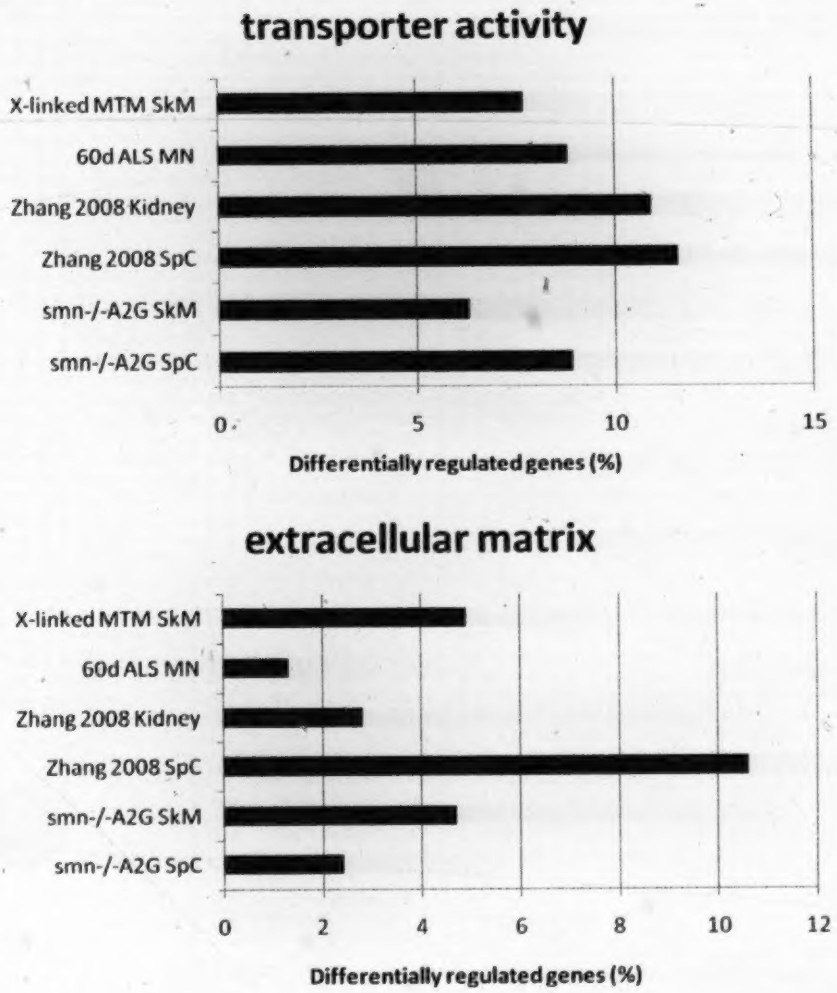

Figure 3.3. Percentage of differentially regulated genes from SMAIII *Smn-/-A2G*-FVB SpC and SkM, ALS 60d MN, and XLMTM SkM with protein product functions involved in transporter activity and the extracellular matrix as determined by GOTM.

3.3.4. Genes showing > 4 fold changes in expression are involved in protein breakdown, energy production, and signaling

Table 3.3 lists genes with a greater than four fold change in expression in SMAIII *Smn-/-A2G-*FVB SpC compared to FVB-WT control SpC. Two genes exhibited fold changes >200. *Echdc1* is UP-regulated 266.98 fold. This gene codes for an enzyme involved in beta-oxidation of fatty acids into acetyl-CoA and energy. The most highly upregulated gene in both SpC and SkM of SMAIII mice is *Dcun1d1* (435.27 fold UP). While there has been little work done on this gene, it belongs to the 'defective in cullin neddylation' family, and likely contributes to neddylation of E3 ubiquitin ligases (Bosu & Kipreos, 2008). Cycles of neddylation and deneddylation positively regulate proteasome activity (Sakata *et al.*, 2007).

Among genes in table 3.3, 18/60 are involved in signaling. Those displaying the greatest fold changes in expression are: *Depdc6, Prdm16, Fut10, Spry2, Rit2, Gnb1, Nbea* and *Igsf11*. *Depdc6* (34.25 fold UP) contains a DEP domain, required for G-protein coupled receptor (GPCR) recognition, and functions in targeting signaling proteins to specific compartments of a cell (Ballon *et al.*, 2006). *Prdm16* (26.5 fold UP) acts downstream of transforming growth factor beta (TGF-β) binding promoters to increase the expression of extracellular matrix (ECM) proteins (Warner *et al.*, 2007). *Fut10* (67.27 fold UP) is a fucosyltransferase enzyme responsible for addition of branched N-glycans to proteins such as cell adhesion molecules (CAMs) like integrins (Zhao *et al.*, 2008). Fucosylation of CAMs is necessary for integrin-mediated cell migration and signal transduction. *Spry2* (20.65 fold UP), a member of the Sprouty family, is expressed predominantly in neurons (Hanafusa *et al.*, 2002) and modulates growth factor signaling through repression of MAP kinase (MAPK) activation (Cabrita & Christofori, 2008). *Spry2* activation is necessary for neural differentiation. *Rit2* (also called *Rin*) is expressed exclusively in neurons, and is involved in integration of MAPK signaling during neuronal development (Hoshino & Nakamura, 2002). It works downstream of nerve growth factor (NGF) and activates the small GTPases Rac1 and Cdc42 to mediate NGF-stimulated neurite outgrowth (Shi *et al.*, 2005). *Nbea* is another neuron-specific protein that modulates signal transduction and vesicular trafficking in neurons; it is essential for synaptic transmission (Su *et al.*, 2004). The protein product of *Nbea*, neurobeachin, contains a regulatory region for protein kinase A (PKA), and mediates its subcellular localization, presumably to synapses to exert its effects (Pawson & Scott, 1997). *Igsf11* (16.61 fold UP) is a member of the immunoglobulin superfamily of CAMs. The protein product of this gene is most likely involved in development and mature functioning of the nervous system (Tzimourakas *et al.*, 2007).

In SkM from SMAIII *Smn-/-A2G*-FVB, 43 differentially regulated genes exhibited a greater than 4 fold change in expression, and 11 of these are involved in signaling (Table 3.4). Five of these genes are also differentially expressed in SpC: *Depdc6* (24.69 fold UP), *Spry2* (10.46 fold UP), *Cdgap* (9.79 fold DOWN), *Gja5* (4.01 fold UP), and *Fut10* (40.45 fold UP). Non-signaling involved genes that are also differentially regulated in SpC include: *Dcun1d1* (201.25 fold UP), *Echdc1* (106.84 fold UP), and *Hal* (63.24 fold DOWN). *Hal* encodes an enzyme that catalyzes the deamination of histidine into urocanic acid (HOLTON *et al.*, 1964;Cornell *et al.*, 1971).

Two genes with a greater than 20 fold difference in regulation are unique to SkM: *Ear1* and *Ntn4*. *Ear1* (56.32 fold UP) is a ribonuclease which degrades single-stranded RNA. *Ntn4* (21.94 fold DOWN) is a neural guidance molecule that additionally forms part of basement membranes through interactions with laminin (Schneiders *et al.*, 2007).

Table 3.3. Genes exhibiting a >4 fold change in expression levels in SpC from SMAIII *Smn-/- A2G*-FVB mice compared to FVB-WT controls determined using GeneSifter (Welch's t-test, adjusted p<0.05, quality = 1, Benjamini and Hochberg correction for FDR, and >4 fold difference)

Ontology	Fold change	Gene Name	Gene ID	Gene Identifier
cell-cell signaling	16.61	Immunoglobulin superfamily, member 11	Igsf11	NM_170599
	4.01	Gap junction membrane channel protein alpha 5	Gja5	AK082993
regulation of cytoskeleton	13.22	Transcribed locus, weakly similar to NP_032661.2 microtubule-associated protein 7 [Mus musculus]	-	AK039098
	-6.83	XM_130232	-	XM_130232
	-5.95	Tropomodulin 4	Tmod4	NM_016712
DNA repair	8.79	DNA segment, Chr 3, ERATO Doi 254, expressed	D3Ertd254e	AK033830
	-4.09	X-ray repair complementing defective repair in Chinese hamster cells 4	Xrcc4	NM_028012
intracellular signaling cascade	34.25	DEP domain containing 6	Depdc6	AK170208
	26.5	PR domain containing 16	Prdm16	NM_027504
	11.15	Diacylglycerol kinase, beta	Dgkb	AK122355
	7.92	Rhotekin 2	Rtkn2	AK045134
	5.16	Serine/threonine kinase 32A	Stk32a	NM_178749
	-4.16	Ankyrin repeat and SOCS box-containing protein 11	Asb11	NM_026853
lipid catabolism	266.98	Enoyl Coenzyme A hydratase domain containing 1	Echdc1	NM_025855
	9.31	DDHD domain containing 1	Ddhd1	AK036369
protein amino acid glycosylation	62.27	Fucosyltransferase 10	Fut10	NM_001012517
	4.09	UDP-GalNAc:betaGlcNAc beta 1,3-galactosaminyltransferase, polypeptide 1	B3galnt1	NM_020026
protein degradation	435.27	DCUN1D1 DCN1, defective in cullin neddylation 1, domain containing 1 (S. cerevisiae)	Dcun1d1	NM_033623
	4.72	Matrix metallopeptidase 8	Mmp8	NM_008611
signal transduction	20.65	Sprouty homolog 2 (Drosophila)	Spry2	BG961926
	19.91	Ras-like without CAAX 2	Rit2	NM_009065
	16.17	Guanine nucleotide binding protein (G protein), beta 1	Gnb1	NM_008142
	12.61	GRAM domain containing 3	Gramd3	NM_026240
	-7.47	Cdc42 GTPase-activating protein	Cdgap	NM_020260
	7.35	Phosphoinositide-3-kinase, class 3	Pik3c3	NM_181414
	6.67	Cnksr family member 3	Cnksr3	NM_172546
	4.17	Paired-Ig-like receptor A3	Pira3	NM_011090
	-4.08	AK078356	Map2k1ip1	AK078356
Transcription	-12.33	Protein arginine N-methyltransferase 6	Prmt6	AK034732
	10.79	Single-stranded DNA binding protein 2	Ssbp2	AK005150
	5.93	AK012660	-	AK012660
Translation	7.28	Ribosomal protein L35a	Rpl35a	NM_021338
	6.32	G elongation factor, mitochondrial 1	Gfm1	AK018125

Transport		6.81	Solute carrier family 7 (cationic amino acid transporter, y+ system), member 8	Slc7a8	NM_016972
		-6.44	Asparagine-linked glycosylation 14 homolog (yeast)	Alg14	NM_024178
vesicle-mediated transport		25.61	Neurobeachin	Nbea	Y18276
		22.65	Mal, T-cell differentiation protein 2	Mal2	NM_178920
miscellaneous	oxidative phosphorylation	-17.72	TC1666890	-	TC1666890
	metal ion binding	15.65	Expressed sequence AI841875	AI841875	NM_001039115
	histidine catabolic process	-7.18	Histidine ammonia lyase	Hal	NM_010401
	myoblast differentiation	-6.4	Triadin	Trdn	AF223417
	nervous system development	6.1	Chordin-like 1	Chrdl1	BC050818
	telomere maintenance	6.06	Werner syndrome homolog (human)	Wrn	NM_011721
	protein transport	5.98	RIKEN cDNA 4930455C21 gene	4930455C21 Rik	NM_024273
	protein folding	4.75	Peptidylprolyl isomerase (cyclophilin)-like 4	Ppil4	NM_026141
Unknown		31.97	RIKEN cDNA 6330407J23 gene	6330407J23 Rik	NM_026138
		-30.67	ENSMUST00000048238	-	
		21.51	Tumor protein D52-like 1	Tpd52l1	NM_009413
		17.59	Transcribed locus	-	AK079569
		14.06	AK042923	-	AK042923
		10.51	Expressed sequence AU021034	AU021034	NM_177629
		-8.69	AK086066	-	AK086066
		7.99	RIKEN cDNA 2610100L16 gene	2610100L16 Rik	AK011787
		7.73	TC1715662	-	TC1715662
		6.95	RIKEN cDNA 5830416P10 gene	5830416P10 Rik	AK158034
		6.9	RIKEN cDNA 2810474C18 gene	2810474C18 Rik	AK013405
		-6.66	CDNA sequence BC030307	BC030307	NM_001003939
		6.6	RIKEN cDNA 1190007I07 gene	1190007I07 Rik	AK045413
		4.96	RIKEN cDNA 1100001G20 gene	1100001G20 Rik	NM_183249
		4.91	Transcribed locus	-	BG969555
		4.03	Resistin like gamma	Retnlg	NM_181596

Table 3.4. Genes exhibiting a >4 fold change in expression levels in SkM from SMAIII *Smn-/- A2G*-FVB mice compared to FVB-WT controls determined using GeneSifter (Welch's t-test, adjusted $p<0.05$, quality = 1, Benjamini and Hochberg correction for FDR, and >4 fold difference)

Ontology		**Ratio**	**Gene Identifier**	**Gene Name**	**Gene ID**
cell-cell signaling		6.33	NM_138673	Stabilin 2	Stab2
		4.17	AK082993	Gap junction membrane channel protein alpha 5	Gja5
intracellular signaling cascade		10.47	NM_027504	PR domain containing 16	Prdm16
		6.13	NM_011932	Dual adaptor for phosphotyrosine and 3-phosphoinositides 1	Dapp1
		5.24	NM_001029841	Src-like adaptor	Sla
nervous system development		-7.74	AY861425	Protocadherin 9	Pcdh9
		4.33	BC050818	Chordin-like 1	Chrdl1
signal transduction		24.69	AK170208	DEP domain containing 6	Depdc6
		10.46	BG961926	Sprouty homolog 2 (Drosophila)	Spry2
		-9.79	NM_020260	Cdc42 GTPase-activating protein	Cdgap
		-4.89	NM_175475	Cytochrome P450, family 26, subfamily b, polypeptide 1	Cyp26b1
		4.13	NM_001002786	RIKEN cDNA 9830134C10 gene	9830134C10Rik
Transcription		7.43	AK005150	Single-stranded DNA binding protein 2	Ssbp2
		4.47	AK171679	Nuclear receptor coactivator 7	Ncoa7
Translation		5.91	NM_021338	Ribosomal protein L35a	Rpl35a
		4.38	AK018125	G elongation factor, mitochondrial 1	Gfm1
		-4.37	NM_172605	Tudor domain containing 3	Tdrd3
Transport		7.17	NM_019818	Translocase of inner mitochondrial membrane 22 homolog (yeast)	Timm22
		4.92	NM_026165	Solute carrier family 25, member 46	Slc25a46
		4.82	NM_024273	RIKEN cDNA 4930455C21 gene	4930455C21Rik
		4.01	NM_016972	Solute carrier family 7 (cationic amino acid transporter, y+ system), member 8	Slc7a8
miscellaneous	protein degradation	201.25	NM_033623	DCUN1D1 DCN1, defective in cullin neddylation 1, domain containing 1 (S. cerevisiae)	Dcun1d1
	lipid catabolism	106.84	NM_025855	Enoyl Coenzyme A hydratase domain containing 1	Echdc1
	histidine catabolic process	-63.24	NM_010401	Histidine ammonia lyase	Hal
	ribonuclease activity	56.32	NM_007894	Eosinophil-associated, ribonuclease A family, member 1	Ear1
	protein amino acid glycosylation	40.45	NM_001012517	Fucosyltransferase 10	Fut10
	axon guidance	-21.94	NM_021320	Netrin 4	Ntn4
	oxidative phosphorylation	-12.59	TC1666890	TC1666890	-
	DNA repair	8.72	NM_133865	DNA cross-link repair 1B,	Dclre1b

				PSO2 homolog (S. cerevisiae)	
	cell cycle	8.06	BC049694	Cyclin-dependent kinase inhibitor 3	Cdkn3
	vesicle-mediated transport	4.75	NM_009498	Vesicle-associated membrane protein 3	Vamp3
	telomerase maintenance	4.74	NM_011721	Werner syndrome homolog (human)	Wrn
	protein folding	4.52	NM_026141	Peptidylprolyl isomerase (cyclophilin)-like 4	Ppil4
	ion transport	-4.15	NM_053198	Sideroflexin 4	Sfxn4
Unknown		-29.88		ENSMUST00000048238	-
		13.41	NM_009413	Tumor protein D52-like 1	Tpd52l1
		7.08	NM_026240	GRAM domain containing 3	Gramd3
		6.87	TC1715662	TC1715662	-
		6.64	AK007195	RIKEN cDNA 1700113H08 gene	1700113H08Rik
		-5.8	NM_011353	Small EDRK-rich factor 1	Serf1
		4.37	NM_025904	RIKEN cDNA 1600012F09 gene	1600012F09Rik
		-4.37	NM_001003939	CDNA sequence BC030307	BC030307
		4.09	NM_175413	Leucine rich repeat containing 39	Lrrc39

3.3.5. Significant overlap exists between differentially regulated genes from SpC and SkM from SMAIII Smn-/-A2G-FVB mice

Table 3.5 lists all 79 genes that are differentially regulated in both SpC and SkM. The large degree of overlap demonstrates that loss of SMN leads to transcriptional changes common to both cell types. It is interesting to note that the direction of transcriptional changes is identical in these two tissue types, and the magnitude is extremely similar, which indicates that loss of SMN leads to exceptionally similar transcriptional responses in SMAIII SpC and SkM

Table 3.5. Genes differentially regulated in both SpC and SkM from SMAIII *Smn-/-A2G*-FVB mice compared to SpC and SkM from FVB-WT controls (log transformed data, Welch's t-test, adjusted p <0.05, Benjamini and Hochberg correction for FDR, quality=1)

Other ID	**Gene Name**	**Gene ID**	**Fold Change SpC**	**Fold Change SkM**
NM_134052	Acireductone dioxygenase 1	Adi1	-2.24	-2.21
NM_172678	Acyl-Coenzyme A dehydrogenase family, member 9	Acad9	3.06	3.33
NM_011994	ATP-binding cassette, sub-family D (ALD), member 2	Abcd2	-1.53	-1.58
NM_025338	Aurora kinase A interacting protein 1	Aurkaip1	2.3	2.2
NM_023465	Catenin beta interacting protein 1	Ctnnbip1	3.01	2
NM_010818	Cd200 antigen	Cd200	1.86	1.9
NM_020260	Cdc42 GTPase-activating protein	Cdgap	-7.47	-9.79
NM_001003939	CDNA sequence BC030307	BC030307	-6.66	-4.37
BC050818	Chordin-like 1	Chrdl1	6.1	4.33
NM_172546	Cnksr family member 3	Cnksr3	6.67	3.9
AK199310	Coiled-coil domain containing 90A	Ccdc90a	2.64	2.18
NM_023243	Cyclin H	Ccnh	2.13	1.75
BC049694	Cyclin-dependent kinase inhibitor 3	Cdkn3	1.63	8.06
NM_033623	DCUN1D1 DCN1, defective in cullin neddylation 1, domain containing 1 (S. cerevisiae)	Dcun1d1	435.27	201.25
AK170208	DEP domain containing 6	Depdc6	34.25	24.69
NM_011932	Dual adaptor for phosphotyrosine and 3-phosphoinositides 1	Dapp1	1.73	6.13
NM_025869	Dual specificity phosphatase 26 (putative)	Dusp26	1.83	1.64
NM_015744	Ectonucleotide pyrophosphatase/phosphodiesterase 2	Enpp2	2.02	2.22
NM_025855	Enoyl Coenzyme A hydratase domain containing 1	Echdc1	266.98	106.84
ENSMUST00000062945	ENSMUST00000062945	-	-3.4	-3.27
NM_181582	Eukaryotic translation initiation factor 5A	Eif5a	2	1.89
NM_145930	Expressed sequence AW549877	AW549877	-1.6	-1.53

NM_010197	Fibroblast growth factor 1	Fgf1	2.39	2.29
NM_001012517	Fucosyltransferase 10	Fut10	62.27	40.45
AK018125	G elongation factor, mitochondrial 1	Gfm1	6.32	4.38
NM_001002268	G protein-coupled receptor 126	Gpr126*	-1.88	-2.15
AK082993	Gap junction membrane channel protein alpha 5	Gja5	4.01	4.17
NM_026240	GRAM domain containing 3	Gramd3	12.61	7.08
NM_008142	Guanine nucleotide binding protein (G protein), beta 1	Gnb1	16.17	24
NM_010401	Histidine ammonia lyase	Hal	-7.18	-63.24
NM_175663	Histone cluster 1, H2ba	Hist1h2ba	2.18	1.92
BF467941	Histone cluster 1, H4i	Hist1h4i	-1.81	-2.11
NM_172380	KTEL (Lys-Tyr-Glu-Leu) containing 1	Ktelc1	-3.15	-1.81
U12147	Laminin, alpha 2	Lama2	-1.55	-1.99
NM_015763	Lipin 1	Lpin1	3.06	3.24
NM_008608	Matrix metallopeptidase 14 (membrane-inserted)	Mmp14*	-1.69	-2.03
BC029173	Mitochondrial ribosomal protein L47	Mrpl47	2.52	2.01
AK171679	Nuclear receptor coactivator 7	Ncoa7	2.67	4.47
NM_027722	Nudix (nucleoside diphosphate linked moiety X)-type motif 4	Nudt4	2.41	2.31
NM_026936	Oxidase assembly 1-like	Oxa1l	2.67	2.3
NM_026141	Peptidylprolyl isomerase (cyclophilin)-like 4	Ppil4	4.75	4.52
NM_011069	Peroxisomal biogenesis factor 11b	Pex11b	1.7	1.57
NM_207229	Placenta specific 9	Plac9	1.58	1.73
NM_027504	PR domain containing 16	Prdm16	26.5	10.47
NM_021880	Protein kinase, cAMP dependent regulatory, type I, alpha	Prkar1a	-2.02	-1.88
AK047681	Protocadherin 9	Pcdh9	-3.19	-7.74
NM_026405	RAB32, member RAS oncogene family	Rab32	2.25	2
NM_023879	Retinitis pigmentosa GTPase regulator interacting protein 1	Rpgrip1	1.92	3.4
NM_007447	Ribonuclease, RNase A family 4	Rnase4	1.68	1.85
NM_021338	Ribosomal protein L35a	Rpl35a	7.28	5.91
AK045413	RIKEN cDNA 1190007I07 gene	1190007I07Rik	6.6	3.11
NM_025904	RIKEN cDNA 1600012F09 gene	1600012F09Rik	2.87	4.37
NM_026136	RIKEN cDNA 4930449I24 gene	4930449I24Rik	-3.13	-2.7
NM_024273	RIKEN cDNA 4930455C21 gene	4930455C21Rik	5.98	4.82
AK084997	RIKEN cDNA B930095G15 gene	B930095G15Rik	3.51	2.55
NM_026518	Ring finger protein 146	Rnf146	2.97	2.65
NM_053198	Sideroflexin 4	Sfxn4	-3.78	-4.15
AK005150	Single-stranded DNA binding protein 2	Ssbp2	10.79	7.43
NM_009196	Solute carrier family 16 (monocarboxylic acid transporters), member 1	Slc16a1	-2.01	-1.95

NM_026165	Solute carrier family 25, member 46	Slc25a46	2.05	4.92
NM_144902	Solute carrier family 35 (UDP-N-acetylglucosamine (UDP-GlcNAc) transporter), member 3	Slc35a3	-1.52	-1.91
NM_016972	Solute carrier family 7 (cationic amino acid transporter, y+ system), member 8	Slc7a8	6.81	4.01
BG961926	Sprouty homolog 2 (Drosophila)	Spry2	20.65	10.46
NM_020618	SWI/SNF related, matrix associated, actin dependent regulator of chromatin, subfamily e, member 1	Smarce1	1.51	2.24
TC1666890	TC1666890	-	-17.72	-12.59
TC1715662	TC1715662	-	7.73	6.87
NM_009351	Telomerase associated protein 1	Tep1	1.97	1.68
NM_001009935	Thioredoxin interacting protein	Txnip	2.1	1.86
BG969555	Transcribed locus	-	4.99	3.78
NM_201373	Tripartite motif-containing 56	Trim56	1.82	2.01
NM_172605	Tudor domain containing 3	Tdrd3	-2.99	-4.37
NM_009413	Tumor protein D52-like 1	Tpd52l1	21.51	13.41
NM_020026	UDP-GalNAc:betaGlcNAc beta 1,3-galactosaminyltransferase, polypeptide 1	B3galnt1	4.09	2.28
BC024687	Vang-like 1 (van gogh, Drosophila)	Vangl1	1.79	1.75
NM_011721	Werner syndrome homolog (human)	Wrn	6.06	4.74
XM_131166	XM_131166 (predicted amylo-1,6-glucosidase, 4-alpha-glucanotransferase, transcript variant 1)	-	1.86	2.79
XM_991662	XM_991662	-	-1.86	-2.14
NM_028012	X-ray repair complementing defective repair in Chinese hamster cells 4	Xrcc4	-4.09	-3.43
NM_013844	Zinc finger protein 68	Zfp68	2.22	1.53

*Determined to be incorrectly spliced in SMAII SpC (Zhang *et al.*, 2008)

3.3.6. Functional grouping of differentially regulated genes in SpC and SkM from SMAIII Smn-/-A2G-FVB mice.

Differentially regulated genes in SpC and SkM from SMAIII *Smn-/-A2G*-FVB mice were grouped according to roles within the cell (gene ontology) to assess areas of cell function most affected among transcriptional changes, and to determine whether overrepresentation of any areas could provide support for existing hypotheses explaining the molecular basis of SMA. An identical analysis was performed on lists of differentially regulated genes from (1) MN of 60d SOD1 G93A ALS mice (Ferraiuolo *et al.*, 2007) and (2) adult SkM samples X-linked MTM (XLMTM) patients (Noguchi *et al.*, 2005) to allow comparison between the representation of a given ontology in SMA and its representation among differentially regulated genes from distinct but related diseases.

ALS is a neuromuscular disease in which loss of spinal MN leads to muscle atrophy. While primary pathology is limited to MN, disease development is dependent upon MN contact with surrounding cell types (Boiller *et al.*, 2006). Ferraiuolo *et al.* (2007) used laser capture microdissection (LCM) to isolate MN from 60d SOD1 G93A ALS mice and subsequently performed MA analysis. XLMTM is a congenital disease of muscle weakness in male infants (Wallgren-Pettersson *et al.*, 1995) caused by mutations in *MTM1*, which codes for myotubularin. Myotubularin is essential for skeletal muscle maintenance (Buj-Bello *et al.*, 2002). Noguchi *et al.*, (2005) performed MA analysis on SkM samples from XLMTM patients. While neither of the above studies utilized the same MA platform employed in the present study, their summary list of differentially regulated genes was submitted to GOTM (Zhang *et al.*, 2004) along with gene lists produced from MA analysis of SMAIII SpC and SkM to allow comparison of overrepresented gene ontologies in these distinct neuromuscular diseases.

3.3.6.1. Representation of genes with protein products involved in development

To assess whether delays in development play a role in SMA at the transcriptional level, we quantified the proportion of differentially regulated genes from SMAIII SpC and SkM, ALS 60d MN, and XLMTM SkM with functions related to cell development. Figure 3.4 shows that a slightly greater percentage of differentially regulated genes in SMAIII tissues are involved in 'cell differentiation', but there is little difference between the proportion of genes involved in 'cell development', 'neuron differentiation' and 'neurite development' in SMAIII tissues compared to those from ALS and XLMTM.

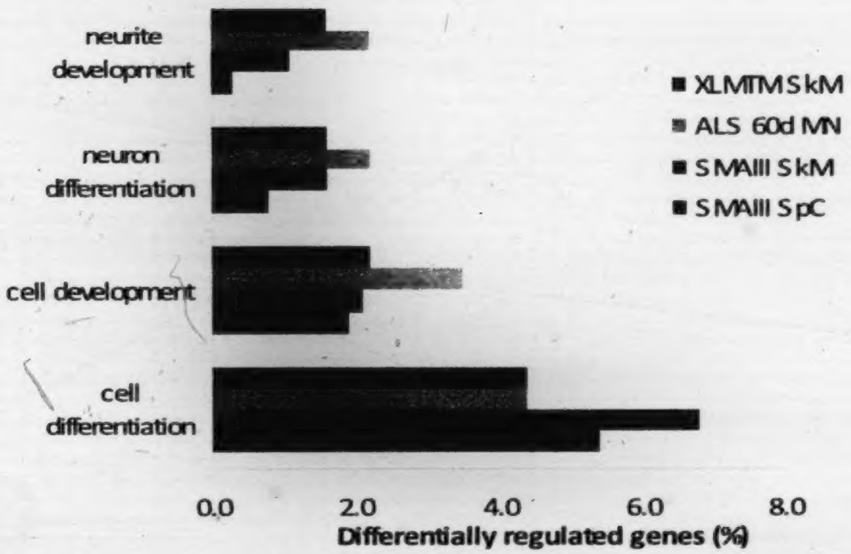

Figure 3.4. Percentage of differentially regulated genes from SMAIII *Smn-/-A2G*-FVB SpC and SkM, ALS 60d MN, and XLMTM SkM determined to have protein product functions related to development determined using GOTM.

3.3.6.2. Representation of genes with protein products involved in RNA transport and localization

SMN has been implicated in β-actin mRNA trafficking and localization (Rossoll *et al.*, 2003), and impairments in mRNA localization lead to neurodegeneration in Fragile X syndrome (Comery *et al.*, 1997). A comparison of differentially regulated genes in SMAIII SpC and SkM with genes differentially regulated in lymphoblasts from Fragile X patients (Bittel *et al.*, 2007) found no commonly affected genes between the two conditions. Figure 3.5 shows representation of genes with RNA transport and localization-related functions in SMAIII SpC and SkM, ALS 60d MN, and XLMTM SkM, and demonstrates that very few genes with protein products involved in RNA transport are affected in SMAIII (n=1, SpC and SkM). Additionally, cell transport in general does not appear to be greatly affected in SMA, as the percentage of differentially regulated genes involved in transport in SMAIII tissues does not differ greatly from percentages observed in ALS 60d MN and XLMTM SkM.

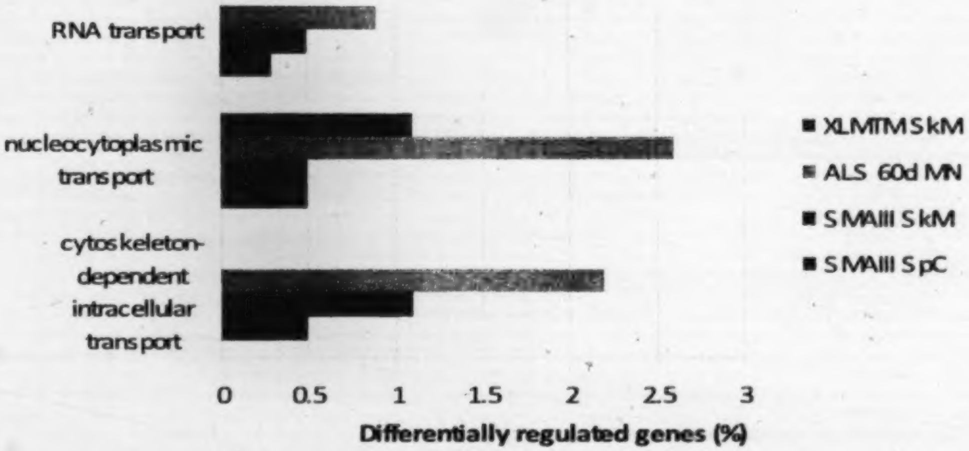

Figure 3.5. Percentage of differentially regulated genes from SMAIII *Smn-/-A2G*-FVB SpC and SkM, ALS 60d MN, and XLMTM SkM determined to have protein product functions related to RNA transport and localization using GOTM.

3.3.6.3. Representation of genes with protein products involved in RNA processing and protein production

SMA can be considered a generalized splicing disorder (Zhang *et al.*, 2008) as the loss of SMN leads to a reduction in formation of snRNPs, essential components of the spliceosome whose effective functioning is required for accurate mRNA intron removal (Li *et al.*, 2007). Although significant splicing defects have been observed in SMA (Zhang *et al.*, 2008), Figure 3.6 shows that there are few genes differentially regulated in SpC and SkM of SMAIII *Smn-/-A2G*-FVB animals involved in mRNA processing and translation. A much larger proportion of genes with these functions are affected in ALS 60d MN and XLMTM SkM, indicating that the modest representation of genes with these protein products is not unique to SMAIII. Similarly, genes with protein products that form ribonucleoprotein complexes are moderately represented in SMAIII, but a much greater percentage of genes is affected in both ALS 60d MN and XLMTM SkM.

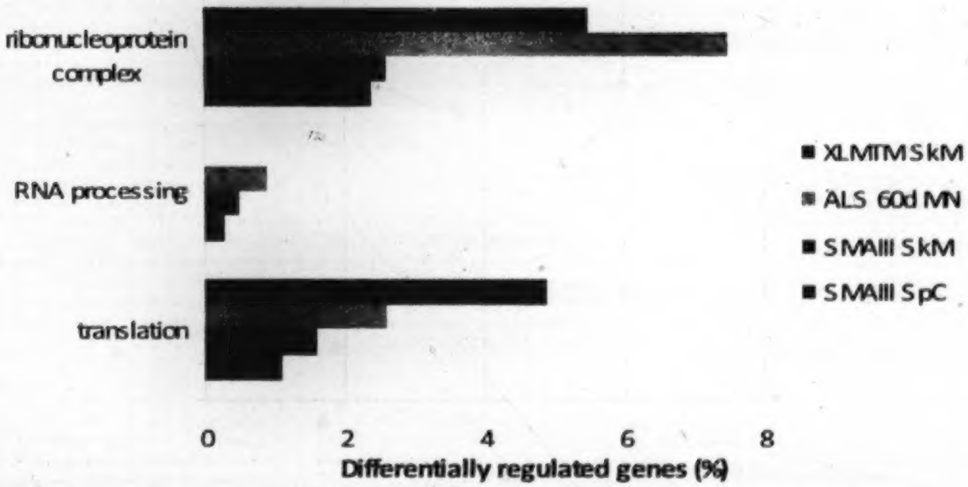

Figure 3.6. Percentage of differentially regulated genes from SMAIII *Smn-/-A2G*-FVB SpC and SkM, ALS 60d MN, and XLMTM SkM with protein product functions related to RNA processing and protein production determined using GOTM.

3.3.6.4. Representation of genes involved in cell cycle and apoptosis

SMA pathology was previously thought to involve over-activation of naturally occurring apoptosis during development (Soler-Botija *et al.*, 2002). Figure 3.7 demonstrates that 3.6% and 2.6% of differentially regulated genes from SMAIII SpC and SkM respectively are related to apoptosis. These numbers are similar to those observed for affected genes in ALS 60d MN (4%) and XLMTM (3.8%), an indication that involvement of apoptotic events is not unique to SMA pathogenesis. Only 3.5 and 3.8% of cell-cycle related genes are differentially regulated in ALS 60d MN and XLMTM SkM respectively compared to 6.8 and 5.3% observed in SMAIII SpC and SkM, indicating an overrepresentation of cell-cycle related genes affected in SMAIII tissues compared to those from ALS and XLMTM.

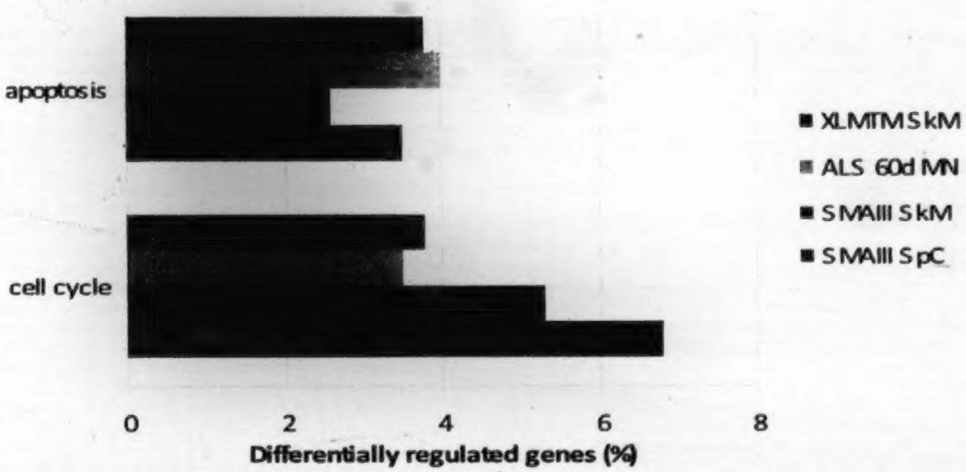

Figure 3.7. Percentage of differentially regulated genes from SMAIII *Smn-/-A2G*-FVB SpC and SkM, ALS 60d MN, and XLMTM SkM with protein product functions related to cell cycle and apoptosis determined using GOTM.

3.3.6.5. Representation of genes with cytoskeleton-related protein products

The recent study by Oprea *et al.* (2008) demonstrated that decreases in SMN levels lead to an increased G:F-actin ratio in SMA MN, and amelioration of this by *T-plastin* overexpression prevents development of disease. Despite this, Figure 3.8 shows that genes with cytoskelton-related functions are not overrepresented in SMA compared to ALS 60d MN and XLMTM SkM. XLMTM is a cytoskeleton-related disorder and so it is not surprising that SkM from XLMTM patients contain the greatest number of differentially regulated actin-binding genes.

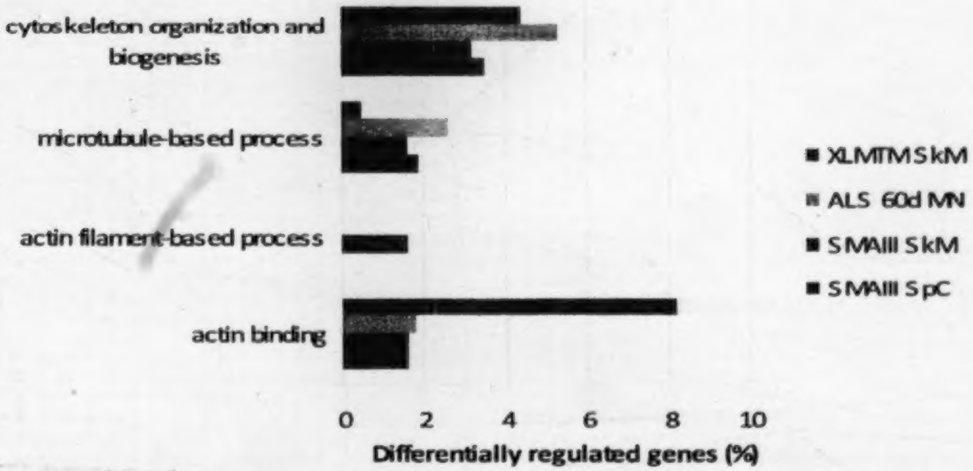

Figure 3.8. Percentage of differentially regulated genes from SMAIII *Smn-/-A2G*-FVB SpC and SkM, ALS 60d MN, and XLMTM SkM with protein product functions related to the cytoskeleton determined using GOTM.

3.3.6.6. Representation of genes with signaling-related protein products

The most overrepresented gene ontologies in SMAIII SpC and SkM are those related to cell communication (Figure 3.9). While cell-cell communication-related genes are not overrepresented among differentially regulated genes in SMAIII SpC and SkM tissues (Figure 3.9), significant proportions of differentially regulated genes in SMAIII SpC (n=51) and SkM (n=34) are involved in signal transduction. This category can be split into 'cell surface receptor-linked signal transduction' and 'intracellular signaling cascade' (Figure 3.9). Overrepresentation of signaling-related gene functions is unique to SpC and SkM from SMAIII tissues (Figure 3.10) when compared with ALS 60d MN and XLMTM SkM.

Of cell surface receptor-linked signaling pathways, genes involved in the 'G-protein coupled receptor protein signaling pathway' and the 'Wnt signaling pathway' are affected to a greater degree in SMAIII SpC and SkM than in ALS 60d MN and XLMTM SkM (Figure 3.11), indicating that deficiencies in SMN cause perturbation of these signaling pathways. Conversely, representation of genes inolved in enzyme-linked receptor protein signaling pathways is similar between SMAIII, ALS and XLMTM tissues (Figure 3.11).

Figure 3.12 shows that representation of genes involved in small GTPase mediated signal transduction is greater in SMAIII SpC and SkM than XLMTM SkM, although the percentage affected in ALS 60d MN is similar. However, in SMAIII SpC, half of the affected genes (n=5) are involved in Ras protein signal transduction (Figure 3.12), a functional classification uniquely overrepresented in SMAIII SpC. There are more differentially regulated genes from SMAIII SpC and SkM involved in second-messenger-mediated signaling (Figure 3.13), and most of these are involved in phophoinositide mediated signaling. Figure 3.13 additionally shows that a small percentage of SMAIII SpC and SkM genes are directly involved in the protein kinase signaling cascade, a function not represented at all among genes affected in ALS 60d MN and XLMTM SkM.

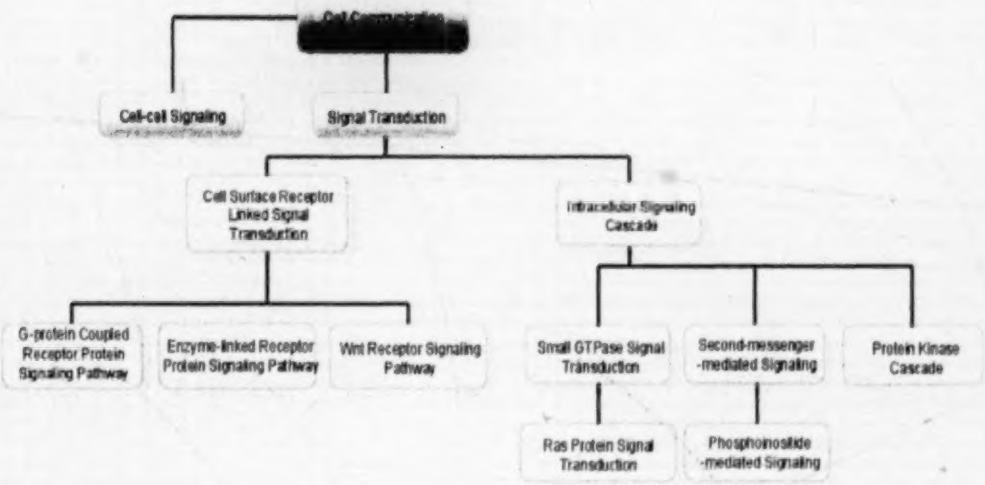
Cell Communication
Cell-cell Signaling
Signal Transduction
Cell Surface Receptor Linked Signal Transduction
Intracellular Signaling Cascade
G-protein Coupled Receptor Protein Signaling Pathway
Enzyme-linked Receptor Protein Signaling Pathway
Wnt Receptor Signaling Pathway
Small GTPase Signal Transduction
Second-messenger -mediated Signaling
Protein Kinase Cascade
Ras Protein Signal Transduction
Phosphoinositide -mediated Signaling

Figure 3.9. Chart describing functional classifications of differentially regulated genes involved in cell communication according to the Gene Ontology Consortium (http://www.geneontology.org/).

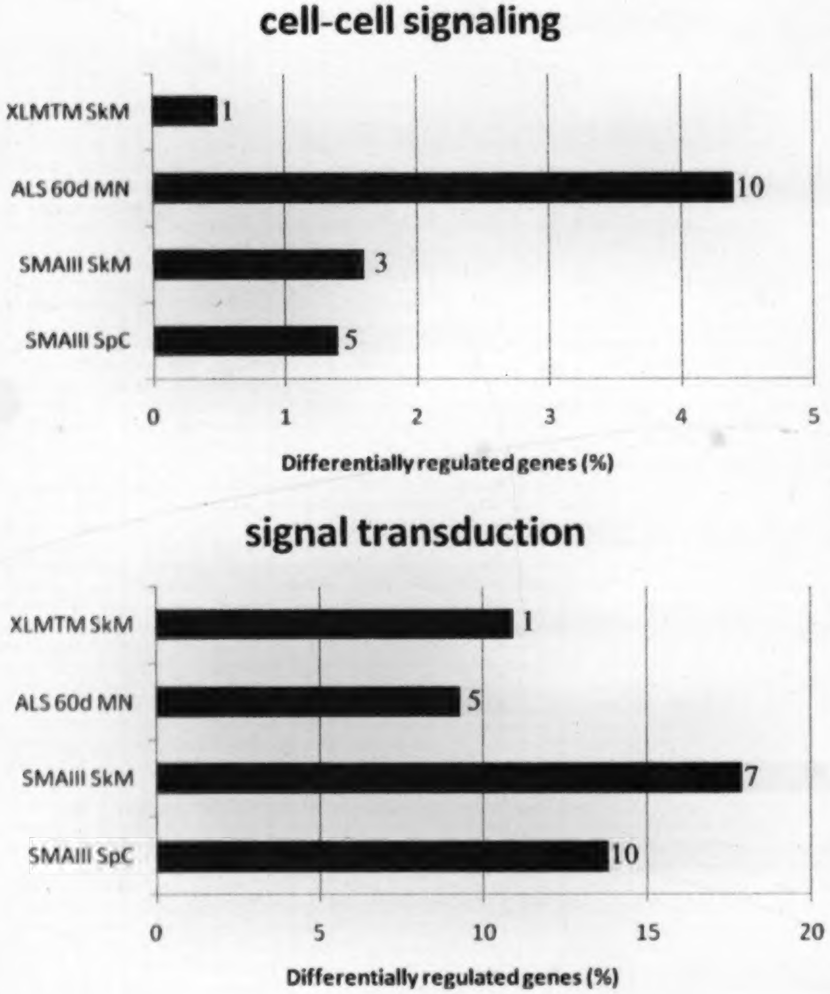

Figure 3.10. Percentage of differentially regulated genes from SMAIII *Smn-/-A2G*-FVB SpC and SkM, ALS 60d MN, and XLMTM SkM with protein product functions involved in cell-cell signaling and signal transduction as determined by GOTM. Numbers shown indicate the actual number of genes involved in a given function.

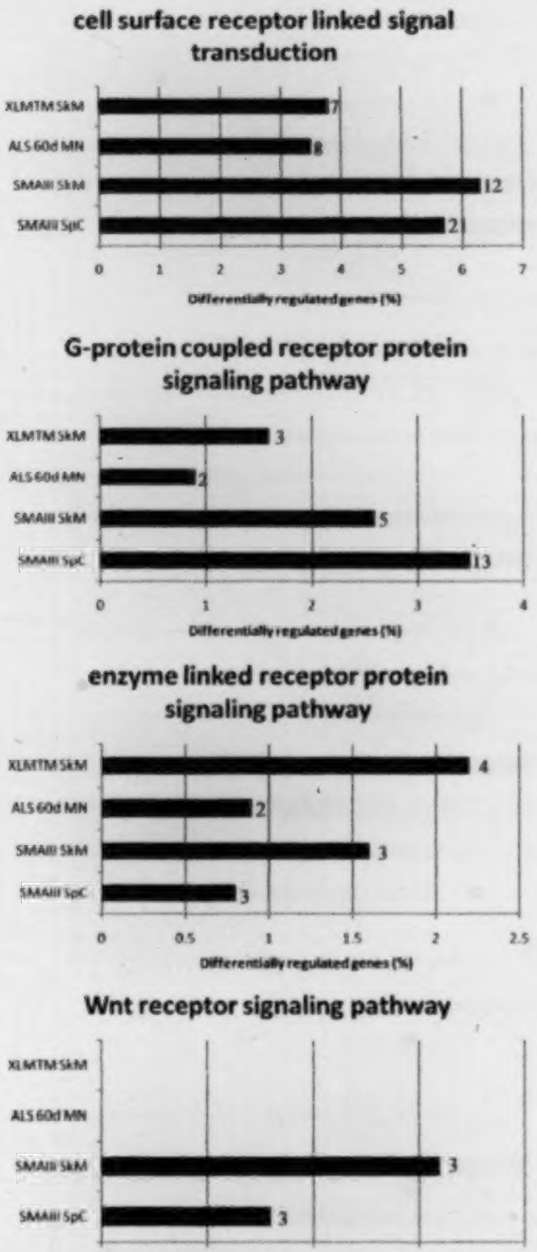

Figure 3.11. Percentage of differentially regulated genes from SMAIII *Smn-/-A2G*-FVB SpC and SkM, ALS 60d MN, and XLMTM SkM with protein product functions involved in cell surface receptor linked signal transduction, the G-protein coupled receptor signaling pathway, enzyme linked receptor protein signaling pathways, and the Wnt receptor signaling pathway as determined by GOTM. Numbers shown indicate the actual number of genes involved in a given function.

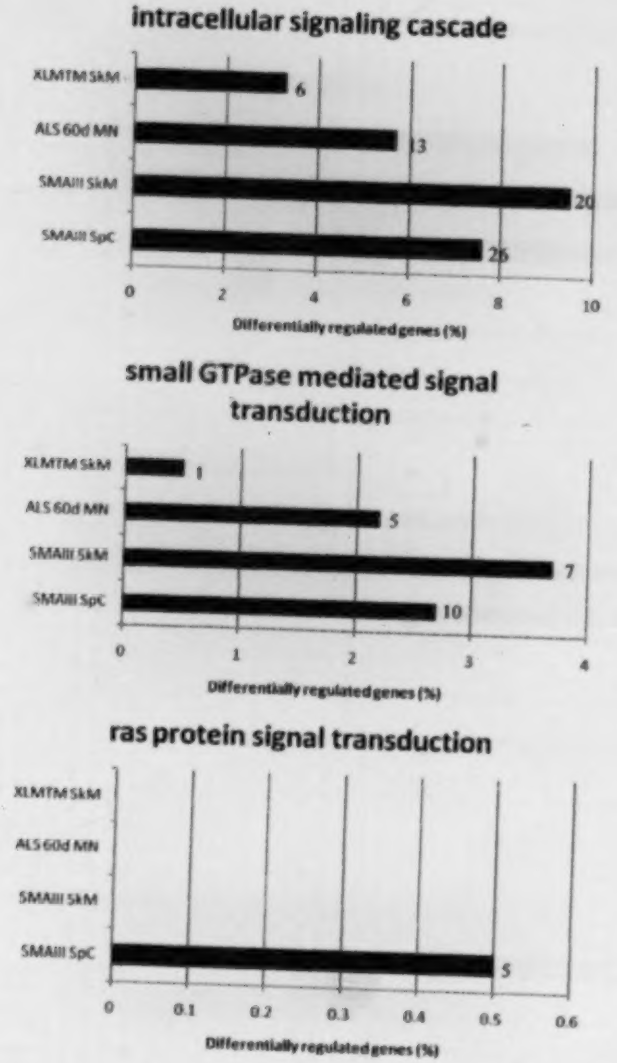

Figure 3.12. Percentage of differentially regulated genes from SMAIII *Smn-/-A2G*-FVB SpC and SkM, ALS 60d MN, and XLMTM SkM with protein product functions involved in intracellular signaling cascades, small GTPase mediated signal transduction, and ras protein signal transduction as determined by GOTM. Numbers shown indicate the actual number of genes involved in a given function.

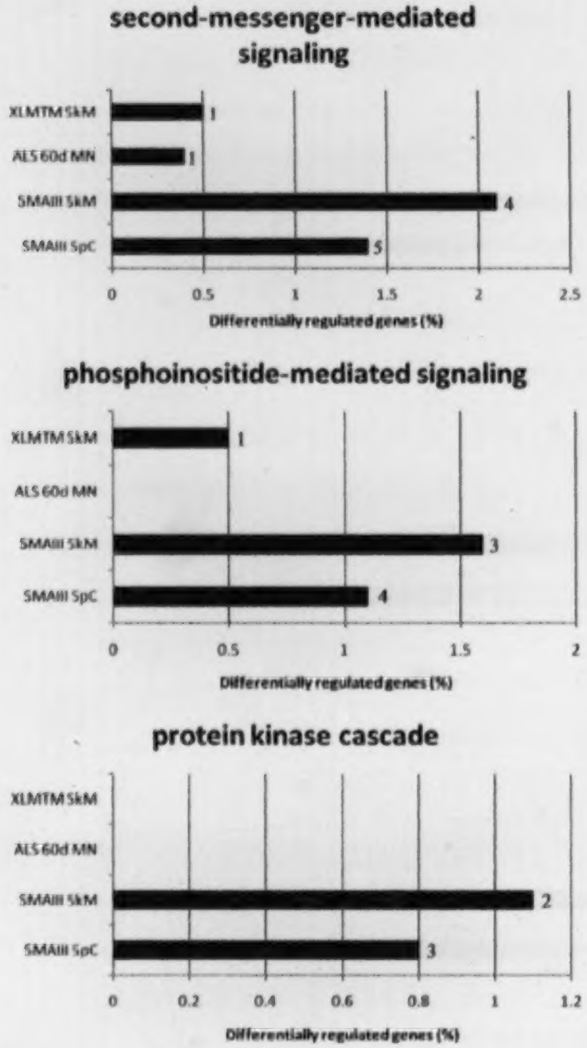

Figure 3.13. Percentage of differentially regulated genes from SMAIII *Smn-/-A2G*-FVB SpC and SkM, ALS 60d MN, and XLMTM SkM with protein product functions involved in second-messenger-mediated signaling, phosphoinositide-mediated signaling, and the protein kinase cascade as determined by GOTM. Numbers shown indicate the actual number of genes involved in a given function.

3.3.7. KEGG pathway analysis of differentially regulated genes in SMAIII Smn-/-A2G-FVB SpC and SkM

The KEGG database connects information regarding molecular interaction networks (Kanehisa *et al.,* 1997) and can be useful for discovery of affected pathways in large amounts of gene or protein expression data. Confirming earlier findings that genes involved in signaling were overrepresented in SMAIII gene expression data, two pathways were determined to be of interest among differentially regulated genes in both SpC and SkM from SMAIII mice: the MAP Kinase (MAPK) signaling cascade and Wnt receptor signaling pathway. Table 3.6 shows that 12 genes involved in MAPK signaling are affected in SMAIII SpC. Two of these, *Rit2* and *Spry2,* were described earlier and are upregulated 19.91 and 20.65 fold respectively. Figure 3.14 shows diagrammatic involvement of some of these genes within the classical MAPK signaling pathway. The significant upregulation of *Spry2* may favor inhibition of ERK and therefore classical MAPK signaling, however there is no consensus regarding a general up or down-regulation of this pathway. We can, however, state with certainty that MAPK signaling is affected in SMAIII. In SMAIII SpC, seven genes associated with the Wnt signaling pathway are affected (Table 3.6). Figure 3.15 provides an illustration of the involvement of some of these in the Wnt pathway. As with the MAPK pathway, it is unclear whether alterations in gene expression would lead to increases or decreases in Wnt signaling, however these results indicate that Wnt signaling is abnormal in SMAIII SpC. The following four repressors of the pathway are up-regulated: *Nlk* (1.7 fold UP), *Sox17* (1.63 fold UP) and *Ctnnbip1* (3.01 fold UP). One pathway promoter, P*rkacb*, is DOWN-regulated (1.69 fold). Two changes in gene expression favor pathway promotion: the repressor *Chd8* is DOWN-regulated (1.57 fold) and *Dvl* (1.53 fold UP). *Dvl* may also lead to promotion of focal adhesions through RhoA and its downstream effector ROCK (discussed in Chapter 2) via the planar cell polarity pathway (Figure 3.15).

The MAPK and Wnt signaling pathways are also affected in SMAIII SkM. There are 14 differentially downregulated genes in SMAIII SkM (Table 3.7). With the exception of *Spry2* UP-regulation (24.69 fold), observed changes appear to promote MAPK signaling, although it is not possible to predict with certainty from this data. Regardless, as in SMAIII SpC, these data indicate that MAPK signaling is affected in SMAIII SkM. Table 3.7 describes nine genes differentially regulated in SMAIII SkM that are involved in Wnt signaling, and figure 3.19 illustrates the involvement of some of these within the pathway. While biological repercussions of these changes cannot be accurately predicted with only the present data, these transcriptional changes appear to favor repression of Wnt signaling with the exception of *Chd8* DOWNregulation (1.57 fold), and the promotion of the planar cell polarity pathway with the exception of *Vangl1* (1.75 fold DOWN).

Table 3.6. Genes involved in MAPK and Wnt signaling pathways differentially regulated in SpC from SMAIII *Smn-/-A2G*-FVB mice compared to FVB-WT controls.

KEGG Pathway	**Gene Name**	**Gene ID**	**Fold Change**
MAPK signaling pathway	Fibroblast growth factor 1	Fgf1	2.39
	Caspase 3	Casp3	-2.06
	Nemo like kinase	Nlk	1.7
	Protein kinase, cAMP dependent, catalytic, beta	Prkacb	-1.69
	Protein tyrosine phosphatase, non-receptor type 7	Ptpn7	1.65
	RAS p21 protein activator 2	Rasa2	-1.6
	TAO kinase 1	Taok1	1.59
	Mitogen-activated protein kinase kinase kinase kinase 1	Map4k1	1.58
	Mitogen-activated protein kinase kinase kinase 6	Map3k6	1.56
	Cell division cycle 25 homolog B (S. pombe)	Cdc25b	1.53
	Sprouty homolog 2 (Drosophila)	Spry2	20.65
	Ras-like without CAAX 2	Rit2	19.91
Wnt signaling pathway	Catenin beta interacting protein 1	Ctnnbip1	3.01
	Vang-like 1 (van gogh, Drosophila)	Vangl1	1.79
	Nemo like kinase	Nlk	1.7
	Protein kinase, cAMP dependent, catalytic, beta	Prkacb	-1.69
	SRY-box containing gene 17	Sox17	1.63
	Chromodomain helicase DNA binding protein 8	Chd8	-1.57
	Dishevelled, dsh homolog 1 (Drosophila)	Dvl1	1.53

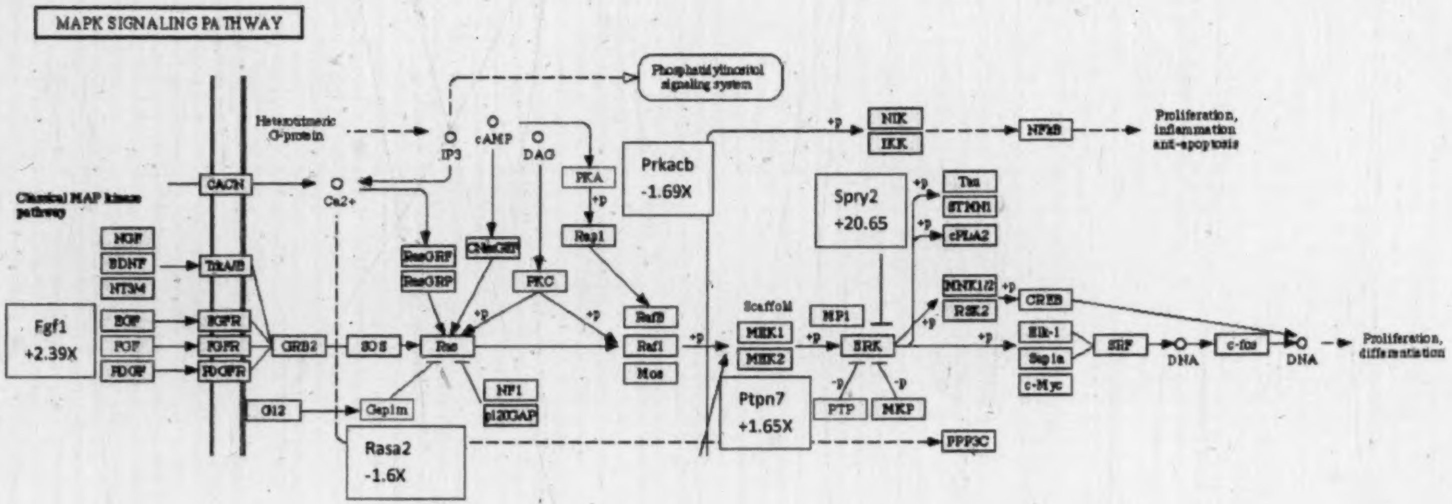
MAPK SIGNALING PATHWAY
Classical MAP kinase pathway
Fgf1
+2.39X
NGF
BDNF
NT3/4
EGF
FGF
PDGF
CACN
TrkA/B
EGFR
FGFR
PDGFR
Heterotrimeric G-protein
Ca2+
IP3
cAMP
DAG
Phosphatidylinositol signaling system
GRB2
SOS
RasGRF
RasGRP
CNrasGEF
PKC
PKA
Rap1
Ras
Gap1m
G12
NF1
p120GAP
Rasa2
-1.6X
Prkacb
-1.69X
RafB
Raf1
Mos
Scaffold
MEK1
MEK2
MP1
ERK
PTP
MKP
Ptpn7
+1.65X
PPP3C
Spry2
+20.65
NIK
IKK
NFκB
Tau
STMN1
cPLA2
MNK1/2
RSK2
CREB
Elk-1
Sap1a
c-Myc
SRF
c-fos
DNA
DNA
+p
-p
Proliferation, inflammation anti-apoptosis
Proliferation, differentiation

Figure 3.14. Involvement of differentially regulated genes from SMAIII *Smn-/-A2G*-FVB SpC in the MAPK signaling pathway. Affected genes are in red, and murine ortholog gene names and fold change in transcription are shown in red-lined boxes.

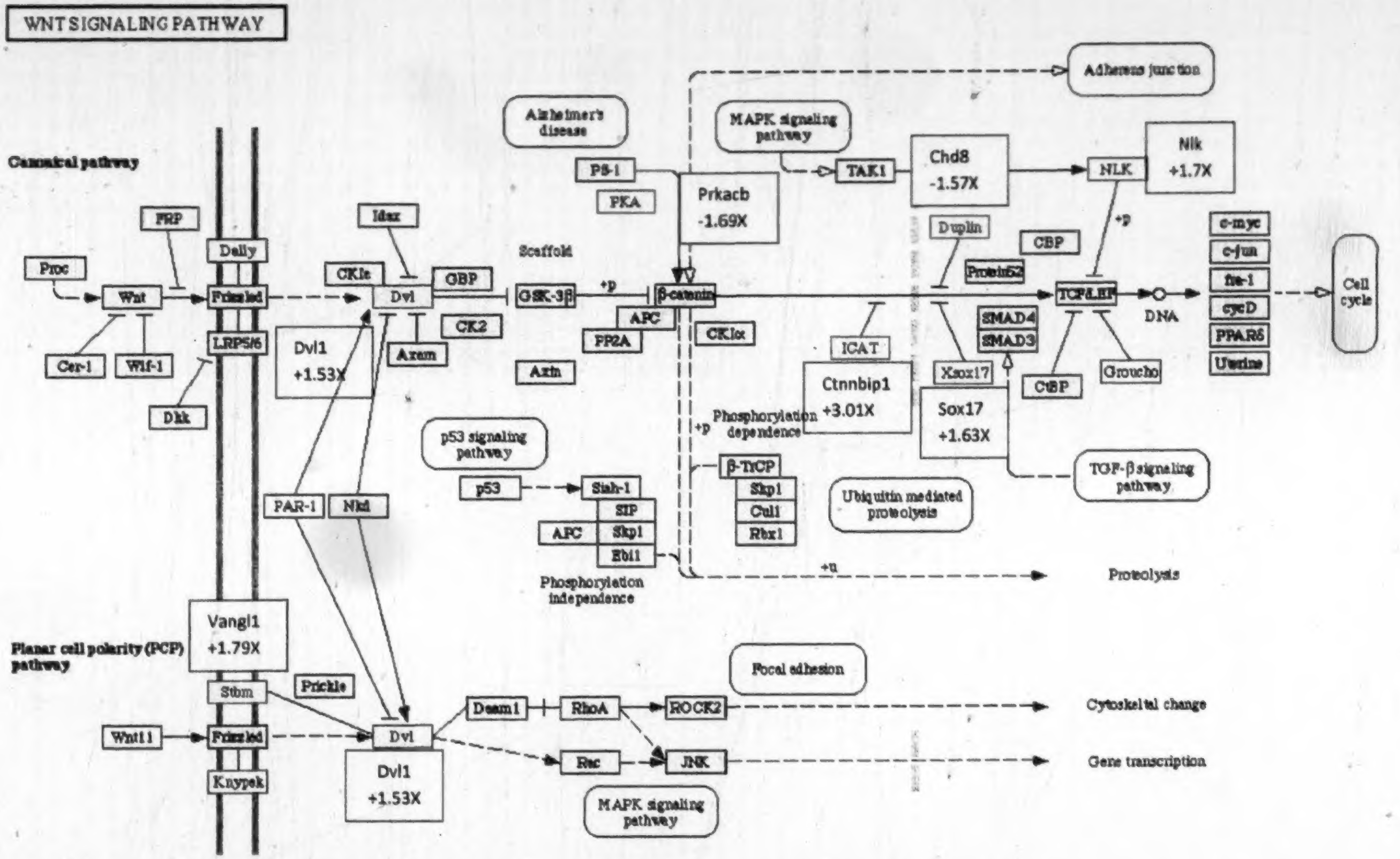
WNT SIGNALING PATHWAY
Canonical pathway
Planar cell polarity (PCP) pathway
Proc
Wnt
FRP
Cer-1
Wif-1
Dkk
Daily
Frizzled
LRP5/6
Vangl1
+1.79X
Stbm
Prickle
Wnt11
Knypek
Idax
CKIε
Dvl
GBP
CK2
Axam
Dvl1
+1.53X
PAR-1
Nkd
Scaffold
GSK-3β
+p
Axin
Alzheimer's disease
PS-1
PKA
Prkacb
-1.69X
APC
PP2A
β-catenin
CKIα
p53 signaling pathway
p53
Siah-1
SIP
Skp1
Ebi1
Phosphorylation independence
β-TrCP
Cul1
Rbx1
Phosphorylation dependence
Ubiquitin mediated proteolysis
+u
Proteolysis
MAPK signaling pathway
TAK1
Chd8
-1.57X
NLK
Nlk
+1.7X
Adherens junction
Duplin
CBP
Protein52
SMAD4
SMAD3
ICAT
Ctnnbip1
+3.01X
Xsox17
Sox17
+1.63X
TCF/LEF
DNA
CtBP
Groucho
TGF-β signaling pathway
c-myc
c-jun
fra-1
cycD
PPARδ
Uterine
Cell cycle
Focal adhesion
Daam1
RhoA
ROCK2
Rac
JNK
Cytoskeletal change
Gene transcription

Figure 3.15. Involvement of differentially regulated genes from SMAIII *Smn-/-A2G*-FVB SpC in the Wnt signaling pathway. Affected genes are in red, and murine ortholog gene names and fold change in transcription are shown in red-lined boxes.

Table 3.7. Genes involved in MAPK and Wnt signaling pathways differentially regulated in SkM from SMAIII *Smn-/-A2G*-FVB mice compared to FVB-WT controls.

KEGG Pathway	**Gene Name**	**Gene ID**	**Fold Change**
MAPK signaling pathway	Fibroblast growth factor 20	Fgf20	-2.78
	Fibroblast growth factor 1	Fgf1	2.29
	RIKEN cDNA 1500003O03 gene	1500003O03Rik	2.17
	Tumor necrosis factor	Tnf	-2.14
	Phospholipase A2, group XIIA	Pla2g12a	2.07
	RAS-related C3 botulinum substrate 2	Rac2	1.95
	Fibroblast growth factor 11	Fgf11	-1.85
	RAS protein-specific guanine nucleotide-releasing factor 2	Rasgrf2	1.57
	Fibroblast growth factor 18	Fgf18	-1.55
	RAS guanyl releasing protein 4	Rasgrp4	1.54
	Protein kinase C, beta 1	Prkcb1	1.53
	Calcium channel, voltage-dependent, T type, alpha 1G subunit	Cacna1g	1.51
	Calcium channel, voltage-dependent, alpha 2/delta subunit 2	Cacna2d2	-1.5
	Sprouty homolog 2 (Drosophila)	Spry2	10.46
Wnt signaling pathway	RIKEN cDNA 1500003O03 gene	1500003O03Rik	2.17
	Catenin beta interacting protein 1	Ctnnbip1	2
	RAS-related C3 botulinum substrate 2	Rac2	1.95
	Secreted frizzled-related protein 2	Sfrp2	1.9
	Vang-like 1 (van gogh, Drosophila)	Vangl1	1.75
	Prickle-like 2 (Drosophila)	Prickle2	-1.7
	Chromodomain helicase DNA binding protein 8	Chd8	-1.63
	Protein kinase C, beta 1	Prkcb1	1.53
	Transcription factor 7-like 2, T-cell specific, HMG-box	Tcf7l2	-1.51

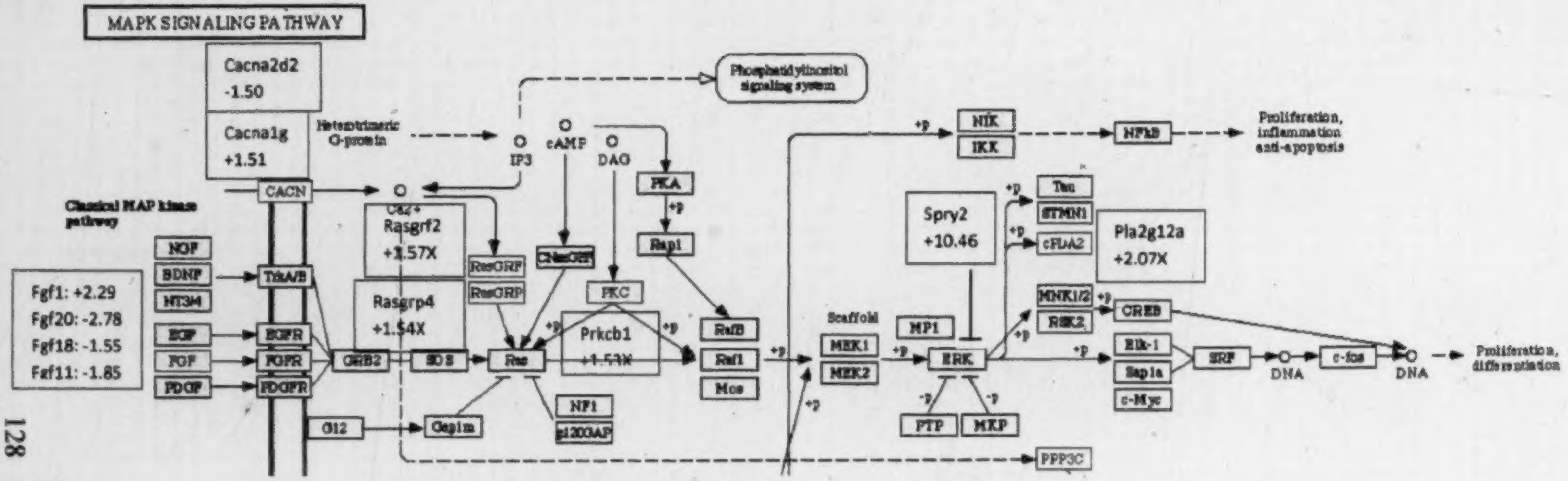
MAPK SIGNALING PATHWAY
Cacna2d2
-1.50
Cacna1g
+1.51
Heterotrimeric G-protein
IP3
cAMP
DAG
Phosphatidylinositol signaling system
CACN
Ca2+
Classical MAP kinase pathway
Fgf1: +2.29
Fgf20: -2.78
Fgf18: -1.55
Fgf11: -1.85
NGF
BDNF
NT3/4
EGF
FGF
PDGF
TrkA/B
EGFR
FGFR
PDGFR
GRB2
SOS
G12
Gap1m
Rasgrf2
+1.57X
Rasgrp4
+1.54X
RasGRF
RasGRP
CNrasGEF
PKA
+p
Rap1
PKC
Prkcb1
+1.53X
Ras
NF1
p120GAP
RafB
Raf1
Mos
Scaffold
MEK1
MEK2
MP1
ERK
-p
PTP
MKP
PPP3C
Spry2
+10.46
NIK
IKK
NFkB
Proliferation, inflammation anti-apoptosis
Tau
STMN1
cPLA2
Pla2g12a
+2.07X
MNK1/2
RSK2
CREB
Elk-1
Sap1a
c-Myc
SRF
DNA
c-fos
DNA
Proliferation, differentiation

Figure 3.16. Involvement of differentially regulated genes from SMAIII *Smn-/-A2G*-FVB SkM in the MAPK signaling pathway. Affected genes are in red, and murine ortholog gene names and fold change in transcription are shown in red-lined boxes.

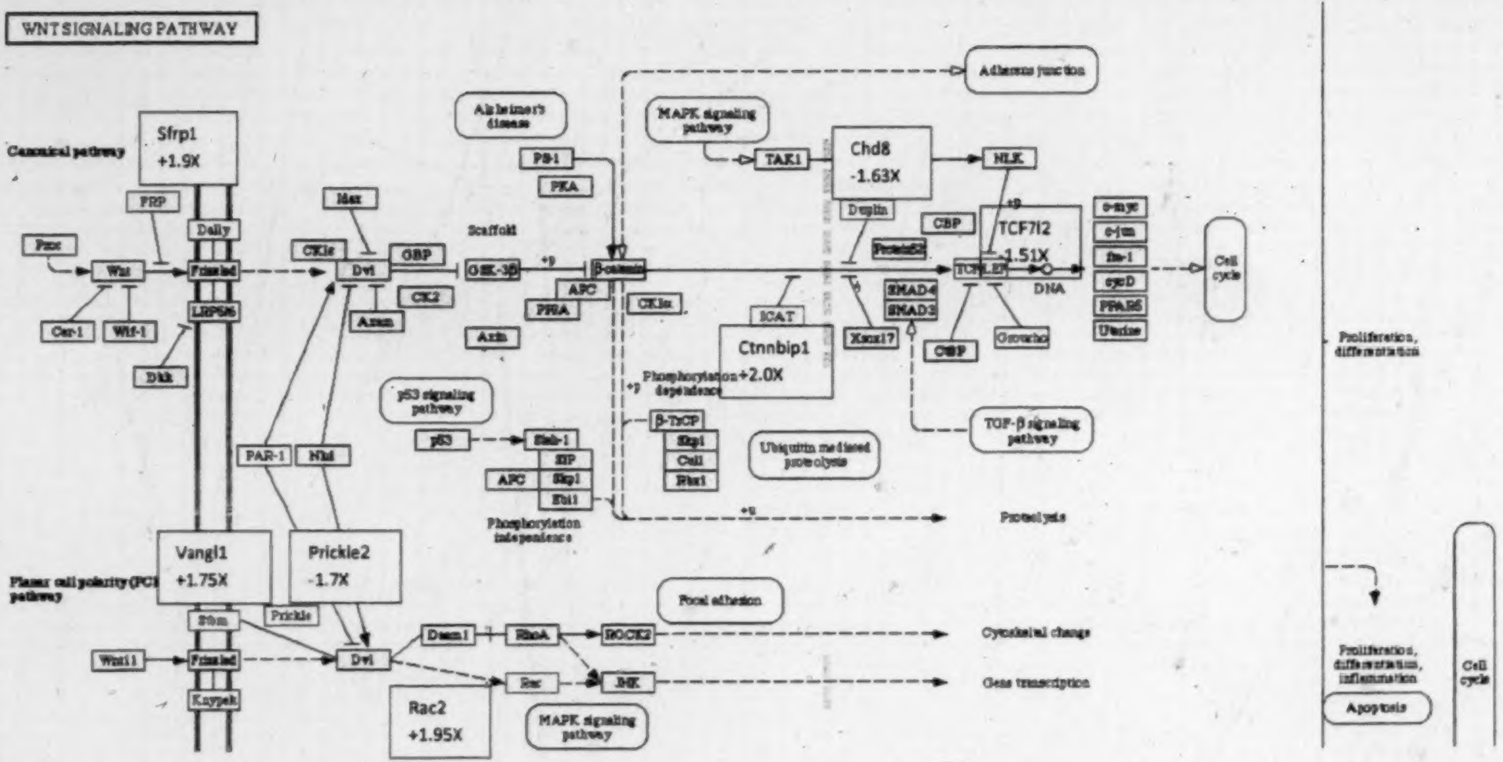
WNT SIGNALING PATHWAY
Canonical pathway
Sfrp1
+1.9X
FRP
Porc
Wnt
Cer-1
Wif-1
Dally
Frizzled
LRP5/6
Dkk
CKIε
Idax
Dvl
GBP
CK2
Axam
Scaffold
GSK-3β
+p
β-catenin
APC
PP2A
Axin
Alzheimer's disease
PS-1
PKA
MAPK signaling pathway
TAK1
Chd8
-1.63X
NLK
Duplin
CBP
Protein82
TCF7l2
-1.51X
TCF/LEF
DNA
SMAD4
SMAD3
Xenx17
CBP
Groucho
ICAT
Ctnnbip1
+2.0X
CKIα
Phosphorylation dependence
+p
β-TrCP
Skp1
Cul1
Rbx1
Ubiquitin mediated proteolysis
TGF-β signaling pathway
p53 signaling pathway
p53
Siah-1
SIP
APC
Skp1
Ebi1
Phosphorylation independence
+u
Proteolysis
c-myc
c-jun
fra-1
cycD
PPARδ
Uterine
Cell cycle
Adherens junction
PAR-1
Nkd
Vangl1
+1.75X
Prickle2
-1.7X
Planar cell polarity (PCP) pathway
Stbm
Prickle
Wnt11
Frizzled
Knypek
Dvl
Daam1
RhoA
ROCK2
Rac
JNK
Rac2
+1.95X
MAPK signaling pathway
Focal adhesion
Cytoskeletal change
Gene transcription
Proliferation, differentiation
Proliferation, differentiation, inflammation
Apoptosis
Cell cycle

Figure 3.17. Involvement of differentially regulated genes from SMAIII *Smn-/-A2G*-FVB SkM in the Wnt signaling pathway. Affected genes are in red, and murine ortholog gene names and fold change in transcription are shown in red-lined boxes.

3.4 DISCUSSION

3.4.1. More genes were differentially regulated in SMAIII SpC than in SkM

All MAs in the present experiment met standard cutoffs (for signal intensity and spot alignment) imposed by Agilent's feature extraction software. Figure 3.1 shows that normalized data falls as it should along a 45 degree line, and indicates that false discovery rate (FDR) cutoffs were stringent enough to exclude most data points (grey). Dye swap experiments for control of dye bias also demonstrated an excellent degree of homology (data not shown). Although fold changes have been noted throughout this report, it is important to recognize that while the direction of a change is typically accurate, the magnitude of transcriptional regulation differences as measured through MA analysis must be confirmed or disproved using more sensitive techniques, such as qRT-PCR, prior to drawing conclusions about the magnitude of change in transcriptional levels. Despite use of stringent p-values, FDR corrections and quality control measures, when working with such large data sets, the number of false-positive hits will understandably be high. Also, stringent cutoffs frequently lead to false-negative errors, excluding relevant and important data. For example, a gene that undergoes highly consistent but small changes in transcriptional levels would have been excluded from the present data sets. There are also significant limitations to MA analysis tools. While gene ontology databases provide an incredible wealth of information that is remarkably up to date, researchers must remain aware of the necessity of double-checking supplied information by cross-referencing literature. During this analysis it became apparent that some listed ontologies are specific to certain cell-types, and the proposed/expected gene function may not apply in all situations. MA technique is not intended to immediately answer experimental questions. Rather, it acts as a guide in the formation of further research ideas, and as such it greatly aids in the resolution of highly complex problems.

According to cutoffs (Welch's t-test, adj. $p < 0.05$, qual=1, Benjamini and Hochberg correction) 421 and 207 genes were differentially regulated in SpC and SkM, respectively (Table 3.1). Of these, 61 and 43 were differentially regulated greater than 4 fold in SpC and SkM respectively (Tables 3.3 and 3.4). Based on these findings, it appears that gene transcription was affected to a greater extent in SpC than in SkM, results in opposition to findings of Lee *et al.* (2008). This discrepancy is likely caused by the dramatic reduction in SMN directed to skeletal muscle in Lee *et al.* (2008), whereas in the model used here, SkM tissue still contains low levels of SMN. The results of the present findings have greater biological relevance because of this, as it has been previously demonstrated that directed loss of SMN to any tissue has significant, negative effects (Vitte *et al.*, 2004).

3.4.1.1. No significant overlap between differentially regulated genes in SMAIII SpC and SkM and genes incorrectly spliced in SMAII SpC

Based on widespread splicing abnormalities identified by Zhang *et al.* (2008) using exon arrays, we expected that these would cause a signifcant number of the transcriptional changes identified here. Yet we found that only a small number of differentially regulated genes identified in the present study were previously determined to be incorrectly spliced. Since incorrectly spliced mRNAs typically undergo rapid nonsense mediated decay (Wen & Brogna, 2008), Zhang *et al.* (2008) believed that their data underestimated the populations of incorrectly spliced transcripts in SMAII tissues. Therefore it is possible that there is more of an overlap between affected genes in the present study and incorrectly spliced genes. Alternatively, there may be fewer splicing problems in the mild SMAIII model examined here (lifespan >300d) compared with the SMAII animals used in Zhang (2008) (lifespan ~15d). Our finding of minimal gene overlap indicates that observed transcriptional changes are *reactive* to (a) existing splicing deficiencies or (b) loss of an additional tissue-specific function of SMN, such as mRNA localization (Rossoll *et al.*, 2003).

A significant proportion of incorrectly spliced genes in SMAII SpC had functions relating to transporter activity or the extracellular matrix (Zhang *et al.*, 2008). However, these functions were **not** overrepresented among differentially regulated genes from SMAIII SpC and SkM when compared to affected genes in 60d ALS MN and XLMTM SkM (Figure 3.3), providing further evidence that the majority of differentially regulated genes identified in the present study are not the result of splicing deficiencies. Exon arrays for detection of splicing impairments should be performed in SMAIII tissues to determine if similar splicing deficiencies exist.

3.4.1.2. Genes differentially regulated >4 fold in SMAIII SpC and SkM have roles in cell signaling, fatty acid oxidation and the proteasome pathway

A significant finding of the present study is that nearly one third of genes differentially regulated greater than four-fold in SpC, and a quarter of those in SkM, are involved in signaling functions, indicating extensive perturbation of cell-cell signaling and signaling pathways in SMAIII tissues (Tables 3.3 and 3.4). This result suggests that loss of or impairments in SMN function somehow interfere with signaling pathways in both SpC and SkM from SMAIII mice. A possible explanation worthy of further investigation is reduced or altered ECM protein composition affecting cell-cell signaling and processing and transduction of extracellular signals into the cell. If ECM genes are incorrectly spliced in SMAIII tissues as they are in those from SMAII mice (Zhang *et al.*, 2008), ECM protein content and protein distribution is likely affected, leading to significant signaling alterations within cells.

In SMAIII SpC and SkM, *Echdc1*and *Dcun1d1* exhibited dramatic upregulation (Table 3.5). Increases in *Echdc1*, involved in fatty acid oxidation, could indicate an increased need for energy in cells, or perhaps increases in cellular fat content that must be metabolized into energy. Drastic upregulation of *Dcun1d1* (UP-regulated 435.27 fold in SpC and 201.25 fold in SkM) may signify an increased need for protein degradation, since this protein catalyzes neddylation, a process which promotes activity of the Ub-proteasome machinery (Bosu & Kipreos, 2008). This explanation is a feasible explanation if incorrect RNA splicing leads to aberrant protein production. Unfortunately, present knowledge of this protein is minimal (Estilo *et al.*, 2003;Sarkaria *et al.*, 2006). Further characterization of its actions in the cell will allow us to better understand the relevance of Dcun1d1 to SMA. Such significant and consistent changes warrant further investigation.

3.4.1.3. Many transcriptional changes are shared and consistent between SMAIII SpC and SkM supporting the idea of a primary lesion common to both tissues in SMA

Perhaps the most striking finding of the present study is the extremely prominent overlap (79) of differentially regulated genes between SpC and SkM SMAIII samples. These parallel changes are of great interest due to their number and shared magnitude and direction (Table 3.5). These results provide overwhelming support for the hypothesis that degeneration of nerve and muscle in SMA is the result of a common cellular defect. It is relevant to perform MAs in other tissues (i.e. cardiac muscle and bone) to determine whether these shared transcriptional changes are also characteristic of SMAIII in tissues outside of the neuromuscular system.

3.4.2. Differentially regulated genes in SMAIII SpC and SkM are NOT overrepresented among RNA-transport, RNA-processing, cell-death, or cytoskeletal-related functions

Grouping of affected genes according to roles allowed determination of cellular functions that may be impacted in SMA. Figures 3.4-3.8 show that in contrast to distinct nerve (ALS) and muscle (XLMTM) diseases, ontologies related to development, RNA transport, cell-death, and the cytoskeleton are not overrepresented in SMAIII SpC or SkM. This indicates that although these cellular functions may be affected in SMA, we do not observe a response at the transcriptional level.

Although there was not differential regulation of a large number of genes related to development (Figure 3.4), the 21.94 fold down-regulation of the developmental gene *Ntn4* may be relevant to SMA pathophysiology. Specifically, animal models of SMA have shown axon pathfinding deficits (McWhorter *et al.*, 2003). *Ntn4*, a basement-membrane component, functions as a neural guidance molecule during development. Its dramatic down-regulation here signifies that despite successful formation of neuromuscular connections in SMAIII, problems exist either in pathfinding and/or in basement membrane organization (Schneiders *et al.*, 2007).

Genes with protein product function relating to RNA transport were minimally represented among differentially regulated genes from SMAIII SpC and SkM (Figure 3.5). However, the gene *trdr3*, UP-regulated in both SpC and SkM (Table 3.5) may indicate disruption of RNA transport in SMAIII tissues. Trdr3 protein contains a tudor domain for RNA binding, an oligosaccharide/nucleotide-binding fold, and an Ub-associated domain (Linder *et al.*, 2008;Goulet *et al.*, 2008). Trdr3 binds FMRP, the affected gene in Fragile X syndrome, which also binds SMN (Piazzon *et al.*, 2008). Disease-causing mutations in FMRP inhibit binding of both SMN and Trdr3 (Piazzon *et al.*, 2007; Linder *et al.*, 2008). SMN and Trdr3 bind FMRP via tudor domains, and it is possible that they may play similar roles in RNA stabilization and localization (Tadesse *et al.*, 2008b), and that the upregulation of *trdr3* in SMAIII tissues compensates for losses in RNA transport resulting from SMN reduction. Present findings of *trdr3* down-regulation should be confirmed via qRT-PCR and western blotting, and Trdr3 should be further assessed to determine its role in SMA. Genes with protein products involved in RNA processing were similarly not overrepresented among differentially regulated genes in SMAIII SpC and SkM, especially when compared with affected genes from 60d ALS MN and XLMTM SkM. Although splicing inefficiencies exist in SMA tissues (Zhang *et al.*, 2008), these do not lead to compensatory transcriptional changes in SMAIII tissues.

Present results do not support a role for apoptosis as a causative factor in SMA (Figure 3.7). Cell death related genes are not significantly represented among differentially regulated genes, and changes among the small number of genes involved in this process provide no evidence of a pro-apoptotic process. This supports the conclusion that involvement of the apoptotic process in neuromuscular degeneration is merely responsive to previously inflicted cellular insults, as it is in many neurodegenerative diseases (Gorman, 2008), although there may be exceptions in SMAI cases with deletions of NAIP (Ingram-Crooks *et al.*, 2002). Findings reported below regarding the potential involvement of MAPK signaling in SMA pathology support a downstream role of apoptosis: increased activation of p38 MAPK signaling in stress-related conditions is associated with apoptosis-mediated cell death . Cell-cycle related genes are represented to a greater degree in SMA SpC and SkM than in 60d ALS MN and XLMTM SkM. Many of these affected genes are involved in signaling, indicating that changes among this functional group are representative of the greater involvement of signaling genes in SMAIII.

Transcriptional changes in SMAIII SpC and SkM do not show overrepresentation of cytoskeleton-related genes, especially when compared with affected genes in 60d ALS MN and XLMTM SkM. Reduction of SMN in SMA leads to disruption of the actin cytoskeleton (Oprea *et al.*, 2008; Bowerman *et al.*, 2007). Since cytoskeleton-related genes are not represented among transcriptional changes, there are three possible explanations for cytoskeletal disruption (i.e. altered G:F-actin ratios) in SMA tissues: (1) changes in availability of actin binding proteins known to interact with SMN (i.e. profilin and α-actinin) (Sharma *et al.*, 2005;Rajendra *et al.*, 2007), (2) loss of SMN as a cytoskeletal component itself (Rajendra *et al.*, 2007), and (3) as a result of altered signaling, supported by transcriptional changes in signaling-related genes observed in the present study. The latter conclusion is also supported by previous findings that the small GTPases RhoA and Cdc42, are misregulated in SMA (Bowerman *et al.*, 2007). Potential misregulation of cytoskeletal actin downstream of signaling defects in SMA is discussed in section 3.4.3.1.

3.4.3. Signaling-related genes are overrepresented and MAPK and Wnt signaling pathways may be affected in SMA

The most significant finding of the present study is the overrepresentation of signaling genes in SMAIII SpC and SkM, even in comparison to affected genes in 60d ALS MN and XLMTM SkM (Figures 3.10-3.13). Overrepresentation of 'cell surface receptor linked signal transduction' and 'intracellular signaling cascade'-related genes is unique to SMAIII tissues (Figures 3.11-3.12). In addition, signaling-related genes made up one-third and one-quarter of most highly (>4 fold changes) affected genes in SpC and SkM respectively (Tables 3.3 and 3.4, Section 3.4.1.2). KEGG pathway analysis confirmed these findings and revealed differential regulation of numerous genes related to MAPK and Wnt signaling pathways, implicating these in SMA pathology (Figures 3.14 and 3.17). Our microarray data independently is insufficient to draw conclusions regarding exactly how signaling is affected in SMA tissues (i.e. are pathways repressed or promoted, and which ones are affected?). Further experimentation must be carried out to determine activation levels of instrumental proteins from three major cellular signal transduction pathways: MAPK, Wnt, (identified here) and PI3K/Akt, which was implicated in our earlier exciting finding of delayed denervation atrophy in SMAIII TA (Chapter 2).

3.4.3.1. Introduction to MAPK and Wnt signaling

The MAPK pathway, simplified and summarized in Figure 3.18, was originally identified as a response to growth factor (GF) stimulation of cultured cells (for review see Aoki *et al.*, 2008). MAPKs are activated by phosphorylation of tyrosine and threonine residues in response to GF binding (epidermal growth factor (EGF), platelet-derived growth factor (PDGF), nerve growth factor (NGF), insulin growth factor (IGF) and insulin-like growth factor (ILGF), T-cell activation, GPCR ligands, thrombin, bombesin, and bradykinin, and also NMDA receptor activation and electrical stimulation (Pacheco-Dominguez *et al.*, 2008). These external signals lead to activation of MAPK kinase kinases (MAPKKKs), MAPK kinases (MAPKKs), and finally to MAPKs (Haddad, 2005;Kolch, 2000) (Figure 3.18). Vertebrates possess three main groups of MAPK proteins: (1) extracellular signal-related kinases (ERKs) consist of ERK1 (p44) and ERK2 (p42), which are MAPKs for the 'classical MAPK pathway' (Frye, 1992;Denhardt, 1996) (2) the Jun N-terminal kinases (JNKs) are named for their ability to activate the transcription factor Jun (Ip & Davis, 1998) and (3) the third group, p38 MAPKs are generally activated under stressful conditions (English *et al.*, 1999), and their activation is generally associated with cell death (Davila & Torres-Aleman, 2008). MAPK signaling is also affected by calcium, which promotes ERK signaling but inhibits JNK activation (Haddad, 2005), an example which also illustrates the diversity in signaling reactions elicited by a single stimulus.

(

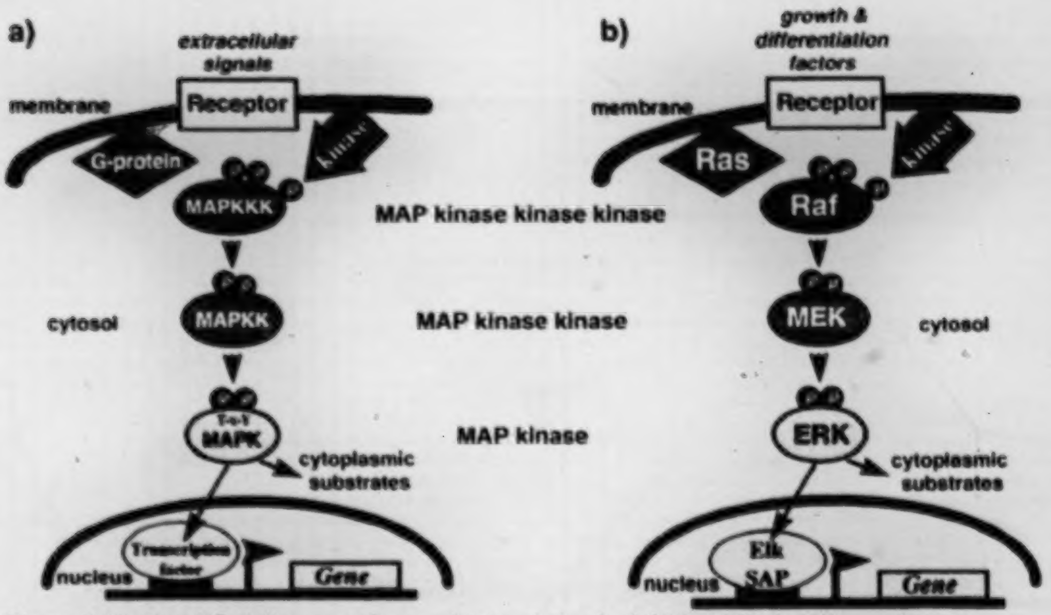
a)
extracellular signals
membrane
Receptor
G-protein
kinase
MAPKKK
MAP kinase kinase kinase
cytosol
MAPKK
MAP kinase kinase
T-x-Y
MAPK
MAP kinase
cytoplasmic substrates
Transcription factor
nucleus
Gene
b)
growth & differentiation factors
membrane
Receptor
Ras
kinase
Raf
MEK
cytosol
ERK
cytoplasmic substrates
Elk
SAP
nucleus
Gene

Figure 3.18. Simplified diagram of general (a) and classical (b) MAPK signaling pathways. ERKs, JNKs, and p38 MAPKs are the three main groups of MAP kinases which act as effectors for external signals in this pathway. From (Kolch, 2000).

Wnt (wingless integration) comprises a family of signaling proteins that are involved in many biological processes including embryonic patterning, development and proliferation (Clevers, 2006). Wnt ligands bind frizzled family receptors to activate either the canonical pathway, which controls gene transcription, or the non-canonical pathways, which either control intracellular calcium levels or dictate planar cell polarity (PCP) (Figure 3.19). Canonical Wnt signaling prevents degradation of β-catenin by glycogen synthase kinase (GSK) 3β-binding, allowing β-catenin to process into the nucleus and influence gene transcription as a coactivator for Tcf transcription factors, which promote transcription or repression of target genes coding for products that include cyclin D1, c-jun, c-myc, E-cadherin, and matrix metalloproteinases (MMPs) (Willert & Jones, 2006) (Chen *et al.*, 2008). Physiological outcomes of Wnt gene regulation are variable and dependent upon cell type and stage of development. In addition to acting as a transcriptional coactivator, β-catenin is also involved in cell-cell adhesion and amounts of this protein available for this function may also be regulated by Wnt signaling (Nelson & Nusse, 2004).

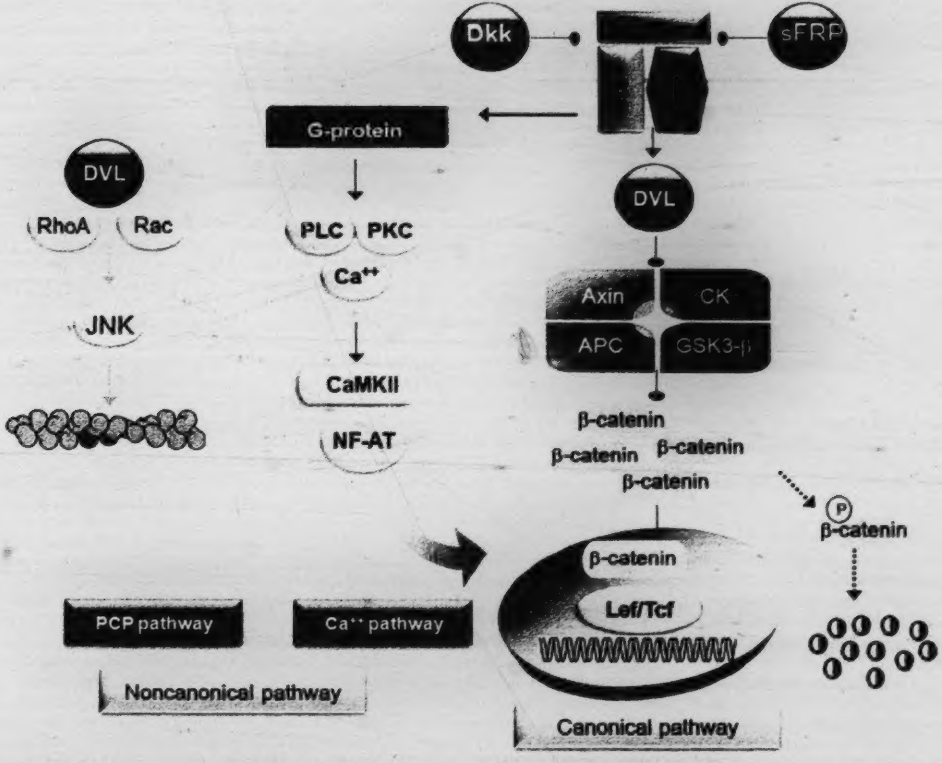
Dkk
sFRP
G-protein
DVL
RhoA
Rac
PLC
PKC
Ca⁺⁺
JNK
CaMKII
NF-AT
DVL
Axin
CK
APC
GSK3-β
β-catenin
β-catenin
β-catenin
β-catenin
P
β-catenin
β-catenin
Lef/Tcf
PCP pathway
Ca⁺⁺ pathway
Noncanonical pathway
Canonical pathway

Figure 3.19. Summary of noncanonical and canonical Wnt signaling pathways. Canonical and calcium noncanonical pathways lead to transcriptional changes within the cell, while disheveled (DVL) acts through the small GTPases RhoA and Rac to influence cell polarity in the PCP noncanonical pathway. From (Chun *et al.*, 2008).

3.4.3.2. MAPK and Wnt signaling are affected in neurodegenerative diseases

Signaling-related problems have been implicated in other neurodegenerative diseases: computational analysis of affected proteins and their interacting partners in Alzheimer's disease (AD), Parkinson disease (PD), ALS, Huntington disease (HD), dentatorubrai-pallidoluysia atrophy (DRPLA) and prion disease (PRND) revealed common involvement of stress-associated MAPK cascades and Wnt signaling (Goni *et al.*, 2008). The stress-associated MAPK (p38) pathway is over-activated at 80, 120 and 140d in an ALS G93A SOD1 mouse model and inhibition of this kinase leads to increased life spans in these animals (Dewil *et al.*, 2007). Activation of the classical (ERK) MAPK pathway has also been observed in ALS (Hu & Krieger, 2002), which the authors interpret as an anti-apoptotic tactic to delay cell death. Wnt signaling has been implicated *in vivo* in both AD and HD (Caricasole *et al.*, 2005), likely owing to its function in neuronal survival, cell death, and oxidative stress. Specifically, reductions in Wnt signaling lead to neurodegeneration and neuronal cell death (Marcus & Carew, 1998;Hetman & Xia, 2000), effects which can be prevented by LiCl administration, an imitator of Wnt activation (Inestrosa *et al.*, 2002). This function partially explains the neuroprotective effects of LiCl in conditions like glutamate-mediated toxicity and HD (Jakopec *et al.*, 2008;Voisine *et al.*, 2007). It is possible that perturbations in Wnt and MAPK signaling observed in SMAIII SpC and SkM are changes common to multiple neurodegenerative disorders. These changes may represent the earliest phenotypic manifestations of the disease in these tissues, as at the three month time point assessed, there are no clinical signs of SMA. It is also possible that signaling involvement in SMA is distinct from signaling associated with cell stress as observed in most cases of neurodegeneration, caused somehow by the loss of SMN.

3.4.4. Differential regulation of signaling-related genes could result from reduced or altered ECM protein expression to explain aspects of molecular pathology observed in SMA

In SMA, reduced or altered ECM protein composition causing reduced integrin clustering and activation may lead to alterations or reductions in MAPK, Wnt and PI3K signaling pathways concurrent with reduced F-actin, F-actin bundling, and focal adhesion (FA) formation, perhaps expressed as the transcriptional changes observed in the present study. This idea is supported by the finding that increased expression of T-plastin, an F-actin bundling and promoting protein, leads to amelioration of SMA in individuals with homozygous loss of function mutations in SMN (Oprea *et al.*, 2008). Zhang *et al.* (2008) found that a disproportionate number (>10%) of incorrectly spliced genes in SMAII SpC were related to the ECM (Figure 3.3) including numerous collagens, laminins, procollagens, and matrix metalloproteinases. Incorrect splicing leads to unstable mature mRNA transcripts, and theoretically, lowered levels of subsequent protein production (Wen & Brogna, 2008).

Cell-cell signaling and ligand-receptor mediated signaling are both greatly affected by the ECM environment, which is detected by the cell through binding of membrane integrin proteins. Integrins are made up of α and β chains which bind and form clusters within the membrane upon binding components of the ECM, subsequently activating multiple intracellular signaling pathways to transduce messages from the external environment into the cell (Humphries, 2000) (Hynes *et al.*, 1997). GF mediated classical MAPK activation involves cell adhesion- dependent nuclear translocation of ERK proteins (Miyamoto *et al.*, 1996) (Aplin, 2003). Effective integrin-ECM binding promotes cell spreading and thereby cellular stability, which may explain why activation of many signaling pathways, including the MAPK pathway, occurs with much higher efficiency when cells are stabilized in this way (Short *et al.*, 1998) (Slack & Siniaia, 2005).

3.4.4.1. Defective signaling can explain reduced a reduced F:G-actin ratio in SMA cells

Defective ECM composition leading to signaling problems could explain some molecular pathology observed in SMA, most notably a reduced F- to G-actin ratio. In mature cells, a large amount of F-actin is involved in focal adhesion structures: large collections of proteins that connect the cell and ECM, allowing transduction of regulatory and mechanical signals, most of which lead to initiation of cell anchorage-dependent signaling changes (Chen *et al.*, 2003) (Figure 3.20). ECM-integrin binding and subsequent integrin clustering leads to focal adhesion kinase (FAK) activation and downstream MAPK signaling, sometimes in cooperation with GF receptors and in addition to PI3K/Akt activation, which inhibits GSK-3β (and so promotes canonical Wnt signaling) (Yamada *et al.*, 2002) (Figure 3.20). MAPK activation stimulated by integrin binding regulates small GTPase activity to promote F-actin, F-actin bundling, and focal adhesion (FA) formation (Oscarsson *et al.*, 2007) (Figure 3.20). F-actin and F-actin bundling and contraction into FAs requires the action of RhoA and its downstream effectors mDia, ROCK and myosin light chain (MLC) kinase along with inhibition of the actin depolymerizing factor (ADF) cofilin (Ridley, 1999) (Figure 3.21). This results in increased F-actin formation and increased bundling of F-actin into stress fibers (Figure 3.21) which are then attached to the membrane to form the basis of FA structures, allowing transduction of mechanical and chemical signals to the cell's cytoskeleton (i.e. cell contracting and spreading response after ECM binding) (Ridley *et al.*, 1999). Changes in ECM composition could impair signaling in FA formation, and lead to reduced levels of F-actin observed in SMA cells. There is evidence to suggest that SMA actin cytoskeleton defects do not result from impairments in actin production, and are rather the result of disorganization of actin within cells: (1) Bowerman (2007) detected a mislocalization of F-actin around the periphery of neuron-like P12 cells, and subsequently reported misregulation of RhoA and Cdc42 activities in these cells; (2) Oprea (2008) detected reductions in F:G-actin ratios, but did not note overall reductions in actin, and this defect (and in fact all SMA symptoms!) could be corrected through the action of an F-actin bundling protein (T-plastin). These findings collectively show that it is the *organization* of the cytoskeleton that is the most significant aspect of SMA molecular pathology. Cytoskeletal *organization* is controlled by signaling, exactly the aspect of cell function that we have determined to be affected with gene expression analysis in SMAIII SpC and SkM.

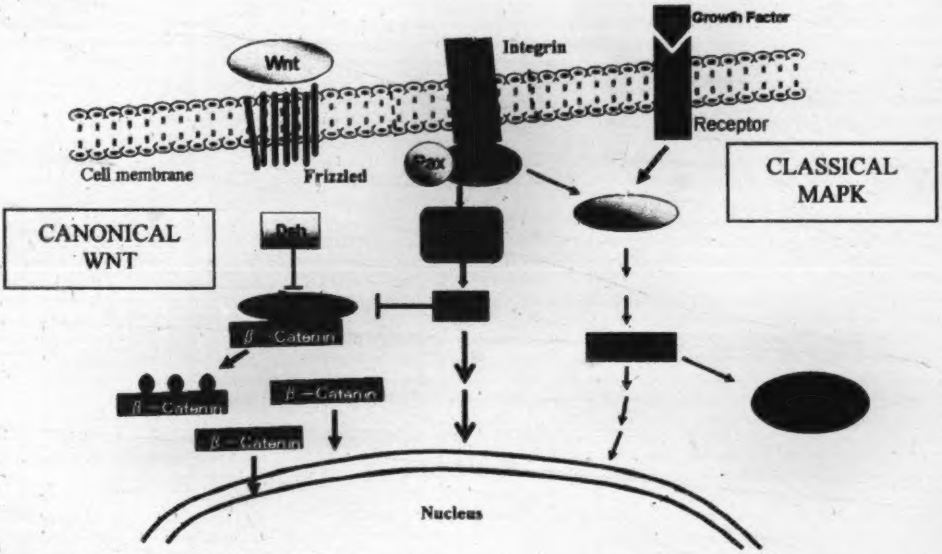
Growth Factor
Integrin
Wnt
Receptor
Cell membrane
Frizzled
Pax
CLASSICAL MAPK
CANONICAL WNT
Dsh
β-Catenin
β-Catenin
β-Catenin
β-Catenin
Nucleus

Figure 3.20. Review of canonical Wnt, PI3K/Akt and the classical MAPK pathway signaling occurring in response to integrin-ECM binding and external signals (GF and Wnt). Modified from (Takeuchi *et al.*, 2008).

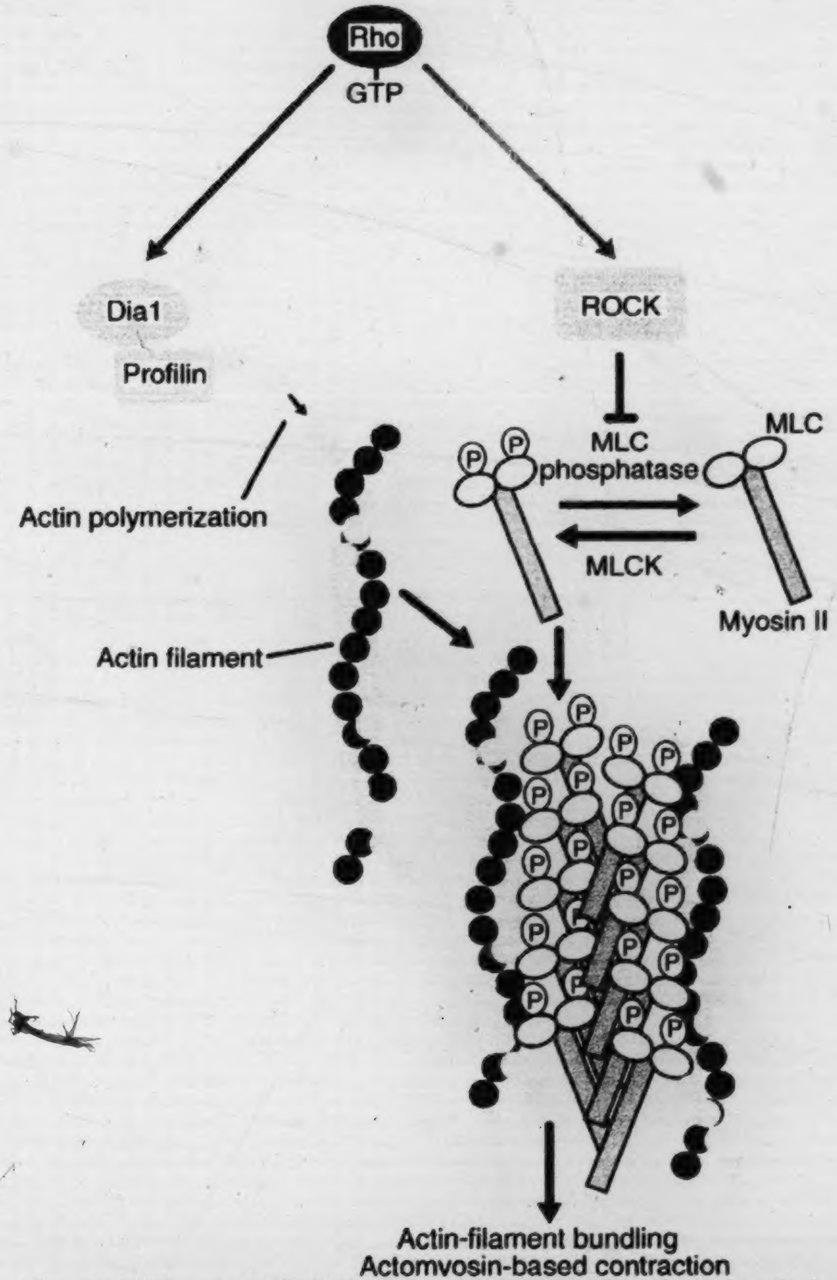
Rho
GTP
Dia1
Profilin
ROCK
Actin polymerization
MLC
phosphatase
MLC
MLCK
Myosin II
Actin filament
P
Actin-filament bundling
Actomyosin-based contraction

Figure 3.21. Summary of RhoA-GTP actions in stress fiber formation via downstream effectors mDia (Dia1) and ROCK. Cofilin is not shown, but functions in depolymerizing the 'minus' end of the actin filament which faces away from the leading edge; its action is inhibited by RhoA-GTP. Stress fibers provide stabilization and allow conduction of mechanical signals and more efficient conduction of ligand-mediated signals (i.e. GFs). From (Ridley, 1999).

Findings that exercise increases lifespan in SMAII mice (Grondard *et al.*, 2005;Biondi *et al.*, 2008) may also relate to this hypothesis: exercise leads to increased collagen production in multiple tissues, most notably skeletal muscle. Neuromuscular activity also promotes MAPK activation. In SMA, perhaps exercise increases collagen production resulting in increased or normalization of integrin binding, activation, F-actin and FA formation and normalization of MAPK, Wnt and PI3K/Akt signaling.

3.4.4.2. Signaling defects can explain aberrant AChR organization at the NMJ

A major molecular pathology hallmark in SMA is the well-documented failure of AChR clustering at the post-synaptic membrane of the NMJ (Murray *et al.*, 2008) (Kariya *et al.*, 2008). AChR clustering is dependent upon agrin signaling (Kummer *et al.*, 2006;Misgeld *et al.*, 2005) (Campagna *et al.*, 1995). Agrin activates muscle specific kinase (MuSK) to promote AChR clustering (Glass *et al.*, 1996), a process mediated by NMJ-specific integrins (Burkin *et al.*, 1998) αVβ1 and α7β1; loss of either inhibits agrin-induced cluster formation (Martin & Sanes, 1997). The N-terminal domain of agrin binds laminins (Denzer *et al.*, 1998) which may play a role in attracting agrin to the basal lamina (Luo *et al.*, 2003). Although the exact signaling pathway has not been conclusively defined, agrin activates PI3K which in turn activates the small GTPases Rac1 and Cdc42 (Nizhynska *et al.*, 2007) which promote F-actin formation and activate p21 activated kinase (PAK) leading to inhibition of cofilin (Luo *et al.*, 2003). As described in Figure 3.20 (Pullikuth & Catling, 2007), integrins promote MAPK, Wnt and PI3K/Akt signaling. It is possible that integrin involvement in AChR clustering is responsible for PI3K activation (Figure 3.22), although at present there is no experimental support for this. Wnt signaling has also been implicated in AChR clustering. Dishevelled (Dvl) is a downstream effector of Wnt signaling that also binds MuSK (Luo *et al.*, 2002). A recent report revealed that over-activation of canonical Wnt signaling and increased nuclear β-catenin leads to dispersal of AChR clusters, likely due to inhibition of rapsyn expression, a protein essential to the process (Wang *et al.*, 2008). However, in its role in cell adhesion complexes (Nelson & Nusse, 2004), β-catenin interacts with rapsyn in an agrin-dependent fashion to promote AChR clustering by connecting AChR clusters to the F-actin cytoskeleton via rapsyn and α-catenin (Zhang *et al.*, 2007). This activity does **not** involve canonical Wnt signaling (Zhang *et al.*, 2007).

In SMA, formation of mature, 'pretzel-shaped' AChR clusters is impaired (Murray *et al.*, 2008;Kariya *et al.*, 2008). Perturbations in transcription levels of signaling-related proteins observed in the present study support the idea that signaling in agrin-mediated AChR clustering (See Figure 3.22 for overview) may be impaired, potentially due to alterations in laminin (*lama2* is DOWN-regulated in both SpC and SkM) or integrin organization owing to altered ECM composition as described above.

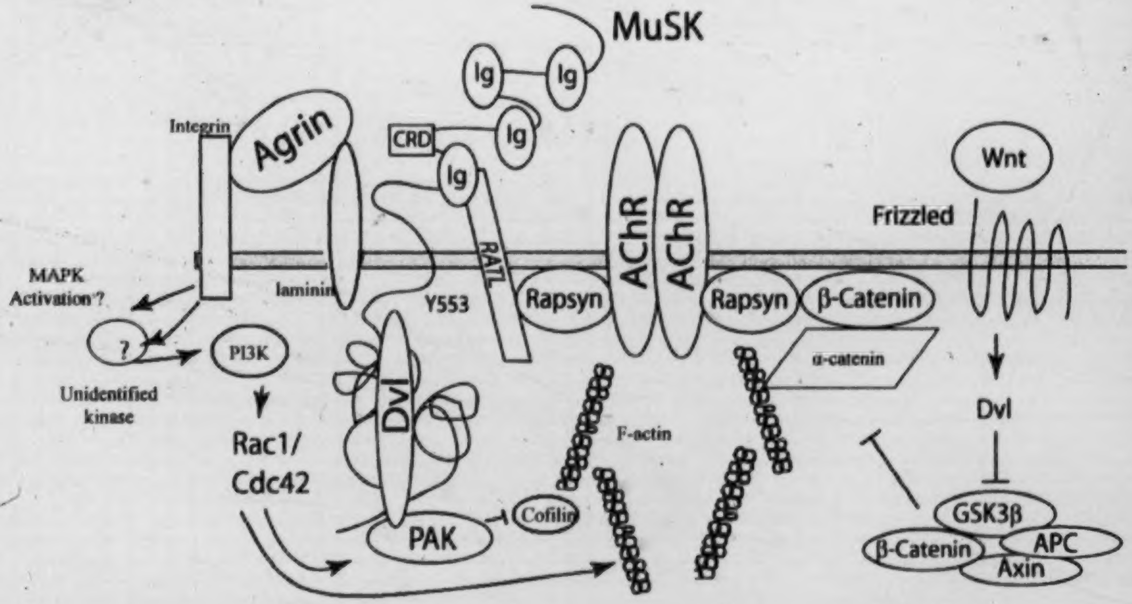
MuSK
Ig
Ig
CRD
Ig
Ig
Integrin
Agrin
Wnt
Frizzled
AChR
AChR
RATL
MAPK Activation?
laminin
Y553
Rapsyn
Rapsyn
β-Catenin
?
PI3K
α-catenin
Unidentified kinase
Dvl
Rac1/ Cdc42
F-actin
Dvl
PAK
Cofilin
GSK3β
β-Catenin
APC
Axin

Figure 3.22. Description of how losses or changes in ECM protein composition could cause aberrant signaling leading to failed AChR organization at the post-synaptic membrane of the NMJ. Reductions in ECM components, such as collagens and laminin, may lead to inefficiencies in agrin binding for MuSK activation, and also to reduced activation of integrin proteins and subsequent down stream signaling (such as MAPK and PI3K), which would affect activation levels of small GTPases Rho (not depicted here), Rac, and Cdc42. Impaired activation of these important regulator proteins will prevent F-actin polymerization and bundling, which is a requirement for AChR stabilization and organizational movement within the membrane. Additionally, cofilin will remain active and continue F-actin depolymerization. Wnt signaling may also be involved, as Wnt activation promotes dispersal of AChR clusters, however increased levels of β-catenin alone promote clustering by acting as a linker molecule between rapsyn/AChRs and α-catenin/F-actin. Picture modified from (Luo *et al.*, 2003).

These ideas are speculative based on MA, and require significant evaluation beginning with assessment of ECM protein levels, qRT-PCR for transcript level detection, western blotting to quantify protein levels, and fluorescent imaging techniques to visualize ECM composition and FA formation in SMA tissues. Involvement of signaling impairments in SMA requires assessment of activation levels of key components of MAPK, Wnt and PI3K/Akt pathways including Dvl, FAK, PI3K, Akt, Ras, ERK (MAPK) and RhoA.

3.4.5. Summary of findings

Genome wide transcriptional analysis of SMAIII SpC and SkM demonstrated a very striking overlap between transcriptional changes in the two distinct tissue types, supportive of a common molecular defect leading to neurodegeneration in both tissues. Our data show minimal transcriptional involvement of genes related to the following cell functions: development, RNA transport, RNA binding, apoptosis, and the cytoskeleton. Among genes differentially regulated more than four fold, we found an overrepresentation of genes with signaling-related functions. Functional classification of differentially regulated genes revealed an overrepresentation of signaling-related genes, especially in comparison with affected genes from 60d ALS MN and XLMTM SkM. KEGG pathway analysis confirmed these findings and highlighted MAPK and Wnt signaling pathways as areas of interest in SMA pathology. SMA may be the result of impaired or altered ECM protein composition leading to significant impairments and/or changes to signal transduction within the cell. This hypothesis could account for the two most significant aspects of molecular pathology in SMA: reduced F:G-actin within cells, and impaired mature organization of AChRs at the postsynaptic membrane of the NMJ.

3.5. Reference List

Anderson KN, Baban D, Oliver PL, Potter A, & Davies KE (2004). Expression profiling in spinal muscular atrophy reveals an RNA binding protein deficit. *Neuromuscul Disord* **14**, 711-722.

Aoki Y, Niihori T, Narumi Y, Kure S, & Matsubara Y (2008). The RAS/MAPK syndromes: novel roles of the RAS pathway in human genetic disorders. *Hum Mutat* **29**, 992-1006.

Aplin AE (2003). Cell adhesion molecule regulation of nucleocytoplasmic trafficking. *FEBS Lett* **534**, 11-14.

Arnold AS, Gueye M, Guettier-Sigrist S, Courdier-Fruh I, Coupin G, Poindron P, & Gies JP (2004). Reduced expression of nicotinic AChRs in myotubes from spinal muscular atrophy I patients. *Lab Invest* **84**, 1271-1278.

Balabanian S, Gendron NH, & MacKenzie AE (2007). Histologic and transcriptional assessment of a mild SMA model. *Neurol Res* **29**, 413-424.

Ballon DR, Flanary PL, Gladue DP, Konopka JB, Dohlman HG, & Thorner J (2006). DEP-domain-mediated regulation of GPCR signaling responses. *Cell* **126**, 1079-1093.

Belanger G, Stocksley MA, Vandromme M, Schaeffer L, Furic L, DesGroseillers L, & Jasmin BJ (2003). Localization of the RNA-binding proteins Staufen1 and Staufen2 at the mammalian neuromuscular junction. *J Neurochem* **86**, 669-677.

Biondi O, Grondard C, Lecolle S, Deforges S, Pariset C, Lopes P, Cifuentes-Diaz C, Li H, della GB, Chanoine C, & Charbonnier F (2008). Exercise-induced activation of NMDA receptor promotes motor unit development and survival in a type 2 spinal muscular atrophy model mouse. *J Neurosci* **28**, 953-962.

Bittel DC, Kibiryeva N, & Butler MG (2007). Whole genome microarray analysis of gene expression in subjects with fragile X syndrome. *Genet Med* **9**, 464-472.

Bloch RJ, Bezakova G, Ursitti JA, Zhou D, & Pumplin DW (1997). A membrane skeleton that clusters nicotinic acetylcholine receptors in muscle. *Soc Gen Physiol Ser* **52**, 177-195.

Bosu DR & Kipreos ET (2008). Cullin-RING ubiquitin ligases: global regulation and activation cycles. *Cell Div* **3**, 7.

Bowerman M, Shafey D, & Kothary R (2007). Smn depletion alters profilin II expression and leads to upregulation of the RhoA/ROCK pathway and defects in neuronal integrity. *J Mol Neurosci* **32**, 120-131.

Braun S, Croizat B, Lagrange MC, Warter JM, & Poindron P (1995). Constitutive muscular abnormalities in culture in spinal muscular atrophy. *Lancet* **345**, 694-695.

Brown V, Jin P, Ceman S, Darnell JC, O'Donnell WT, Tenenbaum SA, Jin X, Feng Y, Wilkinson KD, Keene JD, Darnell RB, & Warren ST (2001). Microarray identification of FMRP-associated brain mRNAs and altered mRNA translational profiles in fragile X syndrome. *Cell* **107**, 477-487.

Buj-Bello A, Laugel V, Messaddeq N, Zahreddine H, Laporte J, Pellissier JF, & Mandel JL (2002). The lipid phosphatase myotubularin is essential for skeletal muscle maintenance but not for myogenesis in mice. *Proc Natl Acad Sci U S A* **99**, 15060-15065.

Burkin DJ, Gu M, Hodges BL, Campanelli JT, & Kaufman SJ (1998). A functional role for specific spliced variants of the alpha7beta1 integrin in acetylcholine receptor clustering. *J Cell Biol* **143**, 1067-1075.

Cabrita MA & Christofori G (2008). Sprouty proteins, masterminds of receptor tyrosine kinase signaling. *Angiogenesis* **11**, 53-62.

Campagna JA, Ruegg MA, & Bixby JL (1995). Agrin is a differentiation-inducing "stop signal" for motoneurons in vitro. *Neuron* **15**, 1365-1374.

Caricasole A, Bakker A, Copani A, Nicoletti F, Gaviraghi G, & Terstappen GC (2005). Two sides of the same coin: Wnt signaling in neurodegeneration and neuro-oncology. *Biosci Rep* **25**, 309-327.

Chan YB, Miguel-Aliaga I, Franks C, Thomas N, Trulzsch B, Sattelle DB, Davies KE, & van den HM (2003). Neuromuscular defects in a Drosophila survival motor neuron gene mutant. *Hum Mol Genet* **12**, 1367-1376.

Chen CS, Alonso JL, Ostuni E, Whitesides GM, & Ingber DE (2003). Cell shape provides global control of focal adhesion assembly. *Biochem Biophys Res Commun* **307**, 355-361.

Chen X, Yang J, Evans PM, & Liu C (2008). Wnt signaling: the good and the bad. *Acta Biochim Biophys Sin (Shanghai)* **40**, 577-594.

Chun JS, Oh H, Yang S, & Park M (2008). Wnt signaling in cartilage development and degeneration. *BMB Rep* **41**, 485-494.

Cifuentes-Diaz C, Frugier T, Tiziano FD, Lacene E, Roblot N, Joshi V, Moreau MH, & Melki J (2001). Deletion of murine SMN exon 7 directed to skeletal muscle leads to severe muscular dystrophy. *J Cell Biol* **152**, 1107-1114.

Clevers H (2006). Wnt/beta-catenin signaling in development and disease. *Cell* **127**, 469-480.

Comery TA, Harris JB, Willems PJ, Oostra BA, Irwin SA, Weiler IJ, & Greenough WT (1997). Abnormal dendritic spines in fragile X knockout mice: maturation and pruning deficits. *Proc Natl Acad Sci U S A* **94**, 5401-5404.

Cornell NW, Josimovich JB, Lien LL, & Davidson KA (1971). Hormonal influences on hepatic histidase. *Endocrinol* **88**, 507-511.

Dahm R, Kiebler M, & Macchi P (2007). RNA localisation in the nervous system. *Semin Cell Dev Biol* **18**, 216-223.

Davila D & Torres-Aleman I (2008). Neuronal Death by Oxidative Stress Involves Activation of FOXO3 through a Two-Arm Pathway That Activates Stress Kinases and Attenuates Insulin-like Growth Factor I Signaling. *Mol Biol Cell* **19**, 2014-2025.

Denhardt DT (1996). Signal-transducing protein phosphorylation cascades mediated by Ras/Rho proteins in the mammalian cell: the potential for multiplex signalling. *Biochem J* **318 (Pt 3)**, 729-747.

Denzer AJ, Schulthess T, Fauser C, Schumacher B, Kammerer RA, Engel J, & Ruegg MA (1998). Electron microscopic structure of agrin and mapping of its binding site in laminin-1. *EMBO J* **17**, 335-343.

Dere E, Boverhof DR, Burgoon LD, & Zacharewski TR (2006). In vivo-in vitro toxicogenomic comparison of TCDD-elicited gene expression in Hepa1c1c7 mouse hepatoma cells and C57BL/6 hepatic tissue. *BMC Genomics* **7**, 80.

Dewil M, la Cruz VF, Van Den BL, & Robberecht W (2007). Inhibition of p38 mitogen activated protein kinase activation and mutant SOD1(G93A)-induced motor neuron death. *Neurobiol Dis* **26**, 332-341.

English J, Pearson G, Wilsbacher J, Swantek J, Karandikar M, Xu S, & Cobb MH (1999). New insights into the control of MAP kinase pathways. *Exp Cell Res* **253**, 255-270.

Estilo CL, Charoenrat P, Ngai I, Patel SG, Reddy PG, Dao S, Shaha AR, Kraus DH, Boyle JO, Wong RJ, Pfister DG, Huryn JM, Zlotolow IM, Shah JP, & Singh B (2003). The role of novel oncogenes squamous cell carcinoma-related oncogene and phosphatidylinositol 3-kinase p110alpha in squamous cell carcinoma of the oral tongue. *Clin Cancer Res* **9**, 2300-2306.

Ferraiuolo L, Heath PR, Holden H, Kasher P, Kirby J, & Shaw PJ (2007). Microarray analysis of the cellular pathways involved in the adaptation to and progression of motor neuron injury in the SOD1 G93A mouse model of familial ALS. *J Neurosci* **27**, 9201-9219.

Frugier T, Tiziano FD, Cifuentes-Diaz C, Miniou P, Roblot N, Dierich A, Le Meur M, & Melki J (2000). Nuclear targeting defect of SMN lacking the C-terminus in a mouse model of spinal muscular atrophy. *Hum Mol Genet* **9**, 849-858.

Frye RA (1992). Involvement of G proteins, cytoplasmic calcium, phospholipases, phospholipid-derived second messengers, and protein kinases in signal transduction from mitogenic cell surface receptors. *Cancer Treat Res* **63**, 281-299.

Gabanella F, Butchbach ME, Saieva L, Carissimi C, Burghes AH, & Pellizzoni L (2007). Ribonucleoprotein assembly defects correlate with spinal muscular atrophy severity and preferentially affect a subset of spliceosomal snRNPs. *PLoS ONE* **2**, e921.

Glass DJ, Bowen DC, Stitt TN, Radziejewski C, Bruno J, Ryan TE, Gies DR, Shah S, Mattsson K, Burden SJ, DiStefano PS, Valenzuela DM, DeChiara TM, & Yancopoulos GD (1996). Agrin acts via a MuSK receptor complex. *Cell* **85**, 513-523.

Goni J, Esteban FJ, de Mendizabal NV, Sepulcre J, rdanza-Trevijano S, Agirrezabal I, & Villoslada P (2008). A computational analysis of protein-protein interaction networks in neurodegenerative diseases. *BMC Syst Biol* **2**, 52.

Gonzalez de Aguilar JL, Niederhauser-Wiederkehr C, Halter B, de TM, Di SF, Demougin P, Dupuis L, Primig M, Meininger V, & Loeffler JP (2008). Gene profiling of skeletal muscle in an amyotrophic lateral sclerosis mouse model. *Physiol Genomics* **32**, 207-218.

Gorman AM (2008). Neuronal cell death in neurodegenerative diseases: recurring themes around protein handling. *J Cell Mol Med.*

Goulet I, Boisvenue S, Mokas S, Mazroui R, & Cote J (2008). TDRD3, a novel Tudor domain-containing protein, localizes to cytoplasmic stress granules. *Hum Mol Genet.*

Grondard C, Biondi O, Armand AS, Lecolle S, della GB, Pariset C, Li H, Gallien CL, Vidal PP, Chanoine C, & Charbonnier F (2005). Regular exercise prolongs survival in a type 2 spinal muscular atrophy model mouse. *J Neurosci* **25**, 7615-7622.

Haddad JJ (2005). N-methyl-D-aspartate (NMDA) and the regulation of mitogen-activated protein kinase (MAPK) signaling pathways: a revolving neurochemical axis for therapeutic intervention? *Prog Neurobiol* **77**, 252-282.

Hanafusa H, Torii S, Yasunaga T, & Nishida E (2002). Sprouty1 and Sprouty2 provide a control mechanism for the Ras/MAPK signalling pathway. *Nat Cell Biol* **4**, 850-858.

Hausmanowa-Petrusewicz I & Vrbova G (2005). Spinal muscular atrophy: a delayed development hypothesis. *NeuroReport* **16**, 657-661.

Hengst U, Cox LJ, Macosko EZ, & Jaffrey SR (2006). Functional and selective RNA interference in developing axons and growth cones. *J Neurosci* **26**, 5727-5732.

Hengst U & Jaffrey SR (2007). Function and translational regulation of mRNA in developing axons. *Semin Cell Dev Biol* **18**, 209-215.

Hetman M & Xia Z (2000). Signaling pathways mediating anti-apoptotic action of neurotrophins. *Acta Neurobiol Exp (Wars)* **60**, 531-545.

HOLTON JB, LEWIS FJ, & MOORE GR (1964). BIOCHEMICAL INVESTIGATION OF HISTIDINAEMIA. *J Clin Pathol* **17**, 671-675.

Hoshino M & Nakamura S (2002). The Ras-like small GTP-binding protein Rin is activated by growth factor stimulation. *Biochem Biophys Res Commun* **295**, 651-656.

Hu JH & Krieger C (2002). Protein phosphorylation networks in motor neuron death. *Prog Drug Res* **59**, 71-109.

Humphries MJ (2000). Integrin structure. *Biochem Soc Trans* **28**, 311-339.

Hynes NM, Bain JR, Thoma A, Veltri K, & Maguire JA (1997). Preservation of denervated muscle by sensory protection in rats. *J Reconstr Microsurg* **13**, 337-343.

Inestrosa N, De Ferrari GV, Garrido JL, Alvarez A, Olivares GH, Barria MI, Bronfman M, & Chacon MA (2002). Wnt signaling involvement in beta-amyloid-dependent neurodegeneration. *Neurochem Int* **41**, 341-344.

Ingram-Crooks J, Holcik M, Drmanic S, & MacKenzie AE (2002). Distinct expression of neuronal apoptosis inhibitory protein (NAIP) during murine development. *NeuroReport* **13**, 397-402.

Ip YT & Davis RJ (1998). Signal transduction by the c-Jun N-terminal kinase (JNK)--from inflammation to development. *Curr Opin Cell Biol* **10**, 205-219.

Jablonka S, Schrank B, Kralewski M, Rossoll W, & Sendtner M (2000). Reduced survival motor neuron (Smn) gene dose in mice leads to motor neuron degeneration: an animal model for spinal muscular atrophy type III. *Hum Mol Genet* **9**, 341-346.

Jakopec S, Karlovic D, Dubravcic K, Batinic D, Soric J, Brozovic A, Buljan D, & Osmak M (2008). Lithium effect on glutamate induced damage in glioblastoma cells. *Coll Antropol* **32 Suppl 1**, 87-91.

Kariya S, Park GH, Maeno-Hikichi Y, Leykekhman O, Lutz C, Arkovitz MS, Landmesser LT, & Monani UR (2008). Reduced SMN protein impairs maturation of the neuromuscular junctions in mouse models of spinal muscular atrophy. *Hum Mol Genet* **17**, 2552-2569.

Kolch W (2000). Meaningful relationships: the regulation of the Ras/Raf/MEK/ERK pathway by protein interactions. *Biochem J* **351** **Pt 2**, 289-305.

Kummer TT, Misgeld T, & Sanes JR (2006). Assembly of the postsynaptic membrane at the neuromuscular junction: paradigm lost. *Curr Opin Neurobiol* **16**, 74-82.

Ladd AN & Cooper TA (2004). Multiple domains control the subcellular localization and activity of ETR-3, a regulator of nuclear and cytoplasmic RNA processing events. *J Cell Sci* **117**, 3519-3529.

Li Q, Lee JA, & Black DL (2007). Neuronal regulation of alternative pre-mRNA splicing. *Nat Rev Neurosci* **8**, 819-831.

Linder B, Plottner O, Kroiss M, Hartmann E, Laggerbauer B, Meister G, Keidel E, & Fischer U (2008). Tdrd3 is a novel stress granule-associated protein interacting with the Fragile-X syndrome protein FMRP. *Hum Mol Genet*.

Luo Z, Wang Q, Dobbins GC, Levy S, Xiong WC, & Mei L (2003). Signaling complexes for postsynaptic differentiation. *J Neurocytol* **32**, 697-708.

Luo ZG, Wang Q, Zhou JZ, Wang J, Luo Z, Liu M, He X, Wynshaw-Boris A, Xiong WC, Lu B, & Mei L (2002). Regulation of AChR clustering by Dishevelled interacting with MuSK and PAK1. *Neuron* **35**, 489-505.

Marcus EA & Carew TJ (1998). Developmental emergence of different forms of neuromodulation in Aplysia sensory neurons. *Proc Natl Acad Sci U S A* **95**, 4726-4731.

Martin PT & Sanes JR (1997). Integrins mediate adhesion to agrin and modulate agrin signaling. *Development* **124**, 3909-3917.

McWhorter ML, Monani UR, Burghes AH, & Beattie CE (2003). Knockdown of the survival motor neuron (Smn) protein in zebrafish causes defects in motor axon outgrowth and pathfinding. *J Cell Biol* **162**, 919-931.

Miguel-Aliaga I, Chan YB, Davies KE, & van den HM (2000). Disruption of SMN function by ectopic expression of the human SMN gene in Drosophila. *FEBS Lett* **486**, 99-102.

Misgeld T, Kummer TT, Lichtman JW, & Sanes JR (2005). Agrin promotes synaptic differentiation by counteracting an inhibitory effect of neurotransmitter. *Proc Natl Acad Sci U S A* **102**, 11088-11093.

Miyamoto S, Teramoto H, Gutkind JS, & Yamada KM (1996). Integrins can collaborate with growth factors for phosphorylation of receptor tyrosine kinases and MAP kinase activation: roles of integrin aggregation and occupancy of receptors. *J Cell Biol* **135**, 1633-1642.

Monani UR, Coovert DD, & Burghes AH (2000). Animal models of spinal muscular atrophy. *Hum Mol Genet* **9**, 2451-2457.

Murray LM, Comley LH, Thomson D, Parkinson N, Talbot K, & Gillingwater TH (2008). Selective vulnerability of motor neurons and dissociation of pre- and post-synaptic pathology at the neuromuscular junction in mouse models of spinal muscular atrophy. *Hum Mol Genet* **17**, 949-962.

Nakayama Y & Aoki Y (2000). Mechanism responsible for the formation of focal swellings on injured neuronal processes using a novel in vitro model of axonal injury. *Forensic Sci Int* **113**, 245-249.

Nelson WJ & Nusse R (2004). Convergence of Wnt, beta-catenin, and cadherin pathways. *Science* **303**, 1483-1487.

Nizhynska V, Neumueller R, & Herbst R (2007). Phosphoinositide 3-kinase acts through RAC and Cdc42 during agrin-induced acetylcholine receptor clustering. *Dev Neurobiol* **67**, 1047-1058.

Noguchi S, Fujita M, Murayama K, Kurokawa R, & Nishino I (2005). Gene expression analyses in X-linked myotubular myopathy. *Neurol* **65**, 732-737.

Oprea GE, Krober S, McWhorter ML, Rossoll W, Muller S, Krawczak M, Bassell GJ, Beattie CE, & Wirth B (2008). Plastin 3 is a protective modifier of autosomal recessive spinal muscular atrophy. *Science* **320**, 524-527.

Oscarsson A, Juhas M, Sjolander A, & Eintrei C (2007). The effect of propofol on actin, ERK-1/2 and GABAA receptor content in neurones. *Acta Anaesthesiol Scand* **51**, 1184-1189.

Pacheco-Dominguez RL, Palma-Nicolas JP, Lopez E, & Lopez-Colome AM (2008). The activation of MEK-ERK1/2 by glutamate receptor-stimulation is involved in the regulation of RPE proliferation and morphologic transformation. *Exp Eye Res* **86**, 207-219.

Pawson T & Scott JD (1997). Signaling through scaffold, anchoring, and adaptor proteins. *Science* **278**, 2075-2080.

Piazzon N, Rage F, Schlotter F, Moine H, Branlant C, & Massenet S (2008). In vitro and in cellulo evidences for association of the survival of motor neuron complex with the fragile X mental retardation protein. *J Biol Chem* **283**, 5598-5610.

Pullikuth AK & Catling AD (2007). Scaffold mediated regulation of MAPK signaling and cytoskeletal dynamics: a perspective. *Cell Signal* **19**, 1621-1632.

Rajendra TK, Gonsalvez GB, Walker MP, Shpargel KB, Salz HK, & Matera AG (2007). A Drosophila melanogaster model of spinal muscular atrophy reveals a function for SMN in striated muscle. *J Cell Biol* **176**, 831-841.

Ridley AJ (1999). Rho family proteins and regulation of the actin cytoskeleton. *Prog Mol Subcell Biol* **22**, 1-22.

Ridley AJ, Allen WE, Peppelenbosch M, & Jones GE (1999). Rho family proteins and cell migration. *Biochem Soc Symp* **65**, 111-123.

Rossoll W, Jablonka S, Andreassi C, Kroning AK, Karle K, Monani UR, & Sendtner M (2003). Smn, the spinal muscular atrophy-determining gene product, modulates axon growth and localization of beta-actin mRNA in growth cones of motoneurons. *J Cell Biol* **163**, 801-812.

Roy S, Dubowitz V, & Wolman L (1971). Ultrastructure of muscle in infantile spinal muscular atrophy. *J Neurol Sci* **12**, 219-232.

Sakata E, Yamaguchi Y, Miyauchi Y, Iwai K, Chiba T, Saeki Y, Matsuda N, Tanaka K, & Kato K (2007). Direct interactions between NEDD8 and ubiquitin E2 conjugating enzymes upregulate cullin-based E3 ligase activity. *Nat Struct Mol Biol* **14**, 167-168.

Sarkaria I, charoenrat P, Talbot SG, Reddy PG, Ngai I, Maghami E, Patel KN, Lee B, Yonekawa Y, Dudas M, Kaufman A, Ryan R, Ghossein R, Rao PH, Stoffel A, Ramanathan Y, & Singh B (2006). Squamous cell carcinoma related oncogene/DCUN1D1 is highly conserved and activated by amplification in squamous cell carcinomas. *Cancer Res* **66**, 9437-9444.

Schneiders FI, Maertens B, Bose K, Li Y, Brunken WJ, Paulsson M, Smyth N, & Koch M (2007). Binding of netrin-4 to laminin short arms regulates basement membrane assembly. *J Biol Chem* **282**, 23750-23758.

Sharma A, Lambrechts A, Hao lT, Le TT, Sewry CA, Ampe C, Burghes AH, & Morris GE (2005). A role for complexes of survival of motor neurons (SMN) protein with gemins and profilin in neurite-like cytoplasmic extensions of cultured nerve cells. *Exp Cell Res* **309**, 185-197.

Shi GX, Han J, & Andres DA (2005). Rin GTPase couples nerve growth factor signaling to p38 and b-Raf/ERK pathways to promote neuronal differentiation. *J Biol Chem* **280**, 37599-37609.

Short SM, Talbott GA, & Juliano RL (1998). Integrin-mediated signaling events in human endothelial cells. *Mol Biol Cell* **9**, 1969-1980.

Slack BE & Siniaia MS (2005). Adhesion-dependent redistribution of MAP kinase and MEK promotes muscarinic receptor-mediated signaling to the nucleus. *J Cell Biochem* **95**, 366-378.

Soler-Botija C, Ferrer I, Gich I, Baiget M, & Tizzano EF (2002). Neuronal death is enhanced and begins during foetal development in type I spinal muscular atrophy spinal cord. *Brain* **125**, 1624-1634.

Su Y, Balice-Gordon RJ, Hess DM, Landsman DS, Minarcik J, Golden J, Hurwitz I, Liebhaber SA, & Cooke NE (2004). Neurobeachin is essential for neuromuscular synaptic transmission. *J Neurosci* **24**, 3627-3636.

Tadesse H, schenes-Furry J, Boisvenue S, & Cote J (2008b). KH-type splicing regulatory protein interacts with survival motor neuron protein and is misregulated in spinal muscular atrophy. *Hum Mol Genet* **17**, 506-524.

Tadesse H, schenes-Furry J, Boisvenue S, & Cote J (2008a). KH-type splicing regulatory protein interacts with survival motor neuron protein and is misregulated in spinal muscular atrophy. *Hum Mol Genet* **17**, 506-524.

Takeuchi R, Ryo A, Komitsu N, Mikuni-Takagaki Y, Fukui A, Takagi Y, Shiraishi T, Morishita S, Yamazaki Y, Kumagai K, Aoki I, & Saito T (2008). Low-intensity pulsed ultrasound activates the phosphatidylinositol 3 kinase/Akt pathway and stimulates the growth of chondrocytes in three-dimensional cultures: a basic science study. *Arthritis Res Ther* **10**, R77.

Tzimourakas A, Giasemi S, Mouratidou M, & Karagogeos D (2007). Structure-function analysis of protein complexes involved in the molecular architecture of juxtaparanodal regions of myelinated fibers. *Biotechnol J* **2**, 577-583.

Vitte JM, Davoult B, Roblot N, Mayer M, Joshi V, Courageot S, Tronche F, Vadrot J, Moreau MH, Kemeny F, & Melki J (2004). Deletion of murine Smn exon 7 directed to liver leads to severe defect of liver development associated with iron overload. *Am J Pathol* **165**, 1731-1741.

Voisine C, Varma H, Walker N, Bates EA, Stockwell BR, & Hart AC (2007). Identification of potential therapeutic drugs for huntington's disease using Caenorhabditis elegans. *PLoS ONE* **2**, e504.

Wallgren-Pettersson C, Jasani B, Newman GR, Morris GE, Jones S, Singhrao S, Clarke A, Virtanen I, Holmberg C, & Rapola J (1995). Alpha-actinin in nemaline bodies in congenital nemaline myopathy: immunological confirmation by light and electron microscopy. *Neuromuscul Disord* **5**, 93-104.

Wang J, Ruan NJ, Qian L, Lei WL, Chen F, & Luo ZG (2008). Wnt/beta-catenin signaling suppresses Rapsyn expression and inhibits acetylcholine receptor clustering at the neuromuscular junction. *J Biol Chem* **283**, 21668-21675.

Wen J & Brogna S (2008). Nonsense-mediated mRNA decay. *Biochem Soc Trans* **36**, 514-516.

Weston C, Gordon C, Teressa G, Hod E, Ren XD, & Prives J (2003). Cooperative regulation by Rac and Rho of agrin-induced acetylcholine receptor clustering in muscle cells. *J Biol Chem* **278**, 6450-6455.

Willert K & Jones KA (2006). Wnt signaling: is the party in the nucleus? *Genes Dev* **20**, 1394-1404.

Yamada H, Tsushima T, Murakami H, Uchigata Y, & Iwamoto Y (2002). Potentiation of mitogenic activity of platelet-derived growth factor by physiological concentrations of insulin via the MAP kinase cascade in rat A10 vascular smooth muscle cells. *Int J Exp Diabetes Res* **3**, 131-144.

Zhang B, Luo S, Dong XP, Zhang X, Liu C, Luo Z, Xiong WC, & Mei L (2007). Beta-catenin regulates acetylcholine receptor clustering in muscle cells through interaction with rapsyn. *J Neurosci* **27**, 3968-3973.

Zhang B, Schmoyer D, Kirov S, & Snoddy J (2004). GOTree Machine (GOTM): a web-based platform for interpreting sets of interesting genes using Gene Ontology hierarchies. *BMC Bioinformatics* **5**, 16.

Zhang HL, Pan F, Hong D, Shenoy SM, Singer RH, & Bassell GJ (2003). Active transport of the survival motor neuron protein and the role of exon-7 in cytoplasmic localization. *J Neurosci* **23**, 6627-6637.

Zhang Z, Lotti F, Dittmar K, Younis I, Wan L, Kasim M, & Dreyfuss G (2008). SMN deficiency causes tissue-specific perturbations in the repertoire of snRNAs and widespread defects in splicing. *Cell* **133**, 585-600.

Zhao YY, Takahashi M, Gu JG, Miyoshi E, Matsumoto A, Kitazume S, & Taniguchi N (2008). Functional roles of N-glycans in cell signaling and cell adhesion in cancer. *Cancer Sci* **99**, 1304-1310.

CHAPTER 4: GENERAL DISCUSSION

Results from two mild SMAIII models, *Smn*-/+-C57Bl and *Smn*-/-A2G-FVB, demonstrated that the developmental transition from a growth-to-transmitting phenotype, as measured by levels of GAP-43 and ChAT in nerve from mature animals, occurred normally. Likewise, reversions from a transmitting-to-growth mode, as measured by GAP-43 upregulation in sciatic nerves post-axotomy, proceeded as in wild-type animals. Our findings indicate that any impairments in mRNA splicing and protein production caused by a modest reduction of SMN and corresponding snRNP biogenesis do not delay GAP-43 downregulation and ChAT upregulation during development. Upregulation of GAP-43 during regeneration triggered by sciatic axotomy was also unimpaired in nerves from SMAIII animals. These findings imply that maturation from a growth-to-transmitting phenotype as well as reversion from a transmitting-to-growth phenotype appears normal in motoneurons from two distinct models of murine SMAIII animals. Similarly, evaluation of skeletal muscle indicated the effective transitions from developmental to mature protein isoforms of MyHC and cytoskeletal proteins takes place in skeletal muscle from SMAIII mice. Hence, results did not identify evidence of inappropriate persistence of immature protein isoforms in neurons or skeletal muscle from mature SMAIII animals, and likewise we did not observe impairments in the ability of tissues from SMAIII animals to express necessary proteins in a timely and effective manner during development.

The most dramatic finding of the present study is that denervation atrophy is delayed in skeletal muscle in the smn-/-A2G-FVB mouse model of SMN. Experimental findings in denervated TA muscle from smn-/-A2G-FVB mice revealed a delayed rate of fiber CSA reduction during denervation atrophy as compared to TA fibers from FVB-wild type controls. Nonetheless, analysis of the skeletal muscle response to denervation-induced atrophy revealed appropriate upregulation of N-CAM in SMAIII mice, but demonstrated a significant delay in the reduction of fiber CSA observed in wild-type samples. This exciting finding provides evidence of reduced rate of response to a stimulus (axotomy) which may be attributable to defective protein upregulation as a result of impaired splicing, or may indicate impairments in another aspect of SMN function affecting the cell signaling pathway required for effective induction of denervation-induced atrophy.

These findings prompted us to undertake microarray (MA) studies to (a) gain a better understanding of results obtained in the first half of the study, including cytoskeletal changes and delayed rates of denervation atrophy, (b) to further assess the delayed development hypothesis in

SMAIII tissues at the transcriptional level, and (c) to evaluate other hypotheses explaining the molecular basis of this complex disease.

Whole genome transcriptional analysis of SpC and SkM tissues from SMAIII smn-/-A2G-FVB animals confirmed earlier findings that ChAT and GAP-43 expression were not affected in this mild model of SMAIII. Gene ontology analysis similarly revealed that genes with protein products involved in development were not overrepresented among differentially regulated genes in SMAIII, especially in comparison with affected genes in tissues from two distinct disorders: 60d ALS MN and XLMTM SkM.

Another important finding of the present study is the significant degree of overlap in differentially regulated genes between SpC and SkM SMAIII tissues. Transcriptional changes were remarkably similar in both magnitude and direction, and this finding strongly supports a common molecular defect in SpC and SkM leading to degeneration of the neuromuscular system in SMA. It will be important to carry out transcriptional analysis on other, more mildly affected tissues, such as cardiac muscle and bone, to determine whether similar changes in gene transcription support a role for these tissues in SMA pathology. MA analysis showed that at the level of transcription, SpC was greater affected than SkM, perhaps because levels of SMN are far lower in this tissue than in SkM, and therefore further reductions in SMN may cause greater distress. A comparison of differentially regulated genes in SMAIII tissues with genes determined to be incorrectly spliced (Zhang *et al.*, 2008) indicated that only a small number of genes affected in SMAIII SpC and SkM could be differentially regulated as a result of splicing problems, implying that changes identified in the present study are responsive to either existing changes in transcript levels, or to loss of other functions of SMN, such as mRNA transport.

Functional grouping of differentially regulated genes allowed evaluation of other existing hypothesis explaining the molecular basis of SMA. Results found no overwhelming transcriptional support for involvement of RNA transport, RNA processing, apoptosis, or cytoskeleton-related functions, indicating that potential failures in these areas are not observed at the level of transcription. Ontology and KEGG pathway analysis together revealed the second extremely important finding within MA results: genes with protein products involved in signaling are strongly overrepresented among those differentially regulated in SMAIII SpC and SkM, even in comparison with affected genes in 60d ALS MN and XLMTM SkM. KEGG analysis found that MAPK and Wnt signaling pathways were specifically affected. Signaling-related genes may be affected merely in response to cellular stress, as in other neurodegenerative diseases (Caricasole *et al.*, 2005). However, findings by Zhang et al (2008) documenting incorrect splicing of large numbers of ECM-related genes in SMAII tissues (SpC, kidney and liver), provide another feasible explanation: reduced or altered ECM composition greatly affects signaling within the cell, a condition that could easily lead to changes in transcription of signaling-related genes as observed here. Future studies are warranted to determine (a) whether ECM composition is indeed affected at the protein level in SMAIII tissues, and (b) to determine resultant effects on signaling pathways within the cell, and (c) to assess subsequent relationships of these changes to the cytoskeleton, potentially explaining altered F:G-actin ratios observed in SMA (Oprea *et al.*, 2008) and perhaps failed acetylcholine receptor organization at the neuromuscular junction.

Figure 2.19 (Sandri *et al.*, 2004) depicts signaling pathways involved in muscle hypertrophy and atrophy, specifically the PI3K/Akt pathway. Interestingly, this same pathway can be affected by integrin-ECM binding (Figure 3.20). Transcriptional changes in signaling-related genes may indicate widespread changes in signaling at the protein level, which could affect this pathway and subsequently lead to delayed denervation-induced atrophy observed in the present study. These exciting findings require further evaluation to determine total and active levels of key proteins in the PI3K/Akt signaling pathway. Similar analysis should be performed on members of the MAPK and Wnt signaling pathways to determine their relevance to SMA.

Results obtained in the present study highlight the complicated nature of SMA. We have shown that neuromuscular degeneration is not the result of developmental delays, and instead have discovered likely impairments in signaling within the cell, most notably the PI3K/Akt pathway involved in denervation-induced atrophy, but also MAPK and Wnt signaling. Significantly, we found striking overlap between differential gene regulation in SpC and SkM tissues, providing great support for a single molecular cause leading to parallel degeneration of both tissues. This work has exposed many areas of great interest for further research, particularly perturbations in cell signaling, which could explain significant previously documented molecular pathology including altered F:G-actin ratios and defects in AChR clustering at the NMJ. We are hopeful that future research in these areas will be successful in determining the molecular basis for this complex disease.

Reference List

Caricasole, A., Bakker, A., Copani, A., Nicoletti, F., Gaviraghi, G., & Terstappen, G. C. (2005). Two sides of the same coin: Wnt signaling in neurodegeneration and neuro-oncology. *Biosci.Rep.* **25**, 309-327.

Oprea, G. E., Krober, S., McWhorter, M. L., Rossoll, W., Muller, S., Krawczak, M., Bassell, G. J:, Beattie, C. E., & Wirth, B. (2008). Plastin 3 is a protective modifier of autosomal recessive spinal muscular atrophy. *Science* **320**, 524-527.

Sandri, M., Sandri, C., Gilbert, A., Skurk, C., Calabria, E., Picard, A., Walsh, K., Schiaffino, S., Lecker, S. H., & Goldberg, A. L. (2004). Foxo transcription factors induce the atrophy-related ubiquitin ligase atrogin-1 and cause skeletal muscle atrophy. *Cell* **117**, 399-412.

Zhang, Z., Lotti, F., Dittmar, K., Younis, I., Wan, L., Kasim, M., & Dreyfuss, G. (2008). SMN deficiency causes tissue-specific perturbations in the repertoire of snRNAs and widespread defects in splicing. *Cell* **133**, 585-600.

APPENDIX 1

Group 1: SMN-/-A2G WT quad
Group 2: SMN-/-A2G TG quad
Statistics: Welchs t-test
Correction: Benjamini and Hochberg

Ratio	Direction	p-value	adj. p-value	Gene identifier	Gene Name	Gene ID
1.68	Up	0.0046761	2.06E-02	NM_007403	A disintegrin and metallopeptidase domain 8	Adam8
1.74	Down	0.0183948	4.80E-02	XM_133543	A kinase (PRKA) anchor protein 13	Akap13
1.68	Up	0.0031611	1.63E-02	NM_021330	Acid phosphatase 1, soluble	Acp1
2.21	Down	6.98E-05	1.71E-03	NM_134052	Acireductone dioxygenase 1	Adi1
1.54	Up	0.0045022	2.03E-02	NM_207625	Acyl-CoA synthetase long-chain family member 4	Acsl4
3.06	Up	4.37E-06	2.88E-04	NM_172678	Acyl-Coenzyme A dehydrogenase family, member 9	Acad9
3.17	Down	0.0122956	3.63E-02	NM_025748	Adenosine deaminase, tRNA-specific 2, TAD2 homolog (S. cerevisiae)	Adat2
1.56	Down	0.0108346	3.32E-02	AF176840	AF176840	-
1.5	Down	0.0184527	4.81E-02	NM_033565	AF4/FMR2 family, member 4	Aff4
5.93	Up	0.0037947	1.88E-02	AK012660	AK012660	-
1.62	Down	0.0009834	7.87E-03	AK014401	AK014401	-
14.06	Up	4.17E-05	1.20E-03	AK042923	AK042923	-
2.41	Up	0.0164043	4.53E-02	AK047112	AK047112	-
1.53	Up	0.0194365	4.94E-02	AK054507	AK054507	-
4.08	Down	0.0044723	2.02E-02	AK078356	AK078356	-
8.69	Down	2.27E-06	2.06E-04	AK086066	AK086066	-
1.67	Down	0.016734	4.56E-02	NM_177614	Amplified in osteosarcoma	Os9
1.56	Up	0.0011249	8.43E-03	AK089032	AN1, ubiquitin-like, homolog (Xenopus laevis)	Anubl1
1.67	Down	0.0060899	2.41E-02	NM_011923	Angiopoietin-like 2	Angptl2
4.16	Down	0.0002674	3.50E-03	NM_026853	Ankyrin repeat and SOCS box-containing protein 11	Asb11
2.23	Up	0.0010099	7.87E-03	X82786	Antigen identified by monoclonal antibody Ki 67	Mki67
1.94	Up	0.0098074	3.14E-02	NM_013900	Antigen p97 (melanoma associated) identified by monoclonal antibodies 133.2 and 96.5	Mfi2
1.74	Up	0.0029367	1.55E-02	NM_023190	Apoptotic chromatin condensation inducer 1	Acin1
1.51	Down	0.0138185	3.98E-02	NM_009700	Aquaporin 4	Aqp4
1.98	Down	0.0045369	2.04E-02	NM_031405	Arsenate resistance protein 2	Ars2

6.44	Down	0.0179168	4.74E-02	NM_024178	Asparagine-linked glycosylation 14 homolog (yeast)	Alg14
1.53	Down	0.0097572	3.14E-02	NM_011994	ATP-binding cassette, sub-family D (ALD), member 2	Abcd2
1.5	Up	0.0008012	6.99E-03	NM_009593	ATP-binding cassette, sub-family G (WHITE), member 1	Abcg1
2.3	Up	0.0001164	2.25E-03	NM_025338	Aurora kinase A interacting protein 1	Aurkaip1
1.58	Up	0.0021597	1.29E-02	NM_001012273	Baculoviral IAP repeat-containing 5	Birc5
1.94	Up	0.0007642	6.77E-03	NM_007566	Baculoviral IAP repeat-containing 6	Birc6
2.04	Up	0.0035457	1.78E-02	BC013561	BC013561	-
1.53	Down	0.0067406	2.58E-02	NM_007570	B-cell translocation gene 2, anti-proliferative	Btg2
1.51	Up	0.0157639	4.40E-02	NM_031368	Bone gamma-carboxyglutamate protein, related sequence 1	Bglap-rs1
1.52	Up	0.0054259	2.26E-02	NM_009765	Breast cancer 2	Brca2
2.55	Up	0.000197	2.90E-03	NM_138678	Butyrophilin related 1	Butr1
1.84	Down	0.0015347	1.03E-02	NM_009813	Calsequestrin 1	Casq1
2.66	Down	0.0191468	4.93E-02	AJ511265	Cardiomyopathy associated 5	Cmya5
1.63	Down	0.0102385	3.23E-02	NM_207653	CASP8 and FADD-like apoptosis regulator	Cflar
2.06	Down	0.0083004	2.93E-02	NM_009810	Caspase 3	Casp3
3.01	Up	0.0011628	8.61E-03	NM_023465	Catenin beta interacting protein 1	Ctnnbip1
3.55	Up	9.77E-06	4.79E-04	NM_009921	Cathelicidin antimicrobial peptide	Camp
2.21	Up	0.0008932	7.36E-03	NM_007799	Cathepsin E	Ctse
2.34	Up	0.0005934	5.68E-03	NM_007800	Cathepsin G	Ctsg
1.86	Up	0.0002079	3.02E-03	NM_010818	Cd200 antigen	Cd200
1.54	Up	0.0068168	2.60E-02	NM_008339	CD79B antigen	Cd79b
7.47	Down	0.0005532	5.49E-03	NM_020260	Cdc42 GTPase-activating protein	Cdgap
1.51	Up	0.0092606	3.11E-02	BC038907	CDNA sequence BC006965	BC006965
6.66	Down	0.0088264	3.01E-02	NM_001003939	CDNA sequence BC030307	BC030307
1.53	Up	0.0008184	7.08E-03	NM_023117	Cell division cycle 25 homolog B (S. pombe)	Cdc25b
1.77	Up	0.0035591	1.78E-02	NM_026410	Cell division cycle associated 5	Cdca5
2.07	Down	0.0007655	6.77E-03	NM_011124	Chemokine (C-C motif) ligand 21b	Ccl21b
1.62	Down	0.0038245	1.88E-02	NM_019577	Chemokine (C-C motif) ligand 24	Ccl24
2.94	Up	0.0020507	1.25E-02	NM_009892	Chitinase 3-like 3	Chi3l3
1.96	Down	0.0082009	2.91E-02	X62895	Chloride channel 1	Clcn1
2	Up	0.0029328	1.55E-02	NM_019701	Chloride channel Kb	Clcnkb
6.1	Up	0.0004662	4.86E-03	BC050818	Chordin-like 1	Chrdl1
1.57	Down	0.0171638	4.59E-02	BC023856	Chromodomain helicase DNA binding protein 8	Chd8
1.62	Down	0.0068041	2.60E-02	NM_009902	Claudin 3	Cldn3
6.67	Up	0.0025955	1.44E-02	NM_172546	Cnksr family member 3	Cnksr3
1.55	Up	0.0083353	2.94E-02	NM_146248	Coiled-coil alpha-helical rod protein 1	Cchcr1

2.64	Up	0.0003201	3.84E-03	AK199310	Coiled-coil domain containing 90A	Ccdc90a
1.67	Up	0.0084543	2.96E-02	NM_007738	Collagen, type VII, alpha 1	Col7a1
1.7	Up	0.0006783	6.29E-03	NM_009926	Collagen, type XI, alpha 2	Col11a2
1.5	Up	0.0098386	3.14E-02	XM_981889	Collagen, type XXII, alpha 1	Col22a1
1.71	Down	0.0182242	4.78E-02	NM_013499	Complement receptor related protein	Crry
1.66	Down	0.0095443	3.14E-02	NM_153166	Copine V	Cpne5
1.6	Up	0.0052538	2.22E-02	NM_007630	Cyclin B2	Ccnb2
2.13	Up	0.0005812	5.65E-03	NM_023243	Cyclin H	Ccnh
1.97	Down	0.0100388	3.18E-02	NM_009875	Cyclin-dependent kinase inhibitor 1B	Cdkn1b
1.63	Up	0.0044544	2.02E-02	BC049694	Cyclin-dependent kinase inhibitor 3	Cdkn3
1.51	Up	0.0098643	3.14E-02	NM_028775	Cytochrome P450, family 2, subfamily s, polypeptide 1	Cyp2s1
435.27	Up	1.15E-06	1.58E-04	NM_033623	DCUN1D1 DCN1, defective in cullin neddylation 1, domain containing 1 (S. cerevisiae)	Dcun1d1
9.31	Up	6.95E-06	3.90E-04	AK036369	DDHD domain containing 1	Ddhd1
1.73	Down	0.0079228	2.86E-02	NM_019553	DEAD (Asp-Glu-Ala-Asp) box polypeptide 21	Ddx21
1.6	Up	0.0120869	3.60E-02	NM_145975	DEAD (Asp-Glu-Ala-Asp) box polypeptide 46	Ddx46
1.55	Down	0.0049354	2.12E-02	NM_172803	Dedicator of cytokinesis 4	Dock4
2.12	Up	0.0039854	1.91E-02	AK018051	Dedicator of cytokinesis 8	Dock8
1.79	Up	0.0005906	5.68E-03	NM_001033326	Dehydrogenase/reductase (SDR family) X chromosome	Dhrsx
1.86	Up	0.019275	4.94E-02	NM_153551	DENN/MADD domain containing 1C	Dennd1c
34.25	Up	0.0003297	3.88E-03	AK170208	DEP domain containing 6	Depdc6
2.48	Down	0.0012954	8.97E-03	NM_010043	Desmin	Des
11.15	Up	5.95E-06	3.69E-04	AK122355	Diacylglycerol kinase, beta	Dgkb
1.57	Up	0.0022321	1.31E-02	AK049335	Diacylglycerol kinase, epsilon	Dgke
2.03	Down	0.0086553	2.98E-02	NM_021294	Diazepam binding inhibitor-like 5	Dbil5
1.53	Up	0.005971	2.39E-02	NM_010091	Dishevelled, dsh homolog 1 (Drosophila)	Dvl1
2.48	Up	0.0053917	2.26E-02	AK047398	DNA segment, Chr 10, Brigham & Womens Genetics 1379 expressed	D10Bwg1379e
8.79	Up	0.0006139	5.78E-03	AK033830	DNA segment, Chr 3, ERATO Doi 254, expressed	D3Ertd254e
2.35	Up	0.0026544	1.46E-02	NM_030143	DNA-damage-inducible transcript 4-like	Ddit4l
1.78	Down	0.0015846	1.05E-02	NM_019978	Doublecortin-like kinase 1	Dclk1
1.73	Up	0.0030494	1.60E-02	NM_011932	Dual adaptor for phosphotyrosine and 3-phosphoinositides 1	Dapp1
1.83	Up	2.26E-05	7.84E-04	NM_025869	Dual specificity phosphatase 26 (putative)	Dusp26
1.56	Down	0.0105145	3.26E-02	NM_001013380	Dynein, cytoplasmic 1 light intermediate chain 2	Dync1li2
1.66	Up	0.0191217	4.93E-02	NM_177733	E2F transcription factor 2	E2f2
2.02	Up	9.14E-05	2.08E-03	NM_015744	Ectonucleotide pyrophosphatase/phosphodiesterase 2	Enpp2

266.98	Up	2.59E-06	2.18E-04	NM_025855	Enoyl Coenzyme A hydratase domain containing 1	Echdc1
1.72	Down	0.0022028	1.30E-02		ENSMUST00000036296	-
1.72	Down	0.0014442	9.77E-03		ENSMUST00000037174	-
1.73	Down	0.0002818	3.57E-03		ENSMUST00000040382	-
30.67	Down	2.02E-07	5.94E-05		ENSMUST00000048238	-
2.04	Up	0.0004447	4.72E-03		ENSMUST00000057926	-
3.4	Down	0.0047609	2.08E-02		ENSMUST00000062945	-
1.53	Up	0.019437	4.94E-02		ENSMUST00000073524	-
1.56	Down	0.0166581	4.56E-02		ENSMUST00000094807	-
1.66	Down	0.019621	4.97E-02		ENSMUST00000097792	-
1.7	Up	0.0002989	3.63E-03	NM_134065	Ependymin related protein 1 (zebrafish)	Epdr1
1.52	Down	0.0056844	2.32E-02	NM_183428	Erythrocyte protein band 4.1	Epb4.1
1.9	Up	0.0022114	1.30E-02	NM_133245	Erythroid associated factor	Eraf
1.71	Up	0.0033351	1.71E-02	NM_010149	Erythropoietin receptor	Epor
2.49	Down	0.0002794	3.57E-03	X17373	Eukaryotic translation initiation factor 3, subunit 10 (theta)	Eif3s10
2	Up	0.0097484	3.14E-02	NM_181582	Eukaryotic translation initiation factor 5A	Eif5a
15.65	Up	0.0001242	2.25E-03	NM_001039115	Expressed sequence AI841875	AI841875
10.51	Up	0.0006868	6.31E-03	NM_177629	Expressed sequence AU021034	AU021034
1.6	Down	0.0012579	8.92E-03	NM_145930	Expressed sequence AW549877	AW549877
1.88	Up	0.0066034	2.55E-02	NM_173439	F-box protein 45	Fbxo45
1.54	Down	0.0177471	4.73E-02	NM_010181	Fibrillin 2	Fbn2
2.39	Up	0.0001652	2.56E-03	NM_010197	Fibroblast growth factor 1	Fgf1
2.11	Down	0.0169781	4.58E-02	NM_008009	Fibroblast growth factor binding protein 1	Fgfbp1
2.12	Down	0.0028376	1.52E-02	NM_007995	Ficolin A	Fcna
1.91	Down	0.0078491	2.85E-02	NM_008035	Folate receptor 2 (fetal)	Folr2
1.66	Up	0.0096056	3.14E-02	NM_178673	Follistatin-like 5	Fstl5
1.57	Up	0.0129213	3.76E-02	NM_010225	Forkhead box F2	Foxf2
2.41	Up	0.0160696	4.45E-02	NM_146187	Free fatty acid receptor 2	Ffar2
1.67	Up	0.0116806	3.51E-02	NM_008026	Friend leukemia integration 1	Fli1
1.58	Down	0.0001557	2.51E-03	NM_013522	FSHD region gene 1	Frg1
62.27	Up	1.48E-08	8.73E-06	NM_001012517	Fucosyltransferase 10	Fut10
6.32	Up	0.0039345	1.91E-02	AK018125	G elongation factor, mitochondrial 1	Gfm1
1.88	Down	0.0085393	2.98E-02	NM_001002268	G protein-coupled receptor 126	Gpr126
2.52	Up	0.0002565	3.42E-03	NM_173036	G protein-coupled receptor 97	Gpr97
1.78	Down	0.0125086	3.67E-02	NM_008066	Gamma-aminobutyric acid (GABA-A) receptor, subunit alpha 2	Gabra2
4.01	Up	0.0015422	1.03E-02	AK082993	Gap junction membrane channel protein alpha 5	Gja5

1.65	Down	0.004616	2.05E-02	NM_080450	Gap junction membrane channel protein epsilon 1	Gje1
1.93	Up	0.0007365	6.62E-03	NM_010208	Gardner-Rasheed feline sarcoma viral (Fgr) oncogene homolog	Fgr
1.71	Down	0.011542	3.48E-02	NM_010279	Glial cell line derived neurotrophic factor family receptor alpha 1	Gfra1
1.54	Down	0.0184098	4.80E-02	NM_177328	Glutamate receptor, metabotropic 7	Grm7
1.6	Down	0.005502	2.29E-02	NM_008078	Glutamic acid decarboxylase 2	Gad2
1.64	Down	9.67E-05	2.08E-03	NM_025374	Glyoxalase 1	Glo1
2.02	Down	0.0072534	2.71E-02	NM_016810	Golgi SNAP receptor complex member 1	Gosr1
12.61	Up	0.0010527	7.99E-03	NM_026240	GRAM domain containing 3	Gramd3
1.6	Down	0.0055756	2.29E-02	NM_207670	GRIP1 associated protein 1	Gripap1
16.17	Up	1.15E-05	5.17E-04	NM_008142	Guanine nucleotide binding protein (G protein), beta 1	Gnb1
1.63	Down	0.0014045	9.67E-03	NM_013531	Guanine nucleotide binding protein (G protein), beta 4	Gnb4
1.9	Up	0.007166	2.70E-02	NM_198110	Guanine nucleotide binding protein-like 3 (nucleolar)-like	Gnl3l
2.79	Up	0.0001693	2.59E-03	NM_017370	Haptoglobin	Hp
2.21	Down	0.0021111	1.27E-02	NM_175199	Heat shock protein 12A	Hspa12a
1.73	Down	0.002769	1.50E-02	AK050997	Heat shock protein 4 like	Hspa4l
1.52	Down	0.0040807	1.93E-02	NM_011631	Heat shock protein 90kDa beta (Grp94), member 1	Hsp90b1
1.67	Down	0.0086515	2.98E-02	XM_974905	HECT domain containing 1	Hectd1
3.45	Up	0.0005307	5.34E-03	NM_053149	Hemogen	Hemgn
7.18	Down	1.35E-05	5.66E-04	NM_010401	Histidine ammonia lyase	Hal
1.57	Down	0.0018039	1.15E-02	NM_008214	Histidyl-tRNA synthetase	Hars
2.62	Down	5.71E-05	1.49E-03	NM_010378	Histocompatibility 2, class II antigen A, alpha	H2-Aa
1.5	Down	0.0019202	1.20E-02	NM_010391	Histocompatibility 2, Q region locus 10	H2-Q10
1.75	Up	0.0194114	4.94E-02	NM_010397	Histocompatibility 2, T region locus 22	H2-T22
1.68	Up	3.31E-05	1.03E-03	NM_015786	Histone cluster 1, H1c	Hist1h1c
2.09	Up	0.0006237	5.83E-03	AK047852	Histone cluster 1, H1e	Hist1h1e
2.18	Up	0.0003925	4.44E-03	NM_175663	Histone cluster 1, H2ba	Hist1h2ba
1.81	Down	0.0004121	4.55E-03	BF467941	Histone cluster 1, H4i	Hist1h4i
1.68	Up	0.0002106	3.02E-03	NM_175652	Histone cluster 4, H4	Hist4h4
1.63	Down	0.0012366	8.91E-03	NM_013751	HRAS-like suppressor	Hrasls
1.69	Down	0.0038583	1.88E-02	NM_008316	Hus1 homolog (S. pombe)	Hus1
1.63	Up	0.0055718	2.29E-02	AK199677	Hydroxyacyl-Coenzyme A dehydrogenase	Hadh
2.12	Up	0.0150235	4.24E-02	BC004786	Immunoglobulin heavy chain complex	Igh
16.61	Up	1.53E-06	1.80E-04	NM_170599	Immunoglobulin superfamily, member 11	Igsf11
1.56	Down	0.0090793	3.07E-02	NM_145467	Integrin, beta-like 1	Itgbl1
1.62	Up	0.0074465	2.76E-02	NM_010531	Interleukin 18 binding protein	Il18bp

1.57	Down	0.0058314	2.34E-02	BC010717	Jumonji, AT rich interactive domain 1A (Rbp2 like)	Jarid1a
1.88	Down	0.0197787	4.97E-02	NM_152895	Jumonji, AT rich interactive domain 1B (Rbp2 like)	Jarid1b
1.58	Up	0.0095372	3.14E-02	AK088732	Kalirin, RhoGEF kinase	Kalrn
1.73	Down	0.0047482	2.08E-02	NM_173427	Kelch domain containing 7A	Klhdc7a
1.7	Down	0.0135326	3.91E-02	NM_028202	Kelch repeat and BTB (POZ) domain containing 5	Kbtbd5
1.8	Down	0.0001539	2.51E-03	NM_053105	Kelch-like 1 (Drosophila)	Klhl1
2.81	Up	0.0025388	1.44E-02	NM_032540	Kell blood group	Kel
1.7	Up	0.0009201	7.52E-03	AK014642	Keratin 28	Krt28
1.57	Up	0.0149355	4.24E-02	NM_009004	Kinesin family member 20A	Kif20a
2.1	Up	0.0046792	2.06E-02	NM_010635	Kruppel-like factor 1 (erythroid)	Klf1
3.15	Down	0.000224	3.14E-03	NM_172380	KTEL (Lys-Tyr-Glu-Leu) containing 1	Ktelc1
2.62	Up	1.79E-06	1.88E-04	NM_008522	Lactotransferrin	Ltf
1.55	Down	0.0178302	4.74E-02	U12147	Laminin, alpha 2	Lama2
1.71	Up	0.0078787	2.85E-02	NM_013589	Latent transforming growth factor beta binding protein 2	Ltbp2
1.51	Up	0.0146675	4.20E-02	NM_153777	Leucine rich repeat containing 56	Lrrc56
2.61	Up	0.0065498	2.55E-02	NM_001025067	Leucine-rich repeats and immunoglobulin-like domains 2	Lrig2
1.52	Down	0.0038157	1.88E-02	NM_008517	Leukotriene A4 hydrolase	Lta4h
1.75	Up	0.0003237	3.85E-03	NM_008519	Leukotriene B4 receptor 1	Ltb4r1
1.54	Down	0.0012459	8.91E-03	NM_001001980	LIM and calponin homology domains 1	Limch1
3.06	Up	8.96E-07	1.51E-04	NM_015763	Lipin 1	Lpin1
1.75	Down	0.0180587	4.76E-02	NM_008489	Lipopolysaccharide binding protein	Lbp
1.72	Up	0.0012492	8.91E-03	NM_030707	Macrophage scavenger receptor 2	Msr2
22.65	Up	9.49E-05	2.08E-03	NM_178920	Mal, T-cell differentiation protein 2	Mal2
1.69	Down	0.000881	7.36E-03	NM_008608	Matrix metallopeptidase 14 (membrane-inserted)	Mmp14
4.72	Up	3.25E-06	2.55E-04	NM_008611	Matrix metallopeptidase 8	Mmp8
1.52	Down	0.0113825	3.44E-02	NM_024263	Matrix-remodelling associated 8	Mxra8
2.82	Down	0.0181642	4.77E-02	NM_013634	Mediator complex subunit 1	Med1
1.66	Down	0.0098648	3.14E-02	AK090111	Metastasis associated lung adenocarcinoma transcript 1 (non-coding RNA)	Malat1
1.54	Down	0.0096323	3.14E-02	AK050582	Methionine adenosyltransferase II, alpha	Mat2a
2.18	Down	8.20E-05	1.95E-03	BE570772	Methionine aminopeptidase 2	Metap2
1.6	Up	0.0011733	8.63E-03	NM_023644	Methylcrotonoyl-Coenzyme A carboxylase 1 (alpha)	Mccc1
1.59	Down	0.0170768	4.59E-02	NM_153761	MHC I like leukocyte 2	Mill2
1.65	Up	0.0075827	2.77E-02	NM_029413	Microrchidia 4	Morc4
1.55	Down	0.0048198	2.10E-02	AK141735	Microtubule-associated protein 1 B	Mtap1b
1.52	Up	0.009424	3.14E-02	NM_008635	Microtubule-associated protein 7	Mtap7
2.52	Up	0.0002881	3.61E-03	BC029173	Mitochondrial ribosomal protein L47	Mrpl47

1.56	Up	0.001079	8.14E-03	NM_016693	Mitogen activated protein kinase kinase kinase 6	Map3k6
1.58	Up	0.0022714	1.32E-02	NM_008279	Mitogen activated protein kinase kinase kinase kinase 1	Map4k1
1.95	Up	0.0003863	4.41E-03	NM_010752	Mitotic arrest deficient 1-like 1	Mad1l1
1.59	Down	0.010949	3.33E-02	NM_172694	Multiple EGF-like-domains 9	Megf9
1.74	Up	0.0151851	4.27E-02	NM_054043	Musashi homolog 2 (Drosophila)	Msi2
2.07	Up	0.0001633	2.56E-03	NM_010848	Myeloblastosis oncogene	Myb
2.35	Up	3.23E-05	1.03E-03	NM_010824	Myeloperoxidase	Mpo
1.57	Down	0.0057761	2.34E-02	NM_001033713	Myocyte enhancer factor 2A	Mef2a
1.96	Up	0.0063299	2.48E-02	NM_178440	Myosin IG	Myo1g
2.41	Up	0.0072148	2.70E-02	NM_178877	Na+/H+ exchanger domain containing 2	Nhedc2
1.53	Up	0.0034678	1.75E-02		NAP036221-1	-
1.65	Down	0.0070192	2.67E-02	NM_008733	Nebulin-related anchoring protein	Nrap
1.57	Down	0.0171263	4.59E-02	NM_016743	NEL-like 2 (chicken)	Nell2
1.7	Up	0.0186564	4.84E-02	NM_008702	Nemo like kinase	Nlk
1.52	Down	0.0193188	4.94E-02	NM_010890	Neural precursor cell expressed, developmentally down-regulted gene 4	Nedd4
25.61	Up	0.0004138	4.55E-03	Y18276	Neurobeachin	Nbea
1.57	Up	0.0075572	2.77E-02	NM_008677	Neutrophil cytosolic factor 4	Ncf4
2.07	Up	0.0041621	1.94E-02	NM_008694	Neutrophilic granule protein	Ngp
3.5	Up	0.0029406	1.55E-02	AK152407	Nicotinamide nucleotide adenylyltransferase 1	Nmnat1
1.94	Down	0.0043239	1.99E-02	NM_010870	NLR family, apoptosis inhibitory protein 5	Naip5
1.56	Down	0.0052045	2.21E-02	NM_013886	NM_013886	-
1.7	Up	0.0012691	8.94E-03	NM_025927	NM_025927	-
1.52	Up	0.0057651	2.34E-02	NM_025832	NMDA receptor regulated 1-like	Narg1l
2.4	Up	3.25E-05	1.03E-03	NM_008685	Nuclear factor, erythroid derived 2	Nfe2
2.67	Up	0.0001489	2.49E-03	AK171679	Nuclear receptor coactivator 7	Ncoa7
1.79	Up	0.0063442	2.48E-02	NM_133851	Nucleolar and spindle associated protein 1	Nusap1
2.41	Up	0.0049398	2.12E-02	NM_027722	Nudix (nucleoside diphosphate linked moiety X)-type motif 4	Nudt4
1.73	Down	0.0185532	4.82E-02	NM_011859	Odd-skipped related 1 (Drosophila)	Osr1
1.72	Up	0.0095943	3.14E-02	NM_172801	Otopetrin 2	Otop2
2.67	Up	0.0012174	8.84E-03	NM_026936	Oxidase assembly 1-like	Oxa1l
1.52	Up	0.0040239	1.91E-02	AK019026	P53-associated parkin-like cytoplasmic protein	Parc
4.17	Up	0.0010346	7.91E-03	NM_011090	Paired-Ig-like receptor A3	Pira3
1.55	Up	0.0017261	1.12E-02	NM_023245	Palmdelphin	Palmd
2.1	Up	0.0014343	9.76E-03	NM_011061	Peptidyl arginine deiminase, type IV	Padi4
4.75	Up	0.0018765	1.17E-02	NM_026141	Peptidylprolyl isomerase (cyclophilin)-like 4	Ppil4

1.7	Up	0.0002981	3.63E-03	NM_011069	Peroxisomal biogenesis factor 11b	Pex11b
1.87	Up	0.0012061	8.82E-03	NM_177201	PHD finger protein 8	Phf8
1.81	Up	0.0002166	3.07E-03	NM_008796	Phosphatidylcholine transfer protein	Pctp
1.61	Down	0.0144014	4.13E-02	NM_013784	Phosphatidylinositol glycan anchor biosynthesis, class N	Pign
2.07	Down	0.0071732	2.70E-02	NM_001009978	Phosphodiesterase 1A, calmodulin-dependent	Pde1a
7.35	Up	6.46E-05	1.62E-03	NM_181414	Phosphoinositide-3-kinase, class 3	Pik3c3
1.82	Up	0.0042694	1.97E-02	NM_171824	PiggyBac transposable element derived 5	Pgbd5
1.58	Up	0.0041576	1.94E-02	NM_207229	Placenta specific 9	Plac9
1.71	Up	0.0035439	1.78E-02	NM_011121	Polo-like kinase 1 (Drosophila)	Plk1
1.64	Down	0.0169285	4.58E-02	NM_019697	Potassium voltage-gated channel, Shal-related family, member 2	Kcnd2
26.5	Up	0.0001053	2.19E-03	NM_027504	PR domain containing 16	Prdm16
1.81	Up	0.0039575	1.91E-02	NM_016982	Pre-B lymphocyte gene 1	Vpreb1
1.57	Up	0.0007323	6.62E-03	XM_001003884	Predicted gene, EG668831	EG668831
1.66	Down	0.0073126	2.72E-02	BC089618	Predicted gene, OTTMUSG00000000971	OTTMUSG00000000971
1.86	Up	0.0031192	1.62E-02	AK030206	Predicted gene, OTTMUSG00000010464	OTTMUSG00000010464
1.52	Up	0.0032577	1.67E-02	NM_152894	Processing of precursor 1, ribonuclease P/MRP family, (S. cerevisiae)	Pop1
2.08	Up	0.0121933	3.61E-02	NM_019976	Proline/serine-rich coiled-coil 1	Psrc1
2.1	Up	0.0008632	7.31E-03	NM_178372	Protease, serine, 34	Prss34
12.33	Down	0.0198695	4.97E-02	AK034732	Protein arginine N-methyltransferase 6	Prmt6
2.02	Down	0.0020194	1.24E-02	NM_021880	Protein kinase, cAMP dependent regulatory, type I, alpha	Prkar1a
1.69	Down	0.0057802	2.34E-02	NM_011100	Protein kinase, cAMP dependent, catalytic, beta	Prkacb
1.65	Up	1.21E-06	1.58E-04	NM_177081	Protein tyrosine phosphatase, non-receptor type 7	Ptpn7
1.99	Up	0.0003672	4.28E-03	NM_008983	Protein tyrosine phosphatase, receptor type, K	Ptprk
2.72	Up	0.0037899	1.88E-02	NM_008920	Proteoglycan 2, bone marrow	Prg2
3.19	Down	0.0055245	2.29E-02	AK047681	Protocadherin 9	Pcdh9
1.76	Up	0.0031326	1.62E-02	NM_053134	Protocadherin beta 9	Pcdhb9
1.51	Up	0.0028406	1.52E-02	NM_013629	Putative homeodomain transcription factor 1	Phtf1
2.25	Up	0.0027863	1.50E-02	NM_026405	RAB32, member RAS oncogene family	Rab32
1.73	Up	0.003998	1.91E-02	NM_021384	Radical S-adenosyl methionine domain containing 2	Rsad2
1.6	Down	0.0124223	3.66E-02	NM_053268	RAS p21 protein activator 2	Rasa2

19.91	Up	0.000107	2.19E-03	NM_009065	Ras-like without CAAX 2	Rit2
1.54	Up	0.0021014	1.27E-02	NM_009061	Regulator of G-protein signaling 2	Rgs2
4.03	Up	4.31E-05	1.21E-03	NM_181596	Resistin like gamma	Retnlg
1.92	Up	1.65E-05	6.68E-04	NM_023879	Retinitis pigmentosa GTPase regulator interacting protein 1	Rpgrip1
2.29	Down	0.0190626	4.93E-02	NM_009030	Retinoblastoma binding protein 4	Rbbp4
1.59	Down	0.0158199	4.40E-02	NM_011254	Retinol binding protein 1, cellular	Rbp1
2.11	Up	0.0117147	3.51E-02	NM_011270	Rh blood group, D antigen	Rhd
2.26	Down	0.0129899	3.78E-02	NM_027871	Rho guanine nucleotide exchange factor (GEF) 3	Arhgef3
7.92	Up	0.0009397	7.63E-03	AK045134	Rhotekin 2	Rtkn2
1.54	Up	0.000841	7.23E-03	NM_026799	Ribonuclease III, nuclear	Rnasen
1.68	Up	0.0010306	7.91E-03	NM_007447	Ribonuclease, RNase A family 4	Rnase4
1.74	Down	0.0023497	1.36E-02	NM_011271	Ribonuclease, RNase A family, 1 (pancreatic)	Rnase1
1.71	Up	0.0020575	1.25E-02	AK170359	Ribosomal protein L22 like 1	Rpl22l1
7.28	Up	1.83E-05	6.73E-04	NM_021338	Ribosomal protein L35a	Rpl35a
1.97	Down	0.0197103	4.97E-02	NM_025425	Ribosomal protein L3-like	Rpl3l
4.96	Up	5.40E-05	1.44E-03	NM_183249	RIKEN cDNA 1100001G20 gene	1100001G20Rik
1.55	Up	0.0149145	4.24E-02	CB575847	RIKEN cDNA 1110038B12 gene	1110038B12Rik
1.9	Up	0.0159032	4.41E-02	AK138072	RIKEN cDNA 1190002F15 gene	1190002F15Rik
6.6	Up	2.68E-08	1.05E-05	AK045413	RIKEN cDNA 1190007I07 gene	1190007I07Rik
2.7	Up	0.0017516	1.13E-02	NM_027918	RIKEN cDNA 1300017J02 gene	1300017J02Rik
2.87	Up	1.19E-05	5.17E-04	NM_025904	RIKEN cDNA 1600012F09 gene	1600012F09Rik
2.53	Down	0.0014289	9.76E-03	NM_028156	RIKEN cDNA 1700001P01 gene	1700001P01Rik
2.7	Up	0.000128	2.28E-03	NM_026985	RIKEN cDNA 1810033B17 gene	1810033B17Rik
1.86	Down	0.0109664	3.33E-02	NM_023220	RIKEN cDNA 2010106G01 gene	2010106G01Rik
1.7	Up	0.0025703	1.44E-02	AK008958	RIKEN cDNA 2210416O15 gene	2210416O15Rik
3.4	Down	0.0117126	3.51E-02	AK009124	RIKEN cDNA 2310002L09 gene	2310002L09Rik
7.99	Up	3.65E-09	4.30E-06	AK011787	RIKEN cDNA 2610100L16 gene	2610100L16Rik
1.83	Down	0.0105227	3.26E-02	NM_001025576	RIKEN cDNA 2610301F02 gene	2610301F02Rik
1.53	Down	0.0075476	2.77E-02	NM_026620	RIKEN cDNA 2610510H03 gene	2610510H03Rik
1.54	Up	0.0151902	4.27E-02	NM_026515	RIKEN cDNA 2810417H13 gene	2810417H13Rik
6.9	Up	0.0034369	1.74E-02	AK013405	RIKEN cDNA 2810474C18 gene	2810474C18Rik
1.52	Down	0.007531	2.77E-02	NM_144518	RIKEN cDNA 2900011O08 gene	2900011O

						08Rik
2.19	Up	2.86E-05	9.61E-04	NM_173181	RIKEN cDNA 3110050N22 gene	3110050N22Rik
1.86	Up	0.000119	2.25E-03	NM_026622	RIKEN cDNA 3110057O12 gene	3110057O12Rik
2.38	Up	0.0026673	1.46E-02	BC025200	RIKEN cDNA 3110073H01 gene	3110073H01Rik
3.13	Down	0.0001299	2.28E-03	NM_026136	RIKEN cDNA 4930449I24 gene	4930449I24Rik
5.98	Up	1.17E-05	5.17E-04	NM_024273	RIKEN cDNA 4930455C21 gene	4930455C21Rik
6.95	Up	0.0001122	2.20E-03	AK158034	RIKEN cDNA 5830416P10 gene	5830416P10Rik
1.59	Down	0.0091494	3.08E-02	AK147575	RIKEN cDNA 5830417I10 gene	5830417I10Rik
31.97	Up	0.0003735	4.31E-03	NM_026138	RIKEN cDNA 6330407J23 gene	6330407J23Rik
2.15	Up	0.0001232	2.25E-03	NM_176952	RIKEN cDNA 6430573F11 gene	6430573F11Rik
1.58	Down	0.0025768	1.44E-02	AK040733	RIKEN cDNA 9330159M07 gene	9330159M07Rik
1.52	Up	0.0005081	5.20E-03	AK036466	RIKEN cDNA 9430076G02 gene	9430076G02Rik
1.58	Up	0.0002989	3.63E-03	AK081752	RIKEN cDNA A230072E10 gene	A230072E10Rik
1.82	Down	0.0088726	3.02E-02	NM_170757	RIKEN cDNA A630007B06 gene	A630007B06Rik
2.01	Down	0.0090124	3.06E-02	BC023719	RIKEN cDNA A930015D03 gene	A930015D03Rik
1.94	Down	1.82E-05	6.73E-04	AK031919	RIKEN cDNA B230215L15 gene	B230215L15Rik
1.55	Up	0.0149288	4.24E-02	AK042827	RIKEN cDNA B230217C12 gene	B230217C12Rik
3.51	Up	2.10E-05	7.47E-04	AK084997	RIKEN cDNA B930095G15 gene	B930095G15Rik
1.71	Down	0.0003967	4.45E-03	NM_001039231	RIKEN cDNA C230055K05 gene	C230055K05Rik
1.59	Up	0.0157974	4.40E-02	AK173328	RIKEN cDNA C230081A13 gene	C230081A13Rik
2.97	Up	0.0009982	7.87E-03	NM_026518	Ring finger protein 146	Rnf146
1.89	Down	0.0004271	4.61E-03	NM_024242	RIO kinase 1 (yeast)	Riok1
1.56	Up	0.0023196	1.34E-02	BC011531	RNA binding motif protein 26	Rbm26
3.09	Up	3.93E-05	1.16E-03	NM_009114	S100 calcium binding protein A9 (calgranulin B)	S100a9
1.83	Down	0.0133163	3.86E-02	NM_011892	Sarcoglycan, gamma (dystrophin-associated glycoprotein)	Sgcg
1.6	Down	0.0048907	2.12E-02	NM_019460	Scm-like with four mbt domains 1	Sfmbt1
2.05	Down	0.0194876	4.94E-02	NM_009245	Serine (or cysteine) peptidase inhibitor, clade A, member 1c	Serpina1c
5.16	Up	0.0017333	1.12E-02	NM_178749	Serine/threonine kinase 32A	Stk32a
1.54	Down	0.0137415	3.96E-02	NM_009762	SET and MYND domain containing 1	Smyd1
1.59	Up	0.0001244	2.25E-03	NM_194344	SH3 domain and tetratricopeptide repeats 1	Sh3tc1

3.12	Up	0.0166593	4.56E-02	NM_009259	Sialophorin	Spn
3.78	Down	6.10E-07	1.20E-04	NM_053198	Sideroflexin 4	Sfxn4
10.79	Up	0.0001856	2.80E-03	AK005150	Single-stranded DNA binding protein 2	Ssbp2
1.68	Up	0.0041939	1.94E-02	NM_027013	Sodium channel modifier 1	Scnm1
2.01	Down	0.0100057	3.17E-02	NM_009196	Solute carrier family 16 (monocarboxylic acid transporters), member 1	Slc16a1
1.56	Up	0.0127798	3.73E-02	NM_019741	Solute carrier family 2 (facilitated glucose transporter), member 5	Slc2a5
1.56	Down	0.0045932	2.05E-02	NM_008766	Solute carrier family 22 (organic anion transporter), member 6	Slc22a6
1.51	Up	0.0198817	4.97E-02	NM_026331	Solute carrier family 25, member 37	Slc25a37
2.05	Up	0.0005679	5.57E-03	NM_026165	Solute carrier family 25, member 46	Slc25a46
2.05	Down	0.0198684	4.97E-02	NM_023596	Solute carrier family 29 (nucleoside transporters), member 3	Slc29a3
1.52	Down	0.0009845	7.87E-03	NM_144902	Solute carrier family 35 (UDP-N-acetylglucosamine (UDP-GlcNAc) transporter), member 3	Slc35a3
2.31	Up	0.0019438	1.20E-02	NM_011403	Solute carrier family 4 (anion exchanger), member 1	Slc4a1
1.64	Down	0.0165022	4.55E-02	NM_018760	Solute carrier family 4 (anion exchanger), member 4	Slc4a4
1.7	Up	0.0018596	1.17E-02	AK082651	Solute carrier family 45, member 1	Slc45a1
1.96	Down	0.0053064	2.23E-02	NM_133661	Solute carrier family 6 (neurotransmitter transporter, betaine/GABA), member 12	Slc6a12
1.5	Down	0.0019464	1.20E-02	NM_144512	Solute carrier family 6 (neurotransmitter transporter, GABA), member 13	Slc6a13
6.81	Up	1.92E-06	1.88E-04	NM_016972	Solute carrier family 7 (cationic amino acid transporter, y+ system), member 8	Slc7a8
1.59	Up	0.0017007	1.11E-02	NM_148933	Solute carrier organic anion transporter family, member 4a1	Slco4a1
1.59	Down	0.007332	2.72E-02	AK147452	Sorting nexin family member 27	Snx27
1.68	Down	0.0121697	3.61E-02	NM_001076554	Spectrin alpha 2	Spna2
20.65	Up	4.02E-07	9.45E-05	BG961926	Sprouty homolog 2 (Drosophila)	Spry2
1.53	Down	0.0066178	2.55E-02	NM_009234	SRY-box containing gene 11	Sox11
1.53	Down	0.0071915	2.70E-02	NM_011374	ST8 alpha-N-acetyl-neuraminide alpha-2,8-sialyltransferase 1	St8sia1
1.64	Down	0.0098212	3.14E-02	AK033099	Sterol-C4-methyl oxidase-like	Sc4mol
1.81	Up	0.0007859	6.90E-03	NM_032400	Succinate receptor 1	Sucnr1
1.63	Up	0.0033499	1.71E-02	AK033206	Suppressor of cytokine signaling 2	Socs2
1.51	Up	0.001278	8.94E-03	NM_020618	SWI/SNF related, matrix associated, actin dependent regulator of chromatin, subfamily e, member 1	Smarce1

1.59	Up	0.0106715	3.28E-02	BC019960	TAO kinase 1	Taok1
1.67	Down	0.0168666	4.58E-02	NM_025816	Tax1 (human T-cell leukemia virus type I) binding protein 1	Tax1bp1
1.51	Up	0.0106455	3.28E-02	TC1608317	TC1608317	-
1.83	Down	4.84E-05	1.33E-03	TC1651824	TC1651824	-
17.72	Down	0.0002584	3.42E-03	TC1666890	TC1666890	-
7.73	Up	0.0011617	8.61E-03	TC1715662	TC1715662	-
1.61	Up	0.0166296	4.56E-02	TC1724170	TC1724170	-
1.97	Up	0.0018132	1.15E-02	NM_009351	Telomerase associated protein 1	Tep1
1.55	Down	0.0085766	2.98E-02	NM_029148	Thioredoxin domain containing 13	Txndc13
2.1	Up	0.0079838	2.86E-02	NM_001009935	Thioredoxin interacting protein	Txnip
1.9	Down	0.0079771	2.86E-02	NM_134097	Topoisomerase I binding, arginine/serine-rich	Topors
17.59	Up	0.0001899	2.83E-03	AK079569	Transcribed locus	-
4.91	Up	4.40E-06	2.88E-04	BG969555	Transcribed locus	-
3.9	Up	0.0001577	2.51E-03	AK043872	Transcribed locus	-
3.44	Up	0.0091574	3.08E-02	AK034660	Transcribed locus	-
1.65	Up	0.019384	4.94E-02	AK077237	Transcribed locus	-
13.22	Up	0.0008927	7.36E-03	AK039098	Transcribed locus, weakly similar to NP_032661.2 microtubule-associated protein 7 [Mus musculus]	-
2.29	Up	0.0104837	3.26E-02	AK040896	Transcribed locus, weakly similar to XP_001152266.1 PREDICTED: similar to gag protein [Pan troglodytes]	-
1.76	Down	0.0008578	7.31E-03	NM_027495	Transmembrane protein 144	Tmem144
1.58	Down	0.0065643	2.55E-02	NM_181401	Transmembrane protein 64	Tmem64
6.4	Down	0.0170975	4.59E-02	AF223417	Triadin	Trdn
2.11	Up	0.0008937	7.36E-03	NM_011280	Tripartite motif protein 10	Trim10
1.52	Down	0.0098656	3.14E-02	NM_197987	Tripartite motif protein 37	Trim37
1.82	Up	3.71E-05	1.12E-03	NM_201373	Tripartite motif-containing 56	Trim56
2.11	Down	0.0094317	3.14E-02	NM_019548	Trophinin	Tro
5.95	Down	0.0081249	2.89E-02	NM_016712	Tropomodulin 4	Tmod4
1.7	Down	0.0006037	5.73E-03	NM_024427	Tropomyosin 1, alpha	Tpm1
2.14	Down	0.0041173	1.94E-02	NM_027462	Tryptophanyl tRNA synthetase 2 (mitochondrial)	Wars2
2.99	Down	0.0001501	2.49E-03	NM_172605	Tudor domain containing 3	Tdrd3
21.51	Up	8.27E-05	1.95E-03	NM_009413	Tumor protein D52-like 1	Tpd52l1
1.76	Down	0.0198478	4.97E-02	NM_030254	Tumor suppressor candidate 3	Tusc3
1.86	Down	0.0098056	3.14E-02	AB099518	UbiE-YGHL1 fusion protein	Ubie
1.91	Up	0.000247	3.40E-03	NM_026785	Ubiquitin-conjugating enzyme E2C	Ube2c
1.9	Down	0.0085465	2.98E-02	NM_016786	Ubiquitin-conjugating enzyme E2K (UBC1 homolog, yeast)	Ube2k

2.35	Up	0.0024951	1.43E-02	NM_010931	Ubiquitin-like, containing PHD and RING finger domains, 1	Uhrf1
1.62	Down	0.0121241	3.60E-02	NM_026390	UBX domain containing 2	Ubxd2
4.09	Up	0.0002485	3.40E-03	NM_020026	UDP-GalNAc:betaGlcNAc beta 1,3-galactosaminyltransferase, polypeptide 1	B3galnt1
1.79	Up	0.0010027	7.87E-03	BC024687	Vang-like 1 (van gogh, Drosophila)	Vangl1
1.61	Up	0.0098727	3.14E-02	NM_172598	WD repeat and HMG-box DNA binding protein 1	Wdhd1
6.06	Up	0.0044027	2.02E-02	NM_011721	Werner syndrome homolog (human)	Wrn
1.68	Up	0.0062391	2.46E-02	AK049137	WSC domain containing 1	Wscd1
2.13	Up	0.0155451	4.36E-02	XM_001002437	XM_001002437	-
1.92	Down	0.0005154	5.23E-03	XM_001002437	XM_001002437	-
1.61	Up	0.0081098	2.89E-02	XM_001005196	XM_001005196	-
6.83	Down	0.0096408	3.14E-02	XM_130232	XM_130232	-
1.86	Up	0.0058212	2.34E-02	XM_131166	XM_131166	-
1.53	Down	0.003995	1.91E-02	XM_132817	XM_132817	-
1.58	Up	0.006625	2.55E-02	XM_139711	XM_139711	-
1.67	Down	0.0007134	6.51E-03	XM_148595	XM_148595	-
2.07	Up	0.0085994	2.98E-02	XM_484075	XM_484075	-
1.6	Down	0.0052796	2.23E-02	XM_485258	XM_485258	-
2.61	Down	0.0002567	3.42E-03	XM_893473	XM_893473	-
1.52	Up	0.0088094	3.01E-02	XM_895138	XM_895138	-
2.14	Down	0.0048467	2.11E-02	XM_898059	XM_898059	-
1.9	Up	0.0045619	2.04E-02	XM_899897	XM_899897	-
1.57	Down	0.0060448	2.40E-02	XM_903055	XM_903055	-
1.53	Down	0.0027194	1.48E-02	XM_982400	XM_982400	-
1.6	Down	0.0169714	4.58E-02	XM_984921	XM_984921	-
1.86	Down	7.94E-06	4.25E-04	XM_991662	XM_991662	-
4.09	Down	0.0001077	2.19E-03	NM_028012	X-ray repair complementing defective repair in Chinese hamster cells 4	Xrcc4
2.79	Up	9.71E-05	2.08E-03	NM_028130	Zinc finger protein 157	Zfp157
1.58	Up	0.0104628	3.26E-02	NM_178679	Zinc finger protein 365	Zfp365
1.59	Up	0.0041363	1.94E-02	NM_175494	Zinc finger protein 367	Zfp367
2.22	Up	6.28E-05	1.61E-03	NM_013844	Zinc finger protein 68	Zfp68
1.71	Down	0.001651	1.09E-02	NM_133218	Zinc finger protein 704	Zfp704
1.58	Down	0.0025673	1.44E-02	NM_153160	Zinc finger, CCHC domain containing 17	Zcchc17

Group 1: **SMN-/-A2G WT quad**

Group 2: **SMN-/-A2G TG quad**

Statistics: **Welchs t-test**

Correction: **Benjamini and Hochberg**

Ratio	Direction	p-value	adj. p-value	Gene Identifier	Gene Name	Gene ID
2.24	Down	0.0001789	5.35E-03	NM_134052	Acireductone dioxygenase 1	Adi1
3.33	Up	1.22E-06	2.35E-04	NM_172678	Acyl-Coenzyme A dehydrogenase family, member 9	Acad9
1.61	Down	0.0027204	2.31E-02	NM_207231	ADP-ribosylation factor-like 5C	Arl5c
1.52	Up	0.0027965	2.31E-02	AF155157	AF155157	-
1.56	Down	0.0004156	6.96E-03	AK031168	AK031168	-
1.86	Down	0.0002691	6.04E-03	AK082951	AK082951	-
2.91	Down	0.0045909	3.24E-02	AK088871	AK088871	-
2.55	Down	0.0008666	1.10E-02	AK011866	Alcohol dehydrogenase, iron containing, 1	Adhfe1
2.69	Up	0.0032187	2.58E-02	NM_001013785	Aldo-keto reductase family 1, member C19	Akr1c19
1.68	Up	0.0055445	3.61E-02	NM_019467	Allograft inflammatory factor 1	Aif1
1.6	Down	0.0014791	1.59E-02	NM_146033	Ankyrin repeat and MYND domain containing 2	Ankmy2
1.93	Down	0.0003522	6.41E-03	AK008728	Ankyrin repeat and SOCS box-containing protein 13	Asb13
1.74	Up	0.0002998	6.30E-03	NM_080856	Ankyrin repeat and SOCS box-containing protein 14	Asb14
2.32	Up	0.0005533	8.28E-03	AK083552	Ankyrin repeat domain 41	Ankrd41
2.48	Down	0.0002573	5.91E-03	NM_145684	Arachidonate lipoxygenase, epidermal	Alox12e
1.68	Down	0.0088732	4.91E-02	NM_031405	Arsenate resistance protein 2	Ars2
1.53	Down	0.0022163	2.01E-02	NM_013464	Aryl-hydrocarbon receptor	Ahr
2.06	Up	0.0001583	5.17E-03	NM_175650	ATPase type 13A5	Atp13a5
1.69	Down	0.0003716	6.65E-03	NM_007508	ATPase, H+ transporting, lysosomal V1 subunit A	Atp6v1a
1.58	Down	0.0067745	4.18E-02	NM_011994	ATP-binding cassette, sub-family D (ALD), member 2	Abcd2
2.2	Up	0.0039911	3.02E-02	NM_025338	Aurora kinase A interacting protein 1	Aurkaip1
2	Up	0.0001207	4.51E-03	NM_013482	Bruton agammaglobulinemia tyrosine kinase	Btk
1.72	Down	0.0031471	2.55E-02	AK030723	Calcium channel, voltage-dependent, alpha 2/delta subunit 4	Cacna2d4
1.64	Up	0.0048585	3.34E-02	NM_009814	Calsequestrin 2	Casq2
1.87	Up	0.0016694	1.73E-02	NM_009797	Capping protein (actin filament) muscle Z-line, alpha 1	Capza1
1.81	Up	0.0027913	2.31E-02	NM_007606	Carbonic anhydrase 3	Car3
2	Up	0.0086703	4.88E-02	NM_023465	Catenin beta interacting protein 1	Ctnnbip1
1.9	Up	0.0011788	1.38E-02	NM_010818	Cd200 antigen	Cd200
1.53	Down	0.0043506	3.17E-02	NM_007642	CD28 antigen	Cd28
1.79	Up	0.0017323	1.78E-02	NM_021293	CD33 antigen	Cd33
9.79	Down	0.0003292	6.33E-03	NM_020260	Cdc42 GTPase-activating protein	Cdgap
1.83	Down	0.0037117	2.87E-02	NM_144927	CDNA sequence BC019943	BC019943
4.37	Down	2.16E-06	3.04E-04	NM_001003939	CDNA sequence BC030307	BC030307

1.89	Up	0.0053037	3.54E-02	NM_183143	CDNA sequence BC048679	BC048679
1.52	Down	0.0019872	1.95E-02	NM_198625	CDNA sequence BC060632	BC060632
1.83	Up	0.0088213	4.91E-02	NM_009863	Cell division cycle 7 (S. cerevisiae)	Cdc7
1.71	Down	0.000612	8.67E-03	NM_009138	Chemokine (C-C motif) ligand 25	Ccl25
4.33	Up	0.0009433	1.19E-02	BC050818	Chordin-like 1	Chrdl1
3.9	Up	0.0059167	3.79E-02	NM_172546	Cnksr family member 3	Cnksr3
2.11	Up	0.0071551	4.34E-02	NM_025779	Coiled-coil domain containing 109B	Ccdc109b
1.9	Down	0.0074931	4.46E-02	AK038056	Coiled-coil domain containing 55	Ccdc55
2.18	Up	0.000341	6.36E-03	AK199310	Coiled-coil domain containing 90A	Ccdc90a
1.84	Up	0.001591	1.67E-02	NM_007740	Collagen, type IX, alpha 1	Col9a1
1.84	Down	8.35E-05	3.40E-03	AK020801	Cyclin H	Ccnh
8.06	Up	1.81E-05	1.52E-03	BC049694	Cyclin-dependent kinase inhibitor 3	Cdkn3
4.89	Down	0.0026644	2.31E-02	NM_175475	Cytochrome P450, family 26, subfamily b, polypeptide 1	Cyp26b1
201.25	Up	1.43E-06	2.41E-04	NM_033623	DCUN1D1 DCN1, defective in cullin neddylation 1, domain containing 1 (S. cerevisiae)	Dcun1d1
24.69	Up	6.55E-07	1.49E-04	AK170208	DEP domain containing 6	Depdc6
2.03	Up	0.0089264	4.92E-02	NM_019670	Diaphanous homolog 3 (Drosophila)	Diap3
1.51	Up	0.0075138	4.46E-02	NM_015814	Dickkopf homolog 3 (Xenopus laevis)	Dkk3
8.72	Up	0.000854	1.09E-02	NM_133865	DNA cross-link repair 1B, PSO2 homolog (S. cerevisiae)	Dclre1b
1.64	Up	0.0020926	1.98E-02	NM_025311	DNA segment, Chr 14, ERATO Doi 449, expressed	D14Ertd449e
1.91	Up	0.0055808	3.61E-02	NM_053078	DNA segment, human D4S114	D0H4S114
6.13	Up	0.0012545	1.44E-02	NM_011932	Dual adaptor for phosphotyrosine and 3-phosphoinositides 1	Dapp1
1.64	Up	0.0082888	4.73E-02	NM_025869	Dual specificity phosphatase 26 (putative)	Dusp26
1.6	Down	0.0070144	4.28E-02	NM_145951	Ecto-NOX disulfide-thiol exchanger 2	Enox2
2.22	Up	0.0077991	4.51E-02	NM_015744	Ectonucleotide pyrophosphatase/phosphodiesterase 2	Enpp2
106.84	Up	2.26E-05	1.52E-03	NM_025855	Enoyl Coenzyme A hydratase domain containing 1	Echdc1
29.88	Down	5.62E-05	2.70E-03		ENSMUST00000048238	-
1.75	Down	0.0055589	3.61E-02		ENSMUST00000049389	-
3.27	Down	0.0021552	2.01E-02		ENSMUST00000062945	-
56.32	Up	4.96E-09	4.38E-06	NM_007894	Eosinophil-associated, ribonuclease A family, member 1	Ear1
1.89	Up	0.006245	3.95E-02	NM_181582	Eukaryotic translation initiation factor 5A	Eif5a
1.53	Down	0.0005474	8.28E-03	NM_145930	Expressed sequence AW549877	AW549877
2.29	Up	0.0070293	4.28E-02	NM_010197	Fibroblast growth factor 1	Fgf1

1.85	Down	0.0003805	6.65E-03	BC066859	Fibroblast growth factor 11	Fgf11
2.78	Down	0.0005304	8.25E-03	NM_030610	Fibroblast growth factor 20	Fgf20
40.45	Up	0.0007362	1.01E-02	NM_001012517	Fucosyltransferase 10	Fut10
4.38	Up	0.0001407	4.99E-03	AK018125	G elongation factor, mitochondrial 1	Gfm1
2.15	Down	0.0021919	2.01E-02	NM_001002268	G protein-coupled receptor 126	Gpr126
1.56	Down	0.0014857	1.59E-02	NM_147217	G protein-coupled receptor, family C, group 5, member C	Gprc5c
4.17	Up	6.48E-05	3.01E-03	AK082993	Gap junction membrane channel protein alpha 5	Gja5
1.51	Down	0.0033886	2.68E-02	NM_010258	GATA binding protein 6	Gata6
7.08	Up	0.0027956	2.31E-02	NM_026240	GRAM domain containing 3	Gramd3
1.54	Down	0.0003294	6.33E-03	NM_011825	Gremlin 2 homolog, cysteine knot superfamily (Xenopus laevis)	Grem2
24	Up	1.18E-05	1.06E-03	NM_008142	Guanine nucleotide binding protein (G protein), beta 1	Gnb1
1.6	Up	0.0004457	7.32E-03	NM_010424	Hemochromatosis	Hfe
1.57	Up	0.0036143	2.83E-02	NM_152803	Heparanase	Hpse
63.24	Down	0.0013405	1.49E-02	NM_010401	Histidine ammonia lyase	Hal
1.92	Up	0.0002878	6.17E-03	NM_175663	Histone cluster 1, H2ba	Hist1h2ba
2.11	Down	4.21E-05	2.36E-03	BF467941	Histone cluster 1, H4i	Hist1h4i
1.56	Down	0.0055586	3.61E-02	NM_146125	Inositol 1,4,5-trisphosphate 3-kinase A	Itpka
1.59	Down	0.0011032	1.31E-02	NM_008351	Interleukin 12a	Il12a
1.63	Up	0.0067551	4.18E-02	NM_008359	Interleukin 17 receptor A	Il17ra
2.74	Up	0.0011435	1.35E-02	NM_027711	IQ motif containing GTPase activating protein 2	Iqgap2
1.56	Down	0.0044373	3.21E-02	NM_172946	Keratin 222	Krt222
1.52	Up	0.0050984	3.47E-02	NM_178357	Kruppel-like factor 11	Klf11
1.81	Down	0.0077555	4.51E-02	NM_172380	KTEL (Lys-Tyr-Glu-Leu) containing 1	Ktelc1
1.99	Down	8.28E-05	3.40E-03	U12147	Laminin, alpha 2	Lama2
2.45	Up	0.0081192	4.67E-02	NM_001001492	Leber congenital amaurosis 5-like	Lca5l
1.6	Up	0.0002233	5.67E-03	NM_010708	Lectin, galactose binding, soluble 9	Lgals9
4.09	Up	0.0005808	8.50E-03	NM_175413	Leucine rich repeat containing 39	Lrrc39
1.7	Down	0.0006087	8.67E-03	NM_146052	Leucine rich repeat containing 3B	Lrrc3b
3.24	Up	2.48E-05	1.57E-03	NM_015763	Lipin 1	Lpin1
1.63	Up	5.30E-05	2.70E-03	NM_181470	LTV1 homolog (S. cerevisiae)	Ltv1
1.97	Down	0.0073963	4.42E-02	NM_010735	Lymphotoxin A	Lta
2.93	Up	0.0020737	1.98E-02	NM_145137	Macrophage galactose N-acetyl-galactosamine specific lectin 2	Mgl2
1.51	Down	0.0012359	1.43E-02	NM_029662	Major facilitator superfamily domain containing 2	Mfsd2
2.03	Down	0.0005391	8.25E-03	NM_008608	Matrix metallopeptidase 14 (membrane-inserted)	Mmp14
2.54	Down	2.68E-05	1.57E-03	BE570772	Methionine aminopeptidase 2	Metap2

3.57	Up	0.0015197	1.61E-02	NM_001029990	Methyltransferase 11 domain containing 1	Mett11d1
1.56	Up	0.0044946	3.21E-02	NM_174850	MICAL-like 2	Micall2
2.01	Up	0.0002537	5.91E-03	BC029173	Mitochondrial ribosomal protein L47	Mrpl47
1.52	Up	0.004312	3.15E-02	NM_030116	Mitochondrial ribosomal protein L9	Mrpl9
1.69	Down	0.0024172	2.13E-02	NM_021509	Monooxygenase, DBH-like 1	Moxd1
1.65	Down	0.0053083	3.54E-02	NM_033564	Mpv17 transgene, kidney disease mutant-like	Mpv17l
1.9	Up	0.0007244	1.01E-02	NM_054043	Musashi homolog 2 (Drosophila)	Msi2
1.59	Up	0.0018133	1.84E-02	AK159160	Myeloid-associated differentiation marker	Myadm
1.58	Down	0.0077699	4.51E-02	NM_028108	N-acetyltransferase 13	Nat13
21.94	Down	0.0001787	5.35E-03	NM_021320	Netrin 4	Ntn4
1.57	Down	0.0013776	1.52E-02	BB665367	Netrin G1	Ntng1
1.6	Down	0.0021763	2.01E-02	NM_008747	Neurotensin receptor 2	Ntsr2
2.35	Up	0.0057423	3.70E-02	NM_010876	Neutrophil cytosolic factor 1	Ncf1
1.57	Up	0.0042036	3.11E-02	NM_177029	NM_177029	-
2.21	Down	0.0085758	4.85E-02	NM_008711	Noggin	Nog
4.47	Up	0.0003753	6.65E-03	AK171679	Nuclear receptor coactivator 7	Ncoa7
1.9	Down	8.35E-05	3.40E-03	NM_010914	Nuclear transcription factor-Y beta	Nfyb
3.14	Up	0.003996	3.02E-02	NM_181345	Nucleophosmin/nucleoplasmin 2	Npm2
2.31	Up	1.93E-05	1.52E-03	NM_027722	Nudix (nucleoside diphosphate linked moiety X)-type motif 4	Nudt4
2.3	Up	2.64E-05	1.57E-03	NM_026936	Oxidase assembly 1-like	Oxa1l
4.52	Up	0.0015969	1.67E-02	NM_026141	Peptidylprolyl isomerase (cyclophilin)-like 4	Ppil4
1.57	Up	0.0047776	3.30E-02	NM_011069	Peroxisomal biogenesis factor 11b	Pex11b
1.9	Down	0.0021008	1.98E-02	NM_175356	Phosphatidylinositol 4-kinase, catalytic, beta polypeptide	Pi4kb
2.07	Up	0.0001003	3.86E-03	NM_183423	Phospholipase A2, group XIIA	Pla2g12a
1.73	Up	0.0003116	6.33E-03	NM_207229	Placenta specific 9	Plac9
1.95	Up	0.0045035	3.21E-02	NM_080465	Potassium intermediate/small conductance calcium-activated channel, subfamily N, member 2	Kcnn2
10.47	Up	0.0008166	1.07E-02	NM_027504	PR domain containing 16	Prdm16
2.88	Down	0.0020665	1.98E-02	BC001981	Predicted gene, ENSMUSG00000050599	ENSMUSG00000050599
1.56	Down	0.0005151	8.25E-03	AK041522	Predicted gene, ENSMUSG00000061510	ENSMUSG00000061510
1.7	Down	0.002224	2.01E-02	AK020123	Prickle-like 2 (Drosophila)	Prickle2
1.91	Up	0.0002512	5.91E-03	NM_011961	Procollagen lysine, 2-oxoglutarate 5-dioxygenase 2	Plod2
1.66	Down	0.0066669	4.17E-02	NM_008965	Prostaglandin E receptor 4 (subtype EP4)	Ptger4
1.77	Down	0.0062476	3.95E-02	NM_008949	Proteasome (prosome, macropain) 26S subunit, ATPase 3, interacting protein	Psmc3ip
1.66	Down	0.0073347	4.42E-02	NM_008860	Protein kinase C, zeta	Prkcz

1.88	Down	0.0001653	5.17E-03	NM_021880	Protein kinase, cAMP dependent regulatory, type I, alpha	Prkar1a
1.78	Up	0.0077285	4.51E-02	NM_011210	Protein tyrosine phosphatase, receptor type, C	Ptprc
7.74	Down	0.0003438	6.36E-03	AY861425	Protocadherin 9	Pcdh9
1.6	Up	0.0066904	4.17E-02	NM_175026	Pyrin and HIN domain family, member 1	Pyhin1
2.09	Up	0.0052192	3.51E-02	NM_013743	Pyruvate dehydrogenase kinase, isoenzyme 4	Pdk4
2	Up	0.0076415	4.49E-02	NM_026817	RAB, member of RAS oncogene family-like 2A	Rabl2a
2.77	Up	0.0013179	1.49E-02	NM_026405	RAB32, member RAS oncogene family	Rab32
1.62	Up	0.0045615	3.23E-02	NM_001013381	Radical S-adenosyl methionine domain containing 1	Rsad1
3.4	Up	0.0001545	5.17E-03	NM_023879	Retinitis pigmentosa GTPase regulator interacting protein 1	Rpgrip1
2.01	Down	5.41E-05	2.70E-03	BC044805	Rho guanine nucleotide exchange factor (GEF) 16	Arhgef16
1.85	Up	0.0005384	8.25E-03	NM_007447	Ribonuclease, RNase A family 4	Rnase4
5.91	Up	2.94E-07	9.88E-05	NM_021338	Ribosomal protein L35a	Rpl35a
3.11	Up	1.04E-08	4.65E-06	AK045413	RIKEN cDNA 1190007I07 gene	1190007I07Rik
1.98	Down	2.21E-05	1.52E-03	NM_028807	RIKEN cDNA 1200009I06 gene	1200009I06Rik
4.37	Up	6.51E-09	4.38E-06	NM_025904	RIKEN cDNA 1600012F09 gene	1600012F09Rik
1.82	Down	0.0020873	1.98E-02	AK007175	RIKEN cDNA 1700112E06 gene	1700112E06Rik
6.64	Up	0.0004896	7.94E-03	AK007195	RIKEN cDNA 1700113H08 gene	1700113H08Rik
1.56	Down	0.0002806	6.17E-03	XM_985599	RIKEN cDNA 2210011C24 gene	2210011C24Rik
2.41	Up	0.0013349	1.49E-02	NM_172417	RIKEN cDNA 2310042D19 gene	2310042D19Rik
1.81	Down	0.0052122	3.51E-02	AK010793	RIKEN cDNA 2410133F24 gene	2410133F24Rik
1.77	Up	0.0068081	4.18E-02	NM_025626	RIKEN cDNA 3110001A13 gene	3110001A13Rik
2.7	Down	0.0010116	1.24E-02	NM_026136	RIKEN cDNA 4930449I24 gene	4930449I24Rik
4.82	Up	9.35E-06	8.99E-04	NM_024273	RIKEN cDNA 4930455C21 gene	4930455C21Rik
1.52	Up	0.0024115	2.13E-02	NM_027627	RIKEN cDNA 4931408A02 gene	4931408A02Rik
2.33	Down	0.0023235	2.07E-02	AK085506	RIKEN cDNA 4933404O12 gene	4933404O12Rik
4.13	Up	0.0041189	3.07E-02	NM_001002786	RIKEN cDNA 9830134C10 gene	9830134C10Rik
2.55	Up	0.0010302	1.25E-02	AK084997	RIKEN cDNA B930095G15 gene	B930095G15Rik
1.6	Up	0.0027036	2.31E-02	NM_175332	RIKEN cDNA E130012A19 gene	E130012A19Rik
2.65	Up	0.0025198	2.20E-02	NM_026518	Ring finger protein 146	Rnf146
1.64	Down	0.0002005	5.60E-03	NM_011347	Selectin, platelet	Selp
1.6	Down	0.0050977	3.47E-02	NM_029023	Serine carboxypeptidase 1	Scpep1

2.55	Up	0.0030806	2.51E-02	NM_011355	SFFV proviral integration 1	Sfpi1
4.15	Down	3.98E-06	4.46E-04	NM_053198	Sideroflexin 4	Sfxn4
7.43	Up	4.97E-06	5.15E-04	AK005150	Single-stranded DNA binding protein 2	Ssbp2
5.8	Down	9.03E-05	3.57E-03	NM_011353	Small EDRK-rich factor 1	Serf1
1.95	Down	0.0032045	2.58E-02	NM_009196	Solute carrier family 16 (monocarboxylic acid transporters), member 1	Slc16a1
4.92	Up	0.0041333	3.07E-02	NM_026165	Solute carrier family 25, member 46	Slc25a46
1.91	Down	0.0008445	1.09E-02	NM_144902	Solute carrier family 35 (UDP-N-acetylglucosamine (UDP-GlcNAc) transporter), member 3	Slc35a3
4.01	Up	5.11E-05	2.70E-03	NM_016972	Solute carrier family 7 (cationic amino acid transporter, y+ system), member 8	Slc7a8
10.46	Up	2.26E-06	3.04E-04	BG961926	Sprouty homolog 2 (Drosophila)	Spry2
5.24	Up	0.0038912	2.99E-02	NM_001029841	Src-like adaptor	Sla
6.33	Up	6.91E-05	3.10E-03	NM_138673	Stabilin 2	Stab2
1.74	Down	0.0022177	2.01E-02	AK021293	Starch binding domain 1	Stbd1
2.24	Up	0.0008161	1.07E-02	NM_020618	SWI/SNF related, matrix associated, actin dependent regulator of chromatin, subfamily e, member 1	Smarce1
12.59	Down	2.21E-05	1.52E-03	TC1666890	TC1666890	-
1.68	Down	0.0020098	1.96E-02	TC1695895	TC1695895	-
6.87	Up	0.0004188	6.96E-03	TC1715662	TC1715662	-
1.68	Up	0.0035889	2.82E-02	NM_009351	Telomerase associated protein 1	Tep1
1.55	Up	0.0008131	1.07E-02	NM_027533	Tetraspanin 2	Tspan2
1.86	Up	0.0014903	1.59E-02	NM_001009935	Thioredoxin interacting protein	Txnip
2.15	Up	0.0002411	5.91E-03	NM_011595	Tissue inhibitor of metalloproteinase 3	Timp3
3.78	Up	0.0002888	6.17E-03	BG969555	Transcribed locus	-
2.09	Up	0.0018379	1.85E-02	AK082375	Transcribed locus	-
1.51	Down	0.003715	2.87E-02	BB653684	Transcribed locus	-
1.51	Down	0.0055534	3.61E-02	NM_009333	Transcription factor 7-like 2, T-cell specific, HMG-box	Tcf7l2
1.63	Up	0.006095	3.89E-02	NM_019754	Transgelin 3	Tagln3
7.17	Up	0.0026822	2.31E-02	NM_019818	Translocase of inner mitochondrial membrane 22 homolog (yeast)	Timm22
2.01	Up	0.0047557	3.30E-02	NM_201373	Tripartite motif-containing 56	Trim56
4.37	Down	2.94E-06	3.60E-04	NM_172605	Tudor domain containing 3	Tdrd3
13.41	Up	0.0002081	5.60E-03	NM_009413	Tumor protein D52-like 1	Tpd52l1
1.61	Down	0.0063099	3.97E-02	NM_011670	Ubiquitin carboxy-terminal hydrolase L1	Uchl1
2.28	Up	0.0010094	1.24E-02	NM_020026	UDP-GalNAc:betaGlcNAc beta 1,3-galactosaminyltransferase, polypeptide 1	B3galnt1
2.38	Down	0.0054147	3.59E-02	NM_199252	Unc-93 homolog A (C. elegans)	Unc93a
1.75	Up	0.0033289	2.65E-02	BC024687	Vang-like 1 (van gogh, Drosophila)	Vangl1
4.75	Up	0.0007498	1.02E-02	NM_009498	Vesicle-associated membrane protein 3	Vamp3

4.74	Up	0.0044736	3.21E-02	NM_011721	Werner syndrome homolog (human)	Wrn
2.79	Up	0.0003449	6.36E-03	XM_131166	XM_131166	-
1.72	Down	0.0017503	1.78E-02	XM_203596	XM_203596	-
2.14	Down	0.0001642	5.17E-03	XM_991662	XM_991662	-
3.43	Down	0.0005228	8.25E-03	NM_028012	X-ray repair complementing defective repair in Chinese hamster cells 4	Xrcc4
1.62	Down	0.0083786	4.76E-02	NM_001004066	Zinc finger protein 386 (Kruppel-like)	Zfp386
1.53	Up	0.0003284	6.33E-03	NM_013844	Zinc finger protein 68	Zfp68
1.54	Down	0.0003183	6.33E-03	NM_001039718	Zinc finger protein 91	Zfp91